Preparation and Characterization of Iridium Hydride and Dihydrogen Complexes Relevant to Biomass Deoxygenation

Jonathan M. Goldberg

A dissertation

submitted in partial fulfillment of the

requirements for the degree of

Doctor of Philosophy

University of Washington

2017

Reading Committee:

D. Michael Heinekey, Chair

Karen I. Goldberg, Chair

Brandi M. Cossairt

Program Authorized to Offer Degree:

Department of Chemistry

University of Washington

Abstract

Preparation and Characterization of Iridium Hydride and Dihydrogen Complexes Relevant to Biomass Deoxygenation

Jonathan M. Goldberg

Chairs of the Supervisory Committee:
Professor D. Michael Heinekey
Professor Karen I. Goldberg
Department of Chemistry

This thesis describes the fundamental organometallic reactivity of iridium pincer complexes and their applications to glycerol deoxygenation catalysis. These investigations provide support for each step of a previously proposed glycerol deoxygenation mechanism. Chapter 1 outlines the motivations for this work, specifically the goal of using biomass as a chemical feedstock over more common petroleum-based sources. A discussion of the importance of transforming glycerol to higher value products, such as 1,3-propanediol, is discussed. Chapter 2 describes investigations into the importance of pincer ligand steric factors on the coordination chemistry of the iridium metal center. Full characterization of a five-coordinate iridium-hydride complex is presented; this species was previously proposed to be a catalyst resting state for

glycerol deoxygenation. Chapter 3 investigates hydrogen addition to ^{R4}(POCOP)Ir(CO) [^{R4}POCOP = κ^3-C_6H_3-2,6-$(OPR_2)_2$ for R = ^{t}Bu, ^{i}Pr] and ^{R4}(PCP)Ir(CO) [^{R4}(PCP) = κ^3-C_6H_3-2,6-$(CH_2PR_2)_2$ for R = ^{t}Bu, ^{i}Pr] to give *cis*- and/or *trans*-dihydride complexes. Two mechanisms of hydrogen addition are presented (concerted oxidative addition and proton-catalyzed addition); the mechanism of hydrogen addition is dependent on the steric environment at the metal center. Chapter 4 presents spectroscopic evidence for two new iridium-dihydrogen complexes only stable under high pressures of hydrogen (40-80 atm) and low temperatures. Furthermore, iridium-catalyzed isotope exchange between H_2 and CD_3OD is presented and its potential implications in supporting the glycerol deoxygenation mechanism. Chapter 5 outlines a fundamental reaction of oxidative addition of iodine to $^{(tBu)4}$(POCOP)Ir(CO) complexes. Characterization of a cationic monoiodo iridium carbonyl complex as a potential oxidative addition intermediate is presented.

TABLE OF CONTENTS

Page

LIST OF FIGURES

Page

LIST OF SCHEMES

Page

LIST OF TABLES

Page

Acknowledgments

I would like to thank everyone who helped me get to where I am today. My time in graduate school went by way too fast and it was an amazing learning experience for me. I am proud to say I have developed into a much better scientist than when I entered as a bright-eyed first year. I have to thank Mr. Biedlingmaier at Churchville-Chili Senior High School who first sparked my interest in chemistry. His daily enthusiasm and excitement about science was contagious. When Mr. B. first dropped sodium into a beaker of water, I knew chemistry was my calling.

I would like to thank my undergraduate advisor Patrick Holland (then at the University of Rochester) for giving me the opportunity to work in his lab. My experiences in the Holland lab sparked my interest to pursue a graduate degree in inorganic chemistry. Pat was a supportive and knowledgeable advisor and always pushed me to be a more thorough and insightful chemist.

To my graduate research advisors, Mike Heinekey and Karen Goldberg, thank you for your guidance, tremendous support, and wisdom. When I first started graduate school, the thought of working for one advisor was daunting, but then I chose two. I am so glad I did. I learned how to attack chemistry problems from two brilliant, but different perspectives. You both pushed me to be a better scientist, mentor, and teacher. I always appreciated your open doors, always willing to chat about chemistry and life. On a personal level, when I lost members of my family, your compassion and kindness helped me get through some very tough times. I always felt like an integral part of both your groups. I am grateful for my time working with both of you.

To my family, my sister Jessica, mom Marcia Nachman, dad Ira, and stepdad Rick Bogdan, thank you for your love and support. You have always pushed me to follow my dreams and I am eternally grateful for having you in my life.

I have met so many amazing people along this graduate school journey. To Gene Wong, who we lost too soon, thank you for taking me under your wing and mentoring me. I am so glad to have known you. To Tim Brewster, Miriam Bowring, and Jason Prantner, thank you for being fantastic resources and always helping me think about research problems. I have been lucky enough to work with wonderful people who I befriended along the way including David Lao, Ash Wright, Carlos Rodriguez, Magnus Johnson, Tom Porter, Jessica Wittman, Amy Chu, Kim Hartstein, Ben Glassy, Danielle Henckel, Betsy Flowers, Mike Pegis, Jennifer Peper, Jenny Stein, Zuzana Culakova, Braden Zahora, Sophie Rubashkin, Alex Phearman, Hannah Zeitler, Byongjoo Bark, and Natalie Hillerson. To Wilson Bailey, Sophia Cherry, Ben Leipzig, Travis Lekich, Karena Smoll, Andrew Chanez, Louise Guard, Kim Quigley, and Tyler Stevens I am grateful for all my adventures with you. I am so thankful for our times exploring the mountains, frequenting a local brewery, or watching a Mariners game. To Sophia, I am so lucky to have met you and be your "work husband." You are my best friend and I will always be grateful for our time together. I am excited for our future adventures.

Dedication

To my family, who has always supported me

and knew I could do this.

Chapter 1

Introduction

1.1 Overview: Under *vs.* Overfunctionalized Chemical Feedstocks

Most carbon-based materials are currently derived from crude oil or natural gas and rely heavily on the availability of petroleum reserves.[1] These materials originate from simple hydrocarbons lacking further functionality (i.e. C-O, C-N bonds); they are often termed *underfunctionalized*.[2] Decades of research have explored how to selectively transform alkanes to functionalized species such as alkenes (dehydrogenation), aldehydes (hydroformylation), and amines (hydroamination).[2] However, a chemical industry based solely on petroleum is not sustainable as oil reserves continue to diminish and eventually will cease to support global demand.[3] Obtaining feedstocks from renewable resources would be a greener, alternative approach to using fossil fuels.[4] Within the last decade, significant advances have been made in using biomass instead of petroleum since Nature provides us with an abundance of renewable carbohydrate-based carbon sources (sugars and related derivatives).[5]

As we move toward a more sustainable future, reducing the amount of CO_2 emissions in the atmosphere is of paramount importance. Plants convert CO_2 and water to sugars (biomass), maintaining the balance of carbon in the atmosphere.[6] Whereas hydrocarbons lack functionality, biomass is *overfunctionalized*, containing a C-O bond on almost every carbon, providing the opposite challenge to petroleum-based feedstocks.[2,7] This highly oxygenated feedstock thus requires selective cleavage of C-O moieties to give hydrocarbons and reduced oxygenated chemical feedstocks via dehydration, hydrogenation or hydrogenolysis reactions.[7] Short-chain

sugars/sugar alcohols (C_3-C_6) have been targeted as the most promising feedstocks since, if selectively reduced, can provide common precursors to commodity chemicals for polyesters, polyurethanes, and solvents.[2,8,9]

1.2 Glycerol as a Chemical Feedstock

In recent years, alternative fuels have been sought to replace petroleum-based products (diesel). Biodiesel has been identified as an alternative fuel source since it can be easily obtained via base catalyzed transesterification of triglycerides (obtained from crops or waste vegetable oil) with methanol (Scheme 1.01), generating glycerol (1,2,3-propanetriol, 10% w/w) as a byproduct.[10] Biodiesel would provide a more sustainable source of fuels and most vehicles would require minimal modifications for its replacement of common diesel.[11]

Scheme 1.01. Transesterification of a Triglyceride with Methanol to Produce Biodiesel and Glycerol[10]

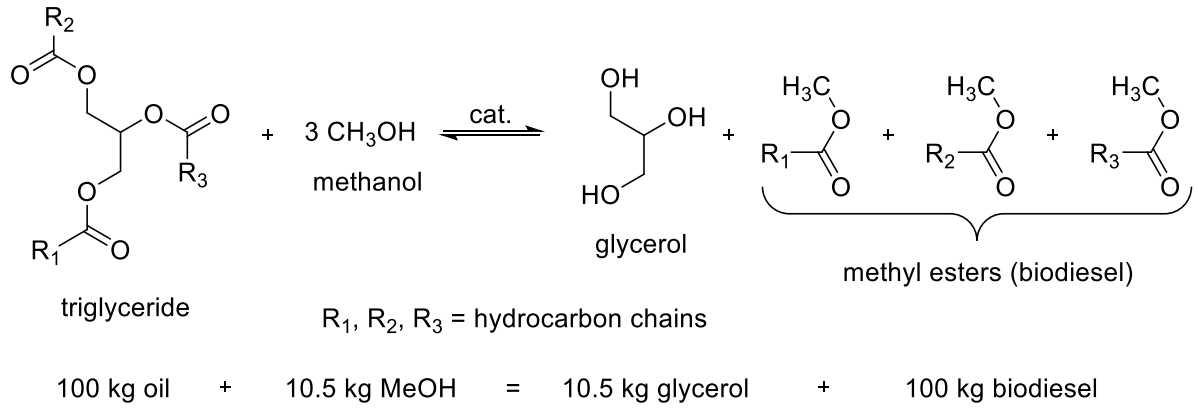

Glycerol finds use in pharmaceuticals, cosmetics, soaps, and toothpaste, but there is a cap in demand for these products.[12] Thus, expanding the usage for crude glycerol is critical for the

sustainability of biodiesel production; crude glycerol is an exceedingly cheap resource, often considered a waste product, and is thus an attractive target for functionalization to other value-added products. Within the last decade, so much glycerol from biodiesel was produced that the world's main suppliers for glycerol changed from major chemical companies like Procter and Gamble to biodiesel companies in Asia.[10] Selective reduction of glycerol to more valuable diols, alcohols, or alkanes could be a promising pathway for usage (Scheme 1.02).[13]

Scheme 1.02. Potential Higher Value Reduced Products from Glycerol Feedstocks[13]

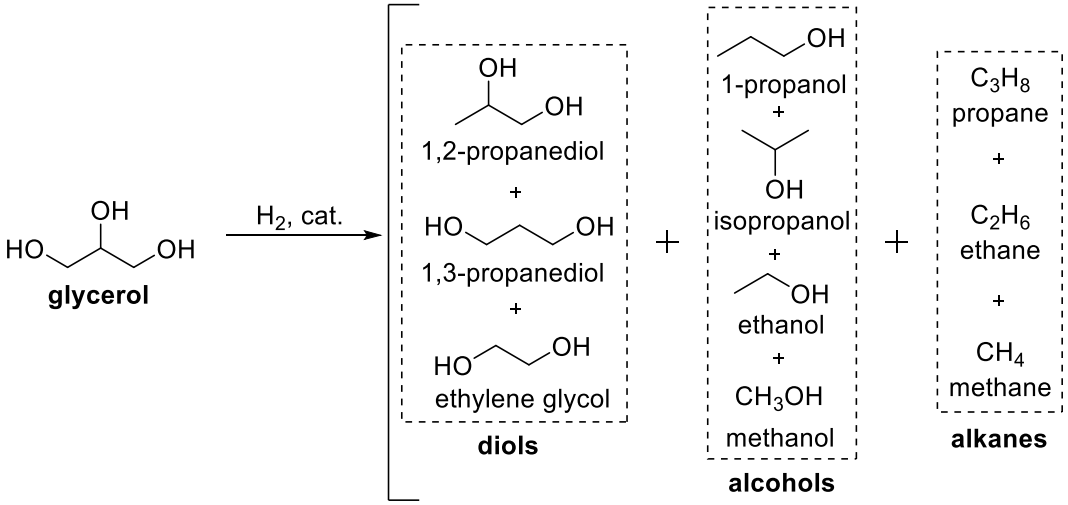

1.3 Glycerol to 1,3-Propanediol

Glycerol could be potentially transformed to a variety of higher value products. 1,3-propanediol (1,3-PD) is one of the most attractive products since it could be most useful in the production of polymers; however, it would also find use in cosmetics and drugs.[14] DuPont and Shell use 1,3-PD as a precursor, in combination with terephthalic acid, to produce polytrimethylene terephthalate (Figure 1.01, PTT), marketed under the commercial name Sorona®

(DuPont) or CORTERRA™ (Shell). PTT is a strong, soft, and stain-resistant polymer used to prepare fibers for carpets and apparel.[15]

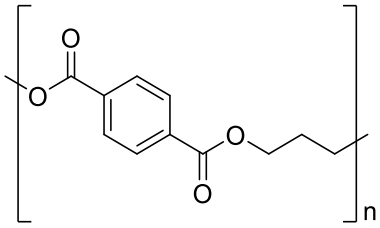

Figure 1.01. Polytrimethylene terephthalate (PTT)

The current state of the art process for 1,3-PD production, developed by DuPont in collaboration with Genencor, does not use glycerol as a feedstock, instead it converts D-glucose to 1,3-PD using engineered *E. coli* strains in a high yielding biotechnological process.[14] Prior to the method developed by DuPont and Genencor, 1,3-PD was previously produced on an industrial scale by hydration of acrolein (eq 1.01, Degussa-DuPont) or via hydroformylation of ethylene oxide followed by hydrogenation (eq 1.02, Shell).[15,16,17] These two methods were based on petroleum feedstocks. Thus, an efficient and selective direct conversion of an abundant bio-based glycerol feedstock to 1,3-PD is still needed.

Degussa-DuPont

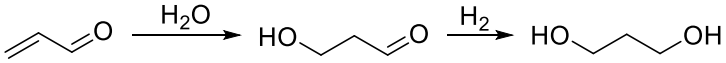

(1.01)

Shell

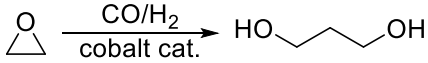

(1.02)

A major challenge to using crude glycerol from biodiesel as a chemical feedstock for 1,3-PD is the requirement to purify the glycerol so that contaminants do not inhibit catalysis. Crude glycerol from biodiesel is heavily contaminated with methanol, metal hydroxides, and water.[18] The

price of glycerol would significantly rise if it needs to be purified via distillation or chemical treatment prior to conversion to 1,3-PD. A successful catalytic system must tolerate potential impurities in crude glycerol.

Transformation of glycerol to value-added products has been approached via many routes, including metabolic engineering with microorganisms[19] and chemical routes. Work from Kivistö and coworkers in biological catalysis has shown viable routes from glycerol to 1,3-PD using an anaerobic bacterial fermentation process.[20] However, the major drawback to this method is inhibition of 1,3-PD production due to the concomitant formation of acetate byproducts. Additionally, many pathways using bacteria are undesirable due to their difficulty with scalability and potential pathogenicity.[17,21] While biological methods have found promising results for converting glycerol to 1,3-PD, we are interested in catalyzing this reaction using transition-metal catalysts since they are often more robust and stable to harsh conditions or potential inhibitory byproducts. The strategy for chemical conversion of glycerol to 1,3-PD involves a tandem pathway of a proton-catalyzed dehydration followed by a hydrogenation step (eq 1.03) to generate 1,3-PD.[2,22] These types of reactions require selective catalysts that must be stable to acidic aqueous conditions and high pressures of hydrogen.

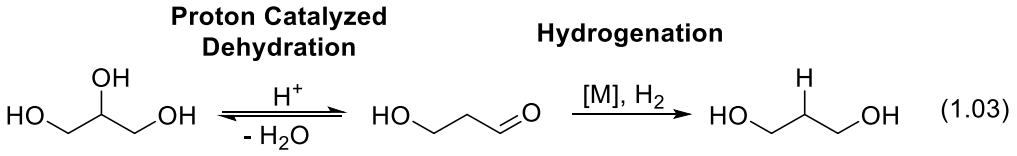

(1.03)

1.4 Transition-Metal Catalyzed Conversion of Glycerol to 1,3-Propanediol

Catalytic chemical conversion of glycerol to 1,3-PD has been previously shown both via heterogeneous and homogenous pathways. Heterogeneous systems for converting glycerol to 1,3-PD have been demonstrated for many supports with a variety of transition-metals including iridium,[23] platinum,[24,25,26] and copper.[27] One of the best heterogeneous systems reported to date achieved 66% yield of 1,3-PD using boehmite-supported platinum nanoparticles and tungsten oxides; formation of 1,2-propanediol (1,2-PD, 2%), 1-propanol (11%), and isopropanol (6%) was also observed.[28] While this system gave selectivity for 1,3-PD, it has since been challenging to improve upon these results. In general, optimization of heterogeneous systems requires the selective formation of 1,3-PD over 1,2-PD.[29]

There are far fewer examples of homogeneous metal catalysts capable of selectively converting glycerol to 1,3-PD. As well, there are few examples of homogenous transition-metal catalyzed deoxygenation of 1,2-propanediol, a model substrate for glycerol, to reduced products (1-propanol or propane). An early report by Che described a homogeneous glycerol to 1,3-PD system with $Rh(CO)_2(acac)$ and H_2WO_4, where 21% conversion to 1,3-PD was observed; however, the other products observed were 1,2-PD (23%), and 1-propanol (1-PO, 3.6%).[30] Controlling the selectivity for 1,3-PD proved to be non-trivial. Similarly, a later example from Drent and Jager using Pd(II)$(acetate)_2$, 1,2-bis(1,5-cyclooctylenephosphino)ethane, and methanesulfonic acid showed similar selectivity difficulties, except 1-propanol was the preferred product; the observed product ratio from conversion of glycerol was 47.4% 1-propanol: 21.8% 1,2-PD: 30.8% 1,3-PD.[31]

Previous work in the Heinekey and Goldberg groups examined deoxygenation of polyols using iridium pincer complexes. An initial report examined the deoxygenation of 1,2-PD to 1-propanol using $^{(tBu)4}(POCOP)IrH_2$ (**1**) [$^{(tBu)4}(POCOP) = \kappa^3$-$C_6H_3$-2,6-$(OP(^tBu)_2)_2$] and triflic acid

(eq 1.04).[32] Iridium pincer complexes were well suited for this transformation since they were previously shown to be thermally robust.[33] This iridium system effectively converted 1,2-PD to 1-propanol in 95% yield and was stable to an acidic aqueous 1,4-dioxane environment. The overall activity and selectivity of the catalyst for producing 1-propanol was best at high water combined with low acid concentrations. Higher acid concentrations or low water containing reactions led to the formation of 15 different products (ethers, ketones, alkanes).[34] Post-reaction analysis showed two iridium species by NMR spectroscopy with data consistent with the complexes being an Ir(I)-CO species $^{(tBu)4}$(POCOP)Ir(CO) (**2**) and a *trans*-dihydride complex *trans*-$^{(tBu)4}$(POCOP)Ir(CO)$(H)_2$ (**3**). It was proposed that **1** decarbonylated the substrate, resulting in the carbonyl ligand in both iridium species. Gratifyingly, **2** was also found to be an effective precatalyst for this transformation, since it is air-stable; complex **1** is only stable under an argon atmosphere.

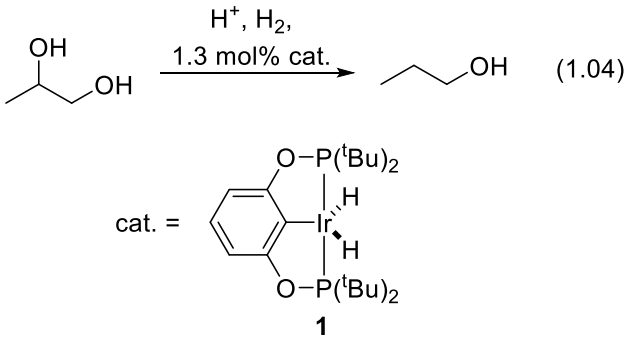

The mechanism for the formation of the *trans*-dihydride complex **3** was proposed to proceed via a water assisted hydrogen addition mechanism (eq 1.05). Formation of **3** was indeed observed upon pressurizing a solution of **2** and acid (anilinium tetraphenylborate) with H_2 pressure.

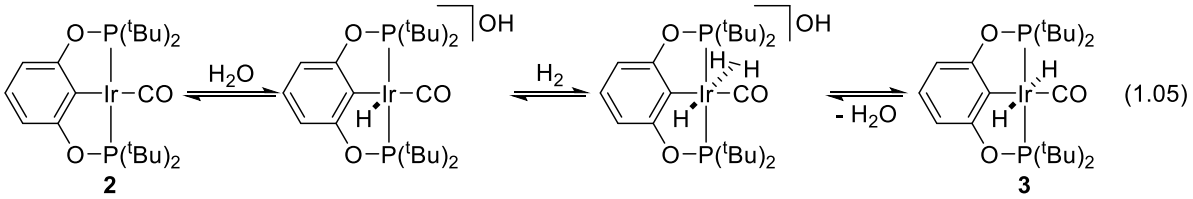

(1.05)

Subsequent work from these groups showed that the same catalyst system with sulfuric acid could convert glycerol to a mixture of 1,3-PD and 1-propanol.[35] A dimethylamino group was substituted in the *para* position of the aromatic backbone [$^{(NMe2)(tBu)4}$(POCOP)Ir(CO) (**4**)] to improve solubility in acidic aqueous 1,4-dioxane (eq 1.06).

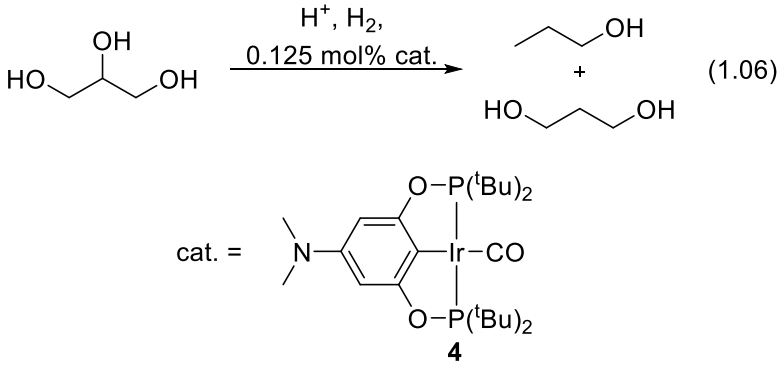

(1.06)

An acid concentration dependence was observed in this system as well. At low acid (0.25% *vs.* glycerol; 2 equiv *vs.* iridium) 2:1 selectivity of 1,3-PD to 1-propanol was observed. Formation of 1,2-PD was also observed in approximately the same ratio as 1,3-PD. However, increasing the acid to 4.0% led to 4:1 selectivity of 1-propanol to 1,3-PD with no 1,2-PD observed. Generally, at lower acid concentrations, overall glycerol conversion was lower. The selectivity and conversion dependence on acid was not fully understood when this work was presented. Post-reaction analysis of glycerol deoxygenation catalysis also showed formation of **2** and **3**, as was observed in reactions with 1,2-PD. Catalyst speciation studies led to the proposal of a mechanism for glycerol deoxygenation to 1,3-PD (Scheme 1.03).

Scheme 1.03. Proposed Mechanism of Glycerol Deoxygenation with $^{(tBu)4}$(POCOP)Ir(CO) Complexes.

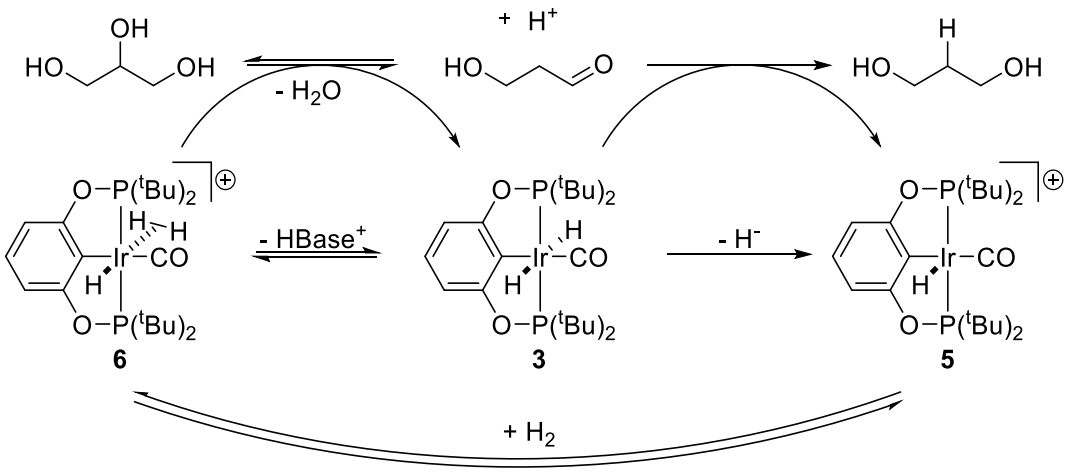

The mechanism for glycerol deoxygenation was previously proposed, however there was not full support for all the hypothesized complexes or steps in the transformation. It was proposed that under acidic conditions, protonation of $^{(tBu)4}$(POCOP)Ir(CO) (**2**) would give a five-coordinate hydride complex, [$^{(tBu)4}$(POCOP)Ir(CO)(H)]$^+$ (**5**), with an open site *trans* to the iridium-hydride. Under a hydrogen atmosphere, an iridium-dihydrogen complex, [$^{(tBu)4}$(POCOP)Ir(CO)(H)(H_2)]$^+$ (**6**), could form. The iridium dihydrogen complex is hypothesized to be quite acidic and will protonate glycerol leading to loss of one equivalent of water. The *in situ* generated aldehyde intermediate would then be readily protonated under acidic conditions and *trans*-dihydride **3** would transfer a hydride to the substrate, forming 1,3-PD and regenerate the catalytic cycle. When this work was reported, evidence for the formation of **3** via proton-assisted hydrogen addition to **2** was shown, as well as preliminary evidence for the five-coordinate hydride **5**. Observation of iridium-dihydrogen complex **6** was attempted by a low temperature protonation of a mixture of complexes **3** and **2**, however, relaxation times (T_1) of the hydride resonances were not consistent with a dihydrogen ligand. Further work is required to characterize each of the proposed reaction intermediates as well as the required elementary steps to reach them.

1.5 Dissertation Summary

The work outlined in this dissertation describes the synthesis, characterization, and reactivity studies of iridium pincer complexes relevant to the mechanism of glycerol deoxygenation catalysis (Scheme 1.03). Chapter 2 describes the importance of POCOP ligand steric factors on the coordination chemistry at iridium. Furthermore, the synthesis and characterization of five-coordinate hydride complexes, such as complex **5** shown above, is described. Chapter 3 investigates hydrogen addition to (POCOP)Ir(CO) and (PCP)Ir(CO) [(PCP) = κ^3-C_6H_3-2,6-$(CH_2PR_2)_2$] complexes. Interestingly, two mechanisms of hydrogen addition are possible (concerted oxidative addition or proton-catalyzed addition), depending on the alkyl group substituted at phosphorus. The synthesis and characterization of *trans*-dihydride complexes, such as complex **3** shown above, is also described. Chapter 4 shows evidence for two new iridium-dihydrogen complexes, such as complex **6** above, stable only under high pressures of hydrogen (40-80 atm) and at low temperatures. Additionally, evidence for iridium catalyzed isotope exchange between H_2 and CD_3OD is discussed. Chapter 5 describes a fundamental study of oxidative addition of iodine to $^{(tBu)4}$(POCOP)Ir(CO) complexes. The effect of changing the *para*-substituent on the pincer ligand on iodine addition to iridium is shown.

1.6 Notes to Chapter

[1] Goldman, A. S.; Roy, A. H.; Huang, Z.; Ahuja, R.; Schinski, W.; Brookhart, M. *Science* **2006**, *312*, 257–261.
[2] Schlaf, M. *Dalton Trans.* **2006**, 4645–4653.
[3] Murray, J.; King, D. *Nature* **2012**, 433-435.
[4] Anastas, P. T.; Warner, J. C. *Green Chemistry: Theory and Practice*, Oxford University Press: New York, 1998; pp 30.
[5] Luterbacher, J. S.; Martin Alonso, D.; Dumesic, J. A. *Green Chem.* **2014**, *16*, 4816–4838.

[6] Ruppert, A, M.; Weinberg, K.; Palkovits, R. *Angew. Chem. Int. Ed.* **2012**, *51*, 2564−2601.
[7] Sutton, A. D.; Waldie, F. D.; Wu, R.; Schlaf, M.; Silks, L. A. P.; Gordon, J. C. *Nat. Chem.* **2013**, *5*, 428–432.
[8] McLaughlin, M. P.; Adduci, L. L.; Becker, J. J.; Gagné, M. R. *J. Am. Chem. Soc.* **2013**, *135*, 1225–1227.
[9] Adduci, L. L.; Bender, T. A.; Dabrowski, J. A.; Gagné, M. R. *Nat. Chem.* **2015**, *7*, 576–581.
[10] Ciriminna, R.; Pina, C. Della; Rossi, M.; Pagliaro, M. *Eur. J. Lipid Sci. Technol.* **2014**, *116*, 1432–1439.
[11] Wood, B. M.; Kirwan, K.; Maggs, S.; Meredith, J.; Coles, S. R. *J. Clean. Prod.* **2015**, *93*, 167–173.
[12] Behr, A.; Eilting, J.; Irawadi, K.; Leschinski, J.; Lindner, F. *Green Chem.* **2008**, *10*, 13–30.
[13] Wang, Y.; Zhou, J.; Guo, X. *RSC Adv.* **2015**, *5*, 74611–74628.
[14] Celińska, E. *Biotechnol. Adv.* **2010**, *28*, 519–530.
[15] Zhou, C. H.; Beltramini, J. N.; Fan, Y. X.; Lu, G. Q. *Chem. Soc. Rev.* **2008**, *37*, 527–549.
[16] Besson, M.; Gallezot, P.; Pigamo, A.; Reifsnyder, S. *Appl. Catal. A: Gen.* **2003**, *250*, 117–124.
[17] Kraus, G. A. *Clean - Soil, Air, Water* **2008**, *36*, 648–651.
[18] Lee, C. S.; Aroua, M. K.; Daud, W. M. A. W.; Cognet, P.; Pérès-Lucchese, Y.; Fabre, P. L.; Reynes, O.; Latapie, L. *Renew. Sustain. Energy Rev.* **2015**, *42*, 963–972.
[19] (a) Chen, Z.; Liu, D. *Biotechnol. Biofuels* **2016**, *9*, 205. (b) Rodriguez, A.; Wojtusik, M.; Masca, F.; Santos, V. E.; Garcia-Ochoa, F. *Biochem. Eng. J.* **2017**, *117*, 57–65.
[20] Kivistö, A.; Santala, V.; Karp, M. *J. Biotechnol.* **2012**, *158*, 242–247.
[21] Tabah, B.; Varvak, A.; Pulidindi, I. N.; Foran, E.; Banin, E.; Gedanken, A. *Green Chem.* **2016**, *18*, 4657–4666.
[22] (a) Schlaf, M.; Ghosh, P.; Fagan, P. J.; Hauptman, E.; Bullock, R. M. *Adv. Synth. Catal.* **2009**, *351*, 789–800. (b) Schlaf, M.; Ghosh, P.; Fagan, P. J.; Hauptman, E.; Bullock, R. M. *Angew. Chem. Int. Ed.* **2001**, *40*, 3887–3890.
[23] Nakagawa, Y.; Ning, X.; Amada, Y.; Tomishige, K. *Appl. Catal. A: Gen.* **2012**, *433–434*, 128–134.
[24] Oh, J.; Dash, S.; Lee, H. *Green Chem.* **2011**, *13*, 2004-2007.
[25] García-Fernández, S.; Gandarias, I.; Requies, J.; Soulimani, F.; Arias, P. L.; Weckhuysen, B. M. *Appl. Catal. B Environ.* **2017**, *204*, 260–272.
[26] Gong, L.; Lu, Y.; Ding, Y.; Lin, R.; Li, J.; Dong, W.; Wang, T.; Chen, W. *Appl. Catal. A: Gen.* **2010**, *390*, 119–126.
[27] Harisekhar, M.; Kumar, V. P.; Priya, S. S.; Chary, K. V. R. *J. Chem. Technol. Biotechnol.* **2015**, *90*, 1906–1917.
[28] Arundhathi, R.; Mizugaki, T.; Mitsudome, T.; Jitsukawa, K.; Kaneda, K. *ChemSusChem* **2013**, *6*, 1345–1347.
[29] Besson, M.; Gallezot, P.; Pinel, C. *Chem. Rev.* **2014**, *114*, 1827–1870.
[30] Che, T. M. Production of propanediols. US 4642394, February 10, 1987.
[31] Drent, E.; Jager, W. W. Hydrogenolysis of glycerol. US 6080898, June 27, 2000.
[32] Ahmed-Foskey, T. J.; Heinekey, D. M.; Goldberg, K. I. *ACS Catal.* **2012**, *2*, 1285–1289.
[33] Choi, J.; MacArthur, A. H. R.; Brookhart, M.; Goldman, A. S. *Chem. Rev.* **2011**, *111*, 1761–1779.
[34] Coll, D.; Delbecq, F.; Aray, Y.; Sautet, P. *Phys. Chem. Chem. Phys.* **2011**, *13*, 1448–1456.
[35] Lao, D. B.; Owens, A. C. E.; Heinekey, D. M.; Goldberg, K. I. *ACS Catal.* **2013**, *3*, 2391–2396.

Chapter 2

The Importance of Steric Factors in Iridium Pincer Complexes

The following has been previously published.[1]

2.1 Introduction

Pincer ligands are ubiquitous in transition and main group metal catalysis due to the stability imparted to the metal complex and the ease with which the pincer framework can be modified.[2] Many pincer ligands feature an aryl backbone with phosphine or phosphinite arms such as those in PCP (where PCP = C_6H_4-1,3-$[CH_2PR_2]_2$) or POCOP (where POCOP = C_6H_4-1,3-$[OPR_2]_2$), respectively (R is often ^{t}Bu or ^{i}Pr).[3,4] Modification of the aryl backbone has been shown to affect the electron density at the metal. For example, Brookhart and co-workers synthesized a series of (POCOP)Ir(CO) complexes and found that the *ν*(CO) changes when the *para* position of the aryl group is substituted with groups of varying electron-donating or -withdrawing ability.[5] Goldman and co-workers found that the thermodynamics of H_2 addition to *para*-substituted (PCP)Ir(CO) depended on the electron-withdrawing or -donating nature of the substituent.[6] While there have been extensive studies on the electronic effects at the iridium center resulting from modifications of the pincer ligand, there are fewer comprehensive studies on the influence of the sterics of the POCOP ligand on the coordination chemistry at iridium.

The steric demands of the substituents bound to phosphorus in both (PCP)Ir and (POCOP)Ir complexes have been shown to be important in both stoichiometric and catalytic reactions. For example, Milstein and co-workers showed how the steric profile of the phosphine alkyl groups in the naphthyl-based (PCP)Rh system influenced reductive elimination of MeI from a Rh(III) complex.[7,8,9] Reductive elimination of MeI was favored from the more sterically

encumbered ^{t}Bu-substituted ligand, whereas the reaction did not occur from the ^{i}Pr-substituted analogue. Goldman, Brookhart, Jensen, and co-workers reported higher activity of (PCP)Ir and (POCOP)Ir catalysts for alkane dehydrogenation when the traditional ^{t}Bu-based phosphine arms were substituted with the smaller ^{i}Pr groups (Figure 2.01).[10] The change in reactivity is proposed to be the result of an increase in the space around the metal center due to reduced steric demand of the phosphine substituent.[11]

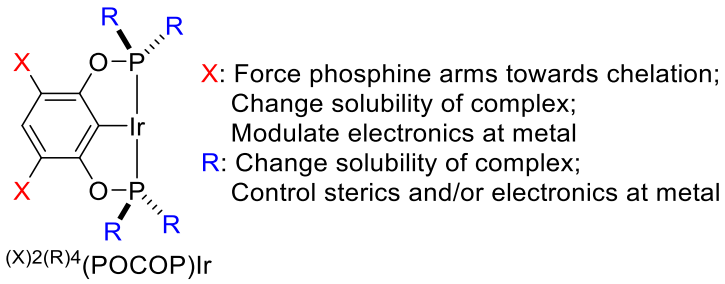

Figure 2.01. POCOP ligand framework.

In the work described herein, the effects of modifications of the POCOP ligand on the synthesis and reactivity of Ir complexes were investigated. (POCOP)Ir complexes are ubiquitous in organometallic catalysis, and we are motivated to design more active catalysts.[12] Here, we report how steric factors of the pincer ligand dictate the coordination chemistry at iridium. POCOP ligands with substituents smaller than ^{i}Pr require substitution of the aryl backbone to prevent formation of polymeric products upon reaction with iridium precursors. Studies of reactions of $Ir(CO)_2Cl$(*p*-toluidine) with POCOP ligands show that R groups smaller than ^{t}Bu favor octahedral hydrido-chloride Ir(III) carbonyl complexes, while R = ^{t}Bu ligands favor square planar Ir(I) carbonyl complexes. For ^{t}Bu-substituted POCOP, the metalation reaction with $Ir(CO)_2Cl$(*p*-toluidine) may proceed via a *cis*- or *trans*-hydrido-chloride Ir(III) intermediate, both of which are

in an equilibrium. Synthesis and characterization of a new series of *meta*-substituted complexes as well as the syntheses of the first bis(phosphite) (POCOP)Ir complexes are presented.

2.2 Results

2.2.1 Synthesis of Iridium Bis(phosphite) Complexes

Addition of two equivalents of *N*,*N*-diisopropylaminobis-(methoxyphosphane) [(^{i}Pr)$_2$NP(OMe)$_2$] to a solution of resorcinol (1,3-dihydroxybenzene) and two equivalents of tetrazole in MeCN affords $^{(OMe)4}$(POCOP) (eq 2.01).[13] Reaction of $^{(OMe)4}$(POCOP) with Ir(CO)$_2$Cl(*p*-toluidine) or [Ir(COE)$_2$(μ-Cl)]$_2$ resulted in the formation of insoluble precipitates. Bedford, Pringle, and co-workers investigated related Pd complexes and also encountered insoluble precipitates, but found that if the *meta*-positions of the aryl backbone were substituted with ^{t}Bu groups, the reactions proceeded to form the desired monomeric species.[14]

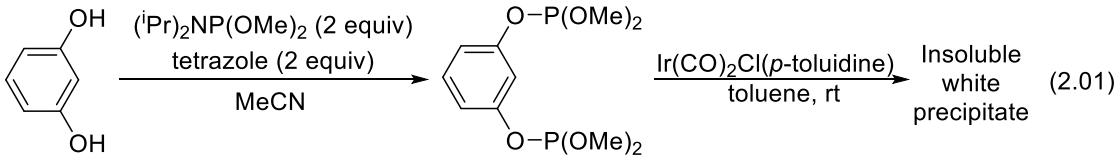

The *meta*-substituted ligand $^{(tBu)2(OMe)4}$(POCOP) (**1a**, Scheme 2.01) was synthesized in a similar manner to the bis(phosphite) POCOP ligands reported by Bedford, Pringle, and co-workers.[14] Excess methanol was added to a solution of one equivalent of [C$_6$H$_2$-4,6-(^{t}Bu)$_2$-1,3-(OPCl$_2$)$_2$] and excess NEt$_3$ at -40 °C. The solution was then warmed to room temperature over 12 h, resulting in formation of the desired product in high purity. The ^{31}P{^{1}H} NMR spectrum of the resulting viscous yellow oil shows a singlet at 135.0 ppm. The ^{1}H NMR spectrum features a

doublet at 3.67 ppm ($^3J_{PH}$ = 10.3 Hz) indicative of coupling between the phosphorus and the methoxy protons, consistent with formation of a P-OCH_3 moiety.

The reaction of the *meta*-substituted ligand **1a** and an Ir(I) precursor led to a soluble monomeric Ir species. The ligand **1a** was treated with $Ir(CO)_2Cl$(*p*-toluidine) at 100 °C in toluene for 18 h, resulting in the formation of $^{(tBu)2(OMe)4}$(POCOP)Ir^{III}(CO)(H)(Cl) (**2a**) (Scheme 2.01). A single phosphorus-containing product was observed by $^{31}P\{^1H\}$ NMR spectroscopy (117.3 ppm). The ^1H NMR spectrum showed two virtual triplets at 4.12 and 3.74 ppm assignable to the two chemically inequivalent OMe environments coupled to two magnetically inequivalent phosphorus atoms. Additionally, a triplet at −18.51 ppm ($^2J_{PH}$ = 13.5 Hz) was assigned to an iridium hydride that is coupled to the two phosphorus atoms. The ^1H NMR spectrum of the reaction mixture also features broad signals between 3.5 and 2.5 ppm, presumably due to decomposition of some of the P-OMe moieties at 100 °C during the metalation reaction. Isolation of pure samples of complex **2a** was achieved in low yields since impurities had similar solubilities. Crystals of **2a** suitable for X-ray diffraction were grown by layering pentane over a dichloromethane solution of **2a** at −20 °C. The molecular structure of **2a** is shown in Figure 2.02.

The analogous bis(phosphite) iridium complex based on 1,2:5,6-di-*O*-isopropylidene-D-mannitol (**2c**, Scheme 2.01) was also prepared. Bedford, Pringle, and co-workers were able to synthesize a Pd−Cl complex based on this ligand; however, it was not structurally characterized.[14] We were able to prepare $^{(tBu)2(diol)2}$(POCOP)Ir^{III}(CO)(H)(Cl) (**2c**) by reaction of the ligand with $Ir(CO)_2Cl$(*p*-toluidine). Crystals suitable for X-ray diffraction were grown by vapor diffusion of hexane into a toluene solution of **2c** at room temperature; the molecular structure is shown in Figure 2.03.

Scheme 2.01. Synthesis of Bis(phosphite) POCOP Ligands and Metalation Reactions[a]

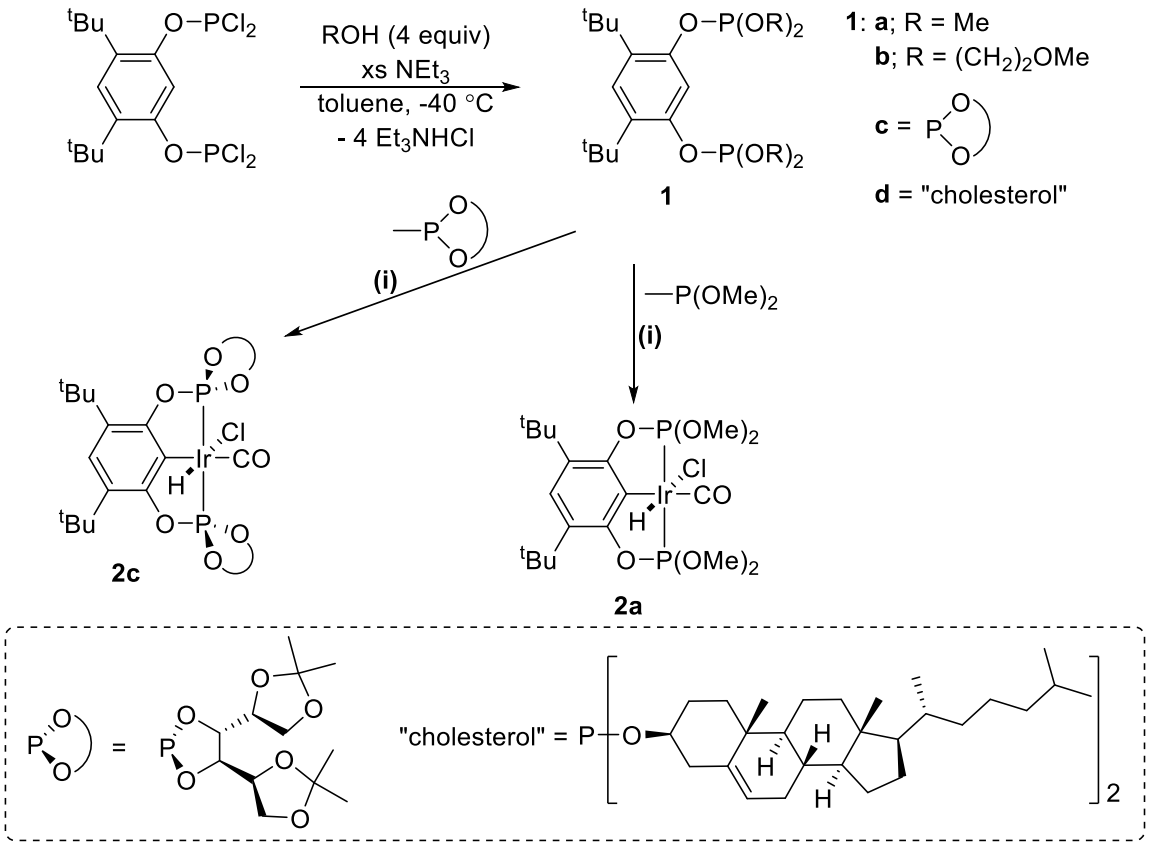

[a](i) Conditions: $Ir(CO)_2Cl$(*p*-toluidine), toluene, 100 °C, 18 h

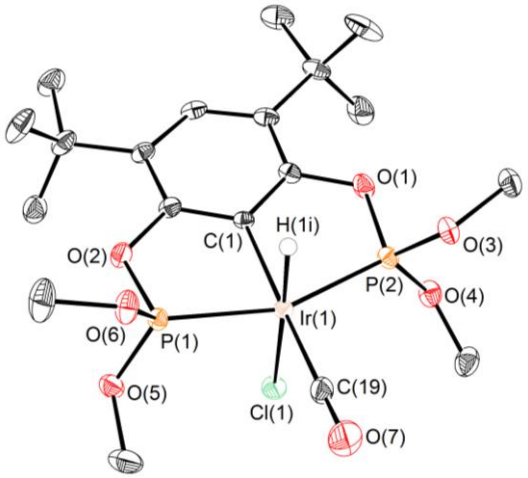

Figure 2.02. ORTEP[15] of $^{(tBu)2(OMe)4}$(POCOP)Ir^{III}(CO)(H)(Cl) (**2a**) shown with 50% thermal ellipsoids. Hydrogen atoms, except for the iridium-bound hydride, are omitted for clarity. Selected bond lengths (Å) and angles (°) for **2a**: Ir(1)-C(1) 2.071(2), Ir(1)-P(1) 2.2676(7), Ir(1)-P(2) 2.2681(7), Ir(1)-C(19) 1.921(3), C(19)-O(7) 1.132(3); C(19)-Ir(1)-C(1) 174.06(11), C(1)-Ir(1)-P(1) 78.45(7), C(1)-Ir(1)-P(2) 78.26(7), P(1)-Ir(1)-P(2) 156.66(2).

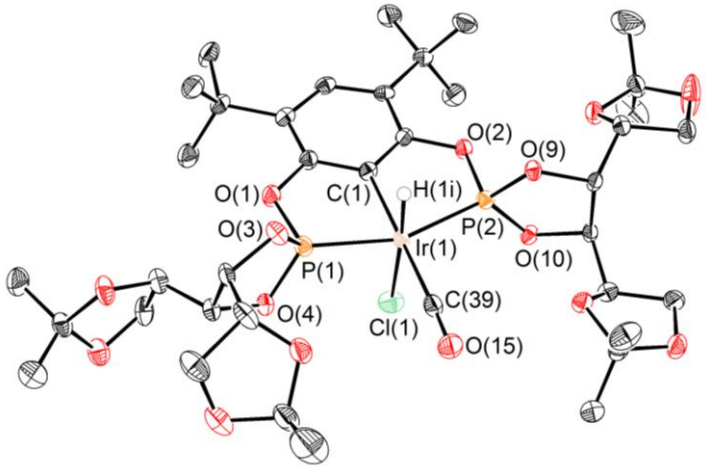

Figure 2.03. ORTEP[15] of $^{(tBu)2(diol)2}$(POCOP)Ir^{III}(CO)(H)(Cl) (**2c**) shown with 50% thermal ellipsoids. Hydrogen atoms, except for the iridium-bound hydride, are omitted for clarity. Selected bond lengths (Å) and angles (°) for **2c**: Ir(1)−C(1) 2.045(3), Ir(1)−P(1) 2.2408(9), Ir(1)−P(2) 2.2626(8), Ir(1)− C(39) 1.949(4), C(39)−O(15) 1.122(4); C(39)-Ir(1)-C(1) 178.30(14), C(1)-Ir(1)-P(1) 79.62(9), C(1)-Ir(1)-P(2) 79.72(9), P(1)-Ir(1)-P(2) 158.64(3).

Reaction of **1b** or **1d** with iridium precursors led to iridium containing products. Heating a toluene-d_8 solution of $[Ir(COE)_2(\mu\text{-}Cl)]_2$ with **1b** under CO at 100 °C for 18 h resulted in a new product by ^{31}P NMR spectroscopy as a singlet resonance at 116.1 ppm. In the ^{1}H NMR spectrum, a triplet hydride resonance was observed at -17.69 ppm ($^{2}J_{PH}$ = 13.1 Hz). These NMR spectra are consistent with an iridium hydrido chloride complex similar to **2a** which we assign as $^{(tBu)2(2\text{-}methoxyethyl)4}$(POCOP)$Ir^{III}$(CO)(H)(Cl). Heating a toluene-d_8 solution of **1d** with $Ir(CO)_2Cl$(*p*-toluidine) at 100 °C for 18 h led to a new product by ^{1}H and ^{31}P NMR spectroscopy. In the ^{1}H NMR spectrum an iridium hydride was observed at -17.39 ppm ($^{2}J_{PH}$ = 13.3 Hz). In the $^{31}P\{^{1}H\}$ NMR spectrum two roofing doublets centered at 114.5 and 107.6 ppm (J_{PP} = 712 Hz) were observed. Since **1d** contains chiral centers, upon metalation, the orientation of the cholesterol moieties may render the two phosphorus nuclei chemically inequivalent, giving rise to two ^{31}P NMR resonances. The spectra are consistent with an iridium containing product, likely a hydrido chloride Ir(III) carbonyl complex similar to **2a**.

2.2.2 Reaction of ^{R4}(POCOP) with $Ir(CO)_2Cl$(p-toluidine)

We previously reported that the square planar Ir(I) complex $^{(tBu)4}$(POCOP)Ir^{I}(CO) (**5**) could be synthesized via metalation of $^{(tBu)4}$(POCOP) (**3**) with $Ir(CO)_2Cl$(*p*-toluidine).[16] Unexpectedly, bis(*phosphite*) POCOP ligands formed Ir(III) complexes upon reaction with $Ir(CO)_2Cl$(*p*-toluidine). Thus, we were interested in studying the reactions of bis(*phosphinite*) POCOP ligands with iridium since the steric and/or electronic features of the phosphite substituent appeared to influence the oxidation state of the iridium product. Upon combining colorless **3** with the purple iridium precursor, $Ir(CO)_2Cl$(*p*-toluidine), a yellow solution was observed accompanied by gas evolution, consistent with dissociation of CO from the precursor and binding of the two

phosphinite arms. Heating this solution at 110 °C for 15 h resulted in formation of the Ir(I) species **5** (Scheme 2.02). The $^{31}P\{^{1}H\}$ NMR spectrum of **5** shows a singlet at 199.0 ppm.

Scheme 2.02. Reactions of ^{R4}(POCOP) Ligands with Ir(CO)$_2$Cl(*p*-toluidine)

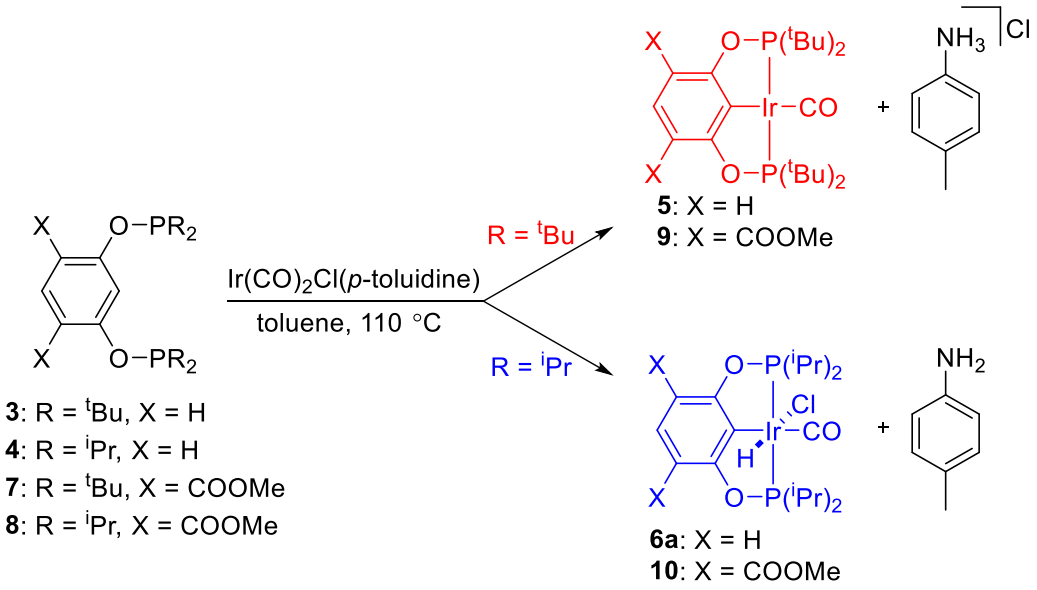

The analogous reaction with $^{(iPr)4}$(POCOP) (**4**) also displayed gas evolution upon combination with Ir(CO)$_2$Cl(*p*-toluidine), consistent with loss of CO.[17] After heating at 110 °C for 30 min, an off-white precipitate was observed, which redissolved upon continued heating (15 h). Observation of the reaction mixture by NMR spectroscopy showed resonances consistent with an Ir(III) hydrido-chloride carbonyl complex as well as free *p*-toluidine. Addition of HCl to the crude reaction mixture resulted in precipitation of *p*-toluidine hydrochloride. The octahedral complex $^{(iPr)4}$(POCOP)Ir^{III}(CO)(H)(Cl) (**6a**) was isolated in good yield. The ^{1}H NMR spectrum of **6a** shows a triplet at −18.49 ppm ($^{2}J_{PH}$ = 13.0 Hz) indicative of an iridium hydride coupled to two phosphorus atoms and four sets of peaks between 1.50 and 0.97 ppm for the four distinct methyl environments. The $^{31}P\{^{1}H\}$ NMR spectrum shows a singlet at 166.4 ppm, consistent with one phosphorus-

containing product. Crystals suitable for X-ray diffraction were grown by slow evaporation of a dichloromethane solution of **6a** (Figure 2.04).

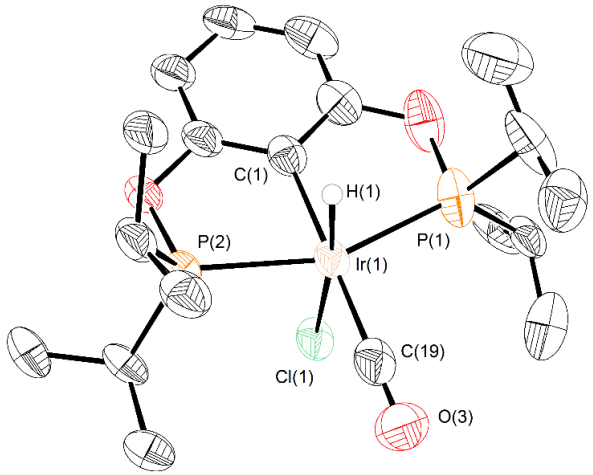

Figure 2.04. ORTEP[15] of $^{(iPr)4}$(POCOP)Ir^{III}(CO)(H)(Cl) (**6a**) at 50% thermal ellipsoids. Hydrogen atoms, except for the iridium bound hydride, are omitted for clarity. Selected bond lengths (Å) and angles (°) for **6a**: Ir(1)-C(1) 2.052(6), Ir(1)-P(1) 2.2959(18), Ir(1)-P(2) 2.3036(15), Ir(1)-C(19) 1.907(8), C(19)-O(3) 1.147(8); C(19)-Ir(1)-C(1) 178.6(3), C(1)-Ir(1)-P(1) 79.12(18), C(1)-Ir(1)-P(2) 78.85(17), P(1)-Ir(1)-P(2) 157.35(7).

The square planar complex $^{(iPr)4}$(POCOP)Ir^{I}(CO) (**6b**) can be isolated by reaction of **6a** with excess NaO^{t}Bu to give a golden yellow solid. The ^{1}H NMR spectrum of **6b** shows the disappearance of the iridium hydride peak and appearance of a multiplet centered at 2.51 ppm, which is assigned to the four equivalent methine (P-C*H*$(CH_3)_2$) protons. The multiplet appears as a set of seven virtual triplets, which results from coupling to six methyl protons from the isopropyl groups and coupling to two magnetically inequivalent phosphorus nuclei (Figure 2.05). The ^{31}P{^{1}H} NMR spectrum shows a singlet at 191.2 ppm, which is ~8.0 ppm upfield from the analogous complex with ^{t}Bu (**5**).

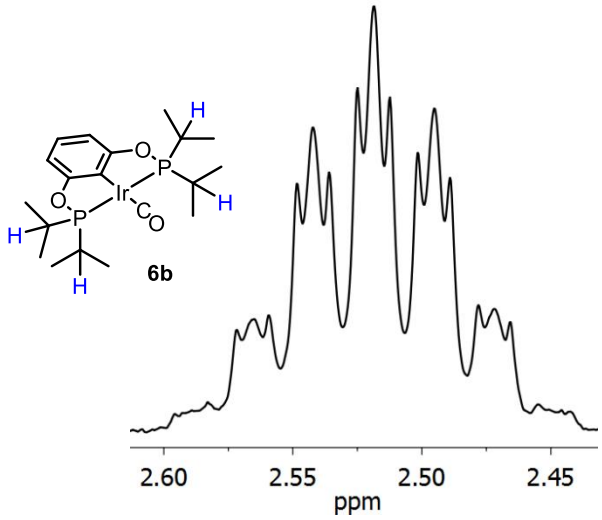

Figure 2.05. ^{1}H NMR spectrum (300 MHz, acetone-d_6) of **6b** showing the resonance for four chemically equivalent methine protons.

*2.2.3 Reactivity of $^{(iPr)4}$(POCOP)Ir(CO) (**6b**) with O_2*

Complex **6b** was found to be an air sensitive compound after solutions in air changed color from golden yellow to brown over the course of days; however, in the solid state, **6b** could be handled in air for a few hours without observable degradation. In contrast, complex **5** was stable to air indefinitely. To probe its oxygen sensitivity, **6b** was treated with 2 atm O_2 in C_6D_6, resulting in clean formation of a new product by NMR spectroscopy after stirring for 3 h at room temperature. There was a color change from golden yellow to dark yellow over the 3 h time period. The ^{1}H NMR spectrum showed four distinct multiplet resonances from 1.31 to 1.03 ppm consistent with a product that has asymmetry above and below the pincer plane. This asymmetry is further supported by two broad methine resonances at 2.93 and 2.26 ppm. Acetone was also observed in the spectrum after this time, suggesting some reaction with the ^{i}Pr moieties. In the ^{31}P NMR spectrum, a new sharp singlet resonance was observed at 144.7 ppm (81%) as well as unreacted

6b at 190.8 ppm (19%). Our proposal for the clean reaction product with O_2 is shown in eq 2.02 where O_2 has been activated to give an iridium peroxo complex. Oxygen addition to Ir complexes has been shown in previous reports.[18] When the reaction was allowed to stir for an additional 15 h, the ^{1}H NMR spectrum showed only two very broad resonances centered at 6.75 ($\omega_{1/2} \approx 150$ Hz) and 1.30 ppm ($\omega_{1/2} \approx 300$ Hz). Additionally, the acetone resonance increased in intensity, supporting further degradation of the pincer framework. The corresponding ^{31}P NMR spectrum had no observable ^{31}P resonances. Similar pincer ligand degradation reactivity resulting in acetone was observed for reaction of $^{(iPr)4}$(PCP)Ni(H) with O_2.[19] We currently do not have a proposal for the iridium product obtained after reaction for longer than 3 h given the extreme broadness of the ^{1}H NMR resonances.

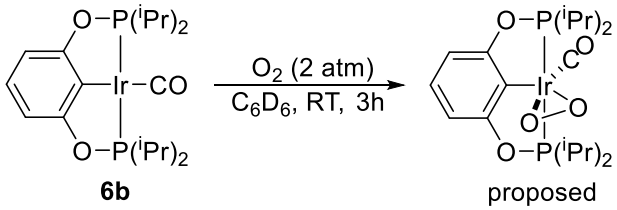

6b proposed (2.02)

2.2.4 Substitution of POCOP with Methyl Esters

Substitution was performed by carboxylation of resorcinol with two equivalents of $KHCO_3$ followed by esterification with MeOH.[20] Two equivalents of R_2PCl (where R = ^{i}Pr or ^{t}Bu) and excess NEt_3 were added to the resorcinol product. The reaction mixture was stirred at room temperature for 1.5 h, resulting in clean formation of the desired ligand $^{(COOMe)2(R4)}$(POCOP) (eq 2.03). The ^{31}P{^{1}H} NMR spectra of $^{(COOMe)2(R4)}$(POCOP) for R = ^{t}Bu (**7**) and R = ^{i}Pr (**8**) feature singlets at 156.9 and 153.4 ppm, respectively. We targeted the synthesis of 4,6-dimethyl 1,3-dihydroxybenzene with methyls substituted on the aryl instead of ^{t}Bu groups since ^{t}Bu groups limit

solubility in polar solvents. Previous methods for preparing 4,6-dimethyl 1,3-dihydroxybenzene required a harsh reaction of 2,4-dimethylphenol with hydrogen peroxide and fluoroantimonic acid.[21] Instead of using this procedure, we hypothesized that the disubstituted carboxylic acid resorcinol precursor or the disubstituted ester resorcinol could be reduced directly to 4,6-dimethyl 1,3-dihydroxybenzene. Following literature precedent for reduction of salicylic acid or methyl salicylate derivatives,[22] all attempts at reduction to 4,6-dimethyl 1,3-dihydroxybenzene were unsuccessful.

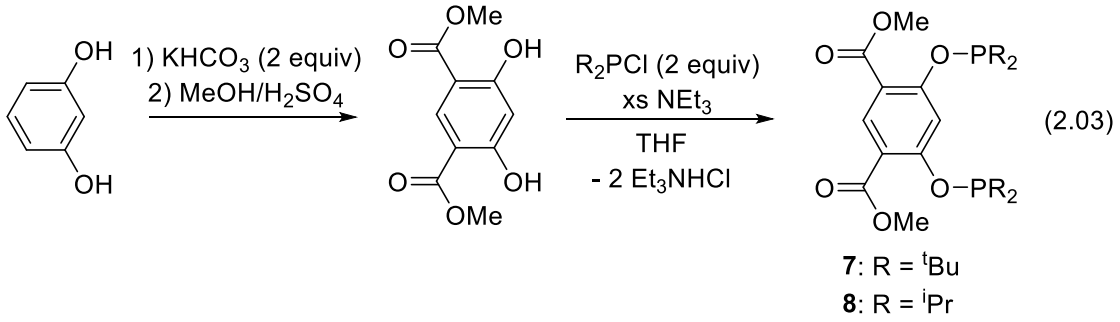

(2.03)

Iridium complexes of ligands **7** and **8** can be prepared using a similar procedure to that used for the syntheses of **5** and **6a** (Scheme 2.02). Notably, a white precipitate was not observed during the course of the reaction. This suggests that polymer formation was prevented by the inclusion of aryl backbone substituents. The substituents on the P atoms were found to affect the reaction product. When R = ^{t}Bu, the Ir(I) carbonyl complex $^{(COOMe)2(tBu)4}$(POCOP)Ir^{I}(CO) (**9**) was formed, whereas when R = ^{i}Pr the Ir(III) complex $^{(COOMe)2(iPr)4}$(POCOP)Ir^{III}(CO)(H)(Cl) (**10**) was generated. The ^{31}P{^{1}H} NMR spectrum of **9** shows a singlet at 204.9 ppm. In the ^{1}H NMR spectrum there is a virtual triplet at 1.29 ppm for the ^{t}Bu groups. The ^{1}H NMR spectrum of **10** exhibits a triplet at −18.29 ppm ($^{2}J_{PH}$ = 13.1 Hz) indicative of an iridium hydride. Additionally, there are four distinct methyl signals between 1.52 and 0.98 ppm and two different methine resonances at 3.35 and 2.60 ppm. The ^{31}P{^{1}H} NMR spectrum reveals only a singlet at 171.7 ppm.

Complexes **9** and **10** have been analyzed by X-ray diffraction, and their solid-state molecular structures are shown in Figure 2.06 and 2.07, respectively. We attempted to prepare the square-planar Ir(I)-CO analogue of **10** by treatment with a variety of bases (NaO^tBu, KHMDS, NEt_3, Ag_2O). For reactions with NaO^tBu, KHMDS, and NEt_3 multiple ester containing products were often obtained and/or ^{31}P NMR spectra showed many unassignable peaks. Reaction of **10** with 3 equiv. Ag_2O in CD_2Cl_2 at 50 °C for 2 days resulted in a new product, which exhibits a singlet resonance at 197.4 ppm in the ^{31}P NMR spectrrum (69% of total ^{31}P NMR integrated resonances). We tentatively assign this product as the desired Ir(I)-CO, $^{(COOMe)2(iPr)4}$(POCOP)Ir^I(CO).

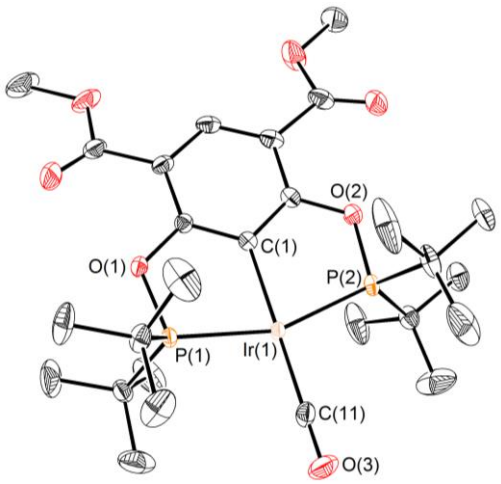

Figure 2.06. ORTEP[15] of $^{(COOMe)2(tBu)4}$(POCOP)Ir^I(CO) (**9**) with 50% thermal ellipsoids. Hydrogen atoms are omitted for clarity. Selected bond lengths (Å) and angles (°) for **9**: Ir(1)−C(1) 2.054(2), Ir(1)−P(1) 2.2679(6), Ir(1)−P(2) 2.2730(6), Ir(1)−C(11) 1.864(3), C(11)−O(3) 1.151(3); C(11)-Ir(1)-C(1) 179.74(11), C(1)-Ir(1)-P(1) 79.10(7), C(1)-Ir(1)-P(2) 79.10(7), P(1)-Ir(1)-P(2) 158.10(2).

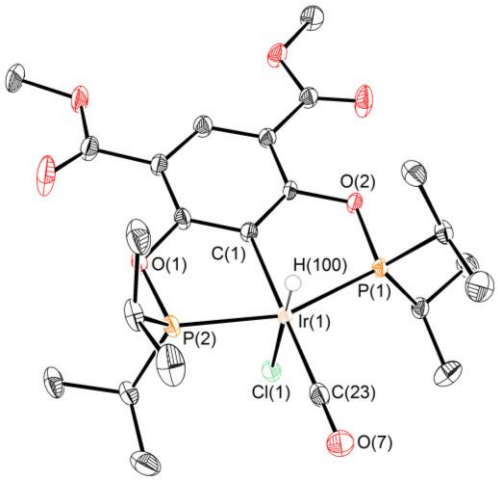

Figure 2.07. ORTEP[15] of $^{(COOMe)2(iPr)4}$(POCOP)Ir^{III}(CO)(H)(Cl) (**10**) with 50% thermal ellipsoids. Hydrogen atoms, except for the iridium-bound hydride, are omitted for clarity. Selected bond lengths (Å) and angles (°) for **10**: Ir(1)−C(1) 2.057(3), Ir(1)−P(1) 2.3000(8), Ir(1)−P(2) 2.2983(8), Ir(1)-C(23) 1.913(4), C(23)−O(7) 1.136(4); C(23)-Ir(1)-C(1) 177.30(16), C(1)-Ir(1)-P(1) 79.33(9), C(1)-Ir(1)-P(2) 79.04(9), P(1)-Ir(1)-P(2) 158.25(3).

2.2.5 Formation of cis- and trans-Hydrido-Chloride Complexes

Reaction of ^{R4}(POCOP) ligands with Ir(CO)$_2$Cl(*p*-toluidine) proceeds to initially form a hydrido-chloride Ir(III) complex. When R = ^{i}Pr, the *trans*-hydrido-chloride Ir(III) complex is isolated as the product. We were interested in the presumed intermediate hydrido-chloride Ir(III) complex for R = ^{t}Bu, since the final product in this case is the square planar Ir(I) complex. Monitoring the metalation reaction of **3** with Ir(CO)$_2$Cl(*p*-toluidine) by ^{31}P{^{1}H} NMR spectroscopy revealed several new resonances between 155.0 and 148.0 ppm (free ligand: 153.5 ppm) prior to heating. When the reaction was heated at 100 °C in toluene-d_8, the new peaks disappeared and were replaced by the product peak at 199.0 ppm. An intermediate hydrido-chloride Ir(III) species was not observed. Reaction of **5** with excess HCl (~10 equiv.) in toluene shows a singlet in the ^{31}P{^{1}H} NMR spectrum at 170.6 ppm and only one triplet hydride peak at −17.60 ppm ($^{2}J_{PH}$ = 13.3 Hz) in the ^{1}H NMR spectrum. These data suggest a *trans* product, *trans*-

$^{(tBu)4}$(POCOP)Ir(CO)(H)(Cl) (***trans*-11**) based on the similar shift of the hydride shifts in complexes **6a** and **10**. The *trans* product, ***trans*-11**, was deprotonated back to the Ir(I)-CO by addition of *p*-toluidine at room temperature within minutes.

Addition of CO to $^{(tBu)4}$(POCOP)Ir^{III}(H)(Cl)^4 in toluene afforded a different complex than addition of HCl to **5**. The new complex exhibits a triplet hydride resonance in the ^{1}H NMR spectrum at −8.27 ppm ($^2J_{PH}$ = 16.1 Hz) and a singlet in the ^{31}P{^{1}H} NMR spectrum at 162.7 ppm. These data suggest a product where CO is in the axial position and the hydride and chloride ligands are in a *cis* configuration.[3] Deprotonation of the *cis* complex, *cis*-$^{(tBu)4}$(POCOP)Ir(CO)(H)(Cl) (***cis*-11**) with *p*-toluidine did not proceed at room temperature under conditions successful for the deprotonation of ***trans*-11**. Interestingly, heating a solution of ***cis*-11** in toluene (in the absence of base) at 100 °C for 12.5 h led to isomerization to ***trans*-11** (79% conversion) and partial HCl loss to form **5** (10%), as evidenced by the ^{31}P{^{1}H} NMR spectrum; the remaining 11% is ***cis*-11** (Scheme 2.03). Prolonged heating over 5 days led to a slight increase in conversion to **5** (15%) and minimal change in ***trans*-11** formation (80%). To determine if the *cis* and *trans* complexes were in equilibrium, ***trans*-11** was heated at 100 °C in toluene-d_8 for 12.5 h, which led to partial formation of ***cis*-11** (confirmed by ^{31}P NMR spectroscopy) and formation of the Ir(I)-CO complex **5**.

Scheme 2.03. Synthetic Routes to *cis*- and *trans*-Hydrido-Chloride Ir(III) Carbonyl Species

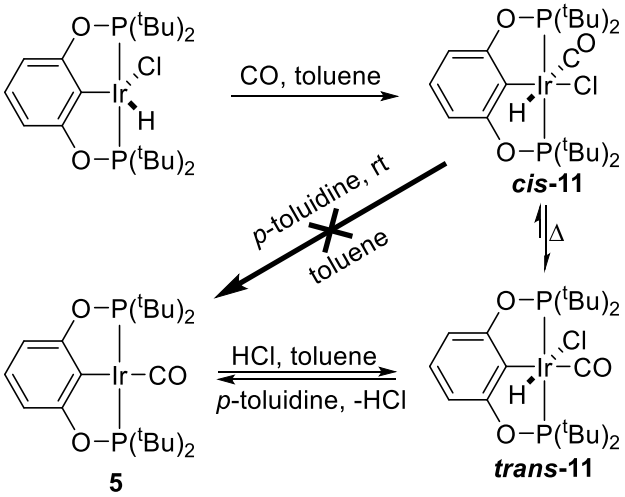

2.2.6 Synthesis of [^{R4}(POCOP)Ir^{III}(CO)(H)]BF$_4$ Complexes

As previously shown, $^{(tBu)4}$(POCOP)Ir^{I}(CO) can be protonated with [H-(OEt$_2$)$_2$]B(C$_6$H$_3$(CF$_3$)$_2$)$_4$ to give the five-coordinate species [$^{(tBu)4}$(POCOP)Ir^{III}(CO)(H)][BArF$_{24}$].[16] Similarly, protonation of **5** with one equivalent of HBF$_4$·Et$_2$O yielded [$^{(tBu)4}$(POCOP)Ir^{III}(CO)(H)]BF$_4$ (**12**, Scheme 2.04). A triplet at −35.70 ppm ($^2J_{PH}$ = 10 Hz) in the ^{1}H NMR spectrum is assigned to the iridium hydride. The ^{31}P{^{1}H} NMR spectrum shows a singlet at 192.0 ppm; this is shifted 7.0 ppm upfield from the Ir(I) starting material. Crystals suitable for X-ray diffraction were grown at −20 °C by layering pentane over a dichloromethane solution (Figure 2.08). In the solid state, the iridium is in a square pyramidal geometry with the hydride in the apical position. The BF$_4$ anion is non-coordinating. The analogous complex with a methyl ester moiety substituted on the aryl backbone, [$^{(COOMe)(tBu)4}$(POCOP)Ir^{III}(CO)(H)]BF$_4$ was also prepared via treatment of $^{(COOMe)(tBu)4}$(POCOP)Ir(CO) with HBF$_4$·Et$_2$O; this complex was crystallographically characterized (Figure 2.09).

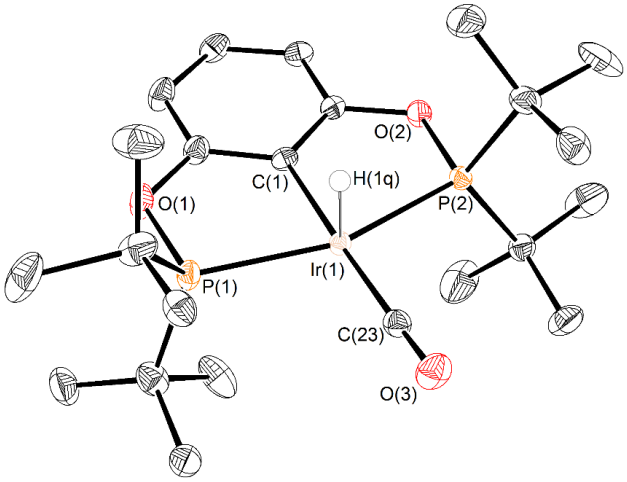

Figure 2.08. ORTEP[15] of [$^{(tBu)4}$(POCOP)Ir^{III}(CO)(H)]BF_4 (**12**) at 50% thermal ellipsoids. A BF_4 anion and hydrogen atoms, except for the iridium bound hydride, were omitted for clarity. Selected bond lengths (Å) and angles (°) for **12**: Ir(1)-C(1) 2.0284(19), Ir(1)-P(1) 2.3258(5), Ir(1)-P(2) 2.3225(5), Ir(1)-C(23) 1.917(2), C(23)-O(3) 1.133(2); C(23)-Ir(1)-C(1) 175.91(8), C(1)-Ir(1)-P(1) 79.28(6), C(1)-Ir(1)-P(2) 79.03(6), P(1)-Ir(1)-P(2) 158.286(19).

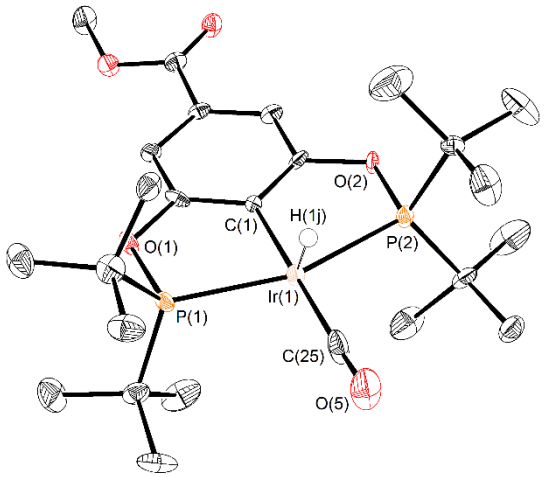

Figure 2.09. ORTEP[15] of [$^{(COOMe)(tBu)4}$(POCOP)Ir^{III}(CO)(H)]BF_4 at 50% thermal ellipsoids. A BF_4 anion and hydrogen atoms, except for the iridium bound hydride, were omitted for clarity. Selected bond lengths (Å) and angles (°) for [$^{(COOMe)(tBu)4}$(POCOP)Ir(CO)(H)]BF_4: Ir(1)-C(1) 2.041(4), Ir(1)-P(1) 2.318(2), Ir(1)-P(2) 2.333(2), Ir(1)-C(25) 1.934(5), C(25)-O(5) 1.131(6); C(25)-Ir(1)-C(1) 178.7(3), C(1)-Ir(1)-P(1) 79.7(3), C(1)-Ir(1)-P(2) 79.1(3), P(1)-Ir(1)-P(2) 158.71(6).

To prepare the ^{i}Pr analogue of **12**, $^{(iPr)4}$(POCOP)Ir^{III}(CO)(H)(Cl) (colorless) was treated with one equivalent of $AgBF_4$ in CD_2Cl_2, resulting in an orange solution and precipitation of a gray solid (Scheme 2.04). The ^{1}H NMR spectrum of [$^{(iPr)4}$(POCOP)Ir^{III}(CO)(H)]BF_4 (**13**) shows a broadened triplet at −29.26 ppm, assigned to the iridium hydride. The ^{31}P{^{1}H} NMR spectrum shows a broad singlet at 174.6 ppm. Attempts to grow crystals of **13** have so far been hampered by the coordination of adventitious water or solvent. It is quite difficult to prevent trace water from coordinating to [$^{(iPr)4}$(POCOP)Ir^{III}(CO)(H)]$^+$, and thus we have isolated only the octahedral hydrido-aquo Ir(III) carbonyl complex (Figure 2.10). A similar halide abstraction with $AgBF_4$ in CD_2Cl_2 was attempted with complex **10**, however multiple products were obtained as observed by ^{31}P NMR spectroscopy, possibly due to reaction with the ester moieties. No further attempts were made to prepare the cationic iridium-hydride complex.

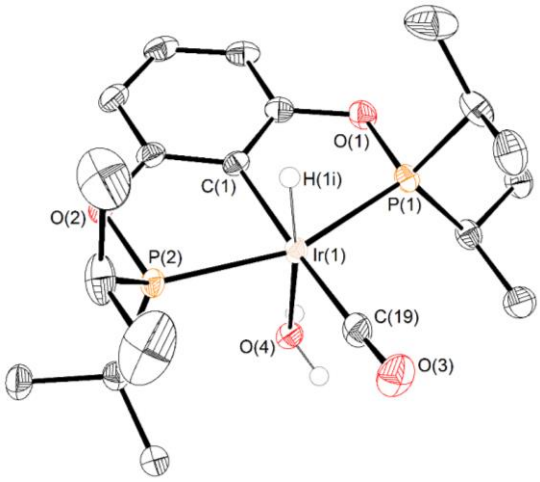

Figure 2.10. ORTEP[15] of [$^{(iPr)4}$(POCOP)Ir^{III}(CO)(H)(H_2O)]BF_4 (**13**) at 50% thermal ellipsoids. A BF_4 anion and hydrogen atoms, except for the iridium bound hydride and the hydrogens in water, were omitted for clarity. Selected bond lengths (Å) and angles (°) for **13**: Ir(1)-C(1) 2.051(2), Ir(1)-P(1) 2.3182(6), Ir(1)-P(2) 2.3145(6), Ir(1)-C(19) 1.925(3), C(19)-O(3) 1.137(3); C(19)-Ir(1)-C(1) 174.22(9), C(1)-Ir(1)-P(1) 78.89(7), C(1)-Ir(1)-P(2) 78.78(7). P(1)-Ir(1)-P(2) 157.62(2).

Scheme 2.04. Synthetic Routes to Cationic Hydrido Ir(III) Carbonyl Complexes

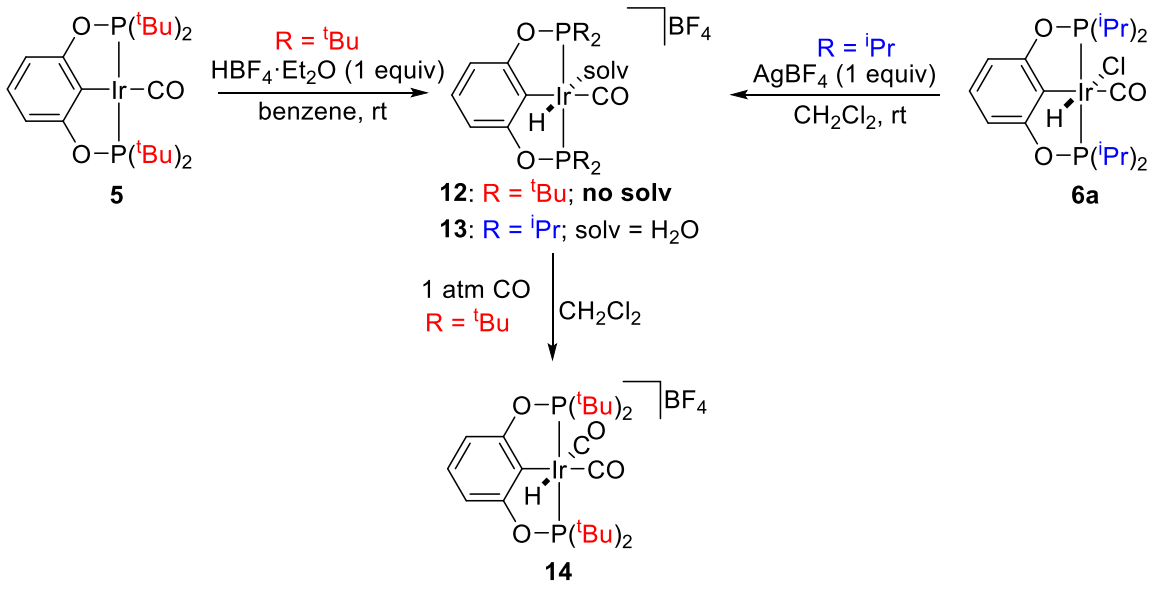

2.2.7 Synthesis of [$^{(tBu)4}$(POCOP)Ir^{III}(CO)$_2$(H)]BF$_4$

Exposing the five-coordinate complex **12** to an atmosphere of CO resulted in a rapid color change from orange to colorless, forming the hydrido-dicarbonyl Ir(III) species [$^{(tBu)4}$(POCOP)Ir^{III}(CO)$_2$(H)]BF$_4$ (**14**) in quantitative yield. In the ^{1}H NMR spectrum, a triplet is observed at −10.49 ppm ($^2J_{PH}$ = 14.9 Hz) for the iridium hydride; this is shifted 25 ppm downfield from the hydride observed in **12**. A singlet is observed in the ^{31}P{^{1}H} NMR spectrum at 174.1 ppm; this is shifted 18 ppm upfield from the starting material. Interestingly, the carbonyl group was not labile to vacuum over the course of several hours. In the infrared spectrum (KBr) of **14**, two CO stretches were observed at 2106 and 2073 cm^{-1}. Crystals suitable for X-ray diffraction were grown by layering pentane over a dichloromethane solution of **14** at −20 °C (Figure 2.11). The molecular structure of **14** shows an octahedral geometry around iridium with the carbonyls in a *cis* configuration.

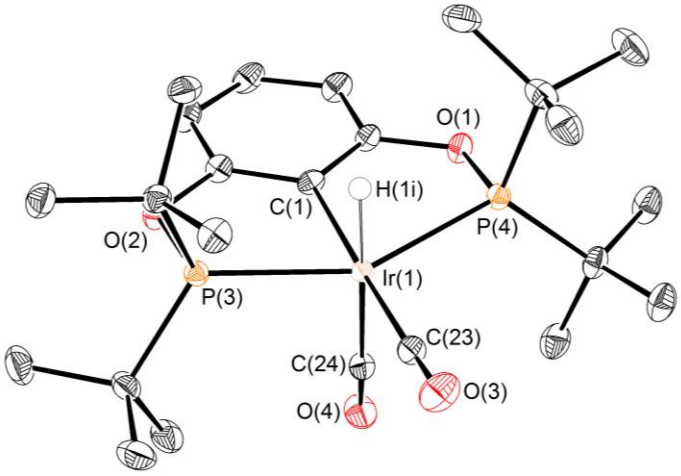

Figure 2.11. ORTEP[15] of [$^{(tBu)4}$(POCOP)Ir^{III}(CO)$_2$(H)]BF_4 (**14**) with 50% thermal ellipsoids. A BF_4 anion and hydrogen atoms, except for the iridium-bound hydride, are omitted for clarity. Selected bond lengths (Å) and angles (°) for **14**: Ir(1)−C(1) 2.0611(18), Ir(1)−P(3) 2.3641(6), Ir(1)−P(4) 2.3625(6), Ir(1)− C(23) 1.941(2), C(23)−O(3) 1.126(2), Ir(1)−C(24) 1.974(2), C(24)−O(4) 1.120(2); C(23)-Ir(1)-C(1) 172.93(8), C(1)-Ir(1)-P(3) 78.46(5), C(1)-Ir(1)-P(4) 78.47(5), P(3)-Ir(1)-P(4) 152.520(17), C(23)-Ir(1)-C(24) 98.76(8).

2.3 Discussion

The (POCOP)Ir complexes presented in this work demonstrate that subtle differences in the steric profiles of the ligand can affect the coordination chemistry at the metal center. For substituents smaller than ^{t}Bu on phosphorus, aryl backbone substituents are useful in preventing precipitates, which are likely coordination polymers. Furthermore, the oxidation state of the iridium complex is dependent on the steric profile of the substituent bound to phosphorus. When the substituent is a bulky ^{t}Bu, square planar Ir(I) complexes are favored, while for R smaller than ^{t}Bu, octahedral Ir(III) complexes are formed.

2.3.1 Comparison of Iridium Bis(phosphite) and Bis(phosphinite) Complexes

The metalation reactions with bis(phosphite) ligands led to formation of new octahedral Ir(III) complexes. Since methoxy groups have different electronic properties than alkyl groups (methoxy is σ-withdrawing and π-donating, whereas alkyls are only σ-donating), we expected slight differences in the Ir−P bond lengths. For complexes in the same oxidation state, one containing bis(phosphite) moieties should have shorter Ir−P bond lengths than one with bis(phosphinite) groups. The Ir(1)−P(1) and Ir(1)−P(2) distances in $^{(tBu)2(OMe)4}$(POCOP)Ir^{III}(CO)(H)(Cl) (**2a**) are 2.2676(7) and 2.2681(7) Å, respectively. These bond lengths are somewhat shorter than those in $^{(iPr)4}$(POCOP)Ir^{III}(CO)(H)(Cl) (**6a**) (2.2958(2) and 2.3036(2) Å, respectively).[23] The difference in bond length could be accounted for by the observations that P-OR functionalities are more effective π-acids.[24] The phosphite groups in **2a** should favor more π-backbonding than in **6a**, consistent with the observed shorter bond lengths.

The X-ray structure of $^{(COOMe)2(tBu)4}$(POCOP)Ir^{I}(CO) (**9**) is similar to the reported structure of $^{(tBu)4}$(POCOP)Ir^{I}(CO); however, the structure of $^{(COOMe)2(iPr)4}$(POCOP)Ir^{III}(CO)(H)(Cl) (**10**) shows how the isopropyl groups can orient themselves depending on the axial ligands bound to iridium. One set of isopropyls is oriented toward the hydride, whereas the other set is oriented away from the chloride. Presumably, since the chloride has a larger van der Waals radius (1.75 Å) than the hydride (1.10 Å), the isopropyls are oriented away to alleviate a steric interaction.[25]

2.3.2 Requirement for Backbone Substitution

Addition of a backbone substituent appears to prevent formation of a polymeric product, but still affords the hydrido-chloride Ir(III) carbonyl complex. The small steric profile of OR

groups bound to phosphorus requires a backbone substituent to prevent the formation of a polymeric precipitate. We propose that when there is no *meta* backbone substituent, there is free rotation around the C_{Ar}–O and P–O bonds and multiple conformers are accessible.[26] This can result in coordination polymers when the phosphine substituent is small. When the aryl backbone is substituted, such as in ligand **1a**, a conformer where the ligand arms are better situated for chelation to the metal is favored (Figure 2.12). This may also prevent potential activation of the *meta* C–H bond on the aryl ring.[27] While the D-mannitoldiol-based ligand **1c** is bulky, in the space closest to the iridium center in **2c**, the steric profile mimics that of OMe. It is possible that **2c** is more open at the metal since the two OR moieties are rigid and part of a five-membered ring.

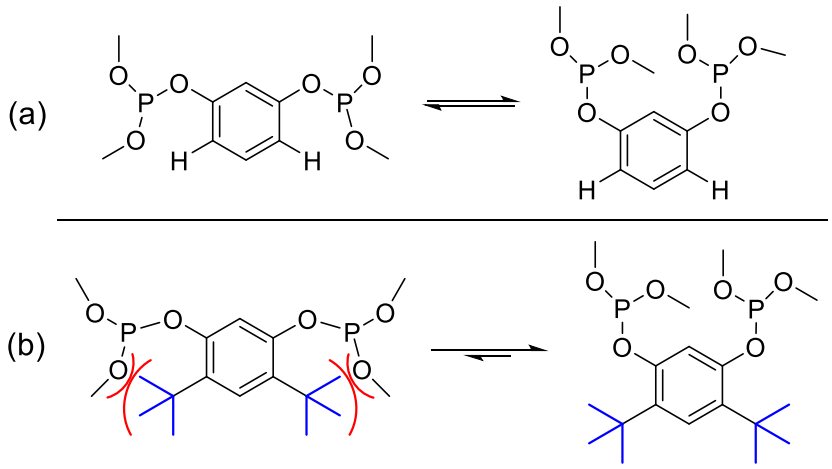

Figure 2.12. Conformations of bis(phosphite) POCOP ligands with (a) an unsubstituted aryl backbone or (b) a substituted aryl backbone.

In the case of $^{(iPr)4}$(POCOP)Ir^{III}(CO)(H)(Cl) (**6a**), the white precipitate that initially forms during metalation is likely a polymeric species that breaks apart upon heating. Similar work by Roddick and co-workers with the less bulky CF_3-substituted PCP iridium complexes showed formation of coordination polymers upon addition of $^{(CF3)4}$(PCP) to [Ir(COD)(μ-Cl)]$_2$. The structure observed in that work is likely similar to the byproduct proposed here (Scheme 2.05).[28]

An alternative to ^{t}Bu as the *meta* substituent on the aryl backbone of the POCOP ligand was investigated. ^{R4}(POCOP) ligands were synthesized with COOMe groups substituted in the *meta* positions of the aryl ring, as we anticipated that this would not only prevent formation of coordination polymers but also give better solubility in polar media. Initial efforts were to replace the backbone ^{t}Bu groups in the bis(phosphite) complexes with COOMe moieties, but all attempts at synthesizing bis(phosphite) ligands with the COOMe-substituted aryl backbone were unsuccessful.

The methyl ester substitution was useful for metalations of ligands with small R groups on phosphorus. During the metalation of $^{(COOMe)2(iPr)4}$(POCOP) (**8**) we did not observe the white precipitate that was observed during the metalation of $^{(iPr)4}$(POCOP) (**4**). While the precipitate from **4** did re-dissolve after continued heating, the COOMe groups in **8** prevent rotational conformers of the pincer ligand and so hinder polymer formation. The COOMe-substituted aryl backbone offers an alternative to the nonpolar ^{t}Bu groups, which have been traditionally employed to prevent polymerizations of pincer ligands with metal precursors. Recent work by Ozerov and co-workers with $^{(iPr)4}$(POCOP)RhI($S^{i}Pr_2$) found that upon addition of vinyl iodide a bimetallic complex was formed.[29] Dimerization was prevented by substitution of the *meta* positions of the aryl backbone with ^{t}Bu, giving the monomeric product $^{(tBu)2(iPr)4}$(POCOP)Rh^{III}($CHCH_2$)(I).

2.3.3 Formation of Ir(I) vs Ir(III) Complexes

Our studies indicate that a small substituent on phosphorus favors formation of an Ir(III) complex upon reaction with $Ir(CO)_2Cl$(*p*-toluidine). In our proposed mechanism of metalation of POCOP ligands, the two phosphine arms bind to the iridium center, with loss of one CO molecule

(Scheme 2.05). This is evidenced by observation of immediate gas evolution upon combining the POCOP ligand with the metal precursor. All reactions of POCOP ligands with $Ir(CO)_2Cl$(*p*-toluidine) involve loss of CO. This is followed by oxidative addition of an aryl C−H bond to iridium, yielding a hydrido-chloride Ir(III) carbonyl species. When R = ^{t}Bu, the hydrido-chloride Ir(III) complex is short-lived and an iridium(I) carbonyl complex is isolated. For R smaller than ^{t}Bu, the *trans* hydrido-chloride Ir(III) carbonyl is formed. This is consistent with the observations of the naphthyl-based (PCP)Rh complexes by Milstein and co-workers, where steric requirements override electronic factors.[7] The more electron-rich ^{t}Bu-substituted ligand would be expected to stabilize octahedral Ir(III), yet the opposite is observed where R = ^{i}Pr favors Ir(III). Notably, the stability of ^{R4}(POCOP)Ir^I(CO) complexes was shown in their stability to oxygen. Less bulky Ir(I) complexes react with oxygen giving putative oxygen addition products followed by degradation of the pincer framework. Sterically encumbered ^{t}Bu substituted complexes do not react with oxygen and are stable indefinitely to ambient atmosphere.

The loss of HCl alleviates a steric interaction between the chloride ligand and the ^{t}Bu groups. The presence of a base, even a relatively weak one such as *p*-toluidine, is enough of a driving force to favor loss of HCl. The slightly smaller ^{i}Pr substitutent mitigates this steric interaction, and HCl loss is not as favored. Stronger bases such as NaO^{t}Bu will readily deprotonate **6a** to $^{(iPr)4}$(POCOP)Ir^I(CO) (**6b**).

Scheme 2.05. Proposed Pathways for Formation of Ir(I) and Ir(III) Complexes

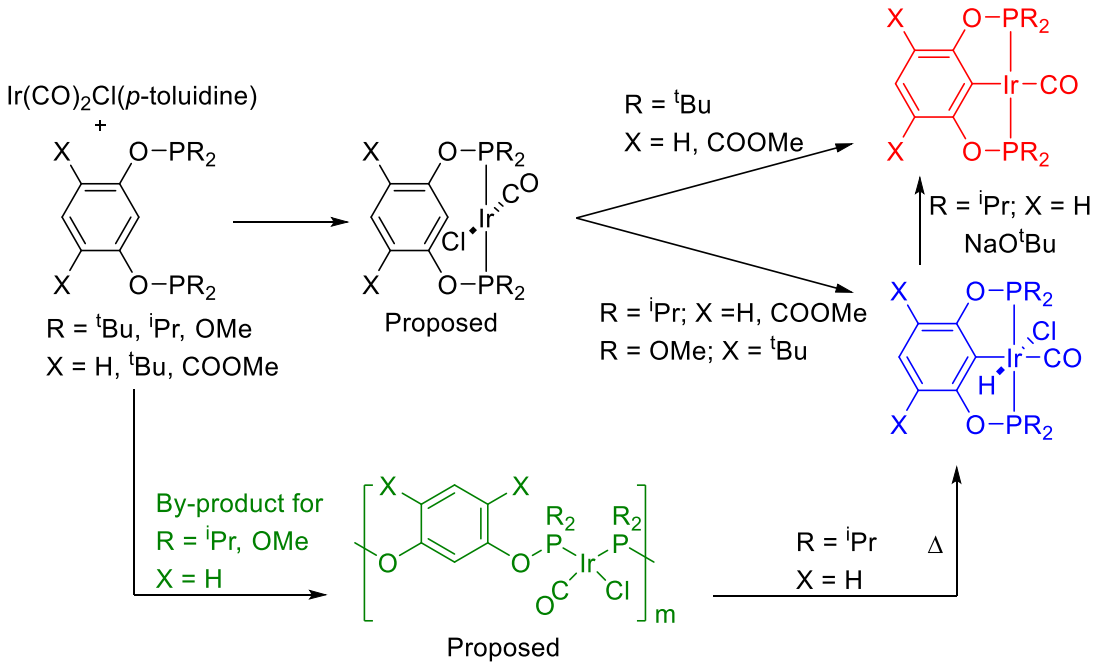

2.3.4 Studies of cis- and trans-Hydrido-Chloride Isomerization

In the proposed pathway for metalation of ^{R4}(POCOP) ligands with Ir(CO)$_2$Cl(*p*-toluidine), there may be an intermediate Ir(Cl)(CO) complex with two bound phosphine arms. Our observations with R groups smaller than ^{t}Bu have shown that the hydrido-chloride Ir(III) carbonyl complexes are favored products. This suggested that an intermediate hydrido-chloride Ir(III) complex is formed for R = ^{t}Bu and is short-lived in the presence of base. Protonation of $^{(tBu)4}$(POCOP)Ir^I(CO) with HCl showed formation of a stable *trans*-hydrido-chloride Ir(III) complex (***trans*-11**) by ^{1}H and ^{31}P NMR spectroscopies.[30] By microscopic reversibility, these data support that metalation of $^{(tBu)4}$(POCOP) with Ir(CO)$_2$Cl(*p*-toluidine) may proceed through a *trans*-hydrido-chloride. Interestingly, the stable *cis*-hydrido-chloride Ir(III) carbonyl complex (***cis*-11**) was observed upon addition of CO to $^{(tBu)4}$(POCOP)Ir^{III}(H)(Cl). When ***cis*-11** was heated, the *trans*

complex, ***trans*-11**, was formed, suggesting that the *cis* isomer is a kinetic product and the *trans* complex is the thermodynamic product. An equilibrium between the *cis* and *trans* isomers, favoring ***trans*-11**, was observed when the *trans* isomer was heated. Moreover, since *p*-toluidine was only able to deprotonate the *trans* isomer at room temperature, these data suggest that the chloride is more labile in the *trans* configuration than in the *cis* configuration. A chloride *trans* to a hydride would result in a weaker Ir-Cl bond because the hydride has a strong *trans* influence.[31] Since the Ir(I)-CO is observed as a minor product after heating either the ***cis*-11** or ***trans*-11** at 100 °C in toluene, we propose that HCl loss from ***trans*-11** is partially favored in order to eliminate a steric interaction with the ^{t}Bu groups. However, an equilibrium between the Ir(I)-CO (**5**), ***cis*-11**, and ***trans*-11** cannot be ruled out since all three species are present in solution after heating over the course of days.

Since different isomers of $^{(tBu)4}$(POCOP)Ir^{III}(CO)(H)(Cl) are observed, we cannot eliminate the possibility of an intermediate *cis*-hydrido-chloride Ir(III) species in the reaction of $^{(tBu)4}$(POCOP) with Ir(CO)$_2$Cl(*p*-toluidine).[32] The data suggest though that if the *cis*-hydrido-chloride Ir(III) complex was formed at 100 °C, it would be short-lived since ***trans*-11** is thermodynamically favored and only ***trans*-11** is deprotonated by *p*-toluidine. However, an isomerization pathway involving an intermediate that can be deprotonated by *p*-toluidine cannot be ruled out. Similar isomerization reactions have been observed, specifically for the Ir(III) dihydride complex $^{(iPr)4}$(PCP)Ir^{III}(CO)(H)$_2$. Work by Milstein and co-workers found that addition of H$_2$ to $^{(iPr)4}$(PCP)Ir^{I}(CO) resulted in complete formation of the *cis*-dihydride complex.[33,34] Upon heating the *cis*-dihydride, quantitative isomerization to the *trans*-dihydride was observed. The observation of *cis*- to *trans*-dihydride isomerization was proposed to be a combination of both

steric and electronic factors. This may be the case for the work described herein since both steric and electronic factors can be implicated in the isomerization pathways.

2.3.5 Properties of [^{R4}(POCOP)Ir^{III}(CO)(H)]BF$_4$ Complexes

The series of five-coordinate hydrido carbonyl species described above provides an opportunity to investigate the influence of the POCOP ligand on the metal center. Previous work with [$^{(tBu)4}$(POCOP)Ir^{III}(CO)(H)][BArF$_{24}$] showed the molecular structure of the five-coordinate complex. Five-coordinate [$^{(tBu)4}$(POCOP)Ir^{III}(CO)(H)]$^+$ was proposed as the active species in glycerol deoxygenation catalysis to 1-propanol and 1,3-propanediol.[16] Here, the analogous BF_4 species was characterized by ^{1}H, ^{31}P, and ^{13}C NMR spectroscopies. The molecular structure of **12** was also confirmed by X-ray crystallography. The structure shows a square pyramidal geometry around iridium with no coordination of adventitious water or solvent. By ^{1}H NMR spectroscopy, a sharp triplet resonance was observed for the iridium hydride, consistent with no exchange of solvent *trans* to the hydride. The opposite is true for the analogous species with R = ^{i}Pr, complex **13**. The X-ray structure of **13** shows coordination of water in the open site. A broadened triplet was observed in the hydride region of the ^{1}H NMR spectrum. The broadened hydride peak is likely due to the averaged spectrum of complexes with bound water, dichloromethane, or the BF_4 anion.[35] Since water is a better ligand than dichloromethane, coordinated water is observed in the solid-state structure of **13**.

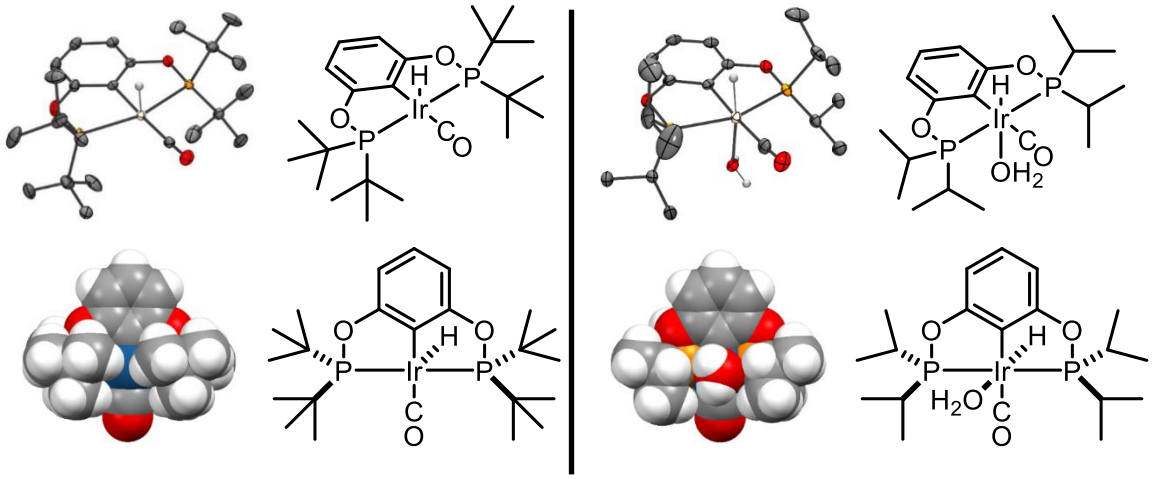

Figure 2.13. Space-filling models of **12** and **13** obtained from the crystal structures of the respective complexes. The view reflected in the space-filling diagram is the site *trans* to the hydride. BF_4 anions and hydrogen atoms, except for the iridium-bound hydrides and the hydrogens in water, have been omitted for clarity from the crystal structures.

Inspection of space-filling models of $[^{R4}(POCOP)Ir^{III}(CO)(H)]BF_4$ show that a change from ^{t}Bu to ^{i}Pr can relieve steric congestion at the open site (Figure 2.13). The ^{t}Bu groups protect the open site at the metal, preventing coordination of possible ligands in solution (water, solvent, BF_4 anion). In contrast, the ^{i}Pr groups can be oriented to allow coordination of water. Four methyl groups of the ^{i}Pr moieties are oriented toward the hydride, while the opposite sets are oriented away from water in **13**. Thus, complex **13** favors an octahedral geometry, whereas in **12** steric congestion prevents solvent coordination and favors the square pyramidal geometry. Similar observations were reported in work by Chianese and co-workers with iridium bis-N-heterocyclic carbene CCC-pincer complexes. In that work, bulky N-substituents (^{t}Bu or adamantyl) favored five-coordinate Ir(III) species, while less bulky N-substituents (2,6-diisopropylphenyl) favored six-coordinate Ir(III) complexes.[36]

Interestingly, a rod-like ligand such as CO can coordinate *trans* to the hydride by reaction of $[^{(tBu)4}(POCOP)Ir^{III}(CO)(H)]BF_4$ (**12**) with CO in dichloromethane to give

[$^{(tBu)4}$(POCOP)Ir^{III}(CO)$_2$(H)]BF$_4$ (**14**, Scheme 2.04). The CO bond lengths (CO_{ap} = 1.120(2) Å and CO_{eq} = 1.126(2) Å) are close to that of free CO in the gas phase (1.1283 Å).[37] Furthermore, the infrared spectrum showed resonances at 2106 and 2073 cm^{-1}, indicative of very little backbonding from the iridium center to the carbonyl moieties. However, CO was not labile to vacuum over the course of hours. The analogous complex of **14** with Rh, [$^{(tBu)4}$(POCOP)Rh^{III}(CO)$_2$(H)]BF$_4$, was stable only at −20 °C and demonstrated reversible binding of CO to give [$^{(tBu)4}$(POCOP)Rh^{III}(CO)(H)]BF$_4$.[38] Structural characterization of the Rh dicarbonyl was possible at −20 °C, but decomposition to $^{(tBu)4}$(POCOP)Rh^{I}(CO) was observed. [$^{(tBu)4}$(POCOP)Rh^{III}(CO)(H)]BF$_4$ decomposed at room temperature, and structural characterization was not possible; however, BF_4 was proposed to weakly coordinate to the Rh center. Later work from Heinekey and co-workers verified that BF_4 did weakly coordinate and that change of supporting anion to B(C$_6$F$_5$)$_4$ (BArF$_{20}$) resulted in an aromatic C-H agostic species.[39] The agostic species, [$^{(tBu)4}$(POCOP)Rh(CO)H][BArF$_{20}$], was crystallographically characterized and proposed to be in an equilibrium with a five-coordinate rhodium hydride complex. In the iridium system, both **12** and **14** are stable as iridium hydride complexes at room temperature and under vacuum. This stability may be attributed to the relative strength of the metal hydride bond since iridium hydride bonds tend to be stronger than rhodium hydride bonds.[40]

2.4 Conclusion

The steric profiles of (POCOP)Ir carbonyl complexes were studied. The first bis(phosphite) (POCOP)Ir complexes were synthesized. Reactions of ^{R4}(POCOP) ligands with Ir(CO)$_2$Cl(*p*-toluidine) where R is smaller than ^{t}Bu result in hydrido-chloride Ir(III) carbonyl species. If R = ^{t}Bu, the metalation results in the Ir(I) carbonyl species. When R is smaller than ^{i}Pr, a white

polymeric material is observed during the reaction. Formation of this polymeric material can be avoided by substituting the aryl backbone. A new *meta*-substituted POCOP ligand with COOMe groups was developed and offers an alternative to ^{t}Bu, which is traditionally used to prevent dimerization or polymerization of metal complexes. The intermediate hydrido-chloride Ir(III) species ^{R4}(POCOP)Ir^{III}(CO)(H)(Cl) formed during the reaction of ^{R4}(POCOP) with Ir(CO)$_2$Cl(*p*-toluidine) is less stable in the presence of base (*p*-toluidine) when R = ^{t}Bu because the metal readily dissociates HCl to alleviate steric crowding. Mechanistic studies indicate that an intermediate hydrido-chloride Ir(III) carbonyl complex with R = ^{t}Bu may be a *cis* or *trans* isomer during the metalation reaction; however, the *trans* isomer is likely the predominant species. With smaller R groups (^{i}Pr and OMe), steric congestion is diminished, leading to the formation of stable *trans*-hydrido-chloride Ir(III) carbonyl complexes and no loss of *p*-toluidine hydrochloride. These observations show that the steric profile of the pincer ligand is important for the structure and oxidation state of the resulting iridium complex.

2.5 Experimental

General Considerations

All experiments and manipulations were performed using standard Schlenk techniques under an argon atmosphere or in an argon- or nitrogen-filled glovebox. Glassware and diatomaceous earth were dried in an oven maintained at 140 °C for at least 24 h. Deuterated solvents were dried over calcium hydride (CD_2Cl_2, $CDCl_3$, and C_6D_6) or sodium/benzophenone (toluene-d_8) and vacuum transferred prior to use. Protiated solvents were passed through columns of activated alumina and molecular sieves. All other reagents were used as received. ^{1}H NMR

spectra were referenced to residual protio signals: dichloromethane (5.32 ppm), chloroform (7.26 ppm), benzene (7.16 ppm), and toluene (7.09 ppm).[41] ^{13}C NMR shifts were referenced to solvent signals: dichloromethane (54.00 ppm) and chloroform (77.16 ppm). ^{31}P NMR shifts were referenced to an 85% H_3PO_4 external standard (0 ppm). Infrared spectra were recorded on a Bruker Tensor 27 FTIR instrument. NMR spectra were recorded on either a Bruker AV-500, DRX-500, or AV-300 NMR instrument. X-ray data were collected at −173 °C on a Bruker APEX II single-crystal X- ray diffractometer, with Mo radiation. Elemental analyses were performed under air-free conditions at the CENTC facility at the University of Rochester.

Synthesis

$^{(OMe)4}$(POCOP),[13] [C_6H_2-4,6-(^{t}Bu)$_2$-1,3-($OPCl_2$)$_2$],[14] $^{(tBu)2(diol)2}$(POCOP),[14] Ir(CO)$_2$Cl(*p*-toluidine),[42] $^{(tBu)4}$(POCOP)Ir^{I}(CO),[16] $^{(tBu)4}$(POCOP)Ir^{III}(H)(Cl),[4] and dimethyl 4,6-dihydroxyisophthalate[20] were synthesized according to published procedures. $^{(iPr)4}$(POCOP) was synthesized via a modified literature procedure employing NEt_3 instead of DMAP.[17]

General procedure for synthesis of bis(phosphite) POCOP ligands. In a 50 mL Schlenk flask, 1 equiv. of [C_6H_2-4,6-(^{t}Bu)$_2$-1,3-($OPCl_2$)$_2$] was dissolved in 10 mL toluene, giving a yellow solution. 5-10 equiv. NEt_3 was added to the toluene solution and was cooled to -40 °C using a dry ice/acetonitrile cold bath. A degassed solution of the corresponding alcohol (4 equiv.) in toluene was added dropwise via syringe to the cooled bis(dichlorophosphane) solution. After stirring at -40 °C for 30 min, the cold bath was removed and the flask warmed to room temperature overnight; precipitation of a white solid was observed. Triethylammonium chloride was removed by filtering

the reaction mixture via cannula through a frit containing a pad of diatomaceous earth. The frit was rinsed with toluene and solvent was removed from the filtrate under vacuum to give the product in high purity.

*$^{(tBu)2(OMe)4}$(POCOP) (**1a**)*. Using the general procedure $^{(tBu)2(OMe)4}$(POCOP) (**1a**) was isolated from a reaction carried out with 204 mg (0.480 mmol) of [C_6H_2-4,6-(^{t}Bu)$_2$-1,3-($OPCl_2$)$_2$], 0.7 mL (5 mmol) NEt_3, and 0.30 mL (7.4 mmol) methanol. The product was isolated as a viscous yellow oil in high purity. An accurate yield was difficult to ascertain since the product is highly viscous and difficult to transfer. Anal. Calcd for $C_{18}H_{32}O_6P_2$: C, 53.20; H, 7.94. Found: C, 53.35; H, 8.02. ^{1}H NMR (CD_2Cl_2, 499.72 MHz, 25 °C): δ 7.28 (s, 1H; Ar-*H*), 6.87 (t, $^4J_{PH}$ = 1.2 Hz, 1H; Ar-*H*), 3.67 (d, $^3J_{PH}$ = 10.3 Hz, 12H; P-OC*H*$_3$), 1.37 (s, 18H, Ar-C(C*H*$_3$)$_3$). ^{31}P{^{1}H} NMR (CD_2Cl_2, 202.29 MHz, 25 °C): δ 135.0 (s). ^{13}C{^{1}H} NMR (CD_2Cl_2, 125.65 MHz, 25 °C): δ 150.23 (m; C_{Ar}), 134.17 (s; C_{Ar}), 126.28 (s; C_{Ar}), 111.15 (t, $^3J_{PC}$ = 17 Hz; C_{Ar}), 50.08 (d, $^2J_{PC}$ = 6.5 Hz; P-O*C*H$_3$), 35.07 (s; Ar-*C*(CH$_3$)$_3$), 30.42 (s; Ar-C(*C*H$_3$)$_3$).

*$^{(tBu)2(2\text{-methoxyethyl})4}$(POCOP) (**1b**)*. Using the general procedure, $^{(tBu)2(2\text{-methoxyethyl})4}$(POCOP) (**1b**) was obtained from a reaction carried out with 215 mg (0.507 mmol) [C_6H_2-4,6-(^{t}Bu)$_2$-1,3-($OPCl_2$)$_2$], 0.7 mL (5 mmol) NEt_3, and 0.4 mL (5 mmol) 2-methoxyethanol. The product was isolated as a viscous yellow oil in high purity. An accurate yield was difficult to ascertain since the product is highly viscous and difficult to transfer. ^{1}H NMR (CD_2Cl_2, 499.72 MHz, 25 °C): 7.27 (s, 1H; Ar-H), 6.93 (s, 1H; Ar-H), 4.10 (m, 8H; P-OC*H*$_2$CH$_2$OCH$_3$), 3.58 (t, $^3J_{HH}$ = 4.9 Hz, 8H; P-OCH$_2$C*H*$_2$OCH$_3$), 3.36 (s, 12H; P-O(CH$_2$)$_2$OC*H*$_3$), 1.37 (s, 12H; ^{t}Bu). ^{31}P{^{1}H} NMR (CD_2Cl_2, 202.29 MHz, 25 °C): δ 134.7 (s).

*$^{(tBu)2(cholesterol)4}$(POCOP) (**1d**)*. Using the general procedure, 770 mg (0.422 mmol, 87% yield) $^{(tBu)2(cholesterol)4}$(POCOP) (**1d**) was obtained from a reaction of 206 mg (0.486 mmol) [C_6H_2-4,6-

(^{t}Bu)$_2$-1,3-(OPCl$_2$)$_2$], 0.7 mL (5 mmol) NEt$_3$, and 779 mg (2.01 mmol) cholesterol. The resulting material was an off-white powder. Product formation was verified by ^{31}P NMR spectroscopy since the ^{1}H NMR spectrum has many resonances from 3 to 0 ppm. ^{31}P{^{1}H} NMR (CDCl$_3$, 202.31 MHz, 25 °C): δ 136.1 (s).

$^{(tBu)2(OMe)4}$(POCOP)Ir^{III}(CO)(H)(Cl) ***(2a)***. To a 100 mL flask sealed with a Teflon stopcock was added 165 mg (0.421 mmol) Ir(CO)$_2$Cl(*p*-toluidine) and 10 mL toluene. A solution of 188 mg (0.462 mmol) $^{(tBu)2(OMe)4}$(POCOP) in 10 mL toluene was added to the iridium solution resulting in a bubbling yellow solution. The yellow solution was heated at 100 °C for 18 h resulting in a paler yellow solution. Toluene was removed under vacuum resulting in a yellow oily residue. The residue was dissolved in 90:10 ethyl acetate/diethyl ether and eluted through a silica plug. The solvent was removed under vacuum giving a yellow oil. The oil was dissolved in dichloromethane and eluted through a neutral alumina plug. Upon rinsing through the alumina plug, the yellow solution turned orange due to partial deprotonation of the crude material to the Ir(I) complex. Dichloromethane was removed under vacuum to give an orange solid. ^{1}H and ^{31}P NMR spectra verified that $^{(tBu)2(OMe)4}$(POCOP)Ir^{III}(CO)(H)(Cl) and $^{(tBu)2(OMe)4}$(POCOP)Ir^{I}(CO) were present as a mixture in the sample. The orange residue was dissolved in dry dichloromethane (~1 mL), filtered through a pad of diatomaceous earth then layered with pentane (~9 mL) and stored at -15 °C. This resulted in yellow crystals suitable for X-ray diffraction of $^{(tBu)2(OMe)4}$(POCOP)Ir^{III}(CO)(H)(Cl). Further attempts at isolating pure samples of $^{(tBu)2(OMe)4}$(POCOP)Ir^{III}(CO)(H)(Cl) were challenging. Dissolving the orange residue in 1 mL toluene, layering with pentane (10 mL) and storing at -20 °C afforded a pale yellow precipitate which was pure $^{(tBu)2(OMe)4}$(POCOP)Ir^{III}(CO)(H)(Cl) by ^{1}H, ^{31}P, and ^{13}C NMR spectroscopies, however this method

was low yielding (3% isolated yield). In a separate experiment, the Ir(I)/Ir(III) mixture obtained after eluting through neutral alumina was dissolved in benzene and excess HCl/Et_2O was added to the mixture. This resulted in complete conversion to Ir(III) and precipitation of *p*-toluidine hydrochloride. Filtration followed by removal of benzene under vacuum gave a pale yellow solid. The solid was washed with pentane and dried under vacuum. The ^1H NMR spectrum showed many broad peaks between 3.0 and 2.0 ppm and thus the material was not as clean as the previously described purification method. This reaction reproducibly gave material which showed many broad peaks in the ^1H NMR spectrum. Complex **2a** did not give a satisfactory elemental analysis presumably due to the presence of impurities from ligand degradation. ^1H NMR ($CDCl_3$, 500 MHz, 25 °C): δ 7.01 (s, 1H; Ar-*H*), 4.12 (vt, $^3J_{PH} + {}^5J_{PH}$ = 12.2 Hz, 6H; P-OC*H*$_3$), 3.74 (vt, $^3J_{PH} + {}^5J_{PH}$ = 12.2 Hz, 6H; P-OC*H*$_3$), 1.37 (s, 18H; ^{t}Bu), -18.51 (t, $^2J_{PH}$ = 13.5 Hz, 1H; Ir-*H*). $^{31}P\{^1H\}$ NMR ($CDCl_3$, 202.40 MHz, 25 °C): δ 117.3 (s). $^{13}C\{^1H\}$ NMR ($CDCl_3$, 125.65 MHz, 25 °C): δ 172.20 (m; C_{Ar}), 154.17 (m; C_{Ar}), 128.56 (m; C_{Ar}), 123.61 (s; C_{Ar}), 56.20 (s; P-O*C*H$_3$), 53.39 (s; P-O*C*H$_3$), 34.78 (s; Ar-*C*(CH$_3$)$_3$), 30.13 (s; Ar-C(*C*H$_3$)$_3$). IR (solution, CH_2Cl_2, cm^{-1}): ν(CO) 2062, ν(Ir-H) 2138.

*$^{(tBu)2(diol)2}$(POCOP)Ir^{III}(CO)(H)(Cl) (**2c**).* To a 100 mL flask sealed with a Teflon stopcock was added 53.3 mg (0.136 mmol) $Ir(CO)_2Cl$(*p*-toluidine), 110 mg (0.136 mmol) of $^{(tBu)2(diol)2}$(POCOP) (**1c**) and 30 mL of toluene. The resulting solution was amber colored. The reaction was heated at 100 °C for 18 h resulting in a color change to yellow. The reaction mixture was filtered through a syringe filter. Solvent was removed under vacuum giving a yellow solid. Crystals suitable for diffraction were grown by slow diffusion of hexane into a toluene solution of **2c**. Product formation was verified by appearance of an iridium hydride peak in the ^1H NMR spectrum. ^1H NMR

(toluene-d_8, 499.71 MHz, 25 °C): δ -16.54 ppm (t, $^2J_{PH}$ = 13.9Hz, 1H; Ir-*H*). Multiple broad resonances between 6.0 and 2.0 ppm are assigned to the sugar moieties. $^{31}P\{^1H\}$ NMR (toluene-d_8, 202.29 MHz, 25 °C): δ 130.9 (s).

*$^{(iPr)4}$(POCOP)Ir^{III}(CO)(H)(Cl) (**6a**)*. To a 100 mL flask sealed with a Teflon stopcock was added 106 mg (0.271 mmol) Ir(CO)$_2$Cl(*p*-toluidine) and a solution of 112 mg (0.327 mmol) $^{(iPr)4}$(POCOP) in 15 mL toluene. This resulted in the evolution of gas from a yellow solution. The solution was heated at 110 °C and after 30 min a white precipitate was observed. After heating for 15.5 h, the precipitate had redissolved and the solution was still yellow. The solution was filtered through diatomaceous earth and the solvent was removed under vacuum giving a yellow oily residue. The residue was dissolved in 5 mL dichloromethane and filtered through a plug of neutral alumina. The solvent was removed under vacuum and the yellow residue was dissolved in 2 mL benzene. Addition of 1 mL of 1.0 M HCl/Et$_2$O precipitated *p*-toluidine hydrochloride, which was removed by filtration through diatomaceous earth. Removal of benzene under vacuum gave an off-white solid. The solid was washed with pentane (~5 mL) and dried under vacuum giving a white air-stable solid; yield: 142 mg (0.237 mmol, 87%). Crystals suitable for diffraction were grown by slow evaporation of a dichloromethane solution. Anal. Calcd for $C_{19}H_{32}ClIrO_3P_2$: C, 38.16; H, 5.39. Found: C, 38.56; H, 5.45. ^1H NMR (CD_2Cl_2, 300.13 MHz, 23 °C): δ 6.88 (m, 1H; *para* Ar-*H*), 6.54 (d, $^3J_{HH}$ = 8.0 Hz, 2H; *meta* Ar-*H*), 3.26 (m, 2H; P-C*H*(CH$_3$)$_2$), 2.49 (m, 2H; P-C*H*(CH$_3$)$_2$), 1.44 (m, 12H; P-CH(C*H*$_3$)$_2$), 1.13 (m, 6H; P-C*H*(CH$_3$)$_2$), 0.97 (m, 6H; P-C*H*(CH$_3$)$_2$), -18.49 (t, $^2J_{PH}$ = 13.0 Hz, 1H; Ir-*H*). $^{31}P\{^1H\}$ NMR (CD_2Cl_2, 121.51 MHz, 23 °C): δ 166.5 (s). $^{13}C\{^1H\}$ NMR (CD_2Cl_2, 125.67 MHz, 27 °C): δ 177.82 (m; Ir-*C*O), 164.43 (m; C_{Ar}), 128.66 (m; C_{Ar}), 127.84 (s; C_{Ar}), 105.82 (m; C_{Ar}), 29.60 (vt, $^1J_{PC}$ + $^3J_{PC}$ = 17.0 Hz; P-*C*H(CH$_3$)$_2$), 28.77 (vt, $^1J_{PC}$ + $^3J_{PC}$ = 17.2

Hz; P-*C*H(CH_3)$_2$), 18.74 (m; P-CH(*C*H_3)$_2$), 18.50 (m; P-CH(*C*H_3)$_2$), 17.90 (s; P-CH(*C*H_3)$_2$), 15.72 (s; P-CH(*C*H_3)$_2$). IR (solution, CH_2Cl_2, cm^{-1}): ν(CO) 2035, ν(Ir-H) 2200.

$^{(iPr)4}$(POCOP)Ir^{I}(CO) (6b). A 20 mL scintillation vial was charged with 44.5 mg (0.0744 mmol) $^{(iPr)4}$(POCOP)Ir^{III}(CO)(H)(Cl) and 19.0 mg (0.198 mmol) NaO^{t}Bu. THF (~5 mL) was added giving an orange solution with white precipitate. After stirring for 2 h at room temperature, solvent was removed under vacuum. The orange residue was dissolved in benzene (~5 mL) and filtered through a neutral alumina plug. Upon lyophilization, 32 mg of golden fluffy solid was isolated. By $^{31}P\{^1H\}$ NMR, the material was ~93% product, with the remainder as unreacted Ir(III) starting material and an unidentified impurity. The material was re-dissolved in THF and an additional 19.0 mg NaO^{t}Bu was added. After the same workup as described above, 15.0 mg (0.267 mmol, 36%) of material was isolated which was pure product by ^1H and $^{31}P\{^1H\}$ NMR spectroscopy. See chapter 3 for an improved synthesis of **6b**. Anal. Calcd for $C_{19}H_{31}IrO_3P_2$: C, 40.63; H, 5.56. Found: C, 41.01; H, 5.57. ^1H NMR (acetone-d_6, 300.13 MHz, 22 °C): δ 6.88 (m, 1H; *para* Ar-*H*), 6.58 (d, $^3J_{HH}$ = 7.9 Hz, 2H; *meta* Ar-*H*), 2.52 (m, 4H; P-C*H*(CH_3)$_2$), 1.27-1.16 (m, 24H; P-CH(C*H*$_3$)$_2$). $^{31}P\{^1H\}$ NMR (acetone-d_6, 121.49 MHz, 22 °C): δ 191.2 (s). $^{13}C\{^1H\}$ NMR (CD_2Cl_2, 75.48 MHz, 25 °C): δ 198.51 (m; Ir-*C*O), 169.22 (m; C_{Ar}), 148.73 (m; C_{Ar}), 129.53 (s; C_{Ar}), 104.16 (m; C_{Ar}), 32.04 (vt, $^1J_{PC}$ + $^3J_{PC}$ = 16.1 Hz; P-*C*H(CH_3)$_2$), 18.75 (s; P-CH(*C*H_3)$_2$), 17.81 (s; P-CH(*C*H_3)$_2$). IR (solution, CH_2Cl_2, cm^{-1}): ν(CO) 1944. The IR spectrum of $^{(tBu)4}$(POCOP)Ir^{I}(CO) (**5**) was recorded in CH_2Cl_2 to make a direct comparison with **6b**; IR (solution, CH_2Cl_2, cm^{-1}): ν(CO) 1937.

General procedure for the synthesis of $^{(COOMe)2(R)4}$(POCOP). A 50 mL flask sealed with a Teflon stopcock was charged with 1 equiv. of dimethyl 4,6-dihydroxyisophthalate and 10 mL THF, resulting in a colorless solution. Under positive argon flow, 10-20 equiv. of NEt_3 and 2-4 equiv. of R_2PCl were added to the flask, giving a colorless solution. The solution was stirred at room temperature for 1.5 h. THF was removed under vacuum giving a yellow/white residue. The residue was dissolved in toluene (~10 mL) and triethylammonium chloride was removed by filtering the reaction mixture via cannula through a frit containing a pad of diatomaceous earth. Toluene was removed under vacuum and the residue was heated at 50 °C while under dynamic vacuum for 1.5 h to remove any remaining volatiles.

*R = ^{t}Bu (**7**).* Using the general procedure, 127 mg (0.247 mmol, 72%) of $^{(COOMe)2(tBu)4}$(POCOP) was isolated from 78.1 mg (0.345 mmol) of dimethyl 4,6-dihydroxyisophthalate, 1.0 mL (7.2 mmol) of NEt_3, and 0.15 mL (0.79 mmol) of $(^{t}Bu)_2PCl$. The resulting material was an off-white powdery solid. Anal. Calcd for $C_{26}H_{44}O_6P_2$: C, 60.69; H, 8.62. Found: C, 60.48; H, 8.42. ^{1}H NMR (C_6D_6, 499.72 MHz, 25 °C): δ 8.91 (s, 1H; Ar-*H*), 8.36 (t, $^4J_{PH}$ = 6.4 Hz, 1H; Ar-*H*), 3.50 (s, 6H; Ar-COOC*H*$_3$), 1.18 (d, $^3J_{PH}$ = 12 Hz, PC(C*H*$_3$)$_3$). ^{31}P{^{1}H} NMR (C_6D_6, 202.29 MHz, 25 °C): δ 156.8 (s). ^{13}C{^{1}H} NMR (CD_2Cl_2, 75.47 MHz, 24 °C): δ 166.13 (s; Ar-*C*OOCH$_3$), 163.97 (dd, $^2J_{PC}$ = 8.9 Hz, $^4J_{PC}$ = 1.8 Hz; *C*$_{Ar}$-O-P), 137.29 (s; *C*$_{Ar}$), 114.23 (s; *C*$_{Ar}$-COOCH$_3$), 107.83 (t, $^3J_{PC}$ = 26.8 Hz; *C*$_{Ar}$), 52.11 (s; C$_{Ar}$-COO*C*H$_3$), 36.43 (d, $^1J_{PC}$ = 26.0 Hz; P-*C*(CH$_3$)$_3$), 27.63 (d, $^2J_{PC}$ = 15.6 Hz; P-C(*C*H$_3$)$_3$).

*R = ^{i}Pr (**8**).* Using the general procedure, 446 mg (0.973 mmol, 80%) of $^{(COOMe)2(iPr)4}$(POCOP) was isolated from 275 mg (0.996 mmol) of dimethyl 4,6-dihydroxyisophthalate, 1.5 mL (11 mmol) of NEt_3, and 0.8 mL (5 mmol) of $(^{i}Pr)_2PCl$. The resulting material was a yellow viscous oil which solidified over weeks. Anal. Calcd for $C_{22}H_{36}O_6P_2$: C, 57.64; H, 7.91. Found: C, 57.43; H, 7.80.

^{1}H NMR (CD_2Cl_2, 300.13 MHz, 22 °C): δ 8.28 (s, 1H; Ar-*H*), 7.58 (t, $^{4}J_{PH}$ = 5.2 Hz, 1H; Ar-*H*), 3.82 (s, 6H; Ar-COOC*H*$_3$), 2.00 (m, 4H; PC*H*$(CH_3)_2$), 1.18 (dd, $^{3}J_{HH}$ = 6.9 Hz, $^{3}J_{PH}$ = 10.8 Hz, 6H; PCH(C*H*$_3)_2$), 1.11 (dd, $^{3}J_{HH}$ = 7.2 Hz, $^{3}J_{PH}$ = 16.0 Hz, 6H; PCH(C*H*$_3)_2$). ^{31}P{^{1}H} NMR (CD_2Cl_2, 121.51 Hz, 22 °C): δ 153.5 (s). ^{13}C{^{1}H} NMR (CD_2Cl_2, 75.48 MHz, 24 °C): δ 165.92 (s; Ar-*C*OOCH$_3$), 163.59 (dd, $^{2}J_{PC}$ = 8.5 Hz, $^{4}J_{PC}$ = 1.6 Hz; *C*$_{Ar}$-O-P), 136.81 (s; *C*$_{Ar}$), 114.74 (s; *C*$_{Ar}$-COOCH$_3$), 108.65 (t, $^{3}J_{PC}$ = 25.2 Hz; *C*$_{Ar}$), 52.09 (s; C$_{Ar}$-COO*C*H$_3$), 28.83 (d, $^{1}J_{PC}$ = 18.2 Hz; P-*C*H$(CH_3)_2$), 17.86 (d, $^{2}J_{PC}$ = 19.8 Hz; P-CH(*C*H$_3)_2$), 17.26 (d, $^{2}J_{PC}$ = 8.2 Hz; P-*C*H$(CH_3)_2$).

$^{(COOMe)2(tBu)4}$(POCOP)Ir^{I}(CO) (***9***). A 50 mL flask sealed with a Teflon stopcock was charged with 51.5 mg (0.132 mmol) Ir$(CO)_2$Cl(*p*-toluidine) and 78.4 mg (0.152 mmol) $^{(COOMe)2(tBu)4}$(POCOP). Toluene (~15 mL) was added to the flask, resulting in a bubbling pale yellow/green solution. The solution was heated at 100 °C for 16 h resulting in a brighter yellow solution and precipitation of *p*-toluidine hydrochloride. The mixture was filtered through diatomaceous earth and toluene was removed under vacuum. The yellow residue was dissolved in dichloromethane and filtered through a neutral alumina plug and washed with 1-2 mL more dichloromethane. Volatiles were removed under vacuum resulting in an air-stable yellow powder in high purity; yield: 89 mg (0.12 mmol, 92%). Slow evaporation of a 3:1 pentane/dichloromethane solution (~8 mL) at room temperature resulted in yellow needle crystals suitable for X-ray diffraction. Anal. Calcd for $C_{27}H_{43}IrO_7P_2$: C, 44.19; H, 5.91. Found: C, 44.04; H, 5.85. ^{1}H NMR (toluene-d_8, 499.72 MHz, 25 °C): δ 8.69 (s, 1H; Ar-*H*), 3.54 (s, 6H; Ar-COOC*H*$_3$), 1.29 (vt, $^{3}J_{PH}$ + $^{5}J_{PH}$ = 14.7 Hz, 18H; PC(C*H*$_3)_3$). ^{31}P{^{1}H} NMR (C_6D_6, 202.42 MHz, 27 °C): δ 205.1 (s). ^{13}C{^{1}H} NMR (CD_2Cl_2, 75.47 MHz, 26 °C): δ 198.50 (t, $^{2}J_{PC}$ = 5.2 Hz; Ir-*C*O), 171.55 (vt, $^{2}J_{PC}$ + $^{4}J_{PC}$ = 7.8 Hz; *C*$_{Ar}$-O-P), 166.27 (s; Ar-*C*OOCH$_3$), 153.31 (t, $^{2}J_{PC}$ = 7.6 Hz; *C*$_{ipso}$), 135.68 (s; *para C*$_{Ar}$), 109.77 (s; *C*$_{Ar}$-COOCH$_3$), 52.03

(s; C_{Ar}-COO*C*H_3), 41.75 (vt, $^1J_{PC} + {}^3J_{PC}$ = 12.2 Hz; P-*C*$(CH_3)_3$), 28.55 (vt, $^2J_{PC} + {}^4J_{PC}$ = 3.2 Hz; P-C(*C*$H_3)_3$). IR (KBr, cm^{-1}): ν(CO) 1946.

*$^{(COOMe)2(iPr)4}$(POCOP)Ir^{III}(CO)(H)(Cl) (**10**)*. A 100 mL flask sealed with a Teflon stopcock was charged with 79.5 mg (0.203 mmol) $Ir(CO)_2Cl$(*p*-toluidine). A solution of 104 mg (0.226 mmol) $^{(COOMe)2(iPr)4}$(POCOP) in 10 mL toluene was added to the flask, giving a bubbling yellow solution. The solution was heated at 100 °C for 14 h. The solution was treated with excess 1.0 M HCl/Et_2O solution to precipitate *p*-toluidine hydrochloride. The precipitate was filtered off and the volatiles from the filtrate were removed under vacuum to give a yellow residue. The residue was dissolved in 5 mL dichloromethane then filtered through a plug of neutral alumina. Removal of dichloromethane under vacuum gave an off-white solid. The solid was rinsed with pentane (~5 mL) and dried under vacuum giving an air-stable white powder; yield: 88 mg (0.12 mmol, 61%). Crystals suitable for diffraction were grown by slow diffusion of pentane into a dichloromethane solution; one molecule of dichloromethane per complex was observed. Anal. Calcd for $C_{23}H_{36}ClIrO_7P_2$ (powder sample, dichloromethane not present): C, 38.68; H, 5.08. Found: C, 38.81; H, 5.06. ^{1}H NMR (CD_2Cl_2, 300.13 MHz, 22 °C): δ 8.21 (s, 1H; Ar-*H*), 3.83 (s, 6H; Ar-COOC*H*$_3$), 3.35 (m, 2H; PC*H*$(CH_3)_2$), 2.60 (m, 2H; PC*H*$(CH_3)_2$), 1.51 (m, 6H; PCH(C*H*$_3)_2$), 1.41 (m, 6H; PCH(C*H*$_3)_2$), 1.16 (m, 6H; PCH(C*H*$_3)_2$), 0.97 (m, 6H; PCH(C*H*$_3)_2$), -18.29 (t, $^2J_{PH}$ = 13.1 Hz, 1H; Ir-*H*). ^{31}P{^{1}H} NMR (CD_2Cl_2, 121.51 MHz, 22 °C): δ 171.7 (s). ^{13}C{^{1}H} NMR (CD_2Cl_2, 125.67 MHz, 25 °C): δ 176.61 (m; Ir-*C*O), 165.75 (m; C_{Ar}), 165.34 (s; Ar-*C*OOCH$_3$), 134.57 (s; *para* C_{Ar}), 133.29 (m; C_{Ar}), 111.11 (m; C_{Ar}), 52.19 (s; Ar-COO*C*H$_3$), 29.49 (vt, $^1J_{PC} + {}^3J_{PC}$ = 16.3 Hz; P-*C*H$(CH_3)_2$), 28.49 (vt, $^1J_{PC} + {}^3J_{PC}$ = 17.2 Hz; P-*C*H$(CH_3)_2$), 18.87 (m; P-CH(*C*H$_3)_2$), 17.93

(m; P-CH(CH_3)$_2$), 17.68 (m; P-CH(CH_3)$_2$), 15.59 (m; P-CH(CH_3)$_2$). IR (solution, CH_2Cl_2, cm^{-1}): ν(CO) 2042, ν(Ir-H) 2193.

*cis-$^{(tBu)4}$(POCOP)Ir^{III}(CO)(H)(Cl) (**cis-11**).* An NMR tube fitted with a J. Young style Teflon valve was charged with 13.3 mg (0.0212 mmol) $^{(tBu)4}$(POCOP)Ir^{III}(H)(Cl). Toluene-d_8 was vacuum transferred into the tube resulting in a red solution with undissolved solid. CO was bubbled through the solution until all solid dissolved and the solution was pale yellow. Representative spectra for identification of ***cis*-11**: ^{1}H NMR (toluene-d_8, 499.71 MHz, 25 °C): δ 6.69 (t, $^3J_{HH}$ = 8.0 Hz, 1H; *para* Ar-*H*), 6.52 (d, $^3J_{HH}$ = 8.0 Hz, 2H; *meta* Ar-*H*), 1.39 (vt, $^3J_{PH}$ + $^5J_{PH}$ = 7.5 Hz, 18H; PC(CH_3)$_3$), 1.31 (vt, $^3J_{PH}$ + $^5J_{PH}$ = 7.5 Hz, 18H; PC(CH_3)$_3$), -8.27 (t, $^2J_{PH}$ = 16.1 Hz, 1H; Ir-*H*). ^{31}P{^{1}H} NMR (toluene-d_8, 202.31 MHz, 25 °C): δ 162.7 (s). IR (solution, CH_2Cl_2, cm^{-1}): ν(CO) 2018.

*trans-$^{(tBu)4}$(POCOP)Ir^{III}(CO)(H)(Cl) (**trans-11**).* A 20 mL scintillation vial was charged with 13.5 mg (0.0219 mmol) $^{(tBu)4}$(POCOP)Ir^{I}(CO). Benzene (~5 mL) was added resulting in a yellow solution. Excess HCl/Et_2O (~10 equiv.) was added to the yellow solution. Upon vigorous mixing, the solution turned colorless. Removal of the solvent under vacuum gave the product as an off-white solid. Representative spectra for identification of ***trans*-11**: ^{1}H NMR (toluene-d_8, 499.72 MHz, 25 °C): δ 6.78 (t, $^3J_{HH}$ = 8.0 Hz, 1H; *para* Ar-*H*), 6.62 (d, $^3J_{HH}$ = 8.0 Hz, 2H; *meta* Ar-*H*), 1.58 (vt, $^3J_{PH}$ + $^5J_{PH}$ = 7.9 Hz, 18H; PC(CH_3)$_3$), 1.08 (vt, $^3J_{PH}$ + $^5J_{PH}$ = 7.4 Hz, 18H; PC(CH_3)$_3$), -17.62 (t, $^2J_{PH}$ = 13.3 Hz, 1H; Ir-*H*). ^{31}P{^{1}H} NMR (toluene-d_8, 202.31 MHz, 25 °C): δ 170.6 (s). IR (solution, CH_2Cl_2, cm^{-1}): ν(CO) 2031.

*[$^{(tBu)4}$(POCOP)Ir^{III}(CO)(H)]BF_4 (**12**).* A 100 mL flask sealed with a Teflon stopcock was charged with 68.8 mg (0.111 mmol) $^{(tBu)4}$(POCOP)Ir^{I}(CO) and 25 mL benzene, giving a yellow solution. 13.6 µL (0.100 mmol) HBF_4•Et_2O was added to the benzene solution and mixed vigorously, giving an orange precipitate. The solvent was removed under vacuum and the orange/yellow residue was dissolved in ~5 mL dichloromethane and filtered through a pad of diatomaceous earth. The dichloromethane solution volume was reduced to 1.5 mL, layered with pentane (~5 mL) and stored at -15 °C for 48 h. This resulted in orange crystals suitable for X-ray diffraction; yield: 50%. Anal. Calcd for $C_{23}H_{40}BF_4IrO_3P_2$: C, 39.15; H, 5.71. Found: C, 38.50; H, 5.46. ^{1}H NMR (CD_2Cl_2, 300.10 MHz, 25 °C): δ 7.36 (t, $^3J_{HH}$ = 7.9 Hz, 1H; *para* Ar-*H*), 6.94 (d, $^3J_{HH}$ = 7.9 Hz, 2H; *meta* Ar-*H*), 1.40 (m, 18H; PC(C*H*$_3$)$_3$), -35.70 (t, $^2J_{PH}$ = 10.5 Hz, 1H; Ir-*H*). ^{31}P{^{1}H} NMR (CD_2Cl_2, 121.49 MHz, 22 °C): δ 191.0 (s). ^{13}C{^{1}H} NMR (CD_2Cl_2, 75.46 MHz, 25 °C): δ 187.06 (m; Ir-*C*O), 170.60 (vt, $^2J_{PC}$ + $^4J_{PC}$ = 10.4 Hz; *C*$_{Ar}$-O-P), 145.01 (s; *para C*$_{Ar}$-H), 135.81 (s; *meta C*$_{Ar}$-H), 107.61 (t, $^2J_{PC}$ = 5.7 Hz; *C*$_{ipso}$), 47.58 (vt, $^1J_{PC}$ + $^3J_{PC}$ = 25.2 Hz; P*C*(CH$_3$)$_3$), 40.97 (vt, $^1J_{PC}$ + $^3J_{PC}$ = 27.2 Hz; P*C*(CH$_3$)$_3$), 28.82 (vt, $^2J_{PC}$ + $^4J_{PC}$ = 5.3 Hz; PC(*C*H$_3$)$_3$), 27.75 (vt, $^2J_{PC}$ + $^4J_{PC}$ = 5.3 Hz; PC(*C*H$_3$)$_3$). IR (solution, CH_2Cl_2, cm^{-1}): *ν*(CO) 2053, *ν*(Ir-H) 2031.

*[$^{(iPr)4}$(POCOP)Ir^{III}(CO)(H)]BF_4 (**13**).* In an NMR tube fitted with a J. Young style Teflon valve, $AgBF_4$ (5.0 mg, 0.026 mmol) was added to a solution of $^{(iPr)4}$(POCOP)Ir^{III}(CO)(H)(Cl) (9.5 mg, 0.016 mmol) in 0.5 mL CD_2Cl_2. Upon shaking the mixture, an orange solution with a gray precipitate was observed. Complex **12** did not give a satisfactory elemental analysis presumably due to the presence of silver salts, resulting in low carbon and hydrogen percentages. ^{1}H NMR (CD_2Cl_2, 300.12 MHz, 22 °C): δ 7.14 (m, 1H; *para* C$_{Ar}$-*H*), 6.73 (d, $^3J_{HH}$ = 8.0 Hz, 2H; *meta* C$_{Ar}$-*H*), 2.96 (m, 2H; P-C*H*(CH$_3$)$_2$), 2.61 (m, 2H; P-C*H*(CH$_3$)$_2$), 1.55-1.35 (m, 12H; P-CH(C*H*$_3$)$_2$), 1.18

(m, 6H; P-CH(CH_3)$_2$), 0.99 (m, 6H; P-CH(CH_3)$_2$), -29.26 (br t, $^2J_{PH}$ = 12.3 Hz, 1H; Ir-*H*) . ^{31}P{^{1}H} (CD_2Cl_2, 121.49 MHz, 22 °C): δ 174.6 (s).

[$^{(tBu)4}$(POCOP)Ir^{III}(CO)$_2$(H)]BF$_4$ ***(14)***. In an NMR tube fitted with a J. Young style Teflon valve, 22.3 mg (0.0316 mmol) [$^{(tBu)4}$(POCOP)Ir^{III}(CO)(H)]BF_4 was dissolved in CD_2Cl_2 (~1 mL) giving a dark orange solution. The tube was freeze-pump-thawed three times then filled with ~1 atm CO. Upon vigorous shaking of the tube, a rapid color change from orange to faint yellow/near colorless was observed. Quantitative conversion to the desired product was verified by ^{1}H and ^{31}P NMR spectroscopies. The CD_2Cl_2 solution (~1 mL) was filtered through a pad of diatomaceous earth, concentrated to 0.5 mL then layered with pentane (~4 mL) and stored at -20 °C for 5 days. This resulted in colorless crystals suitable for X-ray diffraction; one molecule of dichloromethane per complex was observed. Anal. Calcd for $C_{25}H_{42}BF_4Cl_2IrO_4P_2$ (one molecule of dichloromethane present): C, 36.69; H, 5.17. Found: C, 36.52; H, 5.06. ^{1}H NMR (CD_2Cl_2, 300.13 MHz, 22 °C): δ 7.13 (t, $^3J_{HH}$ = 8.2 Hz, 1H; *para* Ar-*H*), 6.79 (d, $^3J_{HH}$ = 8.2 Hz, 2H; *meta* Ar-*H*), 1.57 (vt, $^3J_{PH}$ + $^5J_{PH}$ = 17.2 Hz, 9H; PC(CH_3)$_3$), 1.36 (vt, $^3J_{PH}$ + $^5J_{PH}$ = 16.6 Hz, 9H; PC(CH_3)$_3$), -10.49 (t, $^2J_{PH}$ = 14.8 Hz, 1H; Ir-*H*). ^{31}P{^{1}H} NMR (CD_2Cl_2, 121.49 MHz, 22 °C): δ 174.1 (s). ^{13}C{^{1}H} NMR (CD_2Cl_2, 125.65 MHz, 25 °C): δ 168.08 (t, $^2J_{PC}$ = 4.5 Hz; Ir-*C*O), 166.46 (m; Ir-*C*O), 164.21 (m; *C*$_{Ar}$), 130.86 (s; *C*$_{Ar}$), 111.20 (m; *C*$_{Ar}$), 108.36 (m; *C*$_{Ar}$), 44.31 (vt, $^1J_{PC}$ + $^3J_{PC}$ = 26.19 Hz; P*C*(CH$_3$)$_3$), 44.22 (vt, $^1J_{PC}$ + $^3J_{PC}$ = 24.8 Hz; P*C*(CH$_3$)$_3$), 28.84 (s; PC(*C*H$_3$)$_3$), 27.94 (s; PC(*C*H$_3$)$_3$). IR (KBr, cm^{-1}): *ν*(CO) 2106, 2073, *ν*(Ir-H) 2230.

Experimental Procedures

*Reaction of $^{(iPr)4}$(POCOP)Ir(CO) (**6b**) with O_2.* An NMR tube fitted with a J. Young style Teflon valve was charged with $^{(iPr)4}$(POCOP)Ir(CO) (**6b**) (8.0 mg, 0.014 mmol) and C_6D_6 (0.4 mL) was added to the tube giving a golden yellow solution. The sample was freeze-pump-thawed three times then pressurized with 2 atm O_2. The sample was stirred for 3 h on an NMR tube rotator, resulting in a color change to brown. Observation of the ^{1}H and ^{31}P NMR spectra after 3 h indicated the formation of a new iridium containing product. The NMR resonances observed at the 3 h time point are reported here. ^{1}H NMR (C_6D_6, 499.72 MHz, 25 °C): δ 6.88 (m, 1H; Ar-*H*), 6.73 (d, $^3J_{HH}$ = 7.9 Hz, 2H; Ar-*H*), 2.93 (br m, 2H; PC*H*$(CH_3)_2$), 2.26 (br m, 2H; PC*H*$(CH_3)_2$), 1.29 (m, 6H; P-CH(C*H*$_3)_2$), 1.18 (m, 6H; P-CH(C*H*$_3)_2$), 1.10 (m, 6H; P-CH(C*H*$_3)_2$), 1.06 (m, 6H; P-CH(C*H*$_3)_2$). ^{31}P{^{1}H} NMR (C_6D_6, 202.31 MHz, 25 °C): δ 144.7 (s).

*Isomerization reaction of **cis-11** to **trans-11***. An NMR tube fitted with a J. Young style Teflon valve was charged with 12 mg (0.030 mmol) $^{(tBu)4}$(POCOP) and 13.2 mg (0.015 mmol) [Ir(COE)$_2$(μ-Cl)]$_2$. Toluene-d_8 was vacuum transferred into the tube giving a red solution. The reaction was heated at 100 °C for 14.5 h to generate $^{(tBu)4}$(POCOP)Ir^{III}(H)(Cl) in situ as a burgundy solution with some undissolved red solid. CO was bubbled through the solution resulting in a color change to pale yellow with some undissolved red solid, generating ***cis*-11**. The reaction was heated at 100 °C for 12.5 h, affording a homogeneous yellow solution. ^{1}H and ^{31}P{^{1}H} NMR spectra showed a mixture of ***cis*-11** and as well as $^{(tBu)4}$(POCOP)Ir(CO) (**5**). No $^{(tBu)4}$(POCOP)Ir^{III}(H)(Cl) was observed. Further heating of the solution at 100 °C (5 days total heating) led to further conversion to ***trans*-11** establishing an equilibrium between ***cis*-11** and ***trans*-11**. Some additional **5** was also formed.

*Alternative route for **cis-11** to **trans-11** isomerization reaction.* An NMR tube fitted with a J. Young style Teflon valve was charged with 13.3 mg (0.0212 mmol) $^{(tBu)4}$(POCOP)Ir^{III}(H)(Cl) (no COE present in reaction). Toluene-d_8 was vacuum transferred to the tube giving a red solution with some undissolved red solid. CO was bubbled through the solution resulting in a homogeneous pale yellow solution. Once the color of the solution was consistent, the tube was freeze-pump-thawed three times. ^{1}H and ^{31}P{^{1}H} NMR spectra verified formation of ***cis*-11** with no $^{(tBu)4}$(POCOP)Ir^{III}(H)(Cl) present. The solution was heated at 100 °C for 13.5 h resulting in a light orange solution. ^{1}H and ^{31}P{^{1}H} NMR spectra showed isomerization of ***cis*-11** to ***trans*-11**.

*Isomerization of **trans-11** to **cis-11**.* An NMR tube fitted with a J. Young style Teflon valve was charged with 11.5 mg (0.0176 mmol) *trans*-$^{(tBu)4}$(POCOP)Ir^{III}(CO)(H)(Cl) (***trans*-11**). Toluene-d_8 was vacuum transferred into the tube resulting in a pale yellow solution. The reaction was heated at 100 °C for 12.5 h resulting in a colorless solution with precipitated orange crystals. The identity of the solid precipitate was verified as $^{(tBu)4}$(POCOP)Ir^{I}(CO) (**5**) by X-ray crystallography. ^{1}H and ^{31}P{^{1}H} NMR spectra of the reaction solution showed partial formation of *cis*-$^{(tBu)4}$(POCOP)Ir^{III}(CO)(H)(Cl) (***cis*-11**) indicative of an equilibrium between ***cis*-11** and ***trans*-11**.

2.6 Notes to Chapter

[1] Adapted with permission from Goldberg, J. M.; Wong, G. W.; Brastow, K. E.; Kaminsky, W.; Goldberg, K. I.; Heinekey, D. M. *Organometallics* **2015**, *34*, 753–762. Copyright 2015 American Chemical Society.

[2] (a) *Organometallic Pincer Chemistry*; Topics in Organometallic Chemistry; van Koten, G.; Milstein, D., Eds.; Springer: Heidelberg, 2013; Vol. *40*. (b) O'Reilly, M. E.; Veige, A. S. *Chem. Soc. Rev.* **2014**, *43*, 6325-6369. (c) Henning, J.; Schubert, H.; Eichele, K.; Winter, F.; Pöttgen, R.; Mayer, H. A.; Wesemann, L. *Inorg. Chem.* **2012**, *51*, 5787-5794.

[3] Moulton, C. J.; Shaw, B. L. *J. Chem. Soc., Dalton Trans.* **1976**, 1020-1024.
[4] Göttker-Schnetmann, I.; White, P.; Brookhart, M. *J. Am. Chem. Soc.* **2004**, *126*, 1804-1811.
[5] Göttker-Schnetmann, I.; White, P. S.; Brookhart, M. *Organometallics* **2004**, *23*, 1766-1776.
[6] Krogh-Jespersen, K.; Czerw, M.; Zhu, K.; Singh, B.; Kanzelberger, M.; Darji, N.; Achord, P. D.; Renkema, K. B.; Goldman, A. S. *J. Am. Chem. Soc.* **2002**, *124*, 10797-10809.
[7] (a) Frech, C. M.; Milstein, D. *J. Am. Chem. Soc.* **2006**, *128*, 12434-12435. (b) Feller, M.; Diskin-Posner, Y.; Leitus, G.; Shimon, L. J. W.; Milstein, D. *J. Am. Chem. Soc.* **2013**, *135*, 11040-11047.
[8] Example of steric effects on C−C reductive elimination from (PCP)Ir: Ghosh, R.; Emge, T. J.; Krogh-Jespersen, K.; Goldman, A. S. *J. Am. Chem. Soc.* **2008**, *130*, 11317-11327.
[9] Example of the importance of sterics in (PCP)Pt complexes: Vuzman, D.; Poverenov, E.; Diskin-Posner, Y.; Leitus, G.; Shimon, L. J. W.; Milstein, D. *Dalton Trans.* **2007**, 5692-5700.
[10] (a) Choi, J.; MacArthur, A. H. R.; Brookhart, M.; Goldman, A. S. *Chem. Rev.* **2011**, *111*, 1761-1779. (b) Gupta, M.; Hagen, C.; Flesher, R. J.; Kaska, W. C.; Jensen, C. M. *Chem. Commun.* **1996**, 2083-2084. (c) Liu, F.; Pak, E. B.; Singh, B.; Jensen, C. M.; Goldman, A. S. *J. Am. Chem. Soc.* **1999**, *121*, 4086-4087. (d) Zhu, K.; Achord, P. D.; Zhang, X.; Krogh- Jespersen, K.; Goldman, A. S. *J. Am. Chem. Soc.* **2004**, *126*, 13044-13053. (e) Kundu, S.; Choliy, Y.; Zhuo, G.; Ahuja, R.; Emge, T. J.; Warmuth, R.; Brookhart, M.; Krogh-Jespersen, K.; Goldman, A. S. *Organometallics* **2009**, *28*, 5432-5444. (f) van der Boom, M. E.; Milstein, D. *Chem. Rev.* **2003**, *103*, 1759-1792.
[11] Roddick, D. M. *Top. Organomet. Chem.* **2013**, *40*, 49-88.
[12] Selected publications for catalysis with (POCOP)Ir: (a) Dobereiner, G. E.; Yuan, J.; Schrock, R. R.; Goldman, A. S.; Hackenberg, J. D. *J. Am. Chem. Soc.* **2013**, *135*, 12572-12575. (b) McLaughlin, M. P.; Adduci, L. L.; Becker, J. J.; Gagné, M. R. *J. Am. Chem. Soc.* **2013**, *135*, 1225-1227. (c) Lyons, T. W.; Guironnet, D.; Findlater, M.; Brookhart, M. *J. Am. Chem.* Chem. Soc. **2012**, *134*, 15708-15711. (d) Goldman, A. S.; Roy, A. H.; Huang, Z.; Ahuja, R.; Schinski, W.; Brookhart, M. *Science* **2006**, *312*, 257-261. (e) Denney, M. C.; Pons, V.; Hebden, T. J.; Heinekey, D. M.; Goldberg, K. I. *J. Am. Chem. Soc.* **2006**, *128*, 12048-12049. (f) Ahuja, R.; Punji, B.; Findlater, M.; Supplee, C.; Schinski, W.; Brookhart, M.; Goldman, A. S. *Nat. Chem.* **2011**, *3*, 167-171. (g) Park, S.; Bézier, D.; Brookhart, M. *J. Am. Chem. Soc.* **2012**, *134*, 11404-11407. (h) Huang, Z.; White, P. S.; Brookhart, M. *Nature* **2010**, *465*, 598-601. (i) Polukeev, A. V.; Petrovskii, P. V.; Peregudov, A. S.; Ezernitskaya, M. G.; Koridze, A. A. *Organometallics* **2013**, *32*, 1000-1015.
[13] (a) Mag, M.; Engels, J. W. *Nucleic Acids Res.* **1989**, *17*, 5973-5988. (b) Böhrsch, V.; Serwa, R.; Majkut, P.; Krause, E.; Hackenberger, C. P. R. *Chem. Commun.* **2010**, *46*, 3176-3178.
[14] Baber, R. A.; Bedford, R. B.; Betham, M.; Blake, M. E.; Coles, S. J.; Haddow, M. F.; Hursthouse, M. B.; Orpen, A. G.; Pilarski, L. T.; Pringle, P. G.; Wingad, R. L. *Chem. Commun.* **2006**, *2*, 3880-3882.
[15] (a) Farrugia, L. J. *J. Appl. Cryst.* **2012**, *45*, 849-854. (b) Farrugia, L. J. *J. Appl. Cryst.* **1997**, *30*, 565.
[16] Lao, D. B.; Owens, A. C. E.; Heinekey, D. M.; Goldberg, K. I. *ACS Catal.* **2013**, *3*, 2391-2396.
[17] Morales-Morales, D.; Redón, R.; Yung, C.; Jensen, C. M. *Inorg. Chim. Acta* **2004**, *357*, 2953-2956.
[18] (a) Williams, D. B.; Kaminsky, W.; Mayer, J. M.; Goldberg, K. I. *Chem. Commun.* **2008**, 4195-4197. (b) Vaska, L. *Science* **1963**, *140*, 809–810. (c) Baumgarth, H.; Braun, T.; Braun, B.; Laubenstein, R.; Herrmann, R. *Eur. J. Inorg. Chem.* **2015**, 3157–3168. (c) Ibers, J. A.; La Placa,

S. J. *Science* **1964**, *145*, 920-921. (d) Lebel, H.; Ladjel, C.; Bélanger-Gariépy, F.; Schaper, F. *J. Organomet. Chem.* **2008**, *693*, 2645–2648.

[19] Bailey, W. D.; Parkes, M. V.; Kemp, R. A.; Goldberg, K. I. Reactions of Square Planar d^8 Pincer Complexes with Oxygen and Hydrogen. In *Pincer and Pincer-Type Complexes: Application in Organic Synthesis and Catalysis*; Szabo, K. J., Wendt, O. F., Eds.; Wiley-VCH: Weinheim, Germany, 2014; pp 281−298.

[20] Zeng, H.; Miller, R. S.; Flowers, R. A., II; Gong, B. *J. Am. Chem. Soc.* **2000**, *122*, 2635-2644.

[21] Gessen, J. P.; Jacquesy, J. C.; Jouannetaud, M. P. *J. Chem. Soc., Chem. Commun.* **1980**, 1128-1129.

[22] (a) Mazzini, F.; Salvadori, P. *Synthesis* **2005**, 2479–2481. (b) Underwood, H. W., Jr.; Baril, O. L. *J. Am. Chem. Soc.* **1930**, *52*, 395–397. (c) Underwood, H. W., Jr.; Baril, O. L. *J. Am. Chem. Soc.* **1931**, 53, 2200-2202. (d) Černý, M.; Málek, J. *Tetrahedron Lett.* **1969**, *10*, 1739-1742.

[23] Kuklin, S. A.; Sheloumov, A. M.; Dolgushin, F. M.; Ezernitskaya, M. G.; Peregudov, A. S.; Petrovskii, P. V.; Koridze, A. A.; August, R. V. *Organometallics* **2006**, *25*, 5466-5476.

[24] Leyssens, T.; Peeters, D.; Orpen, A. G.; Harvey, J. N. *Organometallics* **2007**, *26*, 2637-2645.

[25] Mantina, M.; Valero, R.; Cramer, C. J.; Truhlar, D. G. *Atomic Radii of the Elements*; CRC Press: Boca Raton, FL, 2014.

[26] (a) Bedford, R. B.; Chang, Y.-N.; Haddow, M. F.; McMullin, C. L. *Dalton Trans.* **2011**, *40*, 9034-9041. (b) Vabre, B.; Lambert, M. L.; Petit, A.; Ess, D. H.; Zargarian, D. *Organometallics* **2012**, *31*, 6041-6053.

[27] de Geest, D. J.; O'Keefe, B. J.; Steel, P. J. *J. Organomet. Chem.* **1999**, *579*, 97-105.

[28] Adams, J. J.; Lau, A.; Arulsamy, N.; Roddick, D. M. *Organometallics* **2011**, *30*, 689-696.

[29] Timpa, S. D.; Zhou, J.; Bhuvanesh, N.; Ozerov, O. V. *Organometallics* **2014**, *33*, 6210-6217.

[30] (a) Vaska, L. *J. Am. Chem. Soc.* **1966**, *88*, 5325–5327. (b) Collman, J. P. *Acc. Chem. Res.* **1968**, *1*, 136–143. (c) Blum, O.; Milstein, D. *J. Am. Chem. Soc.* **2002**, *124*, 11456–11467.

[31] Hartley, F. R. *Chem. Soc. Rev.* **1973**, *2*, 163-179.

[32] Blake, D. M.; Kubota, M. *Inorg. Chem.* **1970**, *9*, 989-991.

[33] Rybtchinski, B.; Ben-David, Y.; Milstein, D. *Organometallics* **1997**, *16*, 3786-3793.

[34] Other examples of *cis*- and *trans*-dihydride complexes: (a) Kloek, S. M.; Heinekey, D. M.; Goldberg, K. I. *Organometallics* **2006**, *25*, 3007-3011. (b) Iron, M. A.; Ben-Ari, E.; Cohen, R.; Milstein, D. *Dalton Trans.* **2009**, 9433-9439.

[35] Bhagan, S.; Wayland, B. B. *Inorg. Chem.* **2011**, *50*, 11011-11020.

[36] Chianese, A. R.; Shaner, S. E.; Tendler, J. A.; Pudalov, D. M.; Shopov, D. Y.; Kim, D.; Rogers, S. L.; Mo, A. *Organometallics* **2012**, *31*, 7359-7367.

[37] (a) Lide, D. R. *Structure of Free Molecules in the Gas Phase*; CRC Press: Boca Raton, FL, 2014. (b) Hocking, R. K.; Hambley, T. W. *Organometallics* **2007**, *26*, 2815-2823.

[38] (a) Montag, M.; Efremenko, I.; Cohen, R.; Shimon, L. J. W.; Leitus, G.; Diskin-Posner, Y.; Ben-David, Y.; Salem, H.; Martin, J. M. L.; Milstein, D. *Chem. Eur. J.* **2010**, *16*, 328-353. (b) Montag, M.; Schwartsburd, L.; Cohen, R.; Leitus, G.; Ben-David, Y.; Martin, J. M. L.; Milstein, D. *Angew. Chem. Int. Ed.* **2007**, *46*, 1901-1904.

[39] Cherry, S. D. T.; Kaminsky, W.; Heinekey, D. M. *Organometallics* **2016**, *35*, 2165-2169.

[40] Simões, J. A. M.; Beauchamp, J. L. *Chem. Rev.* **1990**, *90*, 629-688.

[41] Fulmer, G. R.; Miller, A. J. M.; Sherden, N. H.; Gottlieb, H. E.; Nudelman, A.; Stoltz, B. M.; Bercaw, J. E.; Goldberg, K. I. *Organometallics* **2010**, *29*, 2176-2179.

[42] Roberto, D.; Cariati, E.; Psaro, R.; Ugo, R. *Organometallics* **1994**, *13*, 4227-4231.

Chapter 3

Hydrogen Addition to (pincer)Ir^{I}(CO) Complexes

The following has been previously published.[1]

Contributions to this project were made by Sophia D. T. Cherry and Louise M. Guard.

3.1 Introduction

Hydrogen addition to transition metal complexes is a fundamental step in many homogeneous catalytic transformations.[2] Early studies with Vaska's complex, and variations thereof, found that oxidative addition of H_2 to *trans*-Ir(Cl)(CO)$(PR_3)_2$ (where R = alkyl or aryl) resulted in almost exclusively *cis*-dihydride products.[3] Subsequent mechanistic studies led to a proposed pathway where H_2 adds to the metal via a side-on bound σ-complex, followed by concerted *cis* oxidative addition (see eq 3.01 for R = Ph).[4] While this mechanism has been accepted for *cis* addition of hydrogen, there have been fewer studies examining the formation of less common *trans*-dihydride complexes.[5,6] It is expected that a *trans*-dihydride would not be as stable as the *cis* analogue since hydride ligands have a very strong *trans* influence.[7]

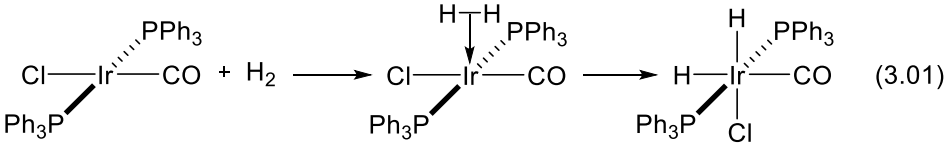

(3.01)

Direct syntheses of Ir trans-dihydride complexes have been shown to proceed through different pathways: metal ligand cooperativity,[8] *cis* oxidative addition of hydrogen followed by isomerization,[9] and proton-catalyzed hydrogen addition.[10] Milstein reported an unusual isomerization reaction where oxidative addition of H_2 to $^{(iPr)4}$(PCP)Ir(CO) [PCP = κ^3-C_6H_3-2,6-$(CH_2P(^iPr)_2)_2$] first resulted in a *cis*-dihydride adduct that upon heating isomerized to a more

thermodynamically stable *trans*-dihydride (eq 3.02).[9] It was proposed that a combination of both steric and electronic factors resulted in the stability of the *trans* species; a carbonyl *cis* to the aryl group is sterically disfavored and a hydride *trans* to the aryl is more destabilizing than a carbonyl.

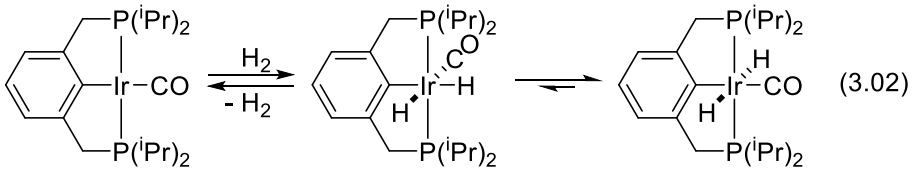

(3.02)

Milstein 1997

Brookhart reported a proton-catalyzed hydrogen addition to $^{(tBu)4}$(PONOP)Ir(CH_3) [PONOP = κ^3-C_5H_3N-2,6-($OP(^tBu)_2)_2$] to give a *trans*-dihydride complex (eq 3.03).[10,11] It was proposed that an acid-catalyzed pathway would result in an intermediate dihydrogen-hydride complex (observed by NMR spectroscopy at low temperature) that could then be deprotonated by the conjugate base in solution to give the *trans*-dihydride product. The proton-catalyzed reaction pathway to the dihydride product is distinct from the *cis* oxidative addition pathway, which is not observed in the Brookhart system.

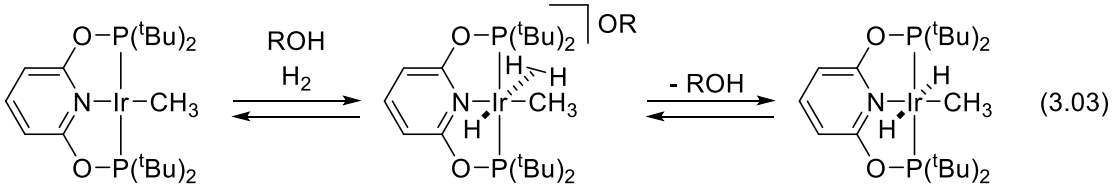

(3.03)

Brookhart 2010

When the isomerization of *cis*- to *trans*-dihydrides in (PCP)Ir(CO) complexes was studied computationally by Hall and coworkers, steric effects were not considered; the phosphine arms were truncated to $–PH_2$.[12] However, we have found that subtle changes in the substituent at phosphorus for (POCOP)Ir(CO) [POCOP = κ^3-C_6H_3-2,6-($OPR_2)_2$ for R = ^{t}Bu, ^{i}Pr, or OMe] complexes can have a profound effect on the chemistry at the metal center; bulky ^{t}Bu substituted

phosphinites favor Ir(I) carbonyl species while less bulky ^{i}Pr and OMe often afford Ir(III) carbonyl complexes under comparable metalation conditions.[13]

We describe how a small change in the R substituent on the phosphine can affect the mechanism of hydrogen addition to (POCOP)- and (PCP)-supported Ir(CO) complexes. While square planar Ir(I) complexes are often able to oxidatively add hydrogen (*vide supra*), we find that ligand steric factors can prevent concerted oxidative addition to Ir for both $^{(tBu)4}$(POCOP)Ir(CO) and $^{(tBu)4}$(PCP)Ir(CO) systems. Previously, we reported that hydrogen addition to $^{(tBu)4}$(POCOP)Ir(CO) proceeds via a proton-catalyzed pathway to give exclusively the *trans*-dihydride adduct which was proposed to be in equilibrium with the Ir(I) carbonyl complex.[14] Here, we have direct evidence of this equilibrium reaction provided by NMR spectroscopy. Goldman previously reported the inability of $^{(tBu)4}$(PCP)Ir(CO) to add hydrogen.[15] We show here that addition of a proton source facilitates hydrogen addition to $^{(tBu)4}$(PCP)Ir(CO).

Previously, Milstein examined $^{(iPr)4}$(PCP)Ir(CO) for oxidative addition of H_2. Here, we have examined hydrogen addition to $^{(iPr)4}$(POCOP)Ir(CO) which proceeds in a similar fashion as the Milstein system; however, hydrogen addition to the $^{(iPr)4}$(POCOP) system requires more forcing conditions. We have been able to determine the thermodynamic parameters for the $^{(iPr)4}$(POCOP)Ir(CO) *cis*/*trans*-dihydride equilibrium. Notably, for $^{(iPr)4}$(POCOP)Ir(CO), hydrogen addition can proceed via a proton-catalyzed pathway or through the concerted oxidative addition mechanism. In line with these results are our observations of hydrogen addition to $^{(iPr)4}$(PCP)Ir(CO), which is found to follow a proton-catalyzed mechanism as well. Previous reports by Milstein only probed the concerted oxidative addition pathway.[9]

3.2 Results

3.2.1 Attempted Observation of cis-$^{(tBu)4}$(POCOP)Ir(CO)(H)$_2$

The observations reported here are made possible by the use of thick-walled NMR tubes and a system for pressurization with hydrogen. Reaction of $^{(tBu)4}$(POCOP)Ir(CO) (**1**) with 8 atm hydrogen in C_6D_6 or THF-d_8 did not result in concerted oxidative addition of hydrogen at room temperature to give *cis*-$^{(tBu)4}$(POCOP)Ir(CO)(H)$_2$. To probe for formation of *cis*-$^{(tBu)4}$(POCOP)Ir(CO)(H)$_2$ at low temperatures, 1 atm CO was added to $^{(tBu)4}$(POCOP)Ir(H)$_2$ (**2**) at -78 °C in toluene-d_8 and inserted to an NMR probe cooled to -63 °C (eq 3.04). The ^{1}H NMR spectrum showed a new broad singlet hydride resonance at -8.32 ppm and a downfield singlet resonance at 9.39 ppm. In the ^{31}P NMR spectrum, new resonances appeared at 183.4 (17.1%), 180.8 (1.8%), and 164.6 ppm (5.2%); unreacted **2** (205.2 ppm, 12.2%) and complex **1** (199.0 ppm, 63.7%) were also present. Upon warming to 0 °C, the new hydride resonance in the ^{1}H NMR spectrum is still present (-8.36 ppm) and the downfield resonance at 9.39 ppm has shifted to 8.36 ppm. At 0 °C, by ^{31}P NMR spectroscopy, the only peaks detected are at 205.0 (11%), 199.0 (75%), and 183.7 (14%). At room temperature, only a mixture of **2** and **1** was observed, which, upon shaking the tube to ensure adequate CO mixing, fully converted to only complex **1**. Based on these low temperature spectra and comparison to previous iridium formyl complexes, the new major species with hydride resonance at -8.36 ppm and ^{31}P NMR shift at ~184 ppm is hypothesized to be an iridium-hydrido-formyl carbonyl complex $^{(tBu)4}$(POCOP)Ir(CHO)(H)(CO) (**3**). Based on the previously reported complex [$^{(tBu)4}$(POCOP)Ir(CO)$_2$(H)]BF$_4$ with hydride resonance -10.49 ppm (CD_2Cl_2),[13] we propose complex **3** has an iridium-hydride *trans* to CO rather than an open site; a five-coordinate iridium-hydride would be shifted to higher field. It is possible the observed downfield resonance at ~9 ppm at low temperatures is formaldehyde resulting from reductive

elimination from **3**. Further experiments are required to verify this proposal. Specifically, the low temperature CO addition experiment should be attempted with ^{13}CO, which will possibly result in detectable ^{13}C-formaldehyde by ^{13}C NMR spectroscopy.

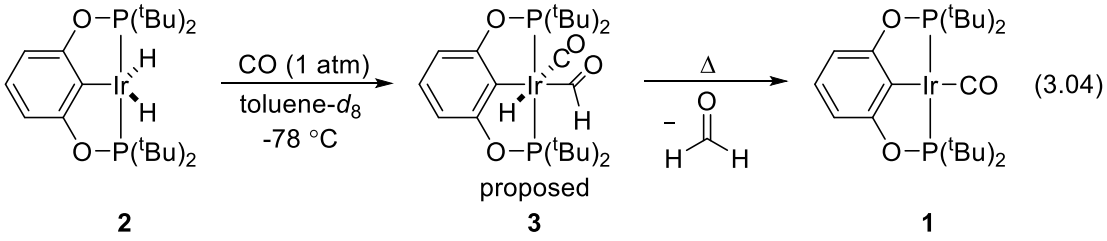

*3.2.2 Hydrogen Addition to $^{(tBu)4}$(POCOP)Ir(CO) (**1**)*

We previously reported the proton-catalyzed addition of hydrogen to $^{(tBu)4}$(POCOP)Ir(CO) (**1**) in a stainless-steel autoclave under high pressures of hydrogen (110 bar = 109 atm) to give *trans*-$^{(tBu)4}$(POCOP)Ir(CO)$(H)_2$ (**4**) in 80% yield. In the absence of catalytic acid, hydrogen addition was not observed. Compound **4** was proposed to be in equilibrium with **1**, since a mixture of **4** and **1** was always obtained.[16] Consistent with previous observations, addition of catalytic acid (0.6 equiv. pyridinium tetrafluoroborate, $[Hpyr]BF_4$) to complex **1** under 8 atm hydrogen in THF-d_8 at room temperature did result in partial conversion to **4** over the course of ~1 week (14% by ^{31}P NMR spectroscopy, eq 3.05).[17]

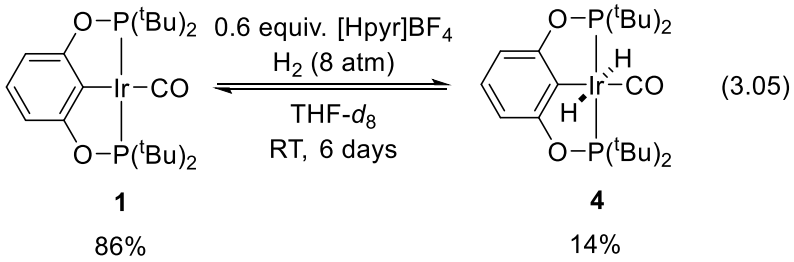

When the reaction was heated at 100 °C overnight, the concentration of **4** decreased from 14% to 2% with a concomitant increase in the concentration of **1**, as observed by ^{31}P NMR spectroscopy. When the reaction was returned to room temperature for a further 3 days, conversion back to **4** was observed (14% conversion). Removal of the hydrogen atmosphere, without quenching the acid in solution, led to hydrogen evolution from the remaining **4** in solution and complete conversion back to **1** over the course of 6 days. The known five-coordinate hydrido species, [$^{(tBu)4}$(POCOP)Ir(CO)(H)]BF_4 (Figure 3.01, **5-BF$_4$**),[13] was never observed by NMR spectroscopy.

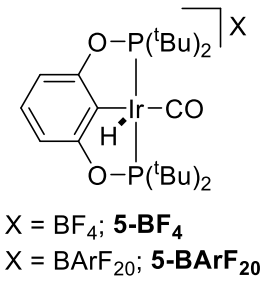

Figure 3.01. [$^{(tBu)4}$(POCOP)Ir(CO)(H)]X, where X = BF_4 or $BArF_{20}$

When monitored by ^{31}P NMR spectroscopy, the proton-catalyzed hydrogen addition to **1** did not reveal any intermediate protonated species. We were curious if **5-BF$_4$** would catalyze hydrogen addition to **1**.[13] When **1** was combined with 0.7 equiv. of crystalline **5-BF$_4$** under 8 atm H_2 in CD_2Cl_2,[18] **4** was observed (eq 3.06). No reaction occurred when **5-BArF$_{20}$**[19] was pressurized with 8 atm H_2 in CD_2Cl_2 in the absence of **1** or base over the course of 1 week.

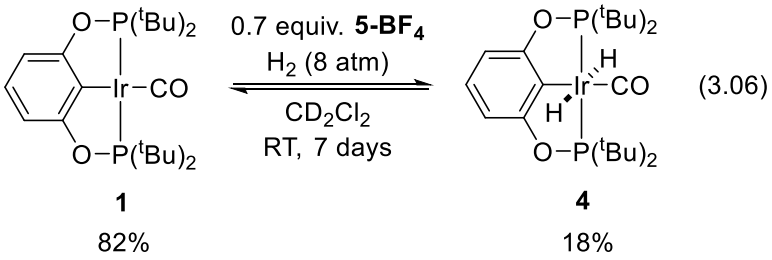

(3.06)

*3.2.3 Formation of cis-$^{(iPr)4}$(POCOP)Ir(CO)(H)$_2$ (**cis-7**)*

Since concerted oxidative addition of H_2 to **1** was not observed, we explored a less sterically encumbered complex, $^{(iPr)4}$(POCOP)Ir(CO) (**6**). Pressurizing a C_6D_6 solution of **6** with 8 atm H_2 results in formation of the *cis*-dihydride Ir(III) complex *cis*-$^{(iPr)4}$(POCOP)Ir(CO)(H)$_2$ (***cis*-7**, eq 3.07). By ^{31}P NMR spectroscopy, 90% conversion to ***cis*-7** was observed after 18 h. Compound ***cis*-7** exhibits a singlet resonance in the $^{31}P\{^1H\}$ NMR spectrum at 167.7 ppm. In the ^{1}H NMR spectrum, two triplet hydride resonances are observed at -10.30 ($^2J_{PH}$ = 9.3 Hz) and -11.16 ($^2J_{PH}$ = 18.4 Hz) ppm, consistent with an Ir complex where the hydrides are *cis* to each other. Removing the hydrogen atmosphere from a sample of ***cis*-7** results in quantitative conversion back to **6**.

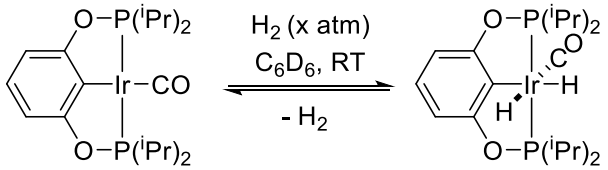

(3.07)

6 ***cis*-7**

10%	x = 8	90%
55%	x = 1	45%

*3.2.4 Isomerization from cis- to trans-$^{(iPr)4}$(POCOP)Ir(CO)(H)$_2$ (**cis-7** to **trans-7**)*

Heating a sample containing 90% ***cis*-7** under 8 atm H_2 at 100 °C in C_6D_6 for 3.5 days results in isomerization to the *trans*-dihydride complex *trans*-$^{(iPr)4}$(POCOP)Ir(CO)(H)$_2$ (***trans*-7**) as observed by ^{31}P NMR spectroscopy (95% ***trans*-7**, 5% ***cis*-7**, Scheme 3.01). All **6** was consumed at 100 °C under H_2 pressure to give dihydride products. A new singlet resonance is observed in the $^{31}P\{^1H\}$ NMR spectrum at 173.2 ppm for ***trans*-7**. In the ^{1}H NMR spectrum, one triplet hydride

resonance is observed at -10.02 ppm ($^2J_{PH}$ = 16.5 Hz) assignable to two equivalent Ir hydrides arising from a complex with approximate C_{2v} symmetry.

The isomerization was also carried out in THF to examine solvent effects on the hydrogen addition to **6**. A high-pressure NMR tube containing a solution of **6** in THF-d_8 was pressurized with 8 atm H_2, which after 2 days resulted in 87% ***cis*-7**, 10% **6**, and ~1.5% each of ***trans*-7** and an unidentified species (165.5 ppm) by ^{31}P NMR spectroscopy. The product ratios did not change after an additional 6 days at room temperature. When the reaction mixture was heated at 100 °C under 8 atm H_2 for 3.5 days, **6** was completely consumed and the only species in solution were ***trans*-7** and ***cis*-7**, 97% and 3%, respectively.

*3.2.5 Independent Synthesis of trans-$^{(iPr)4}$(POCOP)Ir(CO)(H)$_2$ (**trans-7**)*

Current interest in formic acid dehydrogenation with Ir complexes suggested reaction of **6** with formic acid could give ***trans*-7**.[20] Treatment of an acetone-d_6 solution of **6** with 60 equiv. formic acid resulted in two new products in a 1:1 ratio by NMR spectroscopy after 30 min at room temperature (eq 3.08). The ^{1}H NMR spectrum showed two hydride resonances, a triplet at -10.48 ppm ($^2J_{PH}$ = 16.5 Hz) consistent with ***trans*-7**, and a triplet of doublets at -21.63 ppm (triplet, $^2J_{PH}$ = 13.8 Hz; doublet, $^4J_{HH}$ = 3.8 Hz) consistent with an iridium hydrido-formate carbonyl complex $^{(iPr)4}$(POCOP)Ir(CO)(H)(κ^1-OC(O)H) (**8**). The triplet of doublet peak structure for the iridium-hydride likely arises from coupling to the two phosphorus atoms to give a triplet and additional coupling to the formato proton, giving a doublet. Hydrogen was also observed in the ^{1}H NMR spectrum, suggesting there was dehydrogenation of formic acid. By ^{31}P NMR spectroscopy, ***trans*-7** was observed as a singlet at 175.0 ppm and complex **8** as a singlet at 168.3 ppm; no trace of **6**

was detected. Heating the reaction under reduced pressure at 60 °C for 18 h resulted in loss of the hydride resonance at -21.63 ppm and only ***trans*-7** (94%) and ***cis*-7** (6%) were observed by ^{1}H NMR spectroscopy.[21] Since no dicarbonyl complexes were detected, and only hydrogen addition products formed at the end of the reaction, it is hypothesized that the only byproduct is CO_2, however we did not verify formation of CO_2.

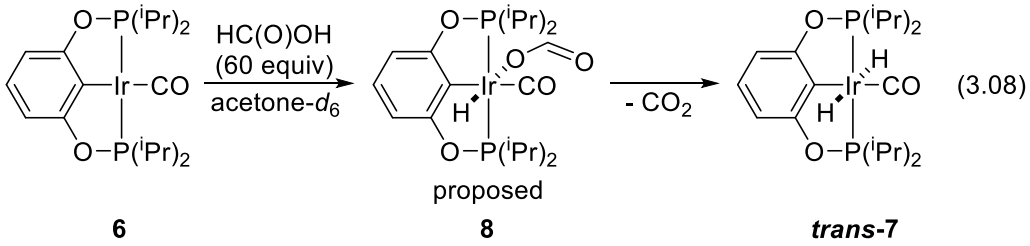

6 **8** ***trans*-7** (3.08)

As both the isomerization reaction from ***cis*-7** to ***trans*-7** and the reaction of **6** with formic acid were not quantitative, ***trans*-7** was independently synthesized and characterized via an alternative route. Reaction of the previously reported hydrido chloride Ir(III) carbonyl complex $^{(iPr)4}$(POCOP)Ir(CO)(H)(Cl) (**9**),[13] with 50 equiv. $NaBH_4$ in a 1:1 mixture of MeCN/EtOH at room temperature resulted in analytically pure ***trans*-7** as a colorless, air-stable powder.[22] Crystals suitable for X-ray diffraction were grown by slow evaporation of a saturated CH_2Cl_2 solution (Figure 3.02). The reaction of ***trans*-7** with excess HCl/Et_2O results in reformation of **9**.

Scheme 3.01. Synthetic routes to *cis*- and *trans*-dihydride complexes

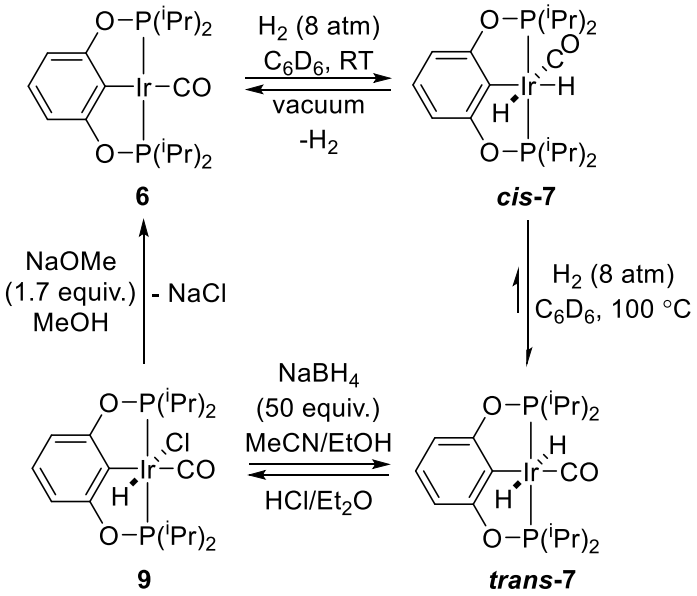

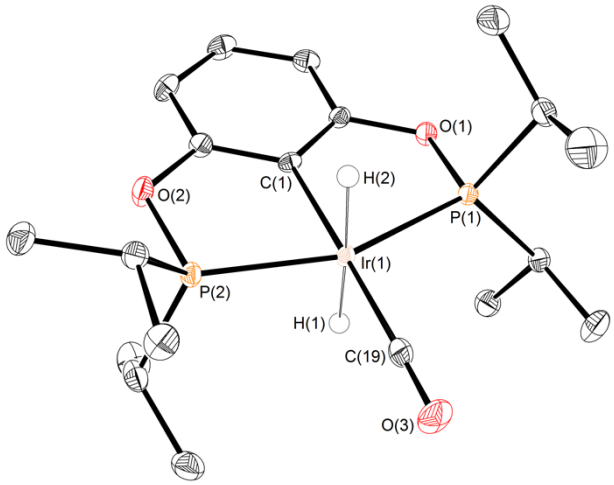

Figure 3.02. ORTEP[23] of ***trans*-7** shown with thermal ellipsoids at 50% probability. Hydrogen atoms, except for the Ir-bound hydrides, are omitted for clarity. Selected bond lengths (Å) and angles (°) for *trans*-$^{(iPr)4}$(POCOP)Ir(CO)(H)$_2$ (***trans*-7**): Ir(1)-C(1) 2.0614(16), Ir(1)-P(1) 2.2894(4), Ir(1)-P(2) 2.2815(4), Ir(1)-C(19) 1.8945(18), C(19)-O(3) 1.145(2); C(19)-Ir(1)-C(1) 178.80(7), C(1)-Ir(1)-P(1) 78.52(5), C(1)-Ir(1)-P(2) 78.66(5), P(1)-Ir(1)-P(2) 157.14(2).

3.2.6 Equilibrium Studies for cis- to trans-Dihydride Isomerization

As the reaction of **6** with hydrogen at 8 atm did not yield complete conversion to ***trans*-7** (95%), we suspected that the *cis* and *trans* isomers were in equilibrium. Pure ***trans*-7** complex was heated at 100 °C under 8 atm H_2 for 18 h in C_6D_6 which led to 3% conversion to ***cis*-7**. No appreciable change in the ratio of products was observed after heating at 100 °C for an additional 24 h. Heating ***trans*-7** requires H_2 pressure to maintain ***cis*-7** in solution, otherwise **6** is formed. The dependence of the equilibrium on the temperature (100 – 130 °C) was monitored and a van't Hoff plot was generated (Figure 3.03). At higher temperatures, some formation of **6** was observed, suggesting an additional equilibrium between ***cis*-7** and **6**. For the isomerization of ***cis*-7** to ***trans*-7**, $\Delta H = -14 \pm 1$ kcal mol^{-1} and $\Delta S = -31 \pm 3$ cal mol^{-1} K^{-1}. Assuming no change in the equilibrium mixture takes place upon cooling the reaction to room temperature (NMR spectra were recorded at 298 K), we find that for the *cis* to *trans* isomerization, $\Delta G_{373} = -2.5 \pm 0.1$ kcal mol^{-1}. Duplicate studies were also performed in mesitylene to eliminate any effect of heating benzene significantly above its boiling point, and within error, the ΔH and ΔS values were the same as in C_6D_6.

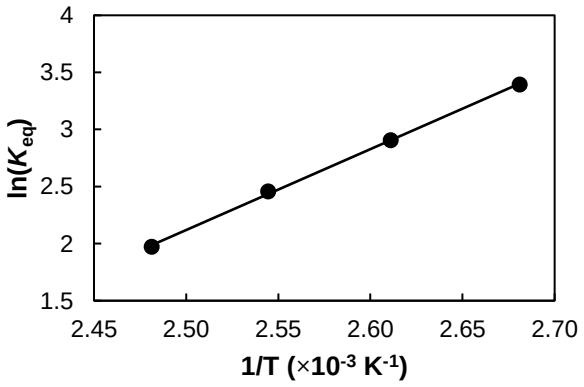

Figure 3.03. van't Hoff plot for equilibrium between ***cis*-7** and ***trans*-7** in C_6D_6 under 8 atm H_2.

The temperature and H_2 pressure dependence was examined for the isomerization of ***cis*-7**/***trans*-7** in mesitylene. As shown in Table 3.01, heating a solution of pure ***trans*-7** under 8 atm at 140 °C led to partial formation of **6**, as well as more ***cis*-7** than the analogous reaction at 100 °C. When examining the pressure dependence on the isomerization, generally, when lower H_2 pressures were used (4 atm) more ***cis*-7** was observed. Increasing the temperature under low pressure led to more ***cis*-7** and a significant increase in **6**. To probe if adventitious protons in solution were the cause for formal loss of hydrogen at higher temperatures (in the form of more **6** at 140 °C), analogous reactions were run in the presence of the proton scavenger 2% cross-linked poly(4-vinylpyridine) (PVP).[24] Under 8 atm at 140 °C in mesitylene with PVP, the relative ratios of the iridium species were identical to those in the absence of PVP.

Table 3.01. Temperature and H_2 Pressure Dependence of *cis*-7/*trans*-7 Isomerization[a]

Temp.	H_2 (atm)	**6**	***cis*-7**	***trans*-7**
100 °C	4	0%	5%	95%
	8	0%	3%	97%
140 °C	4	5%	16%	79%
	8	1%	14%	85%

[a]Initial Reaction conditions: 0.02 mmol ***trans*-7**, H_2 (4 or 8 atm), 0.15 mL mesitylene, 5 mm thick-walled NMR tube. Relative ratios were determined by integrating ^{31}P NMR resonances; the only quantifiable peaks present were those for **6**, ***cis*-7**, and ***trans*-7**.

*3.2.7 Proton-Catalyzed Hydrogen Addition to $^{(iPr)4}$(POCOP)Ir(CO) (**6**)*

When ***cis*-7** was generated in THF-d_8, partial formation of ***trans*-7** was observed after 8 days at room temperature (~2%). To probe for a possible proton-catalyzed pathway to yield ***trans*-**

7, **6** was combined with 0.5 equiv. 2,6-lutidinium tetrafluoroborate ([Hlut]BF_4) in THF-d_8 under 8 atm H_2 resulting in a pale yellow solution (eq 3.09). After 2 days at room temperature, full consumption of **6** was observed to give solely ***trans*-7** by ^{31}P NMR spectroscopy. No intermediate protonated Ir species from reaction of **6** with [Hlut]BF_4 was observed.

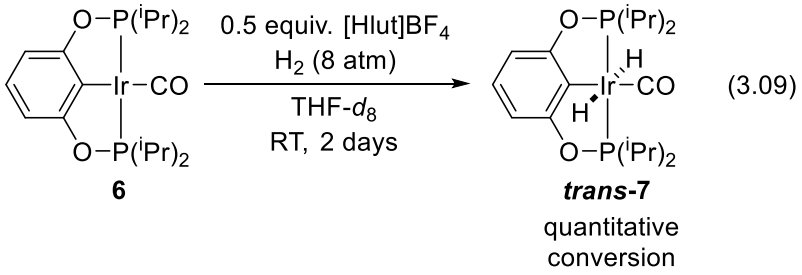

(3.09)

To trap an intermediate Ir-hydride complex in the proton-catalyzed H_2 addition to **6**, complex **6** was combined with the sterically less encumbered acid [Hpyr]BF_4 (0.4 equiv.) in THF-d_8 under 8 atm H_2 pressure yielding a pale yellow solution with some solid ([Hpyr]BF_4 is sparingly soluble in THF). After 30 min, four species were present in solution by ^{31}P NMR spectroscopy. They are assigned as **6** (3.5%), ***trans*-7** (31%), ***cis*-7** (47.5%), and [$^{(iPr)4}$(POCOP)Ir(CO)(H)(pyr)]BF_4 (**10-BF_4**, 18%). Upon standing at room temperature for 15 h (eq 3.10), the solution became colorless and by ^{31}P NMR spectroscopy only ***trans*-7** (87%) and **10-BF_4** (13%) were present. The ^{1}H NMR spectrum shows the triplet hydride signal for **10-BF_4** at -19.42 ppm ($^2J_{PH}$ = 13.3 Hz). No ***cis*-7** or starting material (**6**) were observable.

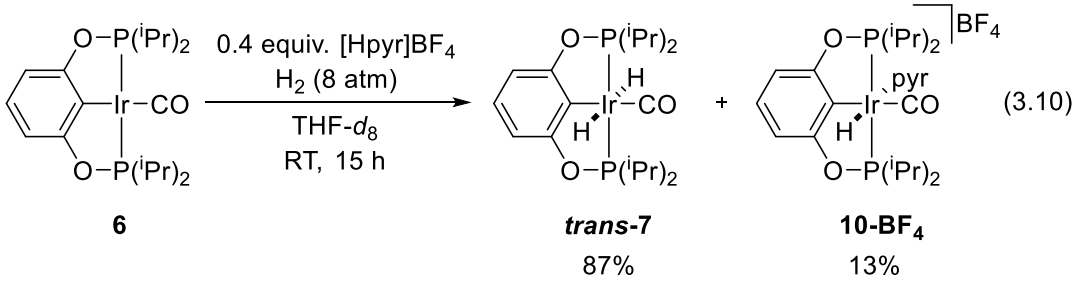

(3.10)

The product ratio did not change after an additional 24 h at room temperature; however, when the reaction was heated at 100 °C for 21 h, the ratio of products was 91% ***trans*-7** to 9% **10-BF$_4$**. No ***cis*-7** was observed following heating. When the reaction mixture was examined 3 days following heating, ~96% ***trans*-7** was observed. Proton-catalyzed hydrogen addition to **6** with [Hpyr]BF$_4$ also proceeded under 1 atm H_2, though it required 9 days for complete consumption of **6** at room temperature.

To eliminate any possible effects of [Hpyr]$^+$ insolubility in THF, complex **6** was combined with 0.5 equiv. [Hpyr]BArF$_{20}$ in THF-d_8 giving a homogeneous yellow solution. Two species are observed by ^{31}P NMR spectroscopy: complex **6** (45%) and [$^{(iPr)4}$(POCOP)Ir(CO)(H)(pyr)]BArF$_{20}$, (**10-BArF$_{20}$**, 55%). Upon addition of 8 atm H_2, the solution turned pale yellow. After 1 hour, four species are present by ^{31}P NMR spectroscopy. They are assigned as **6** (5.3%), ***trans*-7** (4.3%), ***cis*-7** (36%), **10-BArF$_{20}$** (54.4%). After 17 h, all **6** is consumed and only ***trans*-7** (47%) and **10-BArF$_{20}$** (53%) are observed. Upon mixing for 3 weeks, the ratio between the two species changes slightly to 52% ***trans*-7** and 48% **10-BArF$_{20}$**; the change in product ratios was not examined for longer than 3 weeks. When ***trans*-7** was reacted with one equivalent [Hpyr]BArF$_{20}$, in the absence of hydrogen pressure, hydrogen evolution to give **10-BArF$_{20}$** in quantitative conversion was observed.

Complex **10-BF$_4$** was independently synthesized by reaction of **6** with [Hpyr]BF$_4$ in a THF/CH_2Cl_2 mixture (eq 3.11). Isolation of pure **10-BArF$_{20}$** was difficult since oily products were always obtained. In the ^{1}H NMR spectrum of **10-BF$_4$,** a triplet hydride resonance was observed at -19.46 ppm ($^2J_{PH}$ = 13.5 Hz). In the aromatic region, three signals are observed for coordinated pyridine, one sharp triplet resonance at 8.04 ppm and two broad signals centered at 8.90 and 7.45 ppm. In the ^{13}C{^{1}H} NMR spectrum, two broad signals are also observed, centered at 158 and 151

ppm. The $^{31}P\{^{1}H\}$ NMR spectrum showed a singlet resonance at 164.5 ppm, in line with the observed ^{31}P shift in the proton-catalyzed hydrogen addition to **6**. Crystals of **10-BF$_4$** suitable for X-ray diffraction were grown by layering a saturated CH_2Cl_2 solution with pentane at -30 °C (Figure 3.04). Coordination of pyridine *trans* to the Ir bound hydride was unambiguously verified by the solid-state structure.

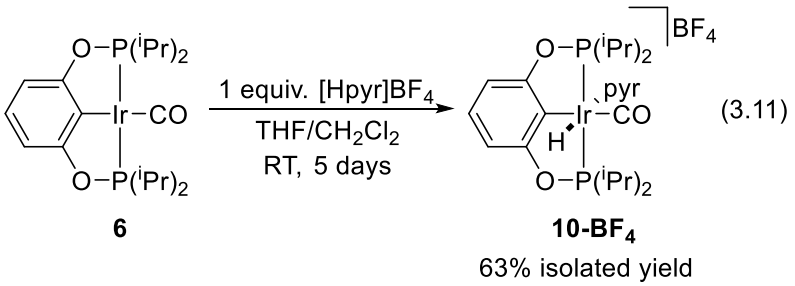

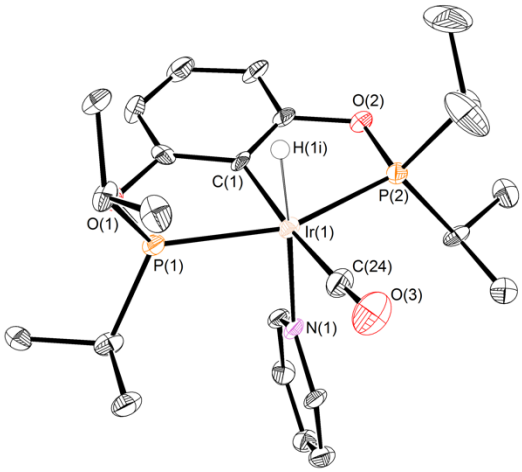

Figure 3.04. ORTEP[23] of **10-BF$_4$** shown with thermal ellipsoids at 50% probability. BF_4 anion and hydrogen atoms, except for the Ir-bound hydride, are omitted for clarity. Selected bond lengths (Å) and angles (°) for [$^{(iPr)4}$(POCOP)Ir(CO)(H)(pyr)]BF_4 (**10-BF$_4$**): Ir(1)-C(1) 2.040(8), Ir(1)-P(1) 2.319(2), Ir(1)-P(2) 2.320(2), Ir(1)-N(1) 2.236(6), Ir(1)-C(24) 1.927(8), C(24)-O(3) 1.142(9); C(24)-Ir(1)-N(1) 95.2(3), C(1)-Ir(1)-N(1) 93.3(3), N(1)-Ir(1)-P(1) 93.4(2), N(1)-Ir(1)-P(2) 92.6(2).

Complex **10-BF$_4$** can serve to catalyze hydrogen addition to **6**. Reaction of **6** with hydrogen (8 atm) in the presence of 0.4 equiv. **10-BF$_4$** led to complete consumption of **6** after 4 days (eq 3.12). The only species present by ^{31}P NMR spectroscopy after this time were ***trans*-7** (89%), **10-BF$_4$** (9%), and minor impurities (148.2 and 139.4 ppm). The rate of consumption of **6** using **10-BF$_4$** as the proton source was slower than when [Hpyr]BF$_4$ was used (15 h). When the hydrogen pressure was removed, only trace **6** (~2%) formed over the course of 6 days; hydrogen loss from ***trans*-7** catalyzed by **10-BF$_4$** is likely very slow. To probe this, we sought to observe pyridine displacement by hydrogen in **10-BF$_4$**. When **10-BF$_4$** was dissolved in THF-d_8 at room temperature, partial loss of [Hpyr]BF$_4$ to give **6** was observed after stirring overnight.[25]

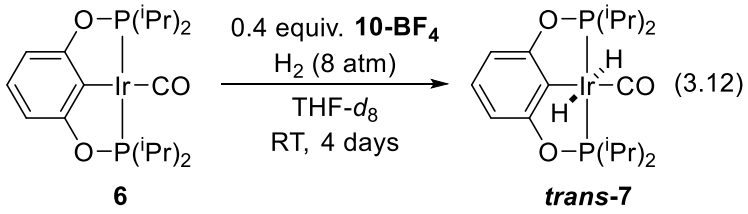

6 ***trans*-7** (3.12)

3.2.8 pK_a of [$^{(tBu)4}$(POCOP)Ir(CO)(H)]$^+$

Reaction of **5-BArF$_{20}$** with 1 equiv. *N*,*N*-dimethylaniline in CH_2Cl_2, resulted in partial deprotonation to give **1** (eq 3.13). Assuming the pK_a values in THF and CH_2Cl_2 are approximately the same (see the Discussion),[26] the pK_a of **5-BArF$_{20}$** was benchmarked based on *N*,*N*-dimethylanilinium (pK_a^{THF} = 4.9)[27] resulting in a pK_a^{CH2Cl2} of 4.0 ± 0.1 (see Experimental for pK_a calculation).

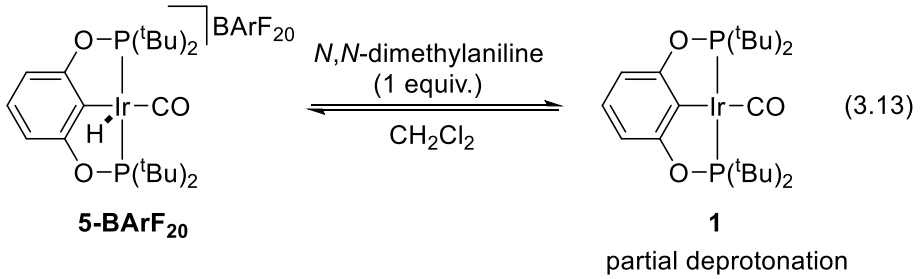

(3.13)

3.2.9 Attempted Observation of a Dihydrogen-Hydride Complex

An NMR tube containing ***trans*-7** and excess *p*-toluenesulfonic acid (*p*TsOH) and CD_2Cl_2 solvent was maintained at -196 °C until it was inserted into a pre-cooled NMR probe at -80 °C. Upon thawing the tube to -78 °C outside the spectrometer, rapid bubbling was observed, indicative of hydrogen evolution. A dihydrogen complex was not observed by ^1H NMR spectroscopy, but rather [$^{(iPr)4}$(POCOP)Ir(CO)(H)]OTs (**12**) (eq 3.14). This was verified by independently synthesizing **12** by direct addition of *p*TsOH to **6**.

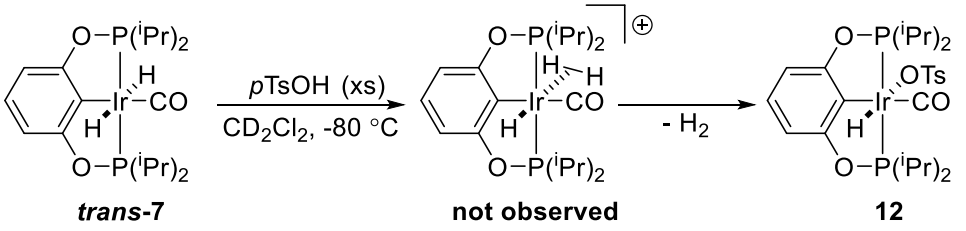

(3.14)

*3.2.10 Hydrogen Addition to $^{(tBu)4}$(PCP)Ir(CO) (**13**)*

The PCP analogue $^{(tBu)4}$(PCP)Ir(CO) (**13**) was prepared *via* a modified procedure from previous reports (see Experimental).[28] No reaction was observed when **13** was pressurized with 8 atm H_2 in C_6D_6 and mixed at either room or at elevated temperature (100 °C) for an extended

period of time. However, when THF-d_8 was used as the solvent, 7% of complex **13** was converted to *trans*-$^{(tBu)4}$(PCP)Ir(CO)(H)$_2$ (**14**) after 8 days at room temperature and **14** was observed in 41% yield after 4 days at 100 °C. A triplet hydride resonance at -9.74 ppm ($^2J_{PH}$ = 14 Hz) in the ^{1}H NMR spectrum is indicative of formation of a *trans*-dihydride Ir complex, where the two hydrides are chemically equivalent. The same reaction in the presence of 0.6 equiv. [Hpyr]BF_4 results in the immediate and quantitative formation of **14** at room temperature (eq 3.15), which differs from the $^{(tBu)4}$(POCOP) case where under analogous conditions only 14% conversion was noted over a period of days.

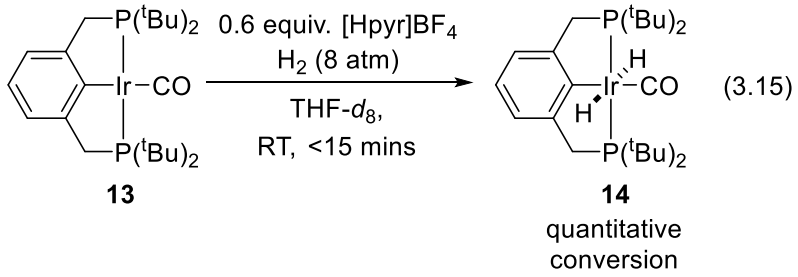

13 **14** quantitative conversion (3.15)

PCP hydrido-pyridine complex [$^{(tBu)4}$(PCP)Ir(CO)(H)(pyr)]BF_4 (**15**) was prepared via reaction of **13** with [Hpyr]BF_4 in CH_2Cl_2 (eq 3.16). The ^{1}H NMR spectrum of **15** displays a triplet resonance at −19.72 ppm ($^2J_{PH}$ = 14 Hz) which is characteristic of a hydride *trans* to a coordinated ligand. Additionally, five distinct proton shifts for the Ir-bound pyridine indicate that ligand rotation is hindered on the NMR timescale.

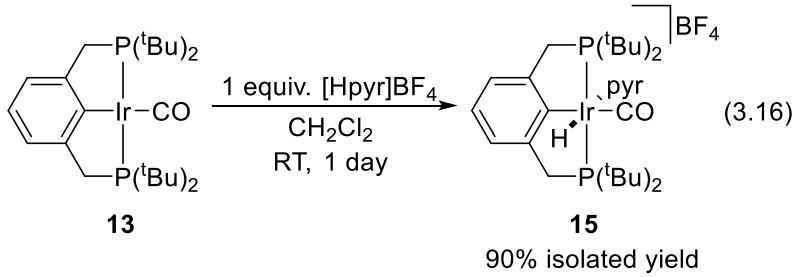

13 **15** 90% isolated yield (3.16)

When a solution of **15** in THF-d_8 was placed under 8 atm of H_2, complete conversion to **14** was noted by ^{1}H NMR spectroscopy, suggesting that **15** is competent for catalyzing H_2 addition to **13**. Perhaps more striking is the apparent displacement of pyridine by H_2, which must occur for this reaction to proceed. A crystal of **15** suitable for diffraction was obtained by crystallization from a ternary mixture of CH_2Cl_2, diethyl ether, and pentane at −30 °C (Figure 3.05).

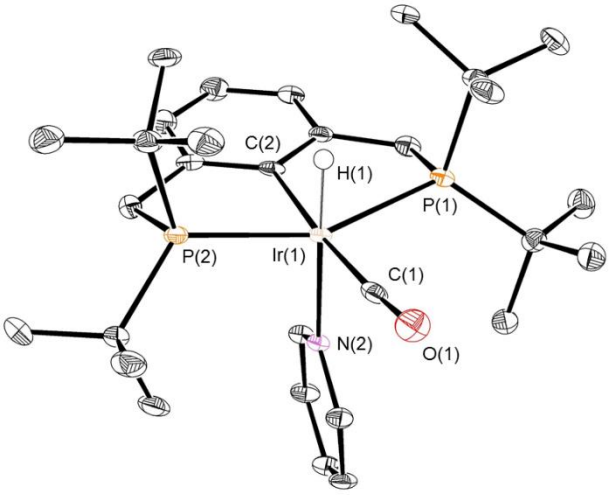

Figure 3.05. ORTEP[23] of **15** shown with thermal ellipsoids at 50% probability. BF_4 anion, solvent of crystallization (CH_2Cl_2) and hydrogen atoms, except for the Ir-bound hydride, are omitted for clarity. There were two molecules in the asymmetric unit, only fragment one is shown. Selected bond lengths (Å) and angles (°) for [$^{(tBu)4}$(PCP)Ir(CO)(H)(pyr)]BF_4 (**15**): Ir(1)-C(2) 2.103(4), Ir(1)-P(1) 2.363(1), Ir(1)-P(2) 2.365(1), Ir(1)-N(2) 2.234(3), Ir(1)-C(1) 1.918(4), C(1)-O(2) 1.138(5), P(1)-Ir(1)-P(2) 156.12(4), P(1)-Ir(1)-N(2) 97.57(8), P(2)-Ir(1)-N(2) 99.12(8), C(2)-Ir(1)-N(2) 88.7(1), C(1)-Ir(1)-N(2) 95.4(2).

Removal of the dihydrogen atmosphere from reactions between **13** and H_2 in the presence of an acid catalyst led to partial conversion back to **13**. The reaction of **13** with 0.4 equiv of [Hpyr]BF_4 under 1 atm of H_2 in THF-d_8 gave **13** (10%), **14** (82%), and **15** (8%), and this ratio did not change after a further 2 days at room temperature. The addition of Et_3N under a flow of H_2

quenched the acid species present allowing the sample to be placed under vacuum without loss of **14**.

*3.2.11 Proton-Catalyzed Hydrogen Addition to $^{(iPr)4}$(PCP)Ir(CO) (**16**)*

Milstein and co-workers have proposed that the reaction of $^{(iPr)4}$(PCP)Ir(CO) (**16**) with H_2 proceeds via concerted oxidative addition to form a *cis*-dihydride complex, which undergoes isomerization to form the *trans*-dihydride complex *trans*-$^{(iPr)4}$(PCP)Ir(CO)$(H)_2$ (**17**).[9] The reaction of **16** with 0.6 equiv. of [Hpyr]BF_4 in THF-d_8 and subsequent pressurization with 8 atm of H_2 resulted in an instantaneous reaction to form **17** and [$^{(iPr)4}$(PCP)Ir(CO)(H)(pyr)]BF_4 (**18**) (in 37 and 63% yield, respectively; eq 3.17). No change in this ratio was observed by ^{31}P NMR spectroscopy over a period of 2 days at room temperature, and no *cis*-dihydride complex was observed.

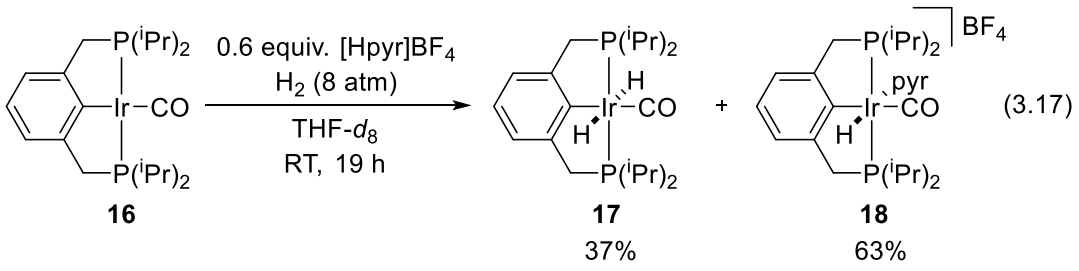

An authentic sample of **18** was prepared by the reaction of **16** with 1 equiv. of [Hpyr]BF_4 in CH_2Cl_2 at room temperature (eq 3.18). The ^{1}H NMR spectrum displays a peak at −19.15 ppm ($^2J_{PH}$ = 12 Hz), corresponding to an Ir-bound hydride trans to pyridine. In contrast to **15**, only three resonances are observed for the metal-bound pyridine.

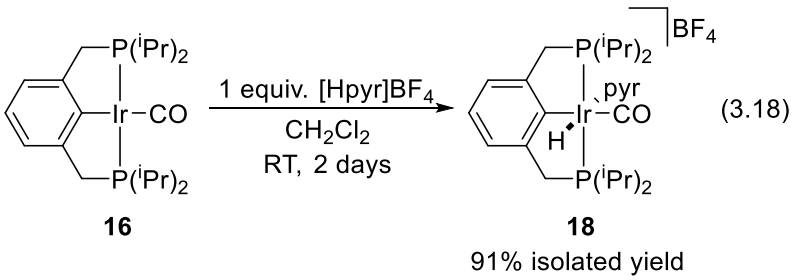

16 **18**

91% isolated yield

(3.18)

3.3 Discussion

Hydrogen addition to Ir(I) is governed by the steric and electronic environment at the metal center. Consistent with previous reports, *trans*-dihydride species are favored over *cis*-dihydride complexes for (pincer)Ir carbonyl complexes.[9,10] For bulky ^{t}Bu-substituted complexes, hydrogen addition proceeds via a proton-catalyzed pathway. When R = ^{i}Pr, hydrogen addition can proceed via concerted oxidative addition to give a *cis*-dihydride, which under hydrogen pressure can be thermally isomerized to a *trans*-dihydride. Additionally, for R = ^{i}Pr, hydrogen addition in the presence of added protons can result in proton-catalyzed hydrogen addition to give *trans*-dihydride complexes.

3.3.1 Concerted Oxidative Addition of H_2 to ^{R4}(POCOP)Ir(CO)

We previously reported the proton-catalyzed hydrogen addition to the Ir(I) carbonyl **1** to give the Ir(III) *trans*-dihydride **4**.[14] No hydride products were observed in the absence of added acid. Since these reactions were performed in stainless-steel autoclaves (*ca.* 109 atm of H_2), we were not able to carry out *in situ* monitoring for intermediates. We suspected that in the absence

of protons a *cis*-dihydride complex could form which when the reactor is vented to release the H_2 pressure likely loses hydrogen to re-form **1**.

When a sample of **1** was pressurized with 8 atm of H_2, hydrogen addition was not observed. We hypothesize that concerted oxidative addition is energetically unfavorable at a sterically congested metal center. When the synthesis of **1** was first reported, one synthetic pathway pursued was the reaction of five-coordinate dihydride complex $^{(tBu)4}$(POCOP)Ir(H)$_2$ (**2**) with CO. Assuming that **2** would react with CO in a manner similar to that of $^{(tBu)4}$(POCOP)Ir(H)(Cl),[13] a *cis*-dihydride carbonyl complex would be expected as an intermediate (eq 3.19); however, the low-temperature addition of CO to **2** did not give a *cis*-dihydride complex,[29] but rather spectra consistent with an iridium hydrido-formyl complex **3**.[30] This complex would result from coordination of CO to **2**, followed by migratory insertion of CO into the metal hydride. Under a CO atmosphere, CO would readily coordinate in the open sixth coordination site. As the reaction is warmed, reductive elimination of formaldehyde would result in formation of **1**. We have not verified formaldehyde formation, however the ^{1}H NMR spectra are consistent with this proposal. We conclude that the *cis*-dihydride complex must be unstable,[31] and formation of **3** is more favored. However, **3** presumably readily loses formaldehyde to give **1** due to steric effects.

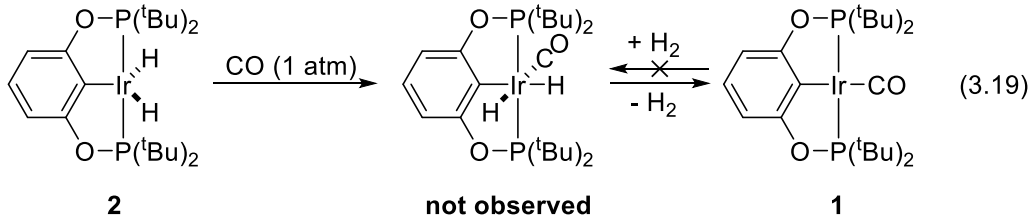

(3.19)

*3.3.2 Isomerization of cis- to trans-$^{(iPr)4}$(POCOP)Ir(CO)(H)$_2$ (**cis-7** to **trans-7**)*

Heating a sample of ***cis*-7** under hydrogen pressure resulted in formation of ***trans*-7**. The stability of the *trans* complex is unexpected because two strong *trans* influence ligands should destabilize each other. The thermodynamic data suggest an enthalpic driving force ($\Delta H = -14 \pm 1$ kcal mol^{-1}), which is required to overcome the significant negative entropy ($\Delta S = -31 \pm 3$ cal mol^{-1} K^{-1}) associated with the isomerization of ***cis*-7** to ***trans*-7**.

Measurement of the thermodynamic parameters for a *cis*-/*trans*-dihydride isomerization is rare, albeit not unprecedented.[32] Early work by Jesson, Muetterties, and Meakin examined the temperature dependence of the *cis*/*trans* equilibria for $H_2Fe(PC_6H_5(OCH_3)_2)_4$; the *cis* form was favored at high temperature.[33] The thermodynamic data for K_{eq} =[*cis*]/[*trans*] suggested that the *trans* isomer was enthalpically favored ($\Delta H = 3$ kcal mol^{-1}) while the *cis* isomer was entropically favored ($\Delta S = 11$ cal mol^{-1} K^{-1}). This trend is in line with what we observe for the $^{(iPr)4}$(POCOP) system; however, the magnitudes of our ΔH and ΔS values are significantly greater. Examination of the temperature and pressure dependence of the isomerization reaction in our system favored the *cis* isomer at high temperature and/or low H_2 pressure; complex 6 was also observed at low H_2 pressure. We do not currently have an explanation for these observations or for the large magnitudes of the ΔH and ΔS values, although there is precedent for enthalpy−entropy compensation, giving rise to modest ΔG values.[34]

3.3.3 Cationic Hydrido-Pyridine (pincer)Ir^{III} Complexes

In the process of studying proton-catalyzed hydrogen addition to ^{R4}(POCOP)Ir(CO), interesting hydrido-pyridine Ir(III) complexes were discovered.[35] For $^{(iPr)4}$(POCOP)Ir(III) species

10-BF$_4$, the coordination of pyridine in the solid state shows five distinct C−H environments; however, the NMR spectra indicate that pyridine is rotating rapidly on the NMR timescale. The chemical shift of the Ir−H signal in the ^{1}H NMR spectrum is diagnostic of pyridine coordination. Previously, we reported open site complex [$^{(iPr)4}$(POCOP)Ir(CO)(H)]BF$_4$ which had a triplet hydride resonance at −29.26 ppm, and **9** which had a triplet hydride signal at −18.49 ppm.[13] The downfield shift of **10-BF$_4$** relative to the open site complex is consistent with coordination of pyridine to the Ir center. Furthermore, the broad signals observed for **10-BF$_4$** in the aromatic region in the ^{1}H and ^{13}C{^{1}H} NMR spectra are consistent with rotation of pyridine in solution.

When reaction of $^{(tBu)4}$(POCOP)Ir(CO) (**1**) was attempted with [Hpyr]BArF$_{20}$ (see the Experimental Section), complete protonation to give [$^{(tBu)4}$(POCOP)Ir(CO)(H)(pyr)]BArF$_{20}$ (**11**) was observed. The NMR spectra of **11** are consistent with pyridine as a static moiety with five distinct C−H environments, in contrast to what is observed for the ^{i}Pr analogue, **10-BF$_4$**, where pyridine is rotating rapidly on the NMR time scale in solution. The difference in pyridine coordination to Ir for ^{t}Bu versus ^{i}Pr is presumably a steric issue, in line with our previous report on the steric environment of cationic (POCOP)Ir(III) complexes (Figure 3.06).[13] A similar difference in pyridine coordination for ^{t}Bu- versus ^{i}Pr-substituted complexes was also observed for [^{R4}(PCP)Ir(CO)(H)(pyr)]$^+$. The static binding of pyridine to ^{t}Bu-substituted (pincer)Ir(CO) complexes is in contrast to the previously reported [*cis*-$^{(tBu)4}$(PNP)Ir(H)$_2$(pyr)]BF$_4$ [PNP = κ^3-C$_5$H$_3$N-2,6-(CH$_2$P(^{t}Bu)$_2$)$_2$] where three broad NMR resonances for pyridine are observed, suggesting rotation in solution despite increased steric congestion at the metal center.[36]

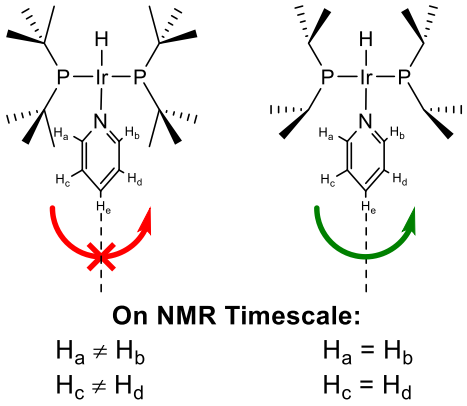

Figure 3.06. Coordination of pyridine in solution to ^{t}Bu (static) and ^{i}Pr (rotating) substituted [(pincer)Ir(CO)(H)(pyr)]$^{+}$ complexes (carbonyls and aryl backbones have been omitted for clarity).

3.3.4 pK_a Studies of [^{R4}(POCOP)Ir(CO)(H)]$^{+}$ Complexes

The pK_a studies described in this work were performed in CH_2Cl_2. Work by Morris, Leito, and others established useful pK_a scales in solvents such as acetonitrile, THF, and CH_2Cl_2.[37] In the course of our studies, **5-X** was observed to be highly soluble and stable in CH_2Cl_2 over a period of weeks, while THF was found to react with the metal complex giving polymeric products. Since other cationic acids have previously been shown to have similar pK_a values in THF and CH_2Cl_2,[38] we assume that the pK_a of **5-X** in CH_2Cl_2 would be roughly the same as that in THF.[39] Reaction of **5-BArF$_{20}$** with *N*,*N*-dimethylaniline in CH_2Cl_2 resulted in partial deprotonation to give **1** (see Appendix B for a discussion of solubility issues encountered during the pK_a studies). pK_a studies with [$^{(iPr)4}$(POCOP)Ir(CO)(H)]BF_4 were hampered by the facile coordination of solvent *trans* to the hydride due to the decreased steric profile at Ir. The pK_a^{CH2Cl2} of 4.0 for **5-BArF$_{20}$** indicates that this complex is slightly more acidic than *N*,*N*-dimethylanilinium and orders of magnitude more acidic than pyridinium [pK_a^{THF} = 5.5] and 2,6-lutidinium [pK_a^{THF} = 7.2].[27]

3.3.5 Proposed Mechanisms: Proton-Catalyzed Addition versus Concerted Oxidative Addition/Isomerization

Initial studies performed in C_6D_6 showed that hydrogen addition to $^{(iPr)4}$(POCOP)Ir(CO) (**6**) first gives the concerted oxidative addition product, ***cis*-7**, which upon heating gives the more stable ***trans*-7**. Essentially the same reaction was observed in THF-d_8 in the absence of added protons; minor conversion to ***trans*-7** under these conditions appeared to be proton-catalyzed. It is hypothesized that the proton source must be sufficiently acidic to partially protonate **6** because when low concentrations of water or phenol were used as the proton source the formation of ***trans*-7** was minimal.

The proposal of **10-X** as the species facilitating hydrogen addition to **6** was verified when [Hpyr]$BArF_{20}$ was used as the proton source and the concentration of **10-$BArF_{20}$** in solution was in line with the amount of acid added. Additionally, hydrogen addition to **6** was facilitated by addition of isolated **10-BF_4** to the reaction. We postulate a mechanistic scenario (Scheme 3.02) with two competing pathways having different rates (where $k_1 > k_2$). The rate of the proton-catalyzed pathway is highly dependent on the solubility of the proton-source. As **6** is consumed by the proton-catalyzed pathway, the equilibrium for **6** and ***cis*-7** shifts back toward **6** until all **6** is consumed to give the more thermodynamically favored ***trans*-7** complex.

Scheme 3.02. Proposed Mechanism for Competing Concerted Oxidative Addition and Proton-Catalyzed Hydrogen Addition to 6

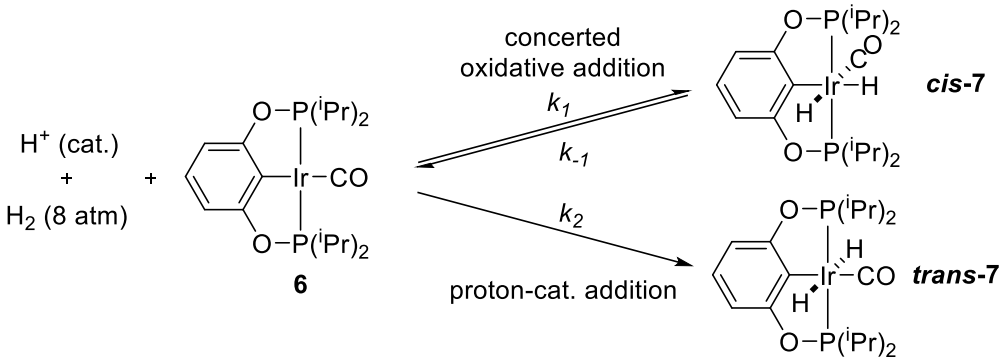

The proton-catalyzed pathway likely proceeds via a mechanism similar to that reported for H_2 addition to $^{(tBu)4}$(PONOP)Ir(CH_3).[10] Addition of H^+ to ^{R4}(POCOP)Ir(CO) results in a cationic hydrido-carbonyl complex (**5-X** or **10-X**). Although the protonated species was only observed for R = ^{i}Pr, in both ^{R4}POCOP systems [Hpyr]BF_4 was competent for hydrogen addition. This protonated species was observed for R = ^{i}Pr (**10-X**) but not for R = ^{t}Bu when [Hpyr]BF_4 was used as the proton source for H_2 addition; however, we found that **5-BF_4** (prepared without coordination of pyridine) did catalyze hydrogen addition to $^{(tBu)4}$(POCOP)Ir(CO).[13] Furthermore, for H_2 addition to **6** catalyzed by [Hlut]BF_4, no intermediate protonated species was observed. When **10-BF_4** was used as the proton source for H_2 addition to **6**, the proton-catalyzed H_2 addition required 4 days for full consumption of **6**, rather than overnight when [Hpyr]BF_4 was the proton source. Complex **10-BF_4** has limited solubility in THF and also loses [Hpyr]BF_4 over time. Since [Hpyr]BF_4 is less soluble than **10-BF_4** in THF, we hypothesize that precipitation is the driving force for partial loss of [Hpyr]BF_4; **6** is highly soluble in THF. To eliminate the solubility issues, [Hpyr]$BArF_{20}$ was used as the proton source to give a homogeneous solution where **10-$BArF_{20}$** (~50% conversion) was generated *in situ*. Upon H_2 addition, ***trans*-7** was formed, with no solid precipitates ever observed over the course of the reaction. We hypothesize that **10-$BArF_{20}$** catalyzes H_2 addition to

the remaining **6** in solution until only a mixture of ***trans*-7** and **10-BArF$_{20}$** is attained. Over the course of weeks, there is slow conversion of **10-BArF$_{20}$** to ***trans*-7** (<5% change in the ratio).

Given the solubility issues faced, we propose two possibilities for how **10-X** can serve as a catalytic proton source. There may be an equilibrium between complex **10-X** and a five-coordinate dissociated pyridine complex, or alternatively, [Hpyr]X (for X = BF_4, $BArF_{20}$) is reductively eliminated and reprotonates another equivalent of **6**. In the presence of H_2, formation of an intermediate dihydrogen-hydride complex, even at low concentration, is feasible when pyridine is not bound to Ir. Direct formation of ***trans*-7** from **10-BArF$_{20}$** and H_2 is much slower than the reaction of **6**, **10-BArF$_{20}$**, and H_2. However, we cannot rule out the former pathway over longer times. This was evident in the approximate 50/50 mixture of ***trans*-7** and **10-BArF$_{20}$** when all **6** was consumed.

When we first observed the proton-catalyzed addition of H_2 to **1**, attempts were made to observe the proposed dihydrogen−hydride complex; however, we could not confirm the presence of a dihydrogen complex.[14] Those studies were performed by a low-temperature protonation of an 80/20 mixture of **4** and **1**, respectively. Here, we performed a similar reaction with the ^{i}Pr analogue (***trans*-7**) since we could prepare pure ***trans*-7** and a less sterically congested metal center was expected to facilitate H_2 coordination. Unfortunately, we were not able to directly observe this species by low-temperature protonation of ***trans*-7**, due to rapid H_2 evolution. Presumably, this is due to weak binding of H_2 at the metal center.

While the discussion above describes competing H_2 addition mechanisms in the presence of added acid, there is also a concerted oxidative addition/isomerization pathway for the formation of ***trans*-7** (Scheme 3.03). Comparable to the $^{(iPr)4}$(PCP)Ir(CO) system reported by Milstein and further computational studies by Hall and co-workers, the *cis*-dihydride may isomerize to the

trans-dihydride via a trigonal twist mechanism where the meridionally coordinated pincer ligand would become facially coordinating to allow isomerization of the ligands at Ir.[12] Experimental evidence from work by Roddick and co-workers on hydrogen addition to $^{(CF3)4}$(PCP)Ir(CO) demonstrates the ability of facial coordination of a pincer ligand to iridium.[40] Alternatively, the evidence for hydrido-formyl complex **3** suggests a CO insertion mechanism could be a possibility as well. Hydrogen addition to **6** would give ***cis*-7** which could undergo a migratory insertion to give a hydrido-formyl complex which could isomerize then undergo de-insertion to give ***trans*-7**. Further investigations to understand the the *cis* to *trans* isomerization would provide more conclusive support for a possible mechanism.

Scheme 3.03. Proposed Mechanisms for Hydrogen Addition to ^{R4}(pincer)Ir(CO)

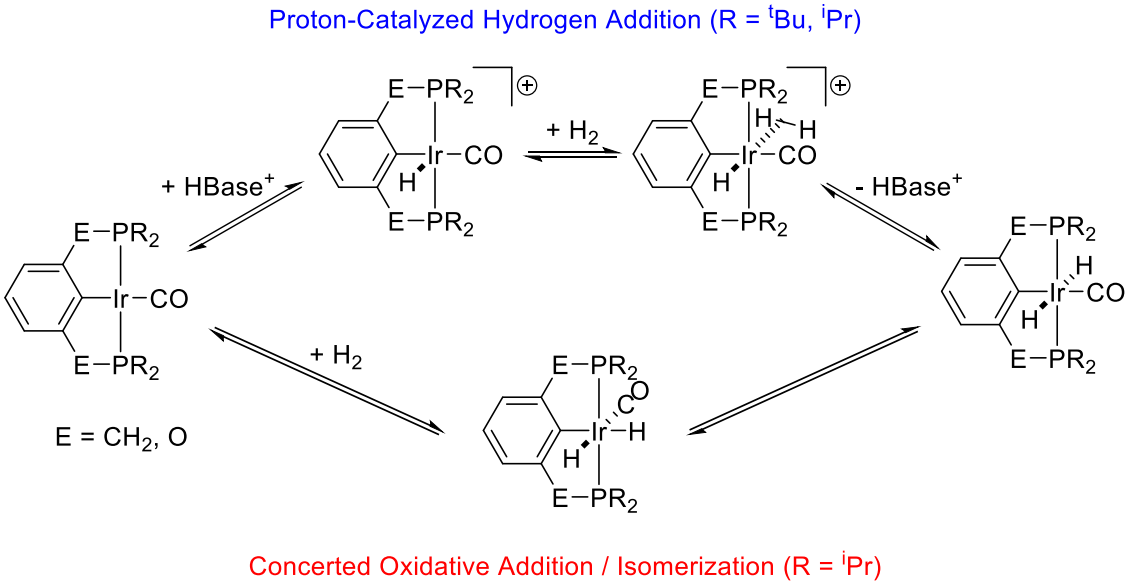

3.3.6 Comparison of H_2 Addition to (POCOP)Ir(CO) versus (PCP)Ir(CO)

A comparison between hydrogen addition to ^{t}Bu-substituted (POCOP) and (PCP)Ir(CO) compounds (**1** and **13**) revealed similar reactivity. Neither compound added hydrogen under increased pressure (8 atm) or elevated temperature (100 °C) in C_6D_6, though both were found to form a *trans*-dihydride complex (**4** or **14**) in varying yields by the proton-catalyzed addition of hydrogen. This reactivity (or lack thereof) is presumably dictated largely by steric factors; the ^{t}Bu substituents on the ligand block dihydrogen from approaching the metal center. The differing conversions in the proton-catalyzed reaction are likely partially attributed to the differing electronic parameters of the ligands. While **14** is formed instantaneously and quantitatively from **13**, **4** is only observed in 14% yield after 6 days from **4**. Presumably a more electron-rich metal center favors both protonation and subsequent formation of the Ir(III) dihydride in the PCP-based system.

The study of the ^{i}Pr analogue of ^{R4}(POCOP)Ir(CO) was conducted for direct comparison with prior reports as well as the synthetic ease over the methyl substituted complexes, which are often used as models for computational studies. Goldman and Krogh-Jespersen previously reported DFT computations showing that the reaction energies for H_2 addition to $^{(Me)4}$(PCP)Ir(CO) or $^{(Me)4}$(POCOP)Ir(CO) were the same within the limits of computational uncertainty (−13.4 and −12.3 kcal mol^{-1}, respectively).[41] Milstein and co-workers reported facile, quantitative addition of H_2 to $^{(iPr)4}$(PCP)Ir(CO) by bubbling H_2 through a solution of the metal complex to give the *cis*-dihydride complex. In contrast, bubbling H_2 through a solution of the POCOP analogue results in only 45% conversion to the *cis*-dihydride. Increasing the H_2 pressure to 8 atm increased the conversion to 90%.

The previous computational work does not fully explain the difference in reactivity between the PCP and POCOP systems; H_2 can be added to (PCP)Ir(CO) under milder conditions than the POCOP analogues. It is interesting that given the small difference computed for reaction energies that there is such a significant difference between the PCP and POCOP systems. Based strictly on the carbonyl stretching frequencies of both *trans*-$^{(iPr)4}$(PCP)Ir(CO)$(H)_2$ and *trans*-$^{(iPr)4}$(POCOP)Ir(CO)$(H)_2$, the PCP complex is expected to be more electron-rich with a ν(CO) of 1980 cm^{-1} as compared to 2003 cm^{-1} for the POCOP analogue. It is expected that a more electron-rich metal center favors H_2 oxidative addition. Interestingly, we were never able to achieve full conversion of ***cis*-7** to ***trans*-7** since we found that they are in equilibrium; the PCP analogue was reported to achieve full conversion from the *cis*- to *trans*-dihydride complex.[9]

The proton-catalyzed H_2 addition pathway was examined for $^{(iPr)4}$(PCP)Ir(CO) (**16**). We found that in addition to the H_2 concerted oxidative addition/isomerization mechanism previously reported by Milstein, in the presence of protons, a proton-catalyzed addition pathway is operative. While more Ir(I) is consumed to give a protonated species (**18**) in the proton-catalyzed H_2 addition to **16** than in the POCOP system, the same reactivity is observed resulting in *trans*-dihydrides (**17** and ***trans*-7**). For both systems, the addition of protons affects the mechanism of H_2 addition to Ir(I).

3.4 Conclusions

Two different H_2 addition pathways to Ir(I) have been explored, facilitated by NMR observations under moderate hydrogen pressure. For $^{(tBu)4}$(POCOP)Ir(CO) and $^{(tBu)4}$(PCP)Ir(CO), concerted oxidative addition of H_2 is not possible; however, in the presence of a proton source,

trans-dihydrides are observed. Proton-catalyzed H_2 addition may be considered as a route for other metal complexes where the barrier to concerted oxidative addition is too high. For $^{(iPr)4}$(POCOP)Ir(CO), both concerted oxidative addition of H_2 followed by isomerization and proton-catalyzed H_2 addition pathways were observed. The isomerization pathway is thermally induced; *cis*- and *trans*-dihydride complexes were found to be in a temperature-dependent equilibrium. The proton-catalyzed H_2 addition pathway for $^{(iPr)4}$(POCOP)Ir(CO) proceeds under mild pressures of H_2 and at room temperature, leading to full consumption of Ir(I). The pK_a value for $[^{(tBu)4}$(POCOP)Ir(CO)(H)$]^+$ was experimentally determined to be slightly more acidic than *N*,*N*-dimethylanilinium in CH_2Cl_2. New cationic hydrido-pyridine Ir(III) carbonyl complexes are described for both the POCOP and PCP systems. These complexes may serve as the catalytic proton sources in the proton-catalyzed H_2 addition pathways. In addition to the previously reported concerted oxidative addition pathway to $^{(iPr)4}$(PCP)Ir(CO) to give the *cis* Ir(III) dihydride, a proton-catalyzed H_2 addition pathway was observed to lead directly to the *trans* Ir(III) dihydride.

3.5 Experimental

General Considerations

All experiments and manipulations were performed using standard Schlenk techniques under an argon atmosphere or in an argon or nitrogen filled glove box. Glassware and diatomaceous earth were dried in an oven maintained at 140 °C for at least 24 h. Deuterated solvents were dried over calcium hydride or molecular sieves (CD_2Cl_2, THF-d_8, and C_6D_6) or sodium/benzophenone (toluene-d_8) and vacuum transferred prior to use. Protio solvents were passed through columns of activated alumina and molecular sieves. All other reagents were used

as received. ^{1}H NMR spectra were referenced to residual protio solvents: dichloromethane (5.32 ppm), THF (1.79 ppm), toluene (2.09 ppm), and benzene (7.16 ppm). ^{13}C NMR shifts were referenced to solvent signals: benzene (128.06 ppm), dichloromethane (54.00 ppm) and THF (26.19 ppm). ^{31}P NMR shifts were referenced to an 85% H_3PO_4 external standard (0 ppm). Infrared spectra were recorded on a Bruker Tensor 27 FTIR instrument. NMR spectra were recorded on either a Bruker AV-700, AV-500, DRX-500, or AV-300 NMR instrument. X-ray data was collected at -173ºC on a Bruker APEX II single crystal X-ray diffractometer, Mo-radiation. Elemental analysis was performed under air-free conditions at the CENTC facility at the University of Rochester or Atlantic Microlabs. Anhydrous *p*-toluenesulfonic acid was prepared by heating the monohydrate under vacuum at 50°C. $^{(tBu)4}$(POCOP)Ir(CO)/$^{(tBu)4}$(POCOP)Ir(H)$_2$,[29] $^{(iPr)4}$(POCOP)Ir(CO)(H)(Cl),[13] $^{(tBu)4}$(PCP)Ir(H)(Cl),[42] and [Hlut]X/[Hpyr]X (for X = BF_4 or $BArF_{20}$)[43] were synthesized according to published procedures.

Synthesis

*Improved Synthesis of [$^{(tBu)4}$(POCOP)Ir(CO)(H)]$BArF_{20}$ (**5-$BArF_{20}$**).*[14] In air, HCl/Et_2O (0.6 mL of 2.0 M solution) was added to a solution of $^{(tBu)4}$(POCOP)Ir(CO) (**1**) (32.3 mg, 0.0523 mmol) in C_6H_6 giving a colorless solution. Upon lyophilization, a white solid was obtained. In a nitrogen-filled glovebox, the white solid was combined with $KBArF_{20}$ (36 mg, 0.050 mmol) and dissolved in CH_2Cl_2 (5 mL) resulting in an orange solution and formation of a white precipitate. After sitting at room temperature for 8 h, the solution was filtered through a pad of diatomaceous earth and concentrated to 1 mL. The solution was layered with pentane (9 mL) and stored at -30 °C, yielding orange crystals. The mother liquor was removed and the orange solid was washed with pentane (3 mL). The solid was dried under vacuum giving a pale orange powder; yield: 52 mg (0.040 mmol,

80%). ^{1}H NMR (CD_2Cl_2, 300.10 MHz, 25 °C): δ 7.37 (t, $^{3}J_{HH}$ = 8.1 Hz, 1H; Ar-*H*), 6.95 (d, $^{3}J_{HH}$ = 8.1 Hz, 2H; Ar-*H*), 1.37 (m, 36H; P-C(C*H*$_3$)$_3$), -35.76 (t, $^{2}J_{PH}$ = 10.4 Hz, 1H; Ir-*H*). ^{31}P{^{1}H} NMR (CD_2Cl_2, 121.51 MHz, 22 °C): δ 191.8 (s).

*Improved Synthesis of $^{(iPr)4}$(POCOP)Ir(CO) (**6**).* A 20 mL scintillation vial was charged with $^{(iPr)4}$(POCOP)Ir(CO)(H)(Cl) (**9**) (38 mg, 0.064 mmol) and methanol (5 mL) giving a pale yellow solution. NaOMe (6 mg, 0.1 mmol) was added to the vial and vigorously mixed, resulting in a yellow/orange solution. Solvent was removed under vacuum giving a yellow/orange residue. The product was extracted with C_6H_6 (2 mL) and filtered through a syringe filter. The solvent was removed under vacuum to give a golden yellow solid; yield: 35 mg (0.062 mmol, 97%). NMR data are consistent with previous reports.[13]

*Synthesis of trans-$^{(iPr)4}$(POCOP)Ir(CO)(H)$_2$ (**trans-7**).* Under an argon atmosphere, $NaBH_4$ (308 mg, 8.14 mmol) and $^{(iPr)4}$(POCOP)Ir(CO)(H)(Cl) (**9**) (96.3 mg, 0.161 mmol) were added to a 100 mL flask sealed with a Teflon stopcock. To the mixture was added degassed CH_3CN (20 mL) followed by degassed ethanol (15 mL). The resulting yellow solution was stirred overnight at room temperature and turned colorless. Solvent was removed under vacuum giving a white residue. The product was extracted with C_6H_6 (10 mL) and filtered through a pad of diatomaceous earth. Upon lyophilization, ***trans*-7** was isolated as an air-stable white powder; yield: 68 mg (0.12 mmol, 75%). No further purification was necessary. Crystals suitable for diffraction were grown by slow evaporation of a dichloromethane solution. Anal. Calcd. for $C_{19}H_{33}IrO_3P_2$: C, 40.49; H, 5.90. Found: C, 40.07; H, 6.03. ^{1}H NMR (C_6D_6, 300.10 MHz, 25 °C): δ 6.80 (t, $^{3}J_{HH}$ = 7.7 Hz, 1H; Ar-

H), 6.68 (d, $^{3}J_{HH}$ = 7.7 Hz, 2H; Ar-*H*), 1.95 (m, 4H; P-C*H*$(CH_3)_2$), 1.15-0.98 (m, 24H; P-CH(C*H*$_3)_2$), -10.02 (t, $^{2}J_{PH}$ = 16.5 Hz, 2H; Ir-*H*). $^{31}P\{^{1}H\}$ NMR (C_6D_6, 121.49 MHz, 25 °C): δ 173.2 (s). $^{13}C\{^{1}H\}$ NMR (C_6D_6, 125.67 MHz, 25 °C): δ 177.42 (m; Ir-*C*O), 163.62 (m; C_{Ar}), 125.33 (s; C_{Ar}), 121.34 (m; C_{Ar}), 104.91 (m; C_{Ar}), 32.55 (vt, $^{1}J_{PC}$ + $^{3}J_{PC}$ = 36.7 Hz; P-*C*H$(CH_3)_2$), 17.88 (s; P-CH(*C*H$_3)_2$), 17.36 (s; P-CH(*C*H$_3)_2$). IR (solution, CH_2Cl_2, cm^{-1}): *ν*(CO) 2008, *ν*(H-Ir-H) 1757. IR (solution, C_6D_6, cm^{-1}): *ν*(CO) 2003, *ν*(H-Ir-H) 1762.

Formation of cis-$^{(iPr)4}$(POCOP)Ir(CO)(H)$_2$ (***cis*-7**). In a nitrogen-filled glovebox, $^{(iPr)4}$(POCOP)Ir(CO) (**6**) (10 mg, 0.018 mmol) was dissolved in freshly distilled C_6D_6 (0.1 mL) giving a dark yellow solution and was added to a 5 mm thick-walled NMR tube fitted with a Teflon valve. The tube was freeze-pump-thawed three times. The reaction was pressurized with 8 atm H_2 and rotated for 20 min to ensure complete mixing, resulting in a lighter yellow solution. By ^{31}P NMR spectroscopy, 90% conversion to ***cis*-7** was observed. After rotating for 16 h at room temperature, no change in the conversion to ***cis*-7** was observed by ^{31}P NMR spectroscopy. ^{1}H NMR (C_6D_6, 300.13 MHz, 22 °C): δ 6.95-6.80 (m, 3H; Ar-*H*), 2.22 (m, 2H; P-C*H*$(CH_3)_2$), 1.92 (m, 2H; P-C*H*$(CH_3)_2$), 1.18-1.06 (m, 12H; P-CH(C*H*$_3)_2$), 1.01-0.92 (m, 12H; P-CH(C*H*$_3)_2$), -10.30 (t, $^{2}J_{PH}$ = 9.3 Hz, 1H; Ir-*H*), -11.16 (t, $^{2}J_{PH}$ = 18.4 Hz, 1H; Ir-*H*). $^{31}P\{^{1}H\}$ NMR (C_6D_6, 121.51 Hz, 22 °C): δ 167.7 (s).

*Synthesis of [$^{(iPr)4}$(POCOP)Ir(CO)(H)(pyr)]BF$_4$ (**10-BF$_4$**).* In a nitrogen filled glovebox, [Hpyr]BF_4 (24.6 mg, 0.147 mmol) was added to a 20 mL vial containing $^{(iPr)4}$(POCOP)Ir(CO) (**6**) (85 mg, 0.15 mmol). THF (5 mL) and CH_2Cl_2 (2 mL) were added giving a golden yellow solution

with undissolved [Hpyr]BF_4. Upon sitting at room temperature for 5 days, the solution color faded to pale yellow and all [Hpyr]BF_4 dissolved. The solution was filtered through a pad of diatomaceous earth and the solvent was removed under vacuum. The yellow/white residue was triturated with pentane then washed with C_6H_6 (3 mL) to remove trace $^{(iPr)4}$(POCOP)Ir(CO) (**6**). The white solid was dried under vacuum then dissolved in CH_2Cl_2 (1 mL) and filtered through diatomaceous earth. Pentane (7 mL) was layered over the CH_2Cl_2 solution and the sample was stored at -30 °C for 5 days giving large colorless plate crystals suitable for diffraction; yield: 68 mg (0.093 mmol, 63%). Anal. Calcd. for $C_{24}H_{37}BF_4IrNO_3P_2$: C, 39.57; H, 5.12; N, 1.92. Found: C, 39.74; H, 5.12; N, 2.01. ^{1}H NMR (CD_2Cl_2, 300.10 MHz, 13 °C): δ 8.90 (br s; C_5H_5N), 8.04 (t, $^3J_{HH}$ = 7.6 Hz, 1H; *para*-C_5H_5N), 7.46 (br s; C_5H_5N), 7.18 (t, $^3J_{HH}$ = 8.0 Hz, 1H; Ar-*H*), 6.76 (d, $^3J_{HH}$ = 8.0 Hz, 2H; Ar-*H*), 2.58 (m, 2H; P-C*H*$(CH_3)_2$), 1.95 (m, 2H; P-C*H*$(CH_3)_2$), 1.24-1.14 (m, 12H; P-CH(C*H*$_3)_2$), 1.06-0.93 (m, 12H; P-CH(C*H*$_3)_2$), -19.46 (t, $^2J_{PH}$ = 13.5 Hz, 1H; Ir-*H*). ^{31}P{^{1}H} NMR (CD_2Cl_2, 121.49 MHz, 13 °C): δ 164.7 (s). ^{13}C{^{1}H} NMR (CD_2Cl_2, 75.47 MHz, 25 °C): δ 177.53 (m; Ir-*C*O), 164.03 (m; C_{Ar}), 140.93 (s; C_{Ar}), 130.74 (s; C_{Ar}), 128.47 (m; C_{Ar}), 107.49 (m; C_{Ar}), 31.34 (vt, $^1J_{PC}$ + $^3J_{PC}$ = 33.0 Hz; P-*C*H$(CH_3)_2$), 30.23 (vt, $^1J_{PC}$ + $^3J_{PC}$ = 36.1 Hz; P-*C*H$(CH_3)_2$), 18.54 (m; P-CH(*C*H$_3)_2$), 17.78 (m; P-CH(*C*H$_3)_2$), 17.61 (m; P-CH(*C*H$_3)_2$), 16.06 (m; P-CH(*C*H$_3)_2$). IR (solution, CH_2Cl_2, cm^{-1}): ν(CO) 2042.

*Preparation of [$^{(tBu)4}$(POCOP)Ir(CO)(H)(pyr)]$BArF_{20}$ (**11**).* An NMR tube fitted with a J. Young style Teflon valve was charged with $^{(tBu)4}$(POCOP)Ir(CO) (**1**) (10 mg, 0.017 mmol), [Hpyr]$BArF_{20}$ (13 mg, 0.017 mmol), and CD_2Cl_2 (0.5 mL) giving a yellow solution. ^{1}H NMR (CD_2Cl_2, 300.13 MHz, 24 °C): δ 8.98 (m, 1H; C_5H_5N), 7.87 (m, 1H; C_5H_5N), 7.46-7.38 (m, 2H; C_5H_5N), 7.25-7.19 (m, 2H; overlapping C_5H_5N and Ar-*H*), 6.84 (m, 2H; Ar-*H*), 1.33 (vt, $^3J_{PH}$ + $^5J_{PH}$ = 15.4 Hz, 18H;

P-C(CH_3)$_3$), 1.02 (vt, $^3J_{PH}$ + $^5J_{PH}$ = 15.7 Hz, 18H; P-C(CH_3)$_3$), -19.42 (t, $^2J_{PH}$ = 14.7 Hz, 1H; Ir-*H*). ^{31}P{^{1}H} NMR (CD_2Cl_2, 121.51 MHz, 24 °C): δ 170.0 (s).

*Preparation of $^{(iPr)4}$(POCOP)Ir(CO)(H)(OTs) (**12**).* In an argon filled glovebox, $^{(iPr)4}$(POCOP)Ir(CO) (**6**) (10 mg, 0.018 mmol) and anhydrous *p*-toluenesulfonic acid (16 mg, 0.093 mmol) were added to an NMR tube fitted with a J. Young style Teflon valve. CD_2Cl_2 (0.5 mL) was vacuum transferred into the tube giving a colorless solution. ^{1}H NMR (CD_2Cl_2, 300.10 MHz, 25 °C): δ 7.02 (t, $^3J_{HH}$ = 8.1 Hz, 1H; Ar-*H*), 6.62 (d, $^3J_{HH}$ = 8.1 Hz, 2H; Ar-*H*), 2.72 (m, 2H; P-C*H*(CH$_3$)$_2$), 2.53 (m, 2H; P-C*H*(CH$_3$)$_2$), 1.32-1.23 (m, 12H; P-CH(CH_3)$_2$), 1.12 (m, 6H; P-CH(CH_3)$_2$), 0.92 (m, 6H; P-CH(CH_3)$_2$), -25.17 (t, $^2J_{PH}$ = 13.6 Hz, 1H; Ir-*H*). The peaks assignable to bound *p*-toluenesulfonate could not be distinguished from excess *p*TsOH in solution. ^{31}P{^{1}H} NMR (CD_2Cl_2, 121.49 MHz, 25 °C): δ 170.6 (s).

*Modified Synthesis of $^{(tBu)4}$(PCP)Ir(CO) (**13**).* A 100 mL flask sealed with a Teflon stopcock was charged with $^{(tBu)4}$(PCP)Ir(H)(Cl) (83.0 mg, 0.133 mmol) in toluene (20 mL), resulting in a red solution. CO was bubbled through the solution, immediately resulting in decolorization. The flask was freeze−pump−thawed three times. NaO^{t}Bu (142 mg, 1.48 mmol) was added to the flask. The mixture was heated at reflux for 15.5 h. Solvent was removed under vacuum giving a yellow residue. The product was extracted with pentane (10 mL) and filtered through a pad of diatomaceous earth. Pentane was removed under vacuum, and the yellow solid was dissolved in benzene (5 mL). The solution was eluted through a plug of basic alumina, and solvent was removed under vacuum. The product was isolated as a bright yellow powder; yield: 70 mg (0.11 mmol,

86%). ^{1}H NMR (C_6D_6, 300.10 MHz, 28 °C): δ 7.26 (d, $^{3}J_{HH}$ = 7.5 Hz, 2H; Ar−*H*), 7.12 (t, $^{3}J_{HH}$ = 7.5 Hz, 1H; Ar−*H*), 3.42 (vt, $^{2}J_{PH}$ + $^{4}J_{PH}$ = 3.7 Hz, 4H; Ar-C*H*$_2$-P), 1.27 (vt, $^{3}J_{PH}$ + $^{5}J_{PH}$ = 6.6 Hz, 36H; P−C(CH$_3$)$_3$). ^{31}P{^{1}H} NMR (C_6D_6, 121.49 MHz, 28 °C): δ 82.9 (s). NMR data are consistent with previous reports.[28] IR (solution, CH_2Cl_2, cm^{-1}) ν(CO) 1913.

*Synthesis of [$^{(tBu)4}$(PCP)Ir(CO)(H)(pyr)]BF$_4$ (**15**).* $^{(tBu)4}$(PCP)Ir(CO) (**13**) (40 mg, 0.065 mmol) was dissolved in CH_2Cl_2 (10 mL) and [Hpyr]BF$_4$ (11 mg, 0.065 mmol) added. The solution was left to stand for 15 hours, upon which the solution had turned from yellow to colorless. The solution was filtered through diatomaceous earth and the solvent removed to yield a colorless solid; yield: 46 mg (0.060 mmol, 90%). X-ray diffraction quality crystals were grown from a ternary mixture of CH_2Cl_2, diethyl ether and pentane at -30 ºC. ^{1}H NMR (CD_2Cl_2, 499.71 MHz): δ 9.01 (d, $^{3}J_{HH}$ = 5.9 Hz, 1H; C_5H_5N), 7.88 (t, $^{3}J_{HH}$ = 7.4 Hz, 1H; C_5H_5N), 7.59 (d, $^{3}J_{HH}$ = 5.3 Hz, 1H; C_5H_5N), 7.39 (t, $^{3}J_{HH}$ = 6.1 Hz, 1H; C_5H_5N), 7.29 (d, $^{3}J_{HH}$ = 7.6 Hz, 2H; Ar-*H*), 7.22 (t, $^{3}J_{HH}$ = 6.5 Hz, 1H; C_5H_5N), 7.16 (t, $^{3}J_{HH}$ = 7.4 Hz, 1H; Ar-*H*), 3.57 (dvt, $^{2}J_{HH}$ = 17.1, $^{2}J_{PH}$ + $^{4}J_{PH}$ = 3.9 Hz, 2H; ArC*H*$_2$PR$_2$), 3.39 (dvt, $^{2}J_{HH}$ = 17.1, $^{2}J_{PH}$ + $^{4}J_{PH}$ = 3.6 Hz, 2H; ArC*H*$_2$PR$_2$), 1.26 (vt, $^{3}J_{PH}$ + $^{5}J_{PH}$ = 6.9 Hz, 18H; PC(C*H*$_3$)$_3$), 1.03 (vt, $^{3}J_{PH}$ + $^{5}J_{PH}$ = 6.8 Hz, 18H; PC(C*H*$_3$)$_3$), -19.72 (t, $^{2}J_{PH}$ = 14 Hz, 1H; Ir-*H*). ^{13}C{^{1}H} NMR (CD_2Cl_2, 125.77 MHz): δ 179.59 (m, Ir-*C*O), 160.15 (s; C_{Ar}), 159.93 (m; C_{Ar}), 150.69 (s; C_{Ar}), 149.50 (m; C_{Ar}), 140.02 (s; C_{Ar}), 127.87 (s; C_{Ar}), 127.85 (s; C_{Ar}), 127.41 (s; C_{Ar}), 123.49 (s; C_{Ar}), 38.30 (m; P-*C*(CH$_3$)$_3$), 37.20 (m; Ar*C*H$_2$PR$_2$), 29.80 (m; P-C(*C*H$_3$)$_3$), 29.57 (m; P-C(*C*H$_3$)$_3$). ^{31}P NMR (CD_2Cl_2, 202.31 MHz): δ 60.8 (s). Anal. Calcd. for $C_{30}H_{49}BF_4IrNOP_2$: C, 46.15; H, 6.33; N, 1.79. Found: C, 46.15; H, 6.15, N, 1.69. IR (solution, CH_2Cl_2, cm^{-1}): ν(CO) 2018.

Synthesis of $^{(iPr)4}$(PCP)Ir(CO)(H)(Cl). In a nitrogen-filled glovebox, $^{(iPr)4}$(PCP)H (400 mg, 1.18 mmol) and $[Ir(COE)_2Cl]_2$ (445 mg, 0.500 mmol) were placed in a 250 mL Kontes valve flask with a stir bar and toluene (20 mL) to give an orange solution. The solution was sparged with H_2 for 15 min, after which a yellow precipitate had formed. The vessel was sealed and the mixture heated at 90 °C under an atmosphere of H_2 for 15 h, resulting in a red solution. The solvent was removed to give a red solid of $^{(iPr)4}$(PCP)Ir(H)(Cl), which was redissolved in toluene (30 mL). The solution was submitted to three freeze−pump−thaw cycles, and an atmosphere of CO was introduced. After stirring for a minute, the solution decolorized and was stirred for an additional 19 h. The solvent was removed from the colorless solution to yield an off-white solid, which was then dissolved in CH_2Cl_2 (10 mL) and filtered through a fritted funnel with 2 cm neutral alumina and 1 cm diatomaceous earth. Removal of the solvent under reduced pressure resulted in a colorless solid, which was found to be a mixture of *cis*- and *trans*-$^{(iPr)4}$(PCP)Ir(H)(CO)(Cl); yield: 500 mg (0.84 mmol, 84%). NMR data are consistent with previous reports.[9]

*Synthesis of $^{(iPr)4}$(PCP)Ir(CO) (**16**).* In a nitrogen-filled glovebox, $^{(iPr)4}$(PCP)Ir(H)(CO)(Cl) (450 mg, 0.76 mmol) was charged to a 250 mL Kontes valve flask with KO^{t}Bu (1.70 g, 15.1 mmol) and a stir bar. The flask was evacuated to remove all nitrogen, and toluene (100 mL) was added under Ar. The mixture was submitted to three freeze−pump−thaw cycles and placed under 1 atm of CO. The mixture was stirred for 5 min at room temperature, after which the solution turned orange, and heated for 72 h at 70 °C. The solvent was removed from the resulting orange solution *in vacuo* to give an orange solid, which was extracted with pentane (20 mL) and filtered through diatomaceous earth. Removal of the solvent under reduced pressure led to the isolation of an orange solid; yield:

335 mg (0.60 mmol, 79%). NMR data are consistent with previous reports. IR (solution, CH_2Cl_2, cm^{-1}) ν(CO) 1920.[9]

*Synthesis of [$^{(iPr)4}$(PCP)Ir(CO)(H)(pyr)]BF_4 (**18**).* $^{(iPr)4}$(PCP)Ir(CO) (**16**) (98 mg, 0.18 mmol) was dissolved in CH_2Cl_2 (5 mL) and [Hpyr]BF_4 (29 mg, 0.18 mmol) added. The solution was left to stand for 48 hours, upon which the solution had turned from orange to yellow. The solution was filtered through diatomaceous earth and the solvent removed to yield a yellow solid which was recrystallized from a ternary mixture of CH_2Cl_2, diethyl ether and pentane at -30 ºC; yield: 115 mg (0.16 mmol, 91 %). ^{1}H NMR (CD_2Cl_2, 300.10 MHz): δ 8.25 (br s, 2H; C_5H_5N), 7.98 (t, $^3J_{HH}$ = 8.0 Hz, 1H; Ar-*H*), 7.39 (t, $^3J_{HH}$ = 6.9 Hz, 2H; C_5H_5N), 7.19 (m, 3H, Ar-*H*), 3.58 (dvt, $^2J_{HH}$= 17.7, $^2J_{PH}$ + $^4J_{PH}$ = 4.6 Hz, 2H; ArCH_2PR$_2$), 3.34 (dvt, $^2J_{HH}$ = 17.7, $^2J_{PH}$ + $^4J_{PH}$ = 4.1 Hz, 2H; ArCH_2PR$_2$), 2.34 (m, 2H; PCH(CH$_3$)$_2$), 1.90 (m, 2H; PCH(CH$_3$)$_2$), 1.07 (m, 24H; PCH(CH_3)$_2$), -19.15 (t, $^2J_{PH}$ = 12 Hz, 1H; Ir-*H*). ^{31}P{^{1}H} NMR (CD_2Cl_2, 121.49 MHz): δ 47.8 (s). IR (solution, CH_2Cl_2, cm^{-1}): ν(CO) 2023.

Experimental Procedures

*Low temperature CO addition to $^{(tBu)4}$(POCOP)Ir(H)$_2$ (**2**).* In an argon-filled glovebox, $^{(tBu)4}$(POCOP)Ir(H)$_2$ (**2**) (8.5 mg, 0.014 mmol) was added to an NMR tube fitted with a J. Young style Teflon valve. Toluene-d_8 (~0.5 mL) was vacuum transferred into the tube, resulting in a red solution. The sample was freeze-pump-thawed three times. The tube was cooled to -78 °C and pressurized with 1 atm CO followed by immediate cooling to -196 °C. The sample was thawed to -78 °C and immediately inserted into a pre-cooled NMR probe at -63 °C. Selected NMR

resonances assigned to $^{(tBu)4}$(POCOP)Ir(CHO)(H)(CO) (**3**). ^{1}H NMR (toluene-d_8, 700.07 MHz, -63 °C): δ -8.32 (s, 1H; Ir-*H*). ^{31}P{^{1}H} NMR (toluene-d_8, 283.45 MHz, -63 °C): δ 183.4 (s).

*Isomerization of cis- to trans-$^{(iPr)4}$(POCOP)Ir(CO)(H)$_2$ (**cis-7** to **trans-7**).* Heating the sample containing ~90% ***cis*-7** for 88 h at 100 °C under 8 atm H_2 in a 5 mm thick-walled NMR tube fitted with a Teflon valve results in 95% conversion to ***trans*-7** by ^{31}P NMR spectroscopy. The remaining 5% is ***cis*-7**.

*Reaction of $^{(iPr)4}$(POCOP)Ir(CO) (**6**) with formic acid*. An NMR tube fitted with a J. Young style Teflon valve was charged with $^{(iPr)4}$(POCOP)Ir(CO) (**6**) (6.0 mg, 0.011 mmol) and acetone-d_6 giving a yellow solution. Formic acid was added in successive amounts until the solution turned colorless (25 µL total, 0.66 mmol). After allowing to react at room temperature for 30 min, resonances consistent with ***trans*-7** and $^{(iPr)4}$(POCOP)Ir(CO)(H)(κ^1-OC(O)H) (**8**) were observed by NMR spectroscopy. Selected NMR resonances assigned to complex **8**. ^{1}H NMR (acetone-d_6, 300.13 MHz, 25 °C): δ -21.63 (td, $^{2}J_{PH}$ = 13.8 Hz, $^{4}J_{HH}$ = 3.8 Hz, 1H; Ir-*H*). ^{31}P{^{1}H} NMR (acetone-d_6, 121.51 MHz, 26 °C): δ 168.3 (s).

*General procedure for proton-catalyzed hydrogen addition to complexes $^{(tBu)4}$(POCOP)Ir(CO) (**1**), $^{(iPr)4}$(POCOP)Ir(CO) (**6**), $^{(tBu)4}$(PCP)Ir(CO) (**13**), and $^{(iPr)4}$(PCP)Ir(CO) (**16**).* In a nitrogen-filled glovebox, a solution of [Hpyr]X/[Hlut]X (X = BF_4 or $BArF_{20}$, ~0.5 equiv.) in CH_3CN was added to a 5 mm thick-walled NMR tube fitted with a Teflon valve. Solvent was removed under vacuum.

A solution of the iridium complex (1 equiv.) in THF-d_8 was added to the tube. The sample was freeze-pump-thawed three times and pressurized with H_2.

*Low temperature protonation of trans-$^{(iPr)4}$(POCOP)Ir(CO)(H)$_2$ (**trans-7**) with pTsOH.* In air, *trans*-$^{(iPr)4}$(POCOP)Ir(CO)(H)$_2$ (***trans*-7**) (11.0 mg, 0.0195 mmol) was added to an NMR tube fitted with a J. Young style Teflon valve and evacuated on a vacuum line. In a nitrogen-filled glovebox, anhydrous *p*-toluenesulfonic acid (~25 mg, 0.15 mmol) was added to the tube. CD_2Cl_2 was vacuum transferred and the sample was maintained at -196 °C. The sample was thawed to -78 °C and immediately inserted into a pre-cooled NMR probe at -80 °C. Formation of $^{(iPr)4}$(POCOP)Ir(CO)(H)(OTs) (**12**) was immediately observed by NMR spectroscopy.

*Reaction of $^{(tBu)4}$(PCP)Ir(CO) (**13**) with H_2 (8 atm, acid catalyzed with [Hpyr]BF$_4$).* [Hpyr]BF_4 (4 μL, 1 M in CH_3CN, 0.004 mmol) was added to a 5 mm thick-walled NMR tube fitted with a Teflon valve using a glass syringe. The solvent was removed in vacuo and $^{(tBu)4}$(PCP)Ir(CO) (**13**) (4 mg, 0.007 mmol) dissolved in THF-d_8 was added to the tube. The sample was subjected to three freeze-pump-thaw cycles and pressurized with 8 atm H_2. An immediate color change from yellow to colorless was observed. NMR spectroscopy revealed quantitative conversion to *trans*-$^{(tBu)4}$(PCP)Ir(CO)(H)$_2$ (**14**). Removal of H_2 atmosphere gave partial conversion back to $^{(tBu)4}$(PCP)Ir(CO) (**13**). *trans*-$^{(tBu)4}$(PCP)Ir(CO)(H)$_2$ (**14**). ^{1}H NMR (THF-d_8, 499.71 MHz): δ 6.77 (d, $^3J_{HH}$ = 7.6 Hz, 2H; Ar-*H*), 6.60 (t, $^3J_{HH}$ = 7.2 Hz, 1H; Ar-*H*), 3.43 (vt, $^2J_{PH}$ + $^4J_{PH}$ = 3.8 Hz, 4H; ArCH_2PR_2), 1.35 (vt, $^2J_{PH}$ + $^4J_{PH}$= 6.5 Hz, 36H; PC(CH_3)$_3$), -9.74 (t, $^2J_{PH}$ = 14 Hz, 2H; Ir-*H*). ^{31}P{^{1}H} NMR (THF-d_8, 202.31 MHz): δ 75.3 (s).

*pK_a Determination of [$^{(tBu)4}$(POCOP)Ir(CO)(H)]$BArF_{20}$ (**5-$BArF_{20}$**).*

In a nitrogen-filled glovebox, 24.1 mg (0.0186 mmol) **5-$BArF_{20}$** was dissolved in a mixture of CD_2Cl_2 and CH_2Cl_2 (0.3 mL and 2 mL respectively) giving a yellow/orange solution. To this solution was added 1 equiv. *N*,*N*-dimethylaniline (100 μL of 0.19 M solution in CH_2Cl_2). Another 2 mL CH_2Cl_2 was added to ensure complete solubility of all species present; $^{(tBu)4}$(POCOP)Ir(CO) (**1**) has lower solubility than **5-$BArF_{20}$** in CH_2Cl_2. A 0.4 mL aliquot was taken from the solution and analyzed by ^{1}H and ^{31}P NMR spectroscopy. The same experiment was repeated with 1.1 equiv. *N*,*N*-dimethylaniline and similar results were obtained (*vide infra*).

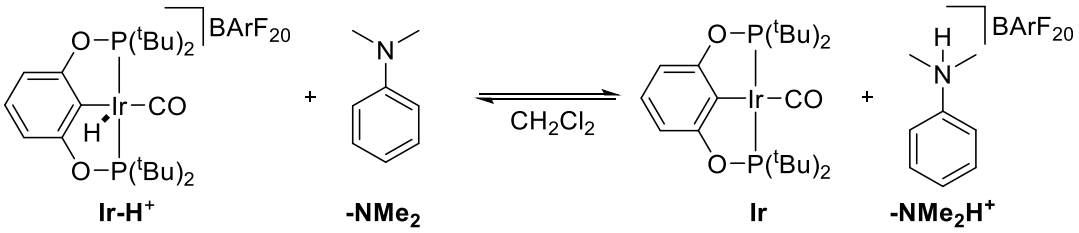

Ir-H$^+$ **-NMe_2** **Ir** **-NMe_2H^+**

1 equiv. **Ir-H$^+$** and 1 equiv. **–NMe_2**; ratios of each species at equilibrium by ^{1}H and ^{31}P NMR:

Ir-H$^+$ = 0.27 **-NMe_2** = 0.27 **Ir** = 0.73 **-NMe_2H^+** = 0.73

The ratios represented are the average of the ratios observed at 1 h and 24 h. There was minimal change in the ratios between 1 h and 24 h. There is an equilibrium between **–NMe_2** and **–NMe_2H^+**, thus only 1 set of signals is observed by ^{1}H NMR for the weighted average of the two species;[44] when integrated versus the total ^{t}Bu protons for **Ir** and **Ir-H$^+$**, the integration of **–NMe_2**/**-NMe_2H^+** represents 1 equiv. The ratios of **Ir** and **Ir-H$^+$** at equilibrium were experimentally determined by integrating the ^{31}P NMR spectra; they were the only ^{31}P containing species present. Characteristic ^{1}H NMR aromatic signals for **Ir** and **Ir-H$^+$** were also integrated and the ratios obtained were in line with those from the ^{31}P NMR spectra. The ratio of **–NMe_2** present at

equilibrium was determined by subtracting the ratio of **Ir** from the number of equivalents of **–NMe$_2$** initially added. The ratio of **–NMe$_2$H$^+$** should be equal to that of **Ir**. The experimentally determined pK_a^{THF}(**-NMe$_2$H$^+$**) is 4.9.[27] It has been previously been shown that for metal-hydride complexes, pK_a^{THF} ≈ pK_a^{CH2Cl2}.[38]

The ratio of each species at equilibrium was substituted into the following equilibrium expression:

$$K = \frac{[\mathrm{Ir}][-\mathrm{NMe_2H^+}]}{[\mathrm{Ir-H^+}][-\mathrm{NMe_2}]} = \frac{(0.73)^2}{(0.27)^2} = 7.31$$

The pK_a of **Ir-H$^+$** was obtained by referencing versus the known pK_a of **–NMe$_2$H$^+$** in the following equation:[45]

pK_a(**Ir-H$^+$**) = pK_a(**-NMe$_2$H$^+$**) – log$K$

pK_a(**Ir-H$^+$**) = 4.9 – log(7.31) = 4.0

The analogous calculation was performed when 1.1 equiv. *N*,*N*-dimethylaniline was used and a pK_a of 4.0 was also obtained. Therefore, pK_a^{CH2Cl2}(**Ir-H$^+$**) = 4.0 ± 0.1.

3.6 Notes to Chapter

[1] Adapted with permission from Goldberg, J. M.; Cherry, S. D. T.; Guard, L. M.; Kaminsky, W.; Goldberg, K. I.; Heinekey, D. M. *Organometallics* **2016**, *35*, 3546–3556. Copyright 2016 American Chemical Society.

[2] (a) Choi, J.; MacArthur, A. H. R.; Brookhart, M.; Goldman, A. S. *Chem. Rev.* **2011**, *111*, 1761−1779. (b) Crabtree, R. H. *Chem. Rev.* **2016**, *116*, 8750−8769.

[3] Deutsch, P. P.; Eisenberg, R. *Chem. Rev.* **1988**, *88*, 1147−1161.

[4] (a) Vaska, L.; Werneke, M. F. *Ann. N. Y. Acad. Sci.* **1971**, *172*, 546−562. (b) Jessop, P. G.; Morris, R. H. *Coord. Chem. Rev.* **1992**, *121*, 155−284.

[5] Ruthenium *trans*-dihydride: Salem, H.; Shimon, L. J. W.; Diskin-Posner, Y.; Leitus, G.; Ben-David, Y.; Milstein, D. *Organometallics* **2009**, *28*, 4791−4806.

[6] Palladium *trans*-dihydride: Fantasia, S.; Egbert, J. D.; Jurčík, V.; Cazin, C. S. J.; Jacobsen, H.; Cavallo, L.; Heinekey, D. M.; Nolan, S. P. *Angew. Chem. Int. Ed.* **2009**, *48*, 5182−5186.

[7] Powell, J.; Shaw, B. L. *J. Chem. Soc. A* **1968**, 617−622.
[8] Examples of metal−ligand cooperation: (a) Ben-Ari, E.; Leitus, G.; Shimon, L. J. W.; Milstein, D. *J. Am. Chem. Soc.* **2006**, *128*, 15390−15391. (b) Iron, M. A.; Ben-Ari, E.; Cohen, R.; Milstein, D. *Dalton Trans.* **2009**, 9433−9439. (c) Schwartsburd, L.; Iron, M. A.; Konstantinovski, L.; Diskin-Posner, Y.; Leitus, G.; Shimon, L. J. W.; Milstein, D. *Organometallics* **2010**, *29*, 3817−3827.
[9] Rybtchinski, B.; Ben-David, Y.; Milstein, D. *Organometallics* **1997**, *16*, 3786−3793.
[10] Findlater, M.; Bernskoetter, W. H.; Brookhart, M. *J. Am. Chem. Soc.* **2010**, *132*, 4534−4535.
[11] Example of acid-catalyzed C−H activation: Hackenberg, J. D.; Kundu, S.; Emge, T. J.; Krogh-Jespersen, K.; Goldman, A. S. *J. Am. Chem. Soc.* **2014**, *136*, 8891−8894.
[12] Li, S.; Hall, M. B. *Organometallics* **1999**, *18*, 5682−5687.
[13] Goldberg, J. M.; Wong, G. W.; Brastow, K. E.; Kaminsky, W.; Goldberg, K. I.; Heinekey, D. M. *Organometallics* **2015**, *34*, 753−762.
[14] Lao, D. B.; Owens, A. C. E.; Heinekey, D. M.; Goldberg, K. I. *ACS Catal.* **2013**, *3*, 2391−2396.
[15] Liu, F.; Goldman, A. S. *Chem. Commun.* **1999**, 655−656.
[16] Polukeev, A. V.; Petrovskii, P. V.; Peregudov, A. S.; Ezernitskaya, M. G.; Koridze, A. A. *Organometallics* **2013**, *32*, 1000−1015.
[17] For all percent conversions reported in this work, the ratios of products were examined by ^{31}P NMR spectroscopy since characteristic peaks overlap in ^{1}H NMR spectra and no other quantifiable byproducts were observed by ^{31}P NMR unless otherwise noted.
[18] **5-X** is soluble in CD_2Cl_2 and reacts with THF when present in higher concentrations.
[19] **5-BArF$_{20}$** was used for the direct reaction with hydrogen and for the pK_a studies to eliminate any solubility issues (see the Appendix).
[20] (a) Celaje, J. J. A.; Lu, Z.; Kedzie, Elyse, A.; Terrile, N. J.; Lo, J. N.; Williams, T. J. *Nat. Commun.* **2016**, *7*, 11308. (b) Schmeier, T. J.; Dobereiner, G. E.; Crabtree, R. H.; Hazari, N. *J. Am. Chem. Soc.* **2011**, *133*, 9274–9277.
[21] Caution must be exercised when heating a reaction in a closed tube that may build up pressure.
[22] Koehne, I.; Schmeier, T. J.; Bielinski, E. A.; Pan, C. J.; Lagaditis, P. O.; Bernskoetter, W. H.; Takase, M. K.; Würtele, C.; Hazari, N.; Schneider, S. *Inorg. Chem.* **2014**, *53*, 2133−2143.
[23] (a) Farrugia, L. J. *J. Appl. Cryst.* **2012**, *45*, 849-854. (b) Farrugia, L. J. *J. Appl. Cryst.* **1997**, *30*, 565.
[24] Williams, B. S.; Goldberg, K. I. *J. Am. Chem. Soc.* **2001**, *123*, 2576–2587.
[25] Complex **10-BF$_4$** has limited solubility in THF.
[26] Morris, R. H. *J. Am. Chem. Soc.* **2014**, *136*, 1948−1959.
[27] Kaljurand, I.; Kütt, A.; Sooväli, L.; Rodima, T.; Mäemets, V.; Leito, I.; Koppel, I. A. *J. Org. Chem.* **2005**, *70*, 1019−1028.
[28] Morales-Morales, D.; Redón, R.; Wang, Z.; Lee, D. W.; Yung, C.; Magnuson, K.; Jensen, C. M. *Can. J. Chem.* **2001**, *79*, 823−829.
[29] (a) Göttker-Schnetmann, I.; White, P. S.; Brookhart, M. *Organometallics* **2004**, *23*, 1766−1776. (b) Kloek, S. M.; Heinekey, D. M.; Goldberg, K. I. *Organometallics* **2006**, *25*, 3007−3011.
[30] Thorn, D. L. *J. Am. Chem. Soc.* **1980**, *102*, 7109–7110.
[31] Romero, P. E.; Whited, M. T.; Grubbs, R. H. *Organometallics* **2008**, *27*, 3422−3429.
[32] Examples of *cis*-/*trans*-dihydride isomerization: (a) Brown, J. M.; Dayrit, F. M.; Lightowler, D. *J. Chem. Soc., Chem. Commun.* **1983**, 414−415. (b) Haibach, M. C.; Wang, D. Y.; Emge, T. J.; Krogh- Jespersen, K.; Goldman, A. S. *Chem. Sci.* **2013**, *4*, 3683−3692. (c) Baumgarth, H.; Braun, T.; Braun, B.; Laubenstein, R.; Herrmann, R. *Eur. J. Inorg. Chem.* **2015**, *2015*, 3157−3168.

[33] Meakin, P.; Muetterties, E. L.; Jesson, J. P. *J. Am. Chem. Soc.* **1973**, *95*, 75−88.
[34] Qian, H.; Hopfield, J. J. *J. Chem. Phys.* **1996**, *105*, 9292−9298.
[35] Titova, E. M.; Silantyev, G. A.; Filippov, O. A.; Gulyaeva, E. S.; Gutsul, E. I.; Dolgushin, F. M.; Belkova, N. V. Eur. J. *Inorg. Chem.* **2016**, *2016*, 56−63.
[36] Holmes, A. J.; Rayner, P. J.; Cowley, M. J.; Green, G. G. R.; Whitwood, A. C.; Duckett, S. B. *Dalton Trans.* **2015**, *44*, 1077−1083.
[37] Morris, R. H. *Chem. Rev.* **2016**, *116*, 8588−8654.
[38] (a) Jia, G.; Lau, C.-P. Coord. *Chem. Rev.* **1999**, *190−192*, 83− 108. (b) Li, T.; Lough, A. J.; Morris, R. H. *Chem. Eur. J.* **2007**, *13*, 3796−3803.
[39] (a) Morris initially coined the term pK_α^{THF} instead of pK_a^{THF} due to discrepancies in values which have been corrected for ion-pairing; however, it was postulated that the values should be equal. See Abdur-Rashid, K.; Fong, T. P.; Greaves, B.; Gusev, D. G.; Hinman, J. G.; Landau, S. E.; Lough, A. J.; Morris, R. H. *J. Am. Chem. Soc.* **2000**, *122*, 9155−9171. (b) Later work by Leito described the scale in terms of pK_α^{THF}. For the purposes of our studies, we are referring to the term as pK_a; however, our work is based on the scale described by Leito. See reference 27 and Rodima, T.; Kaljurand, I.; Pihl, A.; Mäemets, V.; Leito, I.; Koppel, I. A. *J. Org. Chem.* **2002**, *67*, 1873−1881.
[40] (a) Adams, J. J.; Arulsamy, N.; Roddick, D. M. *Organometallics* **2011**, *30*, 697−711. (b) Roddick, D. M. *Top. Organomet. Chem.* **2013**, *40*, 49−88.
[41] (a) Krogh-Jespersen, K.; Czerw, M.; Zhu, K.; Singh, B.; Kanzelberger, M.; Darji, N.; Achord, P. D.; Renkema, K. B.; Goldman, A. S. *J. Am. Chem. Soc.* **2002**, *124*, 10797−10809. (b) Zhu, K.; Achord, P. D.; Zhang, X.; Krogh-Jespersen, K.; Goldman, A. S. *J. Am. Chem. Soc.* **2004**, *126*, 13044−13053.
[42] Moulton, C. J.; Shaw, B. L. *J. Chem. Soc., Dalton Trans.* **1976**, 1020-1024.
[43] Grönberg, K. L. C.; Henderson, R. A.; Oglieve, K. E. *J. Chem. Soc., Dalton Trans.* **1998**, 3093−3104.
[44] Drago, R. S., Physical Methods for Chemists. 2nd ed.; Surfside Scientific Publishers: Gainesville, Fl, 1992.
[45] Saouma, C. T.; Kaminsky, W.; Mayer, J. M. *J. Am. Chem. Soc.* **2012**, *134*, 7293-7296.

Chapter 4

Detection of an Iridium-Dihydrogen Complex: A Proposed Intermediate in Ionic Hydrogenation

4.1 Introduction

Our dependence on diminishing petroleum-based reserves as fuel and chemical sources has sparked interest in using abundant, oxygenated biomass feedstocks.[1] However, the limiting factor in full scale incorporation of biomass as a feedstock is the difficulty of selective deoxygenation.[2] Biodiesel from waste vegetable oil is a viable pathway to generating bio-based fuels from a low-cost resource. However, in the transesterification of vegetable oil to biodiesel, significant amounts of glycerol are generated as a by-product (10% w/w).[3] The conversion of this abundance of glycerol to higher value products represents an opportunity to increase the economic feasibility of biodiesel production.

We previously showed that (POCOP)Ir(CO) [POCOP = κ^3-C_6H_3-2,6- $(OPR_2)_2$ for R = ^{t}Bu] complexes could selectively catalyze the deoxygenation of glycerol to 1,3-propanediol and 1-propanol.[4] The former is a useful precursor for the production of polyesters,[5] and the latter is a potential fuel building block.[6] The proposed pathway for converting glycerol to partially deoxygenated products proceeds through initial acid-catalyzed dehydration followed by an ionic hydrogenation of an intermediate aldehyde.[6] In previous work on polyol deoxygenation, we proposed an iridium-dihydrogen complex could serve as a proton source to dehydrate an alcohol in glycerol. Iridium-dihydrogen complexes have previously been shown to be acidic.[7] Then, an *in situ* generated *trans*-dihydride would serve as a hydride donor in the ionic hydrogenation of an

intermediate aldehyde. A five-coordinate Ir-H complex $[^{(tBu)4}(POCOP)Ir(CO)(H)]^+$ was the proposed catalyst resting state following hydride transfer. (Scheme 4.01).

Scheme 4.01. Proposed Mechanism for Generating Proton and Hydride Equivalents in Ionic Hydrogenation

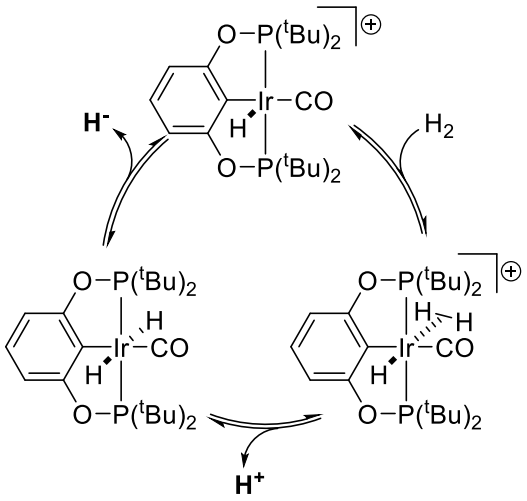

To support this mechanistic proposal, we sought to understand the individual steps of the catalytic cycle as well as to establish the viability of each of the intermediate iridium species. We previously studied the coordination chemistry of five-coordinate Ir-H complexes and found that for ^{t}Bu substituted POCOP ligands, five-coordinate species can be isolated, however for smaller phosphine substituents (R = ^{i}Pr), adventitious coordination of a sixth ligand (i.e. water) was observed.[8] In recent work, we described an extensive study of hydrogen addition to (POCOP)Ir(CO) complexes.[9] We found that a proton source is required for hydrogen addition to bulky $^{(tBu)4}$(POCOP)Ir(CO) to give *trans*-$^{(tBu)4}$(POCOP)Ir(CO)$(H)_2$ and elevated pressures are needed for high conversion to the dihydride product. Additionally, $[^{(tBu)4}(POCOP)Ir(CO)(H)]^+$ can serve as the proton source to facilitate hydrogen addition to $^{(tBu)4}$(POCOP)Ir(CO). In this proton-catalyzed hydrogen addition pathway, it was hypothesized that an intermediate dihydrogen complex would form and be readily deprotonated to give the *trans*-dihydride product. All attempts

to observe the dihydrogen complex were unsuccessful, which we attributed to relatively weak binding of H_2. Herein, we show evidence for this dihydrogen complex made possible by *in situ* NMR spectroscopy under high pressures of hydrogen.[10]

In this contribution, we describe the acid/base chemistry of five-coordinate iridium-hydride complexes and the effect of acid on iridium-hydride ^{1}H NMR resonances. We also show how incorporation of a protonated dimethylamino group on the pincer ligand backbone strengthens binding of hydrogen *trans* to an Ir-H. Two new dihydrogen complexes have been identified by addition of high pressures of H_2 (40-80 atm) at low temperatures to five-coordinate hydride complexes. These results highlight their feasibility as catalytic intermediates in glycerol deoxygenation catalysis. Furthermore, the five-coordinate complexes $[^{(NMe2H)(tBu)4}(POCOP)Ir(CO)(H)]^{2+}$ and $[^{(tBu)4}(POCOP)Ir(CO)(H)]^{+}$ were found to catalyze H/D exchange between H_2 and CD_3OD.

4.2 Results

To generate iridium-dihydrogen complexes, we targeted the synthesis of five-coordinate iridium complexes with a metal bound hydride *trans* to an open site. We previously reported the five coordinate complex $[^{(tBu)4}(POCOP)Ir(CO)(H)]BArF_{20}$ (**1**) [$BArF_{20}$ = $B(C_6F_5)_4$] and were unable to observe coordination of hydrogen (under 8 atm of H_2) to the open site *trans* to the iridium-hydride.[9] Additionally, we found that low temperature protonation of the Ir(III) *trans* dihydride *trans*-$^{(tBu)4}(POCOP)Ir(CO)H_2$ gave rapid evolution of hydrogen.[4] We were unable to directly detect the dihydrogen complex which is proposed as an intermediate in the mechanism for our Ir catalyzed glycerol deoxygenation.[4]

We hypothesized that addition of an electron-withdrawing group in the *para* position of the pincer ligand aryl backbone would make the metal center more Lewis acidic and so favor hydrogen coordination. In previous work from our group on glycerol deoxygenation, a dimethyl amino group was substituted on the aryl backbone to improve solubility in acidic aqueous media.[4] This substitution also presents interesting electronic effects; a dimethylamino group is electron donating (σ_p = -0.83), while the protonated form is electron withdrawing ($\sigma_p \approx 0.60 - 0.83$).[11] Incorporation of a protonated dimethyl amino group should render the iridium center much less basic than a complex without a *para* substituent.

4.2.1 Attempted Halide Abstraction of Hydrido-Chloride Complexes

We first targeted the synthesis of five-coordinate iridium hydride complexes with an open site trans to a hydride, $[^{(NMe2H)(tBu)4}(POCOP)Ir(CO)(H)]^{2+}$. Using the same procedure for the preparation of **1**, $^{(NMe)2(tBu)4}(POCOP)Ir(CO)$ (**2**) was first treated with excess HCl/Et_2O to generate $[^{(NMe2H)(tBu)4}(POCOP)Ir(CO)(H)(Cl)]Cl$ (**3**) as a pale red solid. In the ^1H NMR spectrum, two virtual triplets were observed at 1.61 and 1.30 ppm, consistent with two different ligands above and below the pincer plane. A triplet hydride resonance was observed at -18.04 ppm ($^2J_{PH}$ = 13.5 Hz), consistent with a hydrido-chloride Ir(III) carbonyl complex.[8] In the ^{31}P NMR spectrum, a singlet resonance was observed at 175.8 ppm. Further treatment of **3** with 2 equiv $KBArF_{20}$ in dichloromethane resulted in an intense purple solution. In the ^1H NMR spectrum, a single product was observed, however all peaks were broadened. The ^1H NMR spectrum was consistent with a complex of broken symmetry above and below the pincer plane. A broadened triplet hydride resonance was observed at -19.61 ppm ($^2J_{PH} \approx 15$ Hz) indicating coordination of ligand *trans* to the Ir-H.[8] In the ^{31}P NMR spectrum, a singlet resonance was observed at 179.9 ppm ($\omega_{1/2}$ = 14

Hz). NMR spectra of this purple species were not consistent with a five-coordinate Ir-H *trans* to an open site. However, we were curious if a reaction with CO would occur, suggesting access to a five-coordinate complex. Exposure of the dark purple CD_2Cl_2 solution, resulting from reaction of **3** with $KBArF_{20}$, to 1 atm CO, gave an immediate color change to pale yellow. By ^{1}H NMR spectroscopy, conversion to a new product with sharpened resonances was observed. Two virtual triplets were observed at 1.55 and 1.36 ppm and a triplet hydride resonance appeared at -10.35 ppm ($^2J_{PH}$ = 14.6 Hz). The hydride resonance is consistent with an iridium dicarbonyl complex.[8] In the ^{31}P NMR spectrum, a sharp singlet resonance was observed at 178.4 ppm. Removal of all volatiles under vacuum and dissolving in fresh CD_2Cl_2 resulted in a light purple solution, suggesting loss of CO. However, by ^{1}H NMR spectroscopy, peaks consistent with the proposed iridium dicarbonyl complex were still observed, suggesting only partial CO lability. No further attempts at understanding the nature of these species were carried out.

We also attempted halide abstraction reactions of **3** with excess $AgBF_4$ or AgOTf, but multiple products were obtained as observed by ^{31}P NMR spectroscopy. Reaction of **3** with $NaBF_4$ resulted in no reaction. Interestingly, treatment of **3** with excess $NaBPh_4$ in dichloromethane resulted in a clean reaction mixture. After 30 min at room temperature, by ^{1}H NMR spectroscopy, the iridium hydride disappeared and the two virtual triplets for **3** converged to one virtual triplet at 1.35 ppm. The spectrum was consistent with a single square planar Ir(I) product different from **2**, suggesting formation of the monocationic complex $[^{(NMe2H)(tBu)4}$(POCOP)Ir(CO)]Cl. After letting the reaction mixture sit at room temperature for 17 h, complete conversion to **2** was observed by ^{1}H and ^{31}P NMR spectroscopy. Notably, benzene was observed by ^{1}H NMR spectroscopy at the 30 min and 17 h time points. These data are consistent with reaction of tetraphenylborate first with HCl bound to iridium, followed by deprotonation of the ammonium moiety (Scheme 4.02). Similar

reactivity of tetraphenylborate with acids, yielding benzene, was reported by Morris; phosphonium salts with $pK_a^{CH2Cl2} \leq 6$ were reported to protonate tetraphenylborate.[12] Since halide abstraction of **3** resulted in unusual reactivity as compared to *trans*-$^{(tBu)4}$(POCOP)Ir(CO)(H)(Cl),[8] we instead examined protonation of **2** to generate five-coordinate hydride complexes.

Scheme 4.02. Reaction of [$^{(NMe2H)(tBu)4}$(POCOP)Ir(CO)(H)(Cl)]Cl (3) with Common Halide-Abstraction Reagents

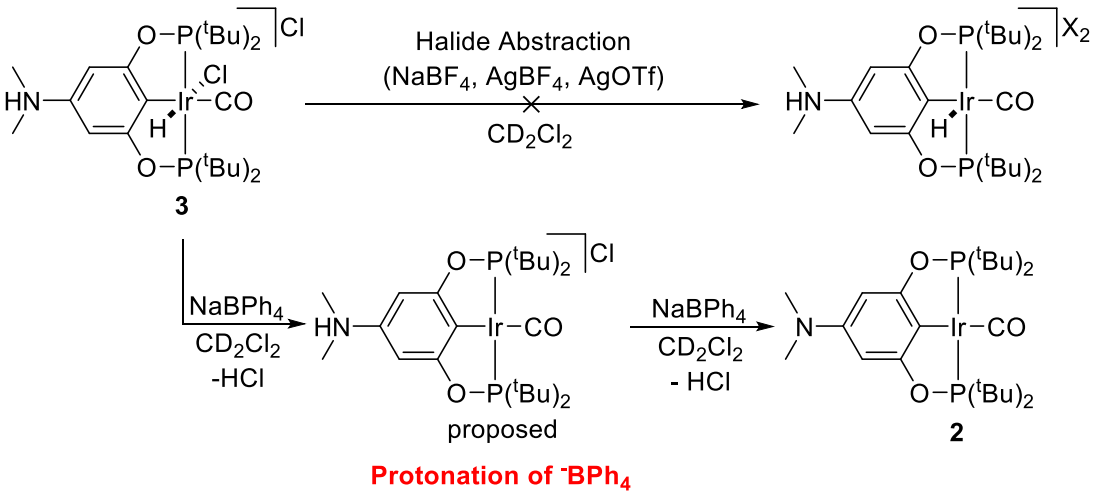

*4.2.2 Protonation of $^{(NMe2)(tBu)4}$(POCOP)Ir(CO) (**2**) with HOTf*

$^{(NMe2)(tBu)4}$(POCOP)Ir(CO) (**2**) was treated with varying amounts of acid (eq 4.01). The strong acid triflic acid (HOTf), was used in dichloromethane, a typically non-coordinating solvent, to ensure complete protonation. As shown in Figure 4.01, reaction of **2** with 1 equiv HOTf results in a single narrow ($\omega_{1/2}$ = 7 Hz) resonance in the ^{31}P NMR spectrum (δ 204.5), replacing the resonance for **2** (δ 200.0). This product was assigned as [$^{(NMe2H)(tBu)4}$(POCOP)Ir(CO)]OTf (**4**), with protonation only at the dimethylamino group. When 2 equiv HOTf was added to **2**, a single broad resonance was observed by ^{31}P NMR at 193.0 ppm ($\omega_{1/2}$ = 96 Hz). When >2 equiv HOTf was added to **2**, the ^{31}P NMR resonance further shifted to 196-197 ppm (the chemical shift depends on

the number of equivalents of excess acid) with a narrow linewidth ($\omega_{1/2} \approx 10$ Hz), indicative of the doubly protonated complex [$^{(NMe2H)(tBu)4}$(POCOP)Ir(CO)(H)](OTf)$_2$ (**5**). Further analysis of the doubly protonated complex will be discussed later.

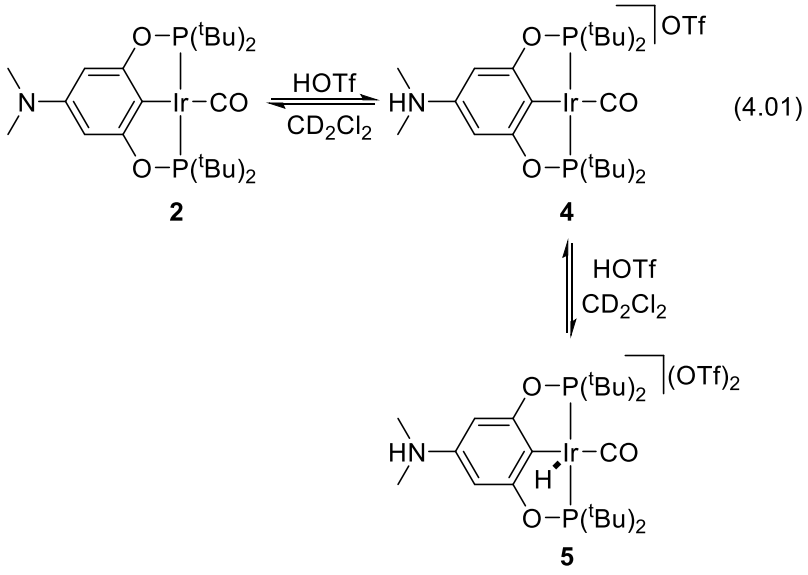

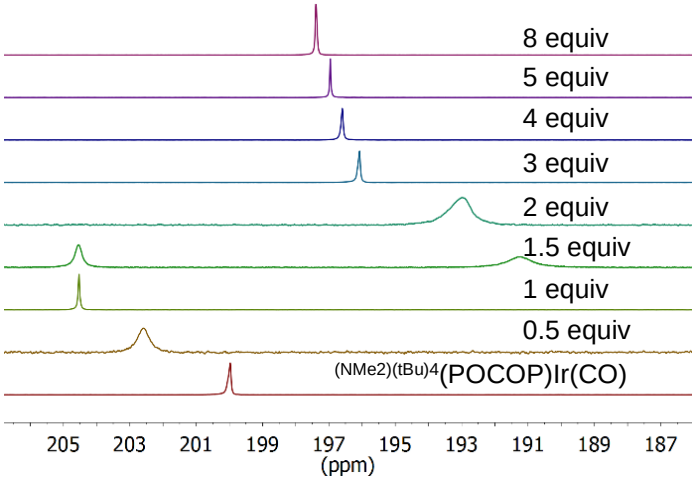

Figure 4.01. Stacked $^{31}P\{^1H\}$ NMR spectra (CD_2Cl_2) of protonation of $^{(NMe2)(tBu)4}$(POCOP)Ir(CO) (**2**) with incremental equivalents of HOTf. A reference spectrum of **2** in CD_2Cl_2 is also shown for comparison.

Since the broad resonance from reaction of **2** with 2 equiv HOTf suggested an exchange process, **2** was treated with only 1.5 equiv HOTf to probe for any intermediate protonated species. The resulting ^{31}P NMR spectrum gave 2 broadened resonances at 204.5 ($\omega_{1/2}$ = 78 Hz) and 191.2 ppm ($\omega_{1/2}$ = 246 Hz). Previously, we reported complex **1** with a ^{31}P NMR resonance at 191.8 ppm, suggesting assignment of the resonance at 191.2 ppm to the iridium-protonated monocation. The ^{31}P NMR spectrum resulting from reaction with 1.5 equiv HOTf was consistent with a mixture of two monoprotonated complexes, **4** at 204.5 ppm and [$^{(NMe2)(tBu)4}$(POCOP)Ir(CO)(H)]OTf (**6**) at 191.2 ppm. It is hypothesized that with less than 2 equiv HOTf in solution, complex **6** results from partial deprotonation of **5** at the ammonium moiety; a protonated iridium center would render the ammonium proton more acidic than in complex **4**.

The solution containing **2** and 1.5 equiv HOTf was cooled to -53 °C. At this temperature, the resonance at 204.5 ppm did not shift, but the linewidth narrowed significantly ($\omega_{1/2}$ = 13 Hz.) The resonance observed at 191.2 ppm at 25 °C narrowed ($\omega_{1/2}$ = 86 Hz) and shifted to 193.3 ppm. The low temperature data suggest the reaction with 1.5 equiv HOTf indeed leads to a mixture of protonated species, however the broad resonances likely arise from proton exchange between three species instead of two: the protonated amine complex **4**, the monoprotonated Ir-H complex [$^{(NMe2)(tBu)4}$(POCOP)Ir(CO)(H)](OTf) (**6**), and the doubly protonated complex **5**. At room temperature, the exact ^{31}P NMR chemical shift of **6** is likely slightly upfield of 191.2 ppm.

When the protonation reactions with complex **2** were monitored by ^{1}H NMR spectroscopy, the number of equivalents of HOTf relative to iridium affected the chemical shift and linewidth of the iridium-hydride resonance. Protonation of **2** with 1 equiv HOTf gave a spectrum consistent with protonation of only the dimethylamino group. As additional HOTf was added to a CD_2Cl_2 solution of **2**, a hydride resonance did not emerge until 1.5 equiv HOTf was added. In the ^{1}H NMR

spectrum, a broad singlet resonance was observed at -32.71 ($\omega_{1/2} \approx 500$ Hz). As further equivalents of HOTf were added, the hydride resonance narrowed and shifted further upfield (Figure 4.02). With 3 equiv HOTf, the hydride appeared as a broadened triplet at -35.69 ppm ($^2J_{PH}$ = 9.7 Hz). At ≥5 equiv HOTf, the hydride no longer shifted significantly and the resonance appeared as a sharp triplet at -36.0 ppm ($^2J_{PH}$ = 10.4 Hz). Notably, a sample containing 8 equiv HOTf was diluted by a factor of two and no change in the Ir-H shift was observed; the only observed changes upon dilution were shifting of the N-H resonance from 9.21 to 9.38 ppm and the HOTf peak from 12.40 to 12.18 ppm. This suggests no Ir-H chemical shift dependence on HOTf concentration.

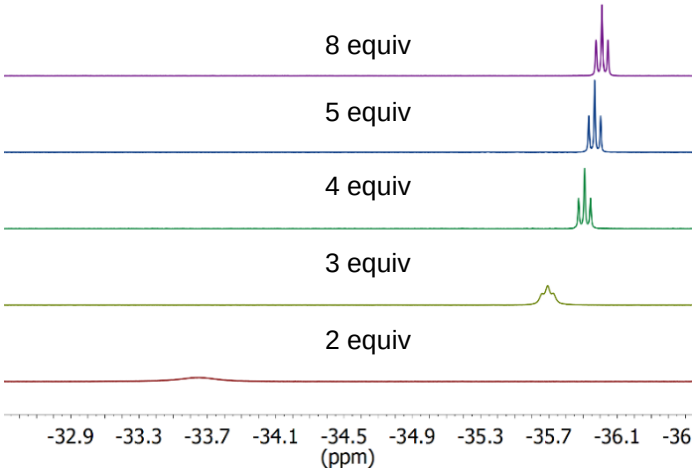

Figure 4.02. Stacked ^{1}H NMR spectra (300.10 MHz, CD_2Cl_2) of the hydride region from the protonation of $^{(NMe2)(tBu)4}$(POCOP)Ir(CO) (**2**) with incremental equivalents of HOTf.

We examined the field dependence of the ^{t}Bu resonances in the ^{1}H NMR spectra of complex **5**. In previous reports, we assigned the resonances observed in five-coordinate Ir(III) complexes for the two sets of ^{t}Bu groups as a multiplet, likely resulting from overlapping signals with similar chemical shifts. Here, we find that at higher field, (800 MHz), the same resonance can be better described as two virtual triplets (Figure 4.03).

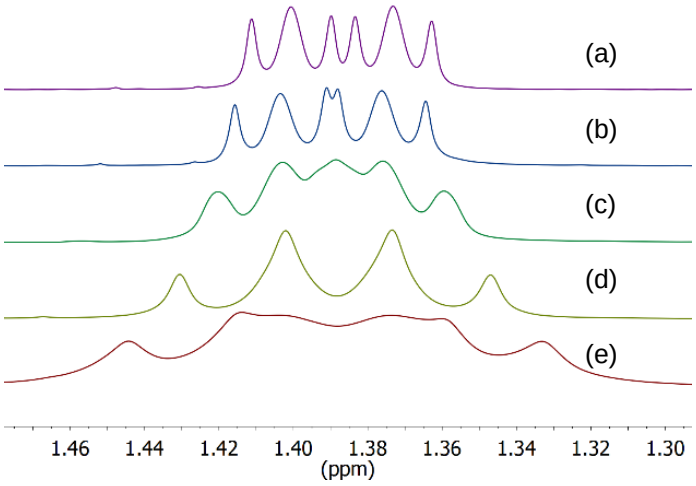

Figure 4.03. Stacked ^{1}H NMR spectra (CD_2Cl_2) of ^{t}Bu region of $[^{(NMe2H)(tBu)4}(POCOP)Ir(CO)(H)](OTf)_2$ (**5**) obtained at different magnetic fields: (a) 800 MHz (b) 700 MHz (c) 500 MHz (d) 300 MHz (e) 200 MHz.

To probe if the Ir-H chemical shift in **5** was dependent on the presence of excess HOTf or OTf^-, a sample of **1** was treated with 2 equiv HOTf followed by 5 equiv $(^{n}Bu)_4N(OTf)$. Before addition of the ammonium salt, by ^{1}H NMR spectroscopy the Ir-H was a broad singlet resonance at -34.22 ppm and by ^{31}P NMR spectroscopy there was a singlet resonance at 193.4 ppm. Note, minor deviations from 2 equiv HOTf (i.e. 2.1 or 1.9 equiv) will have an effect on the Ir-H chemical shift. After addition of $(^{n}Bu)_4N(OTf)$, the Ir-H resonance shifted slightly downfield to -33.80 ppm. The ^{31}P NMR spectrum exhibited two resonances at 204.5 and 193.0 ppm in an approximately 1 to 2 ratio respectively.

To further probe the Ir-H chemical shift dependence on HOTf, a sample containing **2** and 1.5 equiv HOTf was cooled to -53 °C. A new broad hydride resonance was observed at -23.42 ppm. A hydride resonance at this chemical shift is in the range for a hydride *trans* to a weakly coordinated ligand (OTf^-). However, cooling a sample of **2** and 5 equiv HOTf to -53 °C resulted

in only a trace amount of the hydride resonance at -23.42. Additional HOTf in solution prevented formation of a coordinated triflate species.

*4.2.3 Protonation of $^{(tBu)4}$(POCOP)Ir(CO) (**7**) with HOTf*

To determine if the Ir-H chemical shift dependence on HOTf was unique to protonation experiments with **2**, similar experiments were carried out with $^{(tBu)4}$(POCOP)Ir(CO) (**7**, eq 4.02). Treatment of a CD_2Cl_2 solution of **7** with 1 equiv HOTf, resulted in a single product by ^{1}H NMR spectroscopy with broadened triplet and doublet aromatic resonances at 7.34 and 6.92 ppm, respectively. Furthermore, only a single virtual triplet was observed at 1.38 ppm and a broadened singlet hydride resonance was observed at -34.93 ppm. The ^{31}P NMR spectrum showed a new broad singlet resonance at 190.7 ppm with a trace amount of unreacted **7** (199.0 ppm). It was hypothesized that if [$^{(tBu)4}$(POCOP)Ir(CO)(H)]OTf (**8**) was generated as the predominant product, a trace amount of a base in solution could lead to a symmetrized ^{1}H NMR spectrum rather than two distinct ^{t}Bu environments, as exhibited by a single virtual triplet resonance (Figure 4.04).

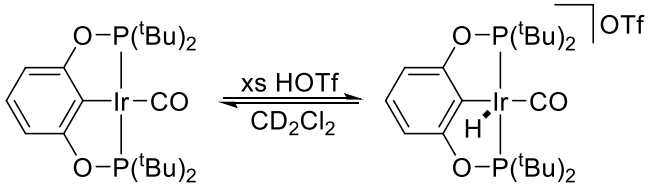

7 **8** (4.02)

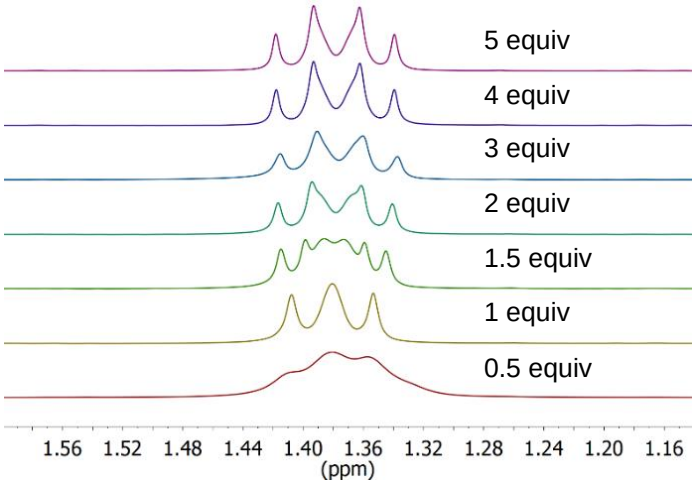

Figure 4.04. Stacked ^{1}H NMR spectra (300 MHz, CD_2Cl_2) of the ^{t}Bu region from the protonation of $^{(tBu)4}$(POCOP)Ir(CO) (**7**) with incremental equivalents of HOTf. Note the 1 equiv spectrum where the ^{t}Bu resonance appears as a single virtual triplet.

Examination of the reaction of **7** with ~0.5 equiv HOTf resulted in a ^{1}H NMR spectrum with two sets of broad aromatic signals, distinctive for two different POCOP products. However, the ^{t}Bu resonance was a broad three-line resonance centered at 1.38 ppm, suggesting either overlapping sets of signals and/or rapid exchange between two species in solution. A broad hydride resonance was observed at -35.10 ppm. As additional equivalents of HOTf were added, the hydride resonance shifted upfield until 2 equiv HOTf where the chemical shift of the hydride no longer changed; however, it remained as a broad singlet. Additional HOTf (>2 equiv) only resulted in sharpening of the resonance to show triplet character (Figure 4.05). These data, in corroboration with the protonation experiments with $^{(NMe2)(tBu)4}$(POCOP)Ir(CO) (**2**), show a hydride chemical shift dependence on the number of equivalents of HOTf until about the point where twice the number of equivalents of HOTf required for complete protonation is in solution. At that point, additional HOTf does not have a profound effect on the hydride chemical shift ($\Delta\delta \approx 0.04$ for complex **5**). However, in the case of protonation with complex **7**, additional HOTf results in

sharpening of the triplet hydride resonance and no change to the chemical shift of the hydride resonance.

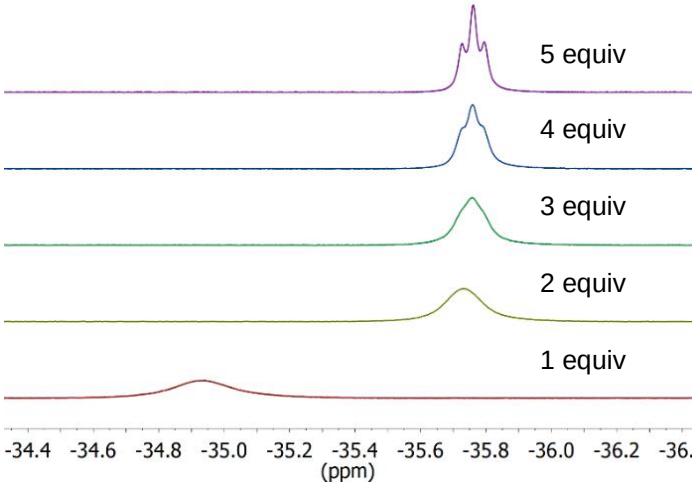

Figure 4.05. Stacked ^{1}H NMR spectra (300.10 MHz, CD_2Cl_2) of the hydride region from the protonation of $^{(tBu)4}$(POCOP)Ir(CO) (**7**) with incremental equivalents of HOTf.

4.2.4 Low Temperature Observation of an Iridium-Dihydrogen Complex

A CD_2Cl_2 solution of **5** was prepared by treatment of **2** with HOTf (10 equiv) in a PEEK NMR cell. At room temperature, by ^{1}H NMR spectroscopy, the Ir-H was observed at -35.92 ppm. Upon addition of 40 atm H_2, the Ir-H broadens and shifts downfield to -35.30 ppm. By ^{31}P NMR spectroscopy, the singlet resonance at 196.5 ppm broadens upon addition of H_2. Upon cooling the NMR probe to -80 °C, two new singlet resonances are observed in the ^{1}H NMR spectrum at -2.38 ($\omega_{1/2}$ = 134 Hz) and -13.64 ppm ($\omega_{1/2}$ = 51 Hz) in an approximate 1.3:1 ratio, respectively. The broad resonance at -2.38 ppm is consistent with iridium bound dihydrogen[13] and the resonance at -13.64 ppm is assigned as the Ir-H in [$^{(NMe2H)(tBu)4}$(POCOP)Ir(CO)(H_2)(H)](OTf)$_2$] (**9**, Figure 4.06). By ^{31}P NMR spectroscopy at -80 °C, a new major product is observed as a singlet resonance at

183.0 ppm; the ratio of the new product to unreacted **5** is approximately 5:1. Complex **9** was stable over the course of hours under H_2 atmosphere (40 atm) at low temperatures.

Standard inversion recovery methods were employed to determine the relaxation times (T_1) for the resonances at -2.38 and -13.64 ppm as well as unreacted iridium-hydride (-36.11 ppm). T_1 values could only be obtained from -80 to -70 °C, as the peaks for the dihydrogen complex were too broad at higher temperatures for accurate integrations. The two upfield resonances for **9** disappeared upon warming the NMR probe to -40 °C. At -80 °C (500 MHz), the T_1 values for **9** are shown in Table 4.01. The T_1(-80 °C) for the unreacted Ir-H at -36.11 ppm was determined to be 565 ms. Analysis of T_1(-80 °C) for the bound dihydrogen resonance, assuming T_{1min} was reached, using the method described by Halpern, resulted in an internuclear dihydrogen distance (r_{HH}) of 1.28 Å (eq 4.03). This simplified equation is only suitable for experiments performed on an instrument where 500 MHz ^{1}H NMR is used; a new expression must be derived for different Larmor frequencies.[14] At temperatures higher than -80 °C, the T_1 values increased, suggesting T_{1min} is at -80 °C or lower. Since T_{1min} could not be unequivocally determined due to limitations in cooling the CD_2Cl_2 solution significantly below -80 °C in the PEEK NMR cells, it is hypothesized that $r_{HH} \leq 1.28$ Å.

$$\frac{1}{T_{1\,min}} = \frac{77.505\ (\text{Å}^6\ s^{-1})}{{r_{HH}}^6} \qquad (4.03)$$

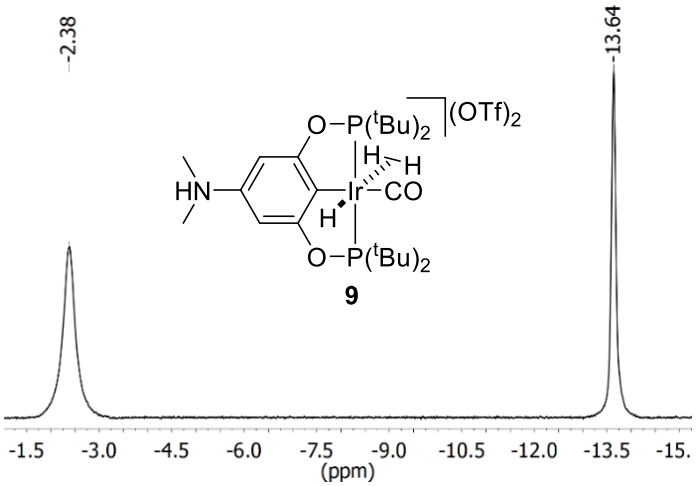

Figure 4.06. ^{1}H NMR spectrum (500 MHz, CD_2Cl_2, -80 °C) of the hydride region (-1.5 to -15 ppm) of [$^{(NMe2H)(tBu)4}$(POCOP)Ir(CO)(H_2)(H)](OTf)$_2$ (**9**).

Table 4.01. ^{1}H NMR Chemical Shifts of Ir-H_2 and Ir-H Resonances and Corresponding T_1 Values

Complex	[$^{(NMe2H)(tBu)4}$(POCOP)Ir(CO)(H_2)(H)]$^{2+}$		[$^{(tBu)4}$(POCOP)Ir(CO)(H_2)(H)]$^{+}$	
δ (ppm)	-2.38 (Ir-H_2)	-13.64 (Ir-H)	-2.39 (Ir-H_2)	-13.41 (Ir-H)
T_1 (ms) -80 °C	58	448	70	433
T_1 (ms) -70 °C	67	451	80	489

Previously, we reported the inability of hydrogen to coordinate to [$^{(tBu)4}$(POCOP)Ir(CO)(H)]BArF$_{20}$ (**1**) under 8 atm H_2.[9] Here, a CD_2Cl_2 solution of **1** was pressurized with 80 atm H_2 in a PEEK NMR cell (eq 4.04).

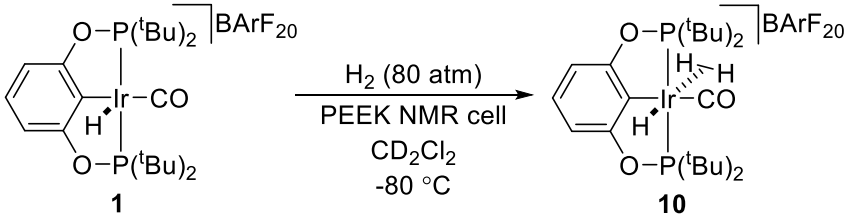

(4.04)

Upon cooling the NMR probe to -80 °C, a new species was observed by ^{1}H NMR spectroscopy, assigned as [$^{(tBu)4}$(POCOP)Ir(CO)(H_2)(H)]$BArF_{20}$ (**10**), with new resonances at -2.39 ($\omega_{1/2} \approx 130$ Hz) and -13.41 ppm ($\omega_{1/2} \approx 70$ Hz). The new peaks are consistent with an iridium-dihydrogen hydride complex where the resonance at -2.39 is assigned to bound dihydrogen and the peak at -13.41 is the new Ir-H. The two upfield resonances for **10** disappeared upon warming the NMR probe above -60 °C. In the ^{31}P NMR spectrum (-80 °C), a new singlet resonance was observed at 178.6 ppm; the ratio of the new product to unreacted **1** was 2:1. The T_1 values (500 MHz) for the new resonances at -80 °C are shown in Table 1. The T_1(-80 °C) for the Ir-H resonance at -34.83 ppm was determined to be 545 ms. Since T_{1min} could not be unequivocally determined for the iridium-bound dihydrogen resonance in **10**, it is hypothesized that $r_{HH} \leq 1.33$ Å.

4.2.5 Isotope Exchange Between H_2 and CD_3OD

A sample of **2** was combined with 2 equiv HOTf giving an Ir-H resonance at -34.55 ppm, a broadened virtual triplet at 1.40 ppm assigned to the ^{t}Bu groups, and a doublet at 3.32 ppm ($^{2}J_{HH}$ = 4.8 Hz) for the dimethylamino group. Upon addition of 11 equiv CD_3OD, the iridium-hydride resonance disappeared, the virtual triplet sharpened (1.37 ppm), and the doublet for the dimethylamino group became a singlet (3.23 ppm). Addition of 3 atm H_2 resulted in a broad hydrogen peak, preventing the observation of the isotope exchange product HD. We hypothesized that the amount of acid in solution was too low to maintain **5** as an Ir-H complex and facilitate hydrogen coordination, further complicated by the presence of CD_3OD as a weak base. Addition of more HOTf (11 equiv total) resulted in deuterium incorporation into the dimethylamino group as -NMe_2D^+, as evidenced by a new singlet resonance at 3.35 ppm (the doublet for the protonated form appeared at the same chemical shift with $^{2}J_{HH}$ = 4.8 Hz). Additionally, with more HOTf in

solution, the iridium-hydride was observed as a broadened triplet in the presence of CD_3OD at -35.83 ppm. Re-pressurization with 3 atm H_2 resulted in a sharp hydrogen signal and observation of a 1:1:1 triplet at 4.47 ppm ($^1J_{HD}$ = 43 Hz) characteristic of HD (eq 4.05), after mixing for 40 min at room temperature. An accurate determination (via integration) of the amount of HD formed could not be accomplished due to overlapping resonances of HD and H_2. Letting the sample stir for an additional 17 h did not result in any changes as evidenced by the ^{1}H NMR spectrum. An analogous isotope exchange experiment facilitated by **7** also resulted in HD gas formation after mixing for 2 h, as detected by ^{1}H NMR spectroscopy. The relative ratio of HD to H_2 was greater in the reaction with **7** than that with **2** since deuterium incorporation into the ligand backbone is not possible for **7**. In the absence of iridium, the hydrogen resonance appeared as a sharp singlet without the observation of HD.

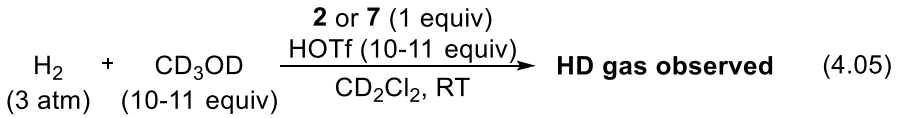

4.3 Discussion

To probe the possible existence of an iridium-dihydrogen complex relevant to glycerol deoxygenation catalysis, we targeted the synthesis of five-coordinate complexes that contain an open site *trans* to an Ir-H. Addition of H^+ to $^{(NMe2)(tBu)4}$(POCOP)Ir(CO) showed two protonation steps. Under high pressures of hydrogen, a bound dihydrogen species was observed at low temperatures by NMR spectroscopy.

4.3.1 Acid/Base Properties of Iridium-Hydride Complexes

Protonation experiments with $^{(NMe2)(tBu)4}$(POCOP)Ir(CO) (**2**) gave rise to interesting acid/base chemistry. Treatment of $^{(NMe2)(tBu)4}$(POCOP)Ir(CO) with 1 equiv HOTf first protonated the dimethylamino group with no evidence, by NMR spectroscopy, of protonation of the Ir metal center itself. It was expected that once the dimethylamino group is protonated, the iridium center would become quite electrophilic. HOTf was chosen as the acid source for these studies to prevent incomplete protonation resulting from weaker Brønsted acid sources. The second protonation indeed resulted in a dicationic metal hydride. When 2 equiv of HOTf was added, the expected triplet hydride resonance (^{1}H NMR) was not observed, rather a broad signal appeared (Figure 4.02). Additional HOTf was required for the Ir-H ^{1}H NMR resonance to sharpen and show triplet character.

We hypothesize that at low acid concentration, triflate is weakly coordinated to the iridium center. The coordination of triflate is enhanced by the presence of a strongly electron withdrawing ammonium group on the ligand backbone, leading to increased Lewis acidity at the metal center. Low temperature NMR data under low acid conditions showed a resonance for an Ir-H *trans* to weakly bound triflate at -23.42 ppm. This signal was greatly diminished in an analogous spectrum recorded with more acid in solution. Adding OTf^- to a solution containing [$^{(NMe2H)(tBu)4}$(POCOP)Ir(CO)(H)](OTf)$_2$ also resulted in partial deprotonation of the Ir-H to give the monocationic complex [$^{(NMe2H)(tBu)4}$(POCOP)Ir(CO)](OTf).

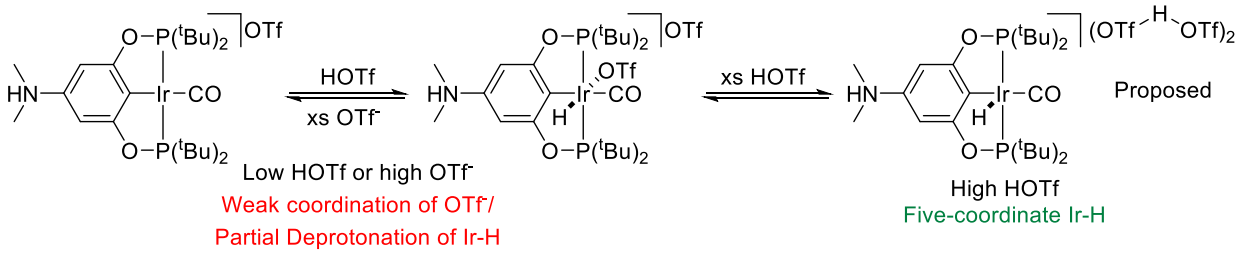

Figure 4.07. Proposed HOTf assisted dissociation of OTf^- from iridium.

Our initial hypothesis was that excess HOTf was required to prevent partial deprotonation of a highly acidic Ir-H by triflate; the protonated dimethylamino backbone would render the Ir-H very acidic (pK_a < 4 in CD_2Cl_2).[9] However, the analogous protonation experiments with $^{(tBu)4}$(POCOP)Ir(CO) showed that excess HOTf relative to iridium was required for the Ir-H to stop shifting upfield. We cannot rule out the possibility that the Ir-H in **5** is very acidic since we observed that addition of excess triflate in the form of $(^nBu)_4N(OTf)$ resulted in partial deprotonation to give more monoprotonated (at amine site) product **4**. These data strongly suggest triflate coordinates to the iridium center at low acid concentrations. However, with higher acid concentration in solution, it is hypothesized that a hydrogen bonding network facilitates dissociation of triflate from the iridium center (Figure 4.07) in the form of the anion $OTfH\bullet\bullet\bullet OTf^-$ resulting in upfield hydride chemical shifts, characteristic of five-coordinate species. In the dimethylamino system, OTf^- potentially serves as a base to partially deprotonate the Ir-H. Furthermore, addition of HOTf over stoichiometric quantities further shifts the Ir-H upfield; at the point of twice the required amount of acid to fully protonate the complex (≥4 equiv HOTf) the Ir-H is no longer broad, and sharpened triplet character is observed. In the unsubstituted system (**8**), there is a point (~2 equiv HOTf) where the hydride no longer shifts upfield but the peak sharpens in the presence of added triflic acid (>2 equiv). This is in contrast to the analogous complex to **8**

with a BF_4^- (previously reported) instead of OTf^- which demonstrated a sharp triplet hydride resonance with stoichiometric protons in solution.[8]

We currently do not have an explanation for these observations, however incorporation of the dimethylamino group on the backbone may introduce the possibility of a hydrogen bonding network that under additional equivalents of HOTf would continue to shift the Ir-H in the form of Ir-H•••HOTf or with a second iridium molecule in the form of Ir-H•••H-N.[15] As more HOTf was added to **2**, the N-H resonance shifted from 11.10 (2 equiv HOTf) to 9.04 ppm (8 equiv HOTf). The analogous phenomenon may not be possible in the unsubstituted system, consistent with the point where the hydride no longer shifts even after additional acid is added. There are known examples of metal hydrides as hydrogen bond acceptors.[16,17,18,19] We initially ruled out the possibility of a bimolecular mechanism since diluting a sample of **5** with excess HOTf to half the concentration did not affect the Ir-H chemical shift. However, our data are consistent with formation of a OTf^-/HOTf network, which should be concentration dependent. At higher HOTf concentrations, formation of TfOH•••OTf^- should be favored, preventing OTf^- binding to iridium (eq 4.06), giving a five-coordinate Ir-H.

Previous work by Bullock proposed a OTf^-/HOTf network in protonation experiments with bis(triphenylphosphine)iminium bases (PPN^+) in CD_2Cl_2.[20] We hypothesize that twice the amount of triflic acid required to fully protonate the iridium species is necessary to facilitate formation of the TfOH•••OTf^- moieties leading to an upfield shift of the Ir-H resonance, typical of a hydride *trans* to an open site. The concentrations of HOTf in our experiments are much higher than those reported by Bullock obviating a direct comparison of TfOH•••OTf^- ^{1}H NMR chemical shifts. For this hypothesis to be true, an additional equilibrium must also be operative resulting in no observable concentration dependence of HOTf on the Ir-H chemical shift. We propose that a

second equilibrium process (eq 4.07) for the binding and dissociation of OTf^- from **5** should also be concentration dependent. At low concentrations, OTf^- dissociation would be favored and therefore an upfield Ir-H shift would be expected consistent with a five-coordinate Ir-H complex. Thus, the opposing equilibria in eq 4.06 and eq 4.07 would show no observable concentration dependence on HOTf in solution. Therefore, we still cannot rule out a bimolecular mechanism causing the Ir-H chemical shift dependence on HOTf resulting from two iridium molecules interacting in the form of Ir-H•••H-N.

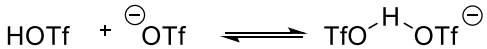

(4.06)

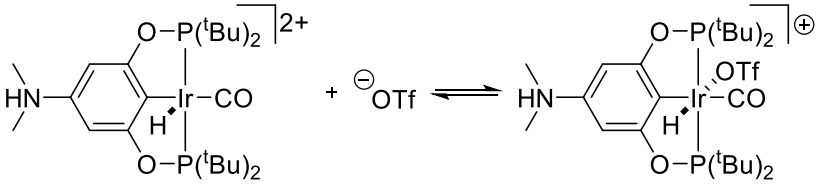

(4.07)

4.3.2 Base-Assisted Exchange Processes

In the course of studying the acid/base properties of complexes **5** and **8**, we often observed simplified ^{1}H NMR spectra when two distinct sets of resonances were expected. For example, in the protonation experiments of $^{(tBu)4}$(POCOP)Ir(CO) (**7**) with HOTf, when 1 equiv HOTf was added, a trace amount of **7** did not fully react. Instead of observing two sets of peaks for complexes **8** and **7**, presumably in the form of a multiplet and a virtual triplet, respectively, only one virtual triplet was observed. Based on the ^{31}P NMR spectrum of this reaction, over 97% iridium in solution was complex **8** (3% **7**). We propose an interpretation of these data in Figure 4.08. When trace amounts of base (i.e. complex **7**) are in solution, the base facilitates rapid deprotonation of the hydride and re-protonation on the opposite side of the molecule. This process would occur rapidly

on the NMR time scale giving rise to a simplified ^{1}H NMR spectrum which appears as a single highly symmetric molecule. Similarly, in protonation experiments of **2** to give complex **5**, the fine structure of the ^{t}Bu resonances in complex **5** were only observed once excess acid was added, suggesting trace amounts of unprotonated iridium facilitated the symmetrization of the ^{t}Bu resonances at low acid to give a simplified spectrum. The chemical shifts of the ^{t}Bu resonances were unchanged in the presence of trace amounts of unprotonated iridium or with excess acid.

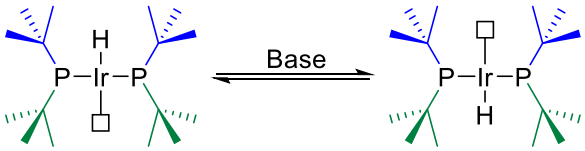

Figure 4.08. Base-assisted simplification of ^{1}H NMR spectra.

4.3.3 Iridium-Dihydrogen-Hydride Complexes

In the proposed mechanism for glycerol deoxygenation to 1,3-propanediol and 1-propanol, an iridium-dihydrogen-hydride complex is proposed to be a key intermediate. In previous work, we were not able to observe a dihydrogen complex by low temperature protonation of an iridium dihydride or addition of 8 atm H_2 to an open site complex.[9] In both these cases, reactions were carried out with the $^{(tBu)4}$(POCOP)Ir(CO) system. We found in these studies that appending a dimethylamino moiety on the pincer ligand backbone introduced new reactivity. Complex **2** was first examined for glycerol deoxygenation due to its enhanced solubility in acidic aqueous media. However, further reactivity studies were not examined. We now find that protonation of the dimethyl amino backbone greatly increases the Lewis acidity of the metal center. Thus, this species is primed for coordination of dihydrogen. Initial studies with complex **5** showed broadening of the Ir-H resonance under low pressures (~3 atm) of H_2. Since glycerol deoxygenation reactions were

performed under high pressures (≥40 atm), we hoped to directly observe a dihydrogen complex under these conditions. Gratifyingly, under 40 atm H_2, complex **9** was observed at -80 °C. At this pressure and temperature, >80% of the iridium in solution can be accounted for as the dihydrogen complex. We were unable to determine a precise value for T_{1min} since the T_1 was still decreasing at the lowest temperature where reliable data could be collected. Previous work from Halpern and co-workers was able to correlate T_{1min} to an H_2 bond length for coordinated dihydrogen.[14] Based on the trend we observe for T_1 values of the iridium bound dihydrogen resonance and the Ir-H resonance, T_{1min} is expected to be at a lower temperature than -80 °C. We propose an upper limit for the H_2 bond length as 1.28 Å based on the T_1(-80 °C) of 58 ms. This is consistent with a stretched dihydrogen complex. It is possible that complex **9** is more of a true Kubas-type dihydrogen complex with r_{HH} = 0.8-1.1 Å but we cannot verify this is the case based on our relaxation times.[21,22]

The enhanced Lewis acidity resulting from incorporating the dimethyl amino group was verified when we observed the analogous dihydrogen complex **10**, albeit at higher hydrogen pressures. Under 80 atm H_2, the ratio of dihydrogen complex versus unreacted hydride was only ~60%, a stark contrast to the required 40 atm H_2 pressure for maintaining complex **9** in solution. This explains the lack of observed dihydrogen coordination in previous work. We propose an upper limit for the H_2 bond length in complex **10** as 1.33 Å based on the T_1(-80 °C) of 70 ms. Complex **10** was found to be less stable than complex **9**; the dihydrogen complex resonances were only observable up to -60 °C as compared to -40 °C for complex **9**. Unfortunately, we cannot make a comparison of the bound dihydrogen bond lengths for complexes **9** and **10** since T_{1min} was also not achieved in our studies of complex **10**.

4.3.4 Proposed Mechanism for H/D Exchange Between H_2 and CD_3OD

The origin of the current investigation came from trying to understand the conversion and selectivity preferences for transforming glycerol to 1,3-propanediol and 1-propanol under varying acid concentrations. Our targeted transformation is conversion of glycerol to 1,3-propanediol, a highly attractive precursor to polyesters. In previous work from our group, we found that in the selective deoxygenation of glycerol, at low acid concentrations (stoichiometric versus iridium), higher selectivity for 1,3-propanediol was observed, however conversion of glycerol was low. In contrast, at high acid concentration, high selectivity for 1-propanol and higher glycerol conversion was observed. Thus, we hypothesized the origin of selectivity was based on the role of the acid in solution. There are two possibilities for the acid sources in solution capable of carrying out the dehydration reaction: added Brønsted acid or *in situ* generated iridium-dihydrogen complex. Examination of an isotope exchange between H_2 and CD_3OD was a model for understanding if protonation of glycerol by an iridium dihydrogen complex was feasible. Since we observed a dihydrogen complex (**9** or **10**) in this work and previously postulated it as a catalytic intermediate in glycerol deoxygenation, we postulated that **5** or **8** would be competent for isotope exchange of H_2 with deuterated alcohols. Based on our proposed catalytic cycle for glycerol deoxygenation with $^{(tBu)4}$(POCOP)Ir(CO) complexes, an iridium dihydrogen complex is expected to be acidic enough to protonate an alcohol moiety in glycerol in order to eliminate an equivalent of water. If a dihydrogen complex forms under acidic conditions in CD_2Cl_2 with CD_3OD, the single exchange product HD and double exchange product D_2 would be expected. Indeed, we were able to observe HD by ^{1}H NMR spectroscopy leading to the proposal of the following mechanism (Scheme 4.03).

Scheme 4.03. Proposed Mechanism for Isotope Exchange Between H_2 and CD_3OD

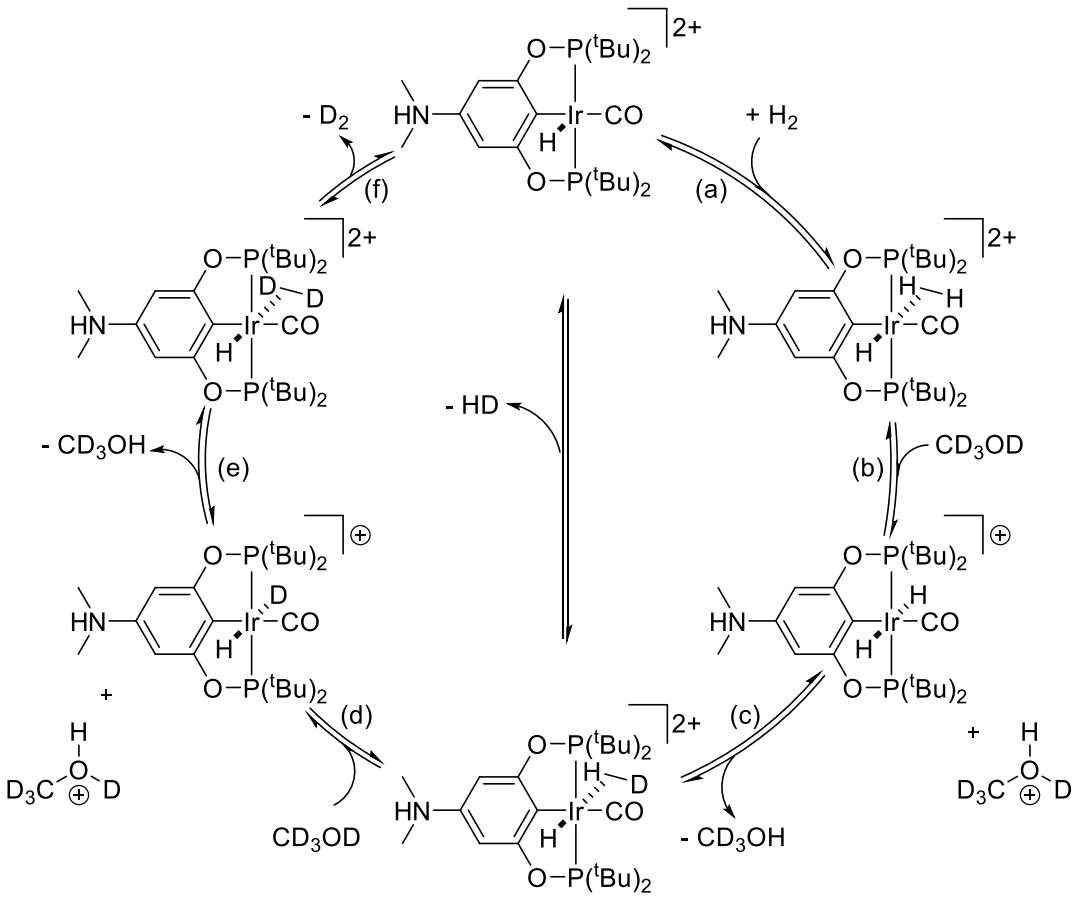

We propose the following mechanism for iridium-catalyzed isotope exchange of deuterated alcohols with H_2. In step (a), assuming the system contains enough acid to generate a five-coordinate Ir-H, hydrogen is added to the iridium center. Then in step (b), the iridium dihydrogen complex is expected to be quite acidic, and readily protonates CD_3OD, also generating an iridium *trans*-dihydride complex. The excess acid in solution could also protonate CD_3OD. Initial exchange of HOTf with CD_3OD to generate DOTf is possible; however, as observed in the ^1H NMR spectra, in the absence of added alcohol, the hydrogen resonance appears as a broadened signal. The protonated alcohol could then add a deuteron to the *trans*-dihydride in step (c) to give an iridium-(HD)-hydride complex. HD gas could then dissociate from iridium and regenerate the cycle. Steps (d)-(f) propose the same protonation/deprotonation steps as (a)-(c) to allow formation

of D_2. We were not able to observe D_2 in this study, but presumably some would form if this mechanism is operative. Similar mechanisms of exchange between hydrogen and alcohols catalyzed by late-metal complexes have been previously reported.[23] It is worth noting, exchange of the Ir-H in complex **5** with CD_3OD to give an iridium-deuteride was not evident by ^2H NMR spectroscopy, however it cannot be ruled out. There are many known examples of late-metal hydrides exchanging with deuterons such as in recent work by Szymczak where a ruthenium hydride supported by the bMepi ligand (bMepi = 1,3-(6′-methyl-2′-pyridylimino)isoindolate) was shown to exchange with D_2O.[24,25]

Since iridium catalyzed isotope exchange was observed, we can draw some conclusions from these studies. In the proposed glycerol deoxygenation pathway, protonation of an alcohol by an iridium dihydrogen complex is one potential route for dehydration of an alcohol. In that case, a *trans*-dihydride complex would also form. Here, the isotope exchange reactions suggest this proposal as feasible since deuteration of a *trans*-dihydride is the likely pathway for formation of HD gas. However, these studies could not be carried out with stoichiometric acid to unequivocally show that the dihydrogen complex is directly protonating the alcohol.

4.3.5 Feasibility of Stable Dihydrogen Complexes Under Catalytic Conditions

While complexes **9** and **10** were detected by NMR spectroscopy at low temperatures and under high pressures of H_2, we must consider their feasibility as intermediates in glycerol deoxygenation catalysis. Indeed, glycerol deoxygenation with (POCOP)Ir(CO) complexes is carried out under 80 atm H_2, however, reactions are run in acidic 1,4-dioxane/H_2O mixtures at 200 °C. The most stable dihydrogen complex, **9**, was only observed to -40 °C; dihydrogen is often

labile at modest temperatures. Furthermore, dihydrogen complexes **9** and **10** are expected to be acidic enough to protonate alcohols, as demonstrated in isotope exchange experiments with CD_3OD and H_2. Thus, if catalysis is performed in H_2O, deprotonation of a dihydrogen complex is expected to be quite facile, making observation of these species quite difficult under catalytic conditions. We hypothesize that complexes **9** and **10** are putative intermediates in glycerol deoxygenation catalysis.

4.4 Conclusions

This work provides further support for mechanistic proposals of glycerol deoxygenation with $^{(tBu)4}$(POCOP)Ir(CO) complexes. Incorporation of a protonated dimethylamino group on $^{(tBu)4}$(POCOP)Ir(CO) complexes increased the Lewis acidity of five-coordinate Ir-H complexes, facilitating stronger hydrogen coordination. This allowed direct observation of hydrogen coordination by low temperature ^{1}H NMR spectroscopy under high pressures of hydrogen. The five-coordinate Ir-H complexes [$^{(NMe2H)(tBu)4}$(POCOP)Ir(CO)(H)](OTf)$_2$ and [$^{(tBu)4}$(POCOP)Ir(CO)(H)]OTf were shown to catalyze H/D exchange between H_2 and CD_3OD. This serves as further evidence for the existence of an iridium-dihydrogen complex under glycerol deoxygenation conditions and the potential ability of an iridium-dihydrogen complex to protonate alcohols.

4.5 Experimental

General Considerations

All experiments and manipulations were performed using standard Schlenk techniques under an argon atmosphere or in an argon- or nitrogen-filled glovebox. Glassware and diatomaceous earth were dried in an oven maintained at 140 °C for at least 24 h. Deuterated solvents were dried over calcium hydride (CD_2Cl_2, CD_3OD). Protiated solvents were passed through columns of activated alumina and molecular sieves. All other reagents were used as received. ^{1}H NMR spectra were referenced to residual protiated solvents: $CHDCl_2$ (5.32 ppm). ^{31}P NMR shifts were referenced to an 85% H_3PO_4 external standard (0 ppm). NMR spectra were recorded on either a Bruker AV-800, AV-700, AV-500, AV-300, or DPX-200 NMR instrument. NMR spectra from high pressure experiments in PEEK NMR cells were recorded on a Varian 500 MHz spectrometer. [$^{(tBu)4}$(POCOP)Ir(CO)(H)]BArF$_{20}$ (**1**),[9] $^{(NMe2)(tBu)4}$(POCOP)Ir(CO) (**2**),[4] and $^{(tBu)4}$(POCOP)Ir(CO) (**7**).[8] were synthesized according to published procedures.

Experimental Procedures

*[$^{(NMe2H)(tBu)4}$(POCOP)Ir(CO)(H)(Cl)]Cl (**3**).* Under ambient atmosphere, a 20 mL scintillation vial was charged with a yellow 10 mL CH_2Cl_2 solution of $^{(NMe2)(tBu)4}$(POCOP)Ir(CO) (**2**) (52 mg, 0.079 mmol). A solution of HCl/Et_2O (7 mL of 2 M solution) was added to the vial, resulting in a color change to pale red. All volatiles were removed under vacuum. The resulting red oil was redissolved in 2 mL CH_2Cl_2 and 2 mL pentane was added to precipitate a red solid. Solvent was removed under vacuum. The resulting red solid was washed with pentane then dried under vacuum. ^{1}H NMR (CD_2Cl_2, 200.13 MHz): δ 14.43 (br s, 1H; Me_2N-*H*), 6.98 (s, 2H; C_{Ar}-*H*), 3.07 (s, 6H; HN(CH_3)$_2$),

1.61 (vt, $^{3}J_{PH} + {}^{5}J_{PH}$ = 16 Hz, 18H; P−C(CH_3)$_3$), 1.30 (vt, $^{3}J_{PH} + {}^{5}J_{PH}$ = 15 Hz, 18H; P−C(CH_3)$_3$), -18.04 (t, $^{2}J_{PH}$ = 13.5 Hz, 1H; Ir-H). ^{31}P{^{1}H} NMR (CD_2Cl_2, 81.02 MHz): δ 175.8 (s).

*Protonation of $^{(NMe2)(tBu)4}$(POCOP)Ir(CO) (**2**) with HOTf.* An NMR tube fitted with a J. Young style Teflon valve was charged with $^{(NMe2)(tBu)4}$(POCOP)Ir(CO) (**2**) (15 mg, 0.023 mmol). CD_2Cl_2 (0.4 mL) was vacuum transferred into the tube giving a yellow solution. In a nitrogen-filled glovebox, successive equivalents of HOTf (1 equiv = 2 µL) were added to the tube via micropipettor. The reaction was monitored via ^{1}H and ^{31}P NMR spectroscopy. Upon addition of 5 equiv HOTf or greater, no significant changes were observed by NMR spectroscopy. Representative spectra for identification of [$^{(NMe2H)(tBu)4}$(POCOP)Ir(CO)(H)](OTf)$_2$ (**5**) from reaction of **2** with 8 equiv HOTf: ^{1}H NMR (CD_2Cl_2, 300.10 MHz, 25 °C): δ 9.03 (br s, 1H; Me_2N-*H*), 7.08 (s, 2H; C_{Ar}-*H*), 3.35 (d, $^{3}J_{HH}$ = 5.1 Hz, 6H; HN(CH_3)$_2$), 1.39 (m, 36H; P−C(CH_3)$_3$), -36.01 (t, $^{2}J_{PH}$ = 10.4 Hz, 1H; Ir-*H*). ^{31}P{^{1}H} NMR (CD_2Cl_2, 121.49 MHz, 27 °C): δ 197.4 (s).

*Protonation of $^{(tBu)4}$(POCOP)Ir(CO) (**7**) with HOTf.* An NMR tube fitted with a J. Young style Teflon valve was charged with $^{(tBu)4}$(POCOP)Ir(CO) (**7**) (14 mg, 0.023 mmol). CD_2Cl_2 (0.4 mL) was vacuum transferred into the tube giving a yellow solution with most of the iridium solid remaining undissolved. In a nitrogen-filled glovebox, successive equivalents of HOTf (1 equiv = 2 µL) were added to the tube via micropipettor. Upon addition of the first equivalent of HOTf, all remaining solid dissolved. The reaction was monitored via ^{1}H and ^{31}P NMR spectroscopy. Representative spectra for identification of [$^{(tBu)4}$(POCOP)Ir(CO)(H)]OTf (**8**) from reaction of **7** with 5 equiv HOTf: ^{1}H NMR (CD_2Cl_2, 300.10 MHz, 24 °C): δ 7.37 (t, $^{3}J_{HH}$ = 8.1 Hz, 1H; Ar-*H*),

6.95 (d, $^{3}J_{HH}$ = 8.1 Hz, 2H; Ar-*H*), 1.38 (m, 36H; P−C(C*H*$_3$)$_3$), -35.76 (t, $^{2}J_{PH}$ = 10.1 Hz, 1H; Ir-*H*). $^{31}P\{^{1}H\}$ NMR (CD_2Cl_2, 121.49 MHz, 25 °C): δ 191.8 (s).

*H/D Exchange Between H_2 and CD_3OD with **2***. An NMR tube fitted with a J. Young style Teflon valve was charged with $^{(NMe2)(tBu)4}$(POCOP)Ir(CO) (**2**) (15 mg, 0.023 mmol). CD_2Cl_2 (0.4 mL) was vacuum transferred into the tube giving a yellow solution. In a nitrogen filled glovebox, C_6H_6 (2.0 µL, 0.022 mmol, internal standard) and HOTf (4.0 µL, 0.045 mmol) were added giving a light orange solution. CD_3OD (10 µL, 0.25 mmol) was added to the tube. The sample was freeze-pump-thawed three times then pressurized with 3 atm H_2. Detection of HD was hampered by overlap of a broad H_2 signal. The sample was degassed and additional HOTf (18 µL, 0.20 mmol) was added. The sample was freeze-pump-thawed three times then pressurized with 3 atm H_2. After mixing for 40 min, formation of HD as a result of isotope exchange between CD_3OD and H_2 was verified by ^{1}H NMR spectroscopy.

*H/D Exchange Between H_2 and CD_3OD with **7***. An NMR tube fitted with a J. Young style Teflon valve was charged with $^{(tBu)4}$(POCOP)Ir(CO) (**7**) (14 mg, 0.023 mmol). CD_2Cl_2 (0.5 mL) was vacuum transferred into the tube giving a yellow solution, and mostly undissolved **7**. In a nitrogen-filled glovebox, HOTf (20 µL, 0.23 mmol) was added to the tube, resulting in a homogenous orange solution (no solids observed). CD_3OD (10 µL, 0.25 mmol) was added to the tube and the sample was freeze-pump-thawed three times. The sample was pressurized with 3 atm H_2. After mixing for 2 h, formation of HD as a result of isotope exchange between CD_3OD and H_2 was verified by ^{1}H NMR spectroscopy.

High Pressure Reactions in PEEK NMR Cells (General Pressurization Procedure). Experiments were run at pressures up to 80 atm and temperatures between -80 to 25°C in PEEK high-pressure NMR spectroscopy tubes designed and built at Pacific Northwest National Laboratory, as reported previously.[10,26] *Operators of high-pressure equipment such as that required for these experiments should take proper precautions to minimize the risk of personal injury.* A reaction solution was added to a PEEK NMR cell inside a nitrogen-filled glovebox. The cell was sealed and connected to a high-pressure line equipped with a vacuum pump and an ISCO syringe pump. The line was purged with hydrogen three times. Opening the PEEK cell to static vacuum (3 × 30 s) degassed headspace above the sample. Hydrogen was delivered to the cell from an ISCO syringe pump running constantly at 40-80 atm. The contents of the PEEK NMR spectroscopy cell were mixed using a vortex mixer until the pressure stabilized.

*Low Temperature Observation of [$^{(NMe2H)(tBu)4}$(POCOP)Ir(CO)(H_2)(H)](OTf)$_2$ (**9**).* A 0.3 mL CD_2Cl_2 solution of $^{(NMe2)(tBu)4}$(POCOP)Ir(CO) (**2**) (22mg, 0.033 mmol) was added to a PEEK NMR cell followed by HOTf (30 µL, 0.34 mmol). Following the general pressurization procedure, 40 atm H_2 was added to the cell. The NMR probe was then cooled to -80 °C. Upon cooling, resonances consistent with an iridium-dihydrogen hydride complex were observed. ^{1}H NMR (CD_2Cl_2, 499.66 MHz, -80 °C): δ -2.38 (br s, 2H; Ir-H_2), -13.64 (s, 1H; Ir-*H*). Note, resonances from 17.0 to 0.0 ppm are broad, likely due to signal averaging between complexes **5** and **9**, thus a complete assignment of these peaks is not possible. ^{31}P{^{1}H} NMR (CD_2Cl_2, 202.30 MHz, -80 °C): δ 183.0 (s).

*Low Temperature Observation of [$^{(tBu)4}$(POCOP)Ir(CO)(H_2)(H)]$BArF_{20}$ (**10**).* A 0.3 mL CD_2Cl_2 solution of [$^{(tBu)4}$(POCOP)Ir(CO)(H)]$BArF_{20}$ (**1**) (28 mg, 0.022 mmol) was added to a PEEK NMR cell. Following the general pressurization procedure, 80 atm H_2 was added to the cell. The NMR probe was then cooled to -80 °C. Upon cooling, resonances consistent with an iridium-dihydrogen complex were observed. Note, resonances from 8.0 to 0.0 ppm are broad, likely due to signal averaging between complexes **1** and **10**, thus a complete assignment of these peaks is not possible. ^{1}H NMR (CD_2Cl_2, 499.66 MHz, -80 °C): δ -2.39 (br s, 2H; Ir-H_2), -13.41 (s, 1H; Ir-*H*). ^{31}P{^{1}H} NMR (CD_2Cl_2, 202.30 MHz, -80 °C): δ 178.6 (s).

4.6 Notes to Chapter

[1] Gallezot, P. *Chem. Soc. Rev.* **2012**, *41*, 1538–1558.
[2] Adduci, L. L.; Bender, T. A.; Dabrowski, J. A.; Gagné, M. R. *Nat. Chem.* **2015**, *7*, 576–581.
[3] Yang, F.; Hanna, M. A.; Sun, R. *Biotechnol. Biofuels* **2012**, *5*, 13.
[4] Lao, D. B.; Owens, A. C. E.; Heinekey, D. M.; Goldberg, K. I. *ACS Catal.* **2013**, *3*, 2391–2396.
[5] Schlaf, M. *Dalton Trans.* **2006**, 4645–4653.
[6] (a) Schlaf, M.; Ghosh, P.; Fagan, P. J.; Hauptman, E.; Bullock, R. M. *Adv. Synth. Catal.* **2009**, *351*, 789–800. (b) Ahmed-Foskey, T. J.; Heinekey, D. M.; Goldberg, K. I. *ACS Catal.* **2012**, *2*, 1285–1289. (c) Ren, D.; Wong, N. T.; Handoko, A. D.; Huang, Y.; Yeo, B. S. *J. Phys. Chem. Lett.* **2016**, *7*, 20–24.
[7] Pons, V.; Heinekey, D. M. *J. Am. Chem. Soc.* **2003**, *125*, 8428–8429.
[8] Goldberg, J. M.; Wong, G. W.; Brastow, K. E.; Kaminsky, W.; Goldberg, K. I.; Heinekey, D. M. *Organometallics* **2015**, *34*, 753–762.
[9] Goldberg, J. M.; Cherry, S. D. T.; Guard, L. M.; Kaminsky, W.; Goldberg, K. I.; Heinekey, D. M. *Organometallics* **2016**, *35*, 3546–3556.
[10] Yonker, C. R.; Linehan, J. C. *Prog. Nucl. Magn. Reson. Spectrosc.* **2005**, *47*, 95–109.
[11] Hansch, C.; Leo, A.; Taft, R. W. *Chem. Rev.* **1991**, *91*, 165–195.
[12] (a) Li, T.; Lough, A. J.; Zuccaccia, C.; Macchioni, A.; Morris, R. H. *Can. J. Chem.* **2006**, *84*, 164–175. (b) Li, T.; Lough, A. J.; Morris, R. H. *Chem. Eur. J.* **2007**, *13*, 3796–3803.
[13] Findlater, M.; Bernskoetter, W. H.; Brookhart, M. *J. Am. Chem. Soc.* **2010**, *132*, 4534–4535.
[14] (a) Desrosiers, P. J.; Cai, L.; Lin, Z.; Richards, R.; Halpern, J. *J. Am. Chem. Soc.* **1991**, *113*, 4173–4184. (b) Bayse, C. A.; Luck, R. L.; Schelter, E. J. *Inorg. Chem.* **2001**, *845*, 3463–3467.
[15] Lough, A. J.; Park, S.; Ramachandran, R.; Morris, R. H. *J. Am. Chem. Soc.* **1994**, *116*, 8356–8357.

[16] Peris, E.; Wessel, J.; Patel, B. P.; Crabtree, R. H. *J. Chem. Soc., Chem. Commun.* **1995**, 2175–2176.
[17] Epstein, L. M.; Shubina, E. S. *Coord. Chem. Rev.* **2002**, *231*, 165–181.
[18] Crabtree, R. H.; Siegbahn, P. E. M.; Eisenstein, O.; Rheingold, A. L.; Koetzle, T. F. *Acc. Chem. Res.* **1996**, *29*, 348–354.
[19] Belkova, N. V; Epstein, L. M.; Filippov, O. A.; Shubina, E. S. *Chem. Rev.* **2016**, *116*, 8545–8587.
[20] Bullock, R. M.; Song, J.-S.; Szalda, D. J. *Organometallics* **1996**, *15*, 2504–2516.
[21] Kubas, G. J. *Proc. Natl. Acad. Sci.* **2007**, *104*, 6901–6907.
[22] Crabtree, R. H. *Chem. Rev.* **2016**, *116*, 8750–8769.
[23] (a) Kovács, G.; Nádasdi, L.; Laurenczy, G.; Joó, F. *Green Chem.* **2003**, *5*, 213–217. (b) Carriker, J. L.; Wagenknecht, P. S.; Hosseini, M. A.; Fleming, P. E. *J. Mol. Catal. A Chem.* **2007**, *267*, 218–223. (c) Kubas, G. J. *Chem. Rev.* **2007**, *107*, 4152–4205.
[24] Hale, L. V. A.; Szymczak, N. K. *J. Am. Chem. Soc.* **2016**, *138*, 13489–13492.
[25] Other notable examples of H/D exchange with metal-hydrides: (a) Paterniti, D. P.; Roman, P. J., Jr.; Atwood, J. D. *Organometallics* **1997**, *16*, 3371–3376. (b) Frost, B. J.; Mebi, C. A. *Organometallics* **2004**, *23*, 5317–5323. (c) Tse, S. K. S.; Xue, P.; Lin, Z.; Jia, G. *Adv. Synth. Catal.* **2010**, *352*, 1512–1522.
[26] Yonker, C. R.; Linehan, J. C. *J. Organomet. Chem.* **2002**, *650*, 249-257.

Chapter 5

Oxidative Addition of Iodine to $^{(tBu)4}$(POCOP)Ir(CO) Complexes

5.1 Introduction

Pincer iridium complexes have been extensively studied for their applications to catalytic transformations,[1] yet there is still an abundance of fundamental organometallic reactions, particularly oxidative reactions, which have not been explored. We recently reported on the importance of steric factors in (POCOP)Ir(CO) (POCOP = κ^3-C_6H_3-2,6- $(OPR_2)_2$ for R = ^{t}Bu, ^{i}Pr) complexes and how a small change in the substituent bound to phosphorus can affect the coordination chemistry.[2] This steric effect was implicit in the alkane dehydrogenation work by Brookhart, Goldman, Jensen and others when ^{i}Pr substituted POCOP ligand gave improved activity over the commonly used ^{t}Bu derivative, however no direct comparison for (POCOP)Ir had previously been studied. Within the realm of (pincer)Ir complexes many reactions have been investigated, such as oxidative addition reactions of dihydrogen,[3] arenes,[4] anilines,[5] alkanes,[6] and C-O[7] and C-F bonds.[8] Surprisingly, oxidative addition reactions of halogens to (POCOP)Ir(CO) complexes have remained unexplored.

Oxidative addition reactions to iridium(I) have been of interest since the discovery of Vaska's complex.[9] An early report by Collman and Sears found that X_2 addition (where X = Cl, Br, I) to *trans*-[IrCl(CO)$(P(Ph)_2CH_3)_2$] favored *trans* addition in solution where the phosphines remained mutually *trans* to each other (eq 5.01).[10] Presumably, as proposed in that study, X_2 addition could have proceeded via a *cis* addition intermediate followed by isomerization. The *cis*-

dihalide complex was not observed. Alternatively, an S_N2 type mechanism could occur where X^+ first adds to the metal followed by association of X^- in the *trans* position.

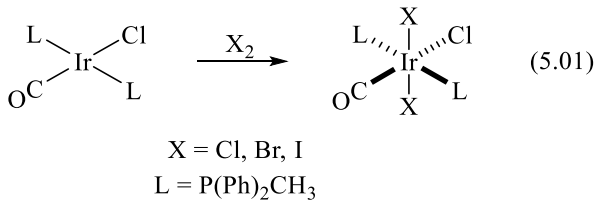

(5.01)

X = Cl, Br, I
L = $P(Ph)_2CH_3$

In contrast, later work by van Koten with (NCN)Pt(R) [where NCN = 2,6-$(Me_2NCH_2)_2C_6H_3$; R = phenyl, 2-tolyl, 4-tolyl] complexes found that oxidative addition of bromine or iodine resulted in *cis*-dihalide complexes (eq 5.02).[11] The difference in reactivity between these two square planar systems sparked our interest in examining analogous reactions of square planar (POOCP)Ir(CO) complexes with iodine.

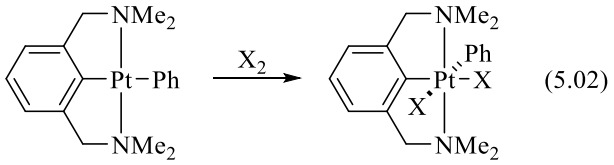

(5.02)

Here, we report that I_2 addition to (POCOP)Ir(CO) complexes is dependent on the *para* substituent on the aryl ring. For strong electron-donor substituents (i.e. NMe_2), iodine addition to Ir(I) favors formation of a five-coordinate Ir(III) iodide-carbonyl complex with an outer sphere polyiodide anion (either I_5^- or I_3^- depending on the amount of iodine used). Interestingly, however, if the *para* substituent on the (POCOP)Ir(CO) is methyl or a more electron-withdrawing moiety, iodine addition results in a *cis*-diiodide complex.

5.2 Results and Discussion

5.2.1 Reactions of $^{(X)(tBu)4}$(POCOP)Ir(CO) (X = H, Me, COOMe) with I_2

Addition of 1-1.5 equiv. iodine to $^{(H)(tBu)4}$(POCOP)Ir(CO) (**1**) in dichloromethane at room temperature results in *cis* addition to the iridium center giving exclusively $^{(H)(tBu)4}$(POCOP)Ir(CO)$(I)_2$ (**4**, eq 5.03). The product was characterized by ^{1}H and ^{31}P NMR spectroscopies. In the ^{1}H NMR spectrum, two virtual triplets are observed at 1.82 and 1.48 ppm resulting from a less symmetric octahedral product as compared to the square planar starting material. The ^{31}P{^{1}H} NMR spectrum shows only one singlet resonance at 138.6 ppm. Crystals of **4** suitable for X-ray diffraction were grown and analysis of the data verified *cis* addition of iodine to the iridium center (Figure 5.01). The carbonyl moiety is located *trans* to an iodide with a C-O bond length of 1.136(8) Å. Iodide addition to iridium results in distortion of the octahedral geometry around iridium. The axial iodide and CO moieties are not perpendicular to the pincer plane, but rather the iodide is bent towards the POCOP framework [C(1)-Ir(1)-I(2) angle is 81.87(15)°], while the carbonyl is bent away [C(1)-Ir(1)-C(23) angle is 104.9(2)°].

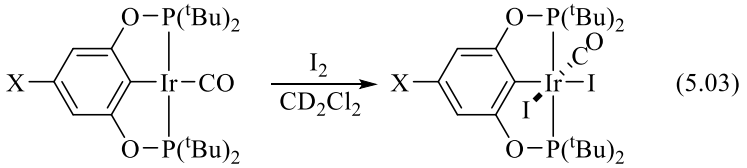

(5.03)

1; X = H
2; X = Me
3; X = COOMe

4; X = H
5; X = Me
6; X = COOMe

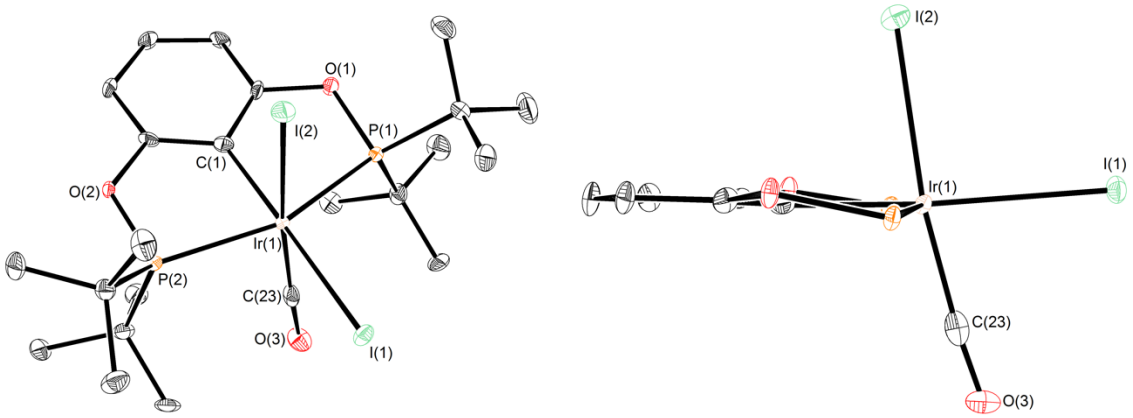

Figure 5.01. ORTEP[12] (full structure and side view) of $^{(H)(tBu)4}$(POCOP)Ir(CO)(I)$_2$ (**4**). Hydrogen atoms were omitted for clarity. In the side view, the ^{t}Bu groups bound to phosphorus were omitted for clarity. Selected bond lengths (Å) and angles (°) for **4**: C(1)-Ir(1) 2.040(6), P(1)-Ir(1) 2.4136(15), P(2)-Ir(1) 2.4075(15), Ir(1)-I(1) 2.7722(4), Ir(1)-I(2) 2.7305(4), C(23)-Ir(1) 1.855(6); C(1)-Ir(1)-I(1) 175.25(16), P(1)-Ir(1)-P(2) 157.04(5), I(1)-Ir(1)-I(2) 94.171(14), C(1)-Ir(1)-C(23) 104.9(2), Ir(1)-C(23)-O(3) 175.6(5).

When the *para* position in the aryl ring was substituted with a methyl or methyl ester group, oxidative addition to give *cis*-diiodide complexes was also observed resulting in $^{(Me)(tBu)4}$(POCOP)Ir(CO)(I)$_2$ (**5**) or $^{(COOMe)(tBu)4}$(POCOP)Ir(CO)(I)$_2$ (**6**), respectively. The ^{31}P{^{1}H} NMR spectra of both complexes showed singlet resonances, 138.9 ppm for **5** and 139.4 ppm for **6**. ^{1}H NMR spectra for both complexes show two virtual triplets between 1.85 – 1.47 ppm indicative of a complex with a break in symmetry above and below the pincer plane. For R = Me, by ^{31}P NMR spectroscopy, 96% of the total peak integration accounts for complex **5** with 4% impurities. When R = COOMe, the only signal observed by ^{31}P NMR spectroscopy is that attributed to **6**. Crystals of **6** suitable for diffraction were grown by slow evaporation of a THF/Et$_2$O solution, verifying formation of the *cis*-diiodide adduct (Figure 5.02).

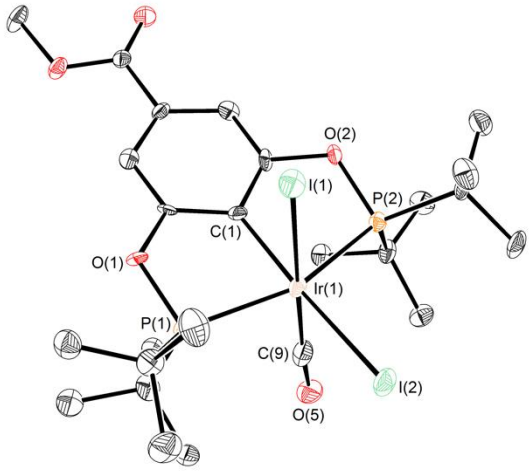

Figure 5.02. ORTEP[12] of $^{(COOMe)(tBu)4}$(POCOP)Ir(CO)$(I)_2$ (**6**). Hydrogen atoms were omitted for clarity. Selected bond lengths (Å) and angles (°) for **6**: C(1)-Ir(1) 2.044(8), P(1)-Ir(1) 2.388(2), P(2)-Ir(1) 2.395(2), Ir(1)-I(1) 2.7546(6), Ir(1)-I(2) 2.7488(6), Ir(1)-C(9) 1.860(10); C(1)-Ir(1)-I(2) 171.8(2), P(1)-Ir(1)-P(2) 156.93(7), I(1)-Ir(1)-I(2) 95.04(2), C(1)-Ir(1)-C(9) 106.0(3), Ir(1)-C(9)-O(5) 175.5(8).

5.2.2 Reaction of $^{(X)(tBu)4}$(POCOP)Ir(CO) (X = NMe_2) with I_2

Reaction of $^{(NMe2)(tBu)4}$(POCOP)Ir(CO) (**7**) with 1.1 equiv. (eq 5.04) iodine results in a single new species as demonstrated by ^{1}H and ^{31}P NMR spectral analysis. Substitution at the *para* position with a dimethylamino moiety changes the nature of the reaction product with respect to the iodine reaction products described above. The $^{31}P\{^1H\}$ NMR spectrum shows a singlet resonance at 186.2 ppm which is shifted ~50 ppm downfield from the complexes where X = COOMe, H, or Me. This lower field shift suggested a complex with a different coordination environment at iridium. Crystals suitable for X-ray diffraction were grown by vapor diffusion of pentane into a saturated dichloromethane solution of **7**. The structure revealed an unusual five-coordinate iridium iodide carbonyl complex, [$^{(NMe2)(tBu)4}$(POCOP)Ir(CO)(I)]$^+$ (**8**) with an outer sphere I_3^- anion. The structure was of poor quality, but was sufficient to define connectivity. When crystals were grown from a reaction mixture where 4 equiv iodine were used, the same five-

coordinate iodide carbonyl species was observed with an outer sphere I_5^- anion (Figure 5.03). This sample gave higher quality diffraction data. The amount of iodine relative to iridium did not affect the coordination chemistry at iridium, but rather the nature of the polyiodide anion. The geometry at the iridium center in the five-coordinate species is best described as distorted square-pyramidal based on $\tau = 0.04$.[13,14] Substitution of the dimethylamino group in the *para* position on the aryl backbone presumably leads to a much more electron-rich metal center as compared to -H, -Me, or -COOMe. Coordination of the second iodide at an electron-rich metal center is less favored.

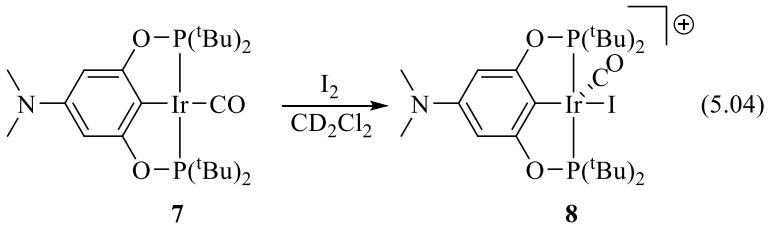

7 **8** (5.04)

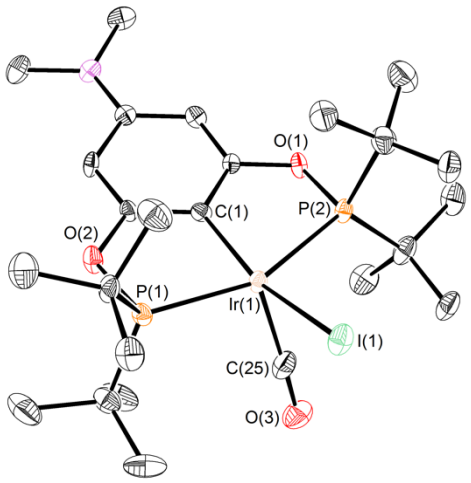

Figure 5.03. ORTEP[12] of $[^{(NMe2)(tBu)4}(POCOP)Ir(CO)(I)]^+$ (**8**). The I_5^- anion and hydrogen atoms were omitted for clarity. Selected bond lengths (Å) and angles (°) for **8**: C(1)-Ir(1) 1.961(6), Ir(1)-I(1) 2.7286(6), P(1)-Ir(1) 2.3503(17), P(2)-Ir(1) 2.339(2), Ir(1)-C(25) 1.845(8); C(1)-Ir(1)-I(1) 155.05(18), P(1)-Ir(1)-P(2) 157.46(7), C(1)-Ir(1)-C(25) 124.5(3), I(1)-Ir(1)-C(25) 80.5(2).

5.2.3 Reaction of $^{(X)(tBu)4}$(POCOP)Ir(CO) (X = OMe) with I_2

Since the strongly electron-donating NMe_2 substituted aryl backbone resulted in a monoiodo five-coordinate product, we presumed that the iridium center was too electron rich for binding of the second iodide. We synthesized the methoxy substituted analogue since it has a Hammett *para* substituent (σ_p) value between methyl (-0.17) and NMe_2 (-0.83).[15] Addition of 1.2 equiv iodine to $^{(OMe)(tBu)4}$(POCOP)Ir(CO) (**9**) in CD_2Cl_2 resulted in a new complex by both ^{1}H and ^{31}P NMR spectroscopies. In the ^{1}H NMR spectrum, there were two virtual triplets at 1.77 and 1.50 ppm consistent with a break in symmetry of the molecule; there are two different ligands above and below the pincer plane. Surprisingly, the $^{31}P\{^1H\}$ NMR spectrum showed a very broad resonance at ~140 ppm ($\omega_{1/2} \approx 2000$ Hz), suggesting a dynamic process in solution. Cooling the solution to -73 °C showed decoalescence of the broad ^{31}P NMR resonance to two narrower, but still broadened, resonances at 188 and 140 ppm in an approximate 1:7 ratio. The resonance at 188 ppm is consistent with a monoiodo complex similar to **8** and the resonance at 140 ppm is consistent with a *cis*-diiodide complex. The resonances at 188 and 140 ppm are both broadened, suggesting some type of exchange process between them. A reasonable explanation based on these data is rapid binding and dissociation of a ligand (i.e. iodide); we propose an equilibrium between a *cis*-diiodide and a five-coordinate monoiodo carbonyl cationic complex (Scheme 5.01). It is possible the methoxy substituent does not result in as electron-rich of a metal center as the NMe_2 analogue, giving rise to weak binding of the iodide.

Scheme 5.01. Proposed Equilibrium Mixture Resulting from Reaction of 9 with I_2

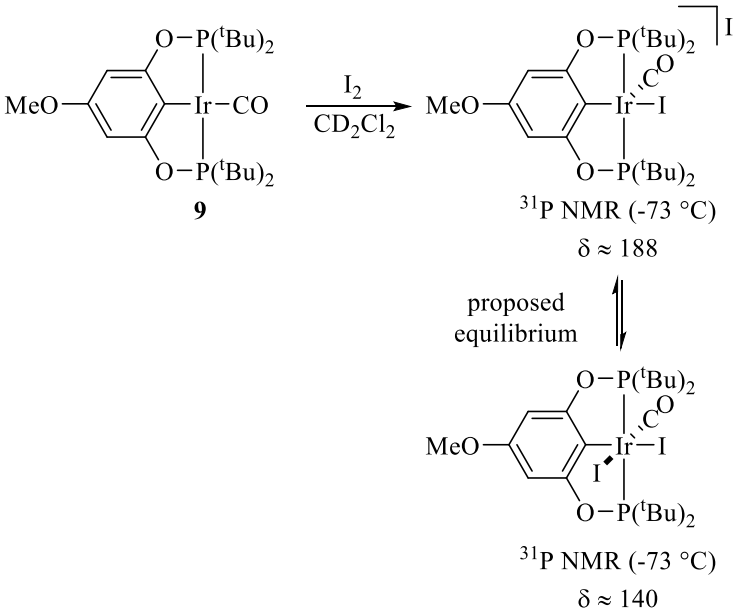

5.2.4 Mechanistic proposals for I_2 addition to $^{(X)(tBu)4}$(POCOP)Ir(CO) complexes

I_2 addition to (POCOP)Ir(CO) complexes showed a dependence on the aryl backbone substituent. For electron-rich substituents (NMe_2), formally, only I^+ was added to the iridium center while for electron-poor substituents, full addition of I_2 to iridium was observed giving *cis*-diiodide complexes. A similar type of formal I^+ addition to iridium was observed by Elsevier and coworkers when iodine was added to an Ir(I)-bis(iminophosphoranyl)methanide complex, resulting in a cationic monoiodo complex with I^-, I_3^- or I_5^- counterions.[16] We observed similar reactivity for reaction of **7** with I_2; the same iridium complex formed regardless of the amount of iodine, only the nature of the polyiodide anion would change with additional iodine. In the Elsevier system, it was proposed that reaction of the Ir(I) with I_2 first results in an end-on η^1-I_2 bound complex then a two-electron oxidation results in cleavage of the I-I bond. An end-on η^1-I_2 complex is plausible since van Koten observed that I_2 addition to (NCN)Pt(I), gave the crystallographically characterized (NCN)Pt(η^1-I_2)(I) complex (Figure 5.04).[17,18]

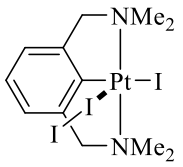

Figure 5.04. (NCN)Pt(η^1-I_2)(I) complex reported by van Koten and coworkers.

We propose a mechanism very similar to that reported by van Koten for X_2 addition to (NCN)Pt(R) complexes.[11,19] $^{(X)(tBu)4}$(POCOP)Ir(CO) first adds I^+ to give a five-coordinate iodo-carbonyl cationic species. Then, if the metal center is sufficiently Lewis acidic, either *cis* or *trans* attack of iodide could result in an iridium diiodide complex. Based on our results, *cis*-attack is more favored; however, we cannot rule out a pathway where *trans*-attack occurs. An additional explanation for the stability of complex **8** may be due to favorable formation of a polyiodide anion[20] rather than coordination of iodide to an unsaturated metal center; both I_3^- and I_5^- anions were observed in reactions of $^{(NMe2)(tBu)4}$(POCOP)Ir(CO) (**7**) with iodine. There may be a combination of ligand electronic effects as well as stabilization of polyiodide moieties that dictate the formation of iridium iodide complexes. The mechanistic proposal for reaction of $^{(X)(tBu)4}$(POCOP)Ir(CO) complexes with I_2 is shown in Scheme 5.02.

Scheme 5.02. Mechanistic Proposals for Formation of Iridium-Iodide Carbonyl Complexes

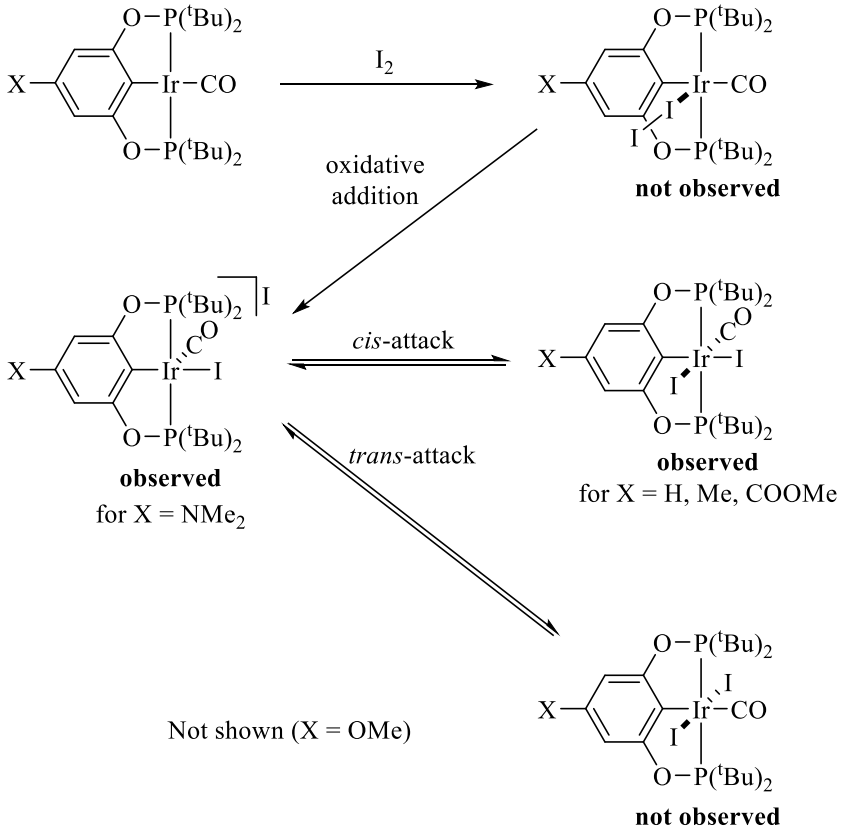

5.2.5 Reaction of $^{(X)(tBu)4}$(POCOP)Ir(CO) (X = NMe_2, COOMe) with Br_2

We were curious if a similar reactivity dependence on the aryl backbone substituent would be observed for reactions of $^{(X)(tBu)4}$(POCOP)Ir(CO) complexes with Br_2. Reaction of $^{(COOMe)(tBu)4}$(POCOP)Ir(CO) (**3**) with excess Br_2 (eq 5.05) resulted in a new clean product by NMR spectroscopy. In the ^{1}H NMR spectrum, loss of an aromatic resonance was observed. Two virtual triplets were observed at 1.73 and 1.50 ppm, consistent with a molecule with broken symmetry above and below the pincer plane. The ^{31}P NMR spectrum showed a singlet resonance at 145.6 ppm. The spectra were consistent with a *cis*-dibromide product; however, the lack of an aromatic signal was peculiar. Crystals suitable for diffraction were grown by vapor diffusion of pentane into

a CH_2Cl_2 solution. The X-ray structure shown in Figure 5.05 shows the *cis*-dibromide adduct $^{(COOMe)(tBu)4}(^{Br2}POCOP)Ir(CO)(Br)_2$ (**10**), however bromine was also incorporated into the C-H bonds on the aromatic backbone, explaining the disappearance of aromatic resonances.

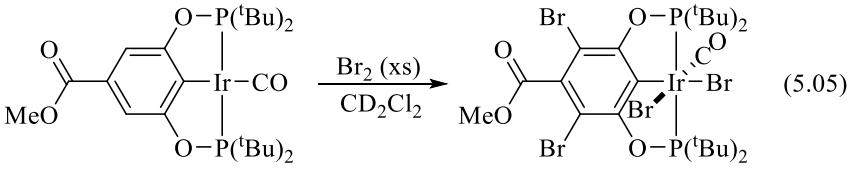

3 **10** (5.05)

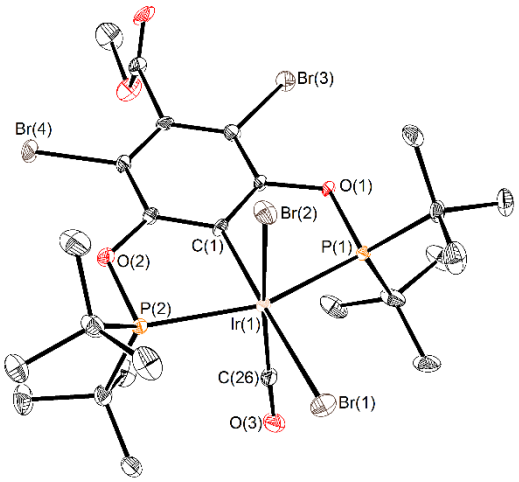

Figure 5.05. ORTEP[12] of $^{(COOMe)(tBu)4}(^{Br2}POCOP)Ir(CO)(Br)_2$ (**10**). Hydrogen atoms and one molecule of CH_2Cl_2 were omitted for clarity. Selected bond lengths (Å) and angles (°) for **10**: C(1)-Ir(1) 2.032(4), P(1)-Ir(1) 2.4067(11), P(2)-Ir(1) 2.4065(11), Ir(1)-Br(1) 2.5661(5), Ir(1)-Br(2) 2.5275(5), Ir(1)-C(26) 1.850(4); C(1)-Ir(1)-Br(1) 176.35(12), P(1)-Ir(1)-P(2) 158.68(4), Br(1)-Ir(1)-Br(2) 91.808(18), C(1)-Ir(1)-C(26) 105.28(18), Ir(1)-C(26)-O(3) 174.1(4).

Reaction of **7** with Br_2 resulted in different reactivity than the analogous reaction with **3**. Treatment of a CD_2Cl_2 solution of **7** with excess Br_2 (eq 5.06) resulted in a complex with broken symmetry, suggested by the observation of two different phosphorus peaks. In the ^{31}P NMR spectrum, a second order pair of doublets are observed at ~149 and 146.7 ppm ($^2J_{PP}$ = 356 Hz, Figure 5.06). The ^1H NMR spectrum in the ^{t}Bu region, shows two different resonances, however

the coupling pattern is quite complex, likely arising because the -P(^{t}Bu)$_2$ moieties are chemically and magnetically inequivalent (Figure 5.07). The dimethylamino resonance appears as a doublet of doublets (J = 5.1 Hz, J = 10.5 Hz). All attempts at growing crystals suitable for diffraction have been unsuccessful.

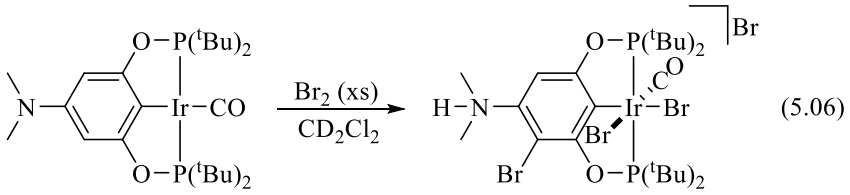

7 proposed (5.06)

It is proposed that the complex may have only one bromine incorporated into the aryl backbone, rendering the molecule asymmetric since the dimethyl amino resonance appears as a doublet of doublets. It is possible that bromination of a single aryl C-H bond results in loss of one equivalent of HBr that may further react at the dimethylamino moiety. A broadened resonance at 9.63 ppm, is consistent with an N-H peak. A protonated dimethylamino moiety would result in two chemically inequivalent methyl groups with similar chemical shifts, each coupled to an N-H proton. The ^{31}P NMR resonances in the range of 149-146 ppm suggest a dibromide carbonyl motif similar to complex **10**. Reaction of (POCOP)Ir(CO) complexes with Br_2 does not appear to give different reactivity at the metal center, regardless of the substituent on the aryl backbone. There are, however, slight deviations in the reactivity at the ligand backbone.

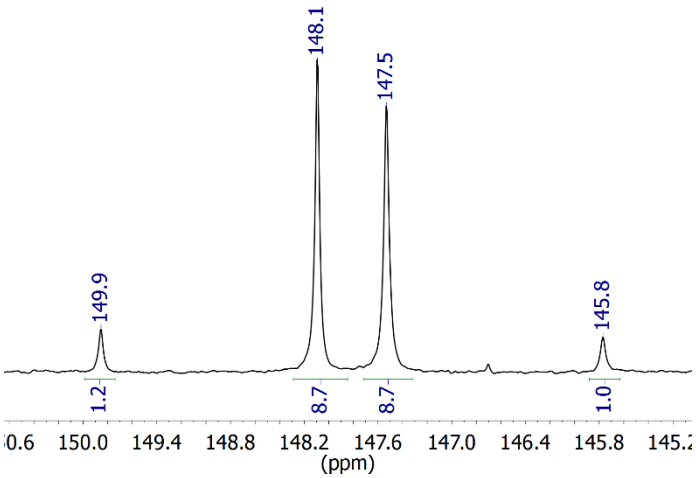

Figure 5.06. $^{31}P\{^{1}H\}$ NMR spectrum obtained after reaction of **7** with Br_2 showing two roofing doublets (202.31 MHz, CD_2Cl_2).

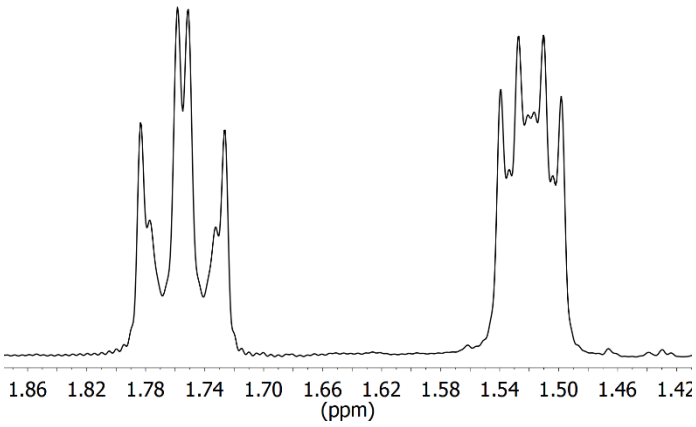

Figure 5.07. ^{1}H NMR spectrum of the ^{t}Bu region obtained after reaction of **7** with Br_2 (499.72 MHz, CD_2Cl_2).

5.3 Conclusions

Reactions of $^{(X)(tBu)4}$(POCOP)Ir(CO) complexes with iodine are reported. When X = H, Me, or COOMe, iodine addition results in *cis*-diiodide Ir(III) carbonyl complexes. When X = NMe_2, only I^+ is added to iridium, resulting in a cationic monoiodo carbonyl complex. The difference in

reactivity is attributed to the electron-density at the metal center imparted by the *para* substituent on the aryl backbone as well as possible stabilization of polyiodide anions for when X = NMe_2. Reaction of $^{(OMe)4(tBu)4}$(POCOP)Ir(CO) with I_2 results in a reaction that appears to contain an equilibrium mixture of a five-coordinate monoiodo carbonyl complex and a *cis*-diiodide complex. The data are consistent with a mechanism of first formal I^+ addition to iridium, followed by *cis* coordination of I^- (if the metal center is sufficiently Lewis acidic). Preliminary reactions of $^{(X)(tBu)4}$(POCOP)Ir(CO) complexes with Br_2 resulted in exclusively *cis*-dibromide adducts, with further bromination observed on the aryl backbone.

5.4 Experimental

General Considerations

All experiments and manipulations were performed using standard Schlenk techniques under an argon atmosphere or in an argon or nitrogen filled glove box unless otherwise noted. Glassware and diatomaceous earth were dried in an oven maintained at 140 °C for at least 24 h. Solvents were passed through columns of activated alumina and molecular sieves. Dichloromethane-d_2 was dried over calcium hydride and vacuum transferred prior to use. All other reagents were used as received. ^{1}H NMR spectra were referenced to residual $CHDCl_2$ at 5.32 ppm. ^{31}P NMR shifts were referenced to an 85% H_3PO_4 external standard (0 ppm). NMR spectra were recorded on either a Bruker AV-500, DRX-500, or AV-300 NMR instrument. Infrared spectra were recorded on a Bruker Tensor 27 FTIR instrument. X-ray data was collected at -173^{o}C on a Bruker APEX II single crystal X-ray diffractometer, Mo-radiation. Elemental analyses were performed under air-free conditions at the CENTC facility at the University of Rochester.

$^{(H)(tBu)4}$(POCOP)Ir(CO) (**1**),[2] $^{(COOMe)(tBu)4}$(POCOP)Ir(CO) (**3**),[21] and $^{(NMe2)(tBu)4}$(POCOP)Ir(CO) (**7**)[22] were synthesized according to published procedures. $^{(OMe)(tBu)4}$(POCOP)Ir(CO) (**9**) and $^{(Me)(tBu)4}$(POCOP)Ir(CO) (**2**) were previously reported,[4] however, here, they were prepared via the same method as **1**.

Preparation of $^{(X)(tBu)4}$(POCOP)Ir(CO)(I)$_2$. In air, 1 equiv. $^{(X)(tBu)4}$(POCOP)Ir(CO) was dissolved in 0.5 mL CD_2Cl_2 and added to a thin-walled NMR tube. To the solution was added 1-1.5 equiv. I_2. The resulting mixture was sonicated to ensure complete dissolution of all reactants. An immediate reaction was observed.

*X = H (**4**).* Using the general procedure 37 mg (0.042 mmol, 76%) $^{(H)(tBu)4}$(POCOP)Ir(CO)(I)$_2$ was isolated from the reaction of 34 mg (0.055 mmol) $^{(tBu)4}$(POCOP)Ir(CO) (**1**) and 20.6 mg (0.0812 mmol) I_2. The solution was brown. The solvent was removed under vacuum, then triturated with dichloromethane (2 x 1 mL). The resulting brown/yellow residue was dissolved in 2 mL benzene and lyophilized to give a pale yellow solid. Crystals suitable for X-ray diffraction were grown by slow evaporation of a dichloromethane/pentane solution. Anal. Calcd for $C_{23}H_{39}I_2IrO_3P_2$: C, 31.70; H, 4.51. Found: C, 31.63; H, 4.46. ^{1}H NMR (CD_2Cl_2, 300.10 MHz, 25 °C): δ 6.91 (t, $^3J_{HH}$ = 8.0 Hz, 1H; Ar-*H*), 6.63 (d, $^3J_{HH}$ = 8.0 Hz, 2H; Ar-*H*), 1.82 (vt, $^3J_{PH}$ + $^5J_{PH}$ = 15.8 Hz, 18H; PC(C*H*$_3$)$_3$), 1.48 (vt, $^3J_{PH}$ + $^5J_{PH}$ = 14.2 Hz, 18H; PC(C*H*$_3$)$_3$). ^{31}P{^{1}H} NMR (CD_2Cl_2, 121.49 MHz, 25 °C): δ 138.6 (s). IR (solution, CH_2Cl_2, cm^{-1}): ν(CO) 2031.

*X = Me (**5**).* Using the general procedure, $^{(Me)(tBu)4}$(POCOP)Ir(CO)(I)$_2$ was prepared from the reaction of 17 mg (0.027 mmol) $^{(Me)(tBu)4}$(POCOP)Ir(CO) (**2**) and 7.4 mg (0.029 mmol) I_2. The resulting solution was olive green. ^{1}H NMR (CD_2Cl_2, 499.72 MHz, 25 °C): δ 6.50 (s, 2H; Ar-*H*),

2.28 (s, 3H; Ar-CH_3), 1.81 (vt, $^3J_{PH}$ + $^5J_{PH}$ = 15.8 Hz, 18H; PC(CH_3)$_3$), 1.48 (vt, $^3J_{PH}$ + $^5J_{PH}$ = 14.1 Hz, 18H; PC(CH_3)$_3$). $^{31}P\{^1H\}$ NMR (CD_2Cl_2, 202.31 MHz, 25 °C): δ 138.9 (s). IR (solution, CH_2Cl_2, cm^{-1}): ν(CO) 2029.

*X = COOMe (**6**).* Using the general procedure, $^{(COOMe)(tBu)4}$(POCOP)Ir(CO)(I)$_2$ was prepared from the reaction of 15 mg (0.022 mmol) $^{(COOMe)(tBu)4}$(POCOP)Ir(CO) (**3**) and 6.7 mg (0.026 mmol) I_2. The resulting solution was red. Crystals suitable for X-ray diffraction were grown by slow evaporation of a THF/Et_2O solution. ^1H NMR (CD_2Cl_2, 499.72 MHz, 25 °C): δ 7.29 (s, 2H; Ar-*H*), 3.84 (s, 3H; Ar-COOCH_3), 1.83 (vt, $^3J_{PH}$ + $^5J_{PH}$ = 16.0 Hz, 18H; PC(CH_3)$_3$), 1.49 (vt, $^3J_{PH}$ + $^5J_{PH}$ = 14.2 Hz, 18H; PC(CH_3)$_3$). $^{31}P\{^1H\}$ NMR (CD_2Cl_2, 202.31 MHz, 25 °C): δ 139.4 (s). IR (solution, CH_2Cl_2, cm^{-1}): ν(CO) 2034.

*Preparation of [$^{(NMe2)(tBu)4}$(POCOP)Ir(CO)(I)]$^+$ (**8**).* In air, 13 mg (0.020 mmol) $^{(NMe2)(tBu)4}$(POCOP)Ir(CO) (**7**) was dissolved in 0.5 mL CD_2Cl_2 in a thin-walled NMR tube. To the yellow solution was added 5.5 mg (0.022 mmol) I_2, resulting in a dark blue solution upon mixing. The solvent was removed under vacuum then redissolved in CH_2Cl_2 and filtered through a 0.2 µm syringe filter. Vapor diffusion of pentane into a CH_2Cl_2 solution of **8** at room temperature resulted in dark brown/purple needle crystals suitable for X-ray diffraction. X-ray analysis revealed a five-coordinate complex with an outer sphere I_3 anion. Redissolving the crystals in solution gave the same spectra as before crystallization. Crystals grown via the same method from a reaction mixture containing 4 equiv. iodine resulted in the same cationic five-coordinate complex, however with an outer sphere I_5 anion. ^1H and $^{31}P\{^1H\}$ NMR spectra of the I_3^- and I_5^- species were identical. ^1H NMR (CD_2Cl_2, 300.13 MHz, 22 °C): δ 6.55 (s, 2H; Ar-*H*), 2.83 (s, 6H; N(CH_3)$_2$), 1.58 (m, 36H; PC(CH_3)$_3$). $^{31}P\{^1H\}$ NMR (CD_2Cl_2, 121.51 MHz, 22 °C): δ 186.2 (s).

*Reaction of $^{(OMe)(tBu)4}$(POCOP)Ir(CO) (**9**) with I_2.* An NMR tube fitted with a J. Young style Teflon valve was charged with 19 mg (0.029 mmol) $^{(OMe)(tBu)4}$(POCOP)Ir(CO) (**9**) and 9.0 mg (0.035 mmol) I_2. 0.4 mL CD_2Cl_2 was added into the tube resulting in a dark green solution. The sample was freeze-pump-thawed three times to remove air. ^{1}H NMR (CD_2Cl_2, 499.71 MHz, 25 °C): δ 6.36 (s, 2H; Ar-*H*), 3.77 (s, 3H; Ar-OC*H*$_3$), 1.77 (vt, $^3J_{PH} + {}^5J_{PH}$ = 15.6 Hz, 18H; PC(C*H*$_3$)$_3$), 1.50 (vt, $^3J_{PH} + {}^5J_{PH}$ = 14.2 Hz, 18H; PC(C*H*$_3$)$_3$). ^{31}P{^{1}H} NMR (CD_2Cl_2, 202.31 MHz, 25 °C): very broad resonance centered at ~140 ppm. Unknown impurities were observed in the ^{31}P NMR spectrum at 144, 142, 133, and 17 ppm, however upon cooling the sample to -73 °C, no change in these resonances was observed. Only decoalescence of the broad ^{31}P NMR resonance at ~140 ppm was observed.

*$^{(COOMe)(tBu)4}$(^{Br2}POCOP)Ir(CO)(Br)$_2$ (**10**).* In air, 13 mg (0.019 mmol) $^{(COOMe)(tBu)4}$(POCOP)Ir(CO) (**3**) was dissolved in 0.4 mL CD_2Cl_2 giving an orange solution. Added 12 µL (0.23 mmol) Br_2 resulting in a dark orange solution. Crystals of **10** suitable for diffraction were grown by first removing all volatiles followed by preparing a vapor diffusion of pentane into a CH_2Cl_2 solution of **10**. ^{1}H NMR (CD_2Cl_2, 300.10 MHz, 12 °C): δ 3.93 (s, 3H; COOC*H*$_3$), 1.73 (vt, $^3J_{PH} + {}^5J_{PH}$ = 16.4 Hz, 18H; PC(C*H*$_3$)$_3$), 1.50 (vt, $^3J_{PH} + {}^5J_{PH}$ = 14.8 Hz, 18H; PC(C*H*$_3$)$_3$). ^{31}P{^{1}H} NMR (CD_2Cl_2, 121.49 MHz, 12 °C): δ 145.6 (s).

*Reaction of $^{(NMe2)(tBu)4}$(POCOP)Ir(CO) (**7**) with Br_2.* In air, an NMR tube was charged with 16 mg (0.024 mmol) $^{(NMe2)(tBu)4}$(POCOP)Ir(CO) (**7**) and 0.4 mL CD_2Cl_2 giving a dark yellow solution. 8 µL (0.16 mmol) Br_2 was added to the tube giving an orange solution. ^{1}H NMR (CD_2Cl_2, 499.72

MHz, 25 °C): δ 9.63 (br s, 1H; N-*H*), 7.06 (s, 1H; Ar-*H*), 3.48 (dd, J = 5.1 Hz, J = 10.5 Hz, 6H; N(CH_3)$_2$), 1.75 (m, 18H; PC(CH_3)$_3$), 1.52 (m, 18H; PC(CH_3)$_3$). ^{31}P{^{1}H} NMR (CD_2Cl_2, 202.31 MHz, 25 °C): δ 149 (d, $^2J_{PP}$ = 356 Hz, 1P; *P*C(CH$_3$)$_3$), 146.7 (d, $^2J_{PP}$ = 356 Hz, 1P; *P*C(CH$_3$)$_3$).

5.5 Notes to Chapter

[1] Choi, J.; MacArthur, A. H. R.; Brookhart, M.; Goldman, A. S. *Chem. Rev.* **2011**, *111*, 1761–1779.

[2] Goldberg, J. M.; Wong, G. W.; Brastow, K. E.; Kaminsky, W.; Goldberg, K. I.; Heinekey, D. M. *Organometallics* **2015**, *34*, 753-762.

[3] (a) Krogh-Jespersen, K.; Czerw, M.; Zhu, K.; Singh, B.; Kanzelberger, M.; Darji, N.; Achord, P. D.; Renkema, K. B.; Goldman, A. S. *J. Am. Chem. Soc.* **2002**, *124*, 10797-10809. (b) Goldberg, J. M.; Cherry, S. D. T.; Guard, L. M.; Kaminsky, W.; Goldberg, K. I.; Heinekey, D. M. *Organometallics* **2016**, *35*, 3546–3556.

[4] Göttker-Schnetmann, I.; White, P. S.; Brookhart, M. *Organometallics* **2004**, *23*, 1766-1776.

[5] Sykes, A. C.; White, P.; Brookhart, M. *Organometallics* **2006**, *25*, 1664-1675.

[6] (a) Goldman, A. S.; Roy, A. H.; Huang, Z.; Ahuja, R.; Schinski, W.; Brookhart, M. *Science* **2006**, *312*, 257-261. (b) Zhu, K.; Achord, P. D.; Zhang, X.; Krogh-Jespersen, K.; Goldman, A. S. *J. Am. Chem. Soc.* **2004**, *126*, 13044-13053.

[7] Kundu, S.; Choi, J.; Wang, D. Y.; Choliy, Y.; Emge, T. J.; Krogh-Jespersen, K.; Goldman, A. S. *J. Am. Chem. Soc.* **2013**, *135*, 5127-5143.

[8] Choi, J.; Wang, D. Y.; Kundu, S.; Choliy, Y.; Emge, T. J.; Krogh-Jespersen, K.; Goldman, A. S. *Science* **2011**, *332*, 1545-1548.

[9] (a) Chock, P. B.; Halpern, J. *J. Am. Chem. Soc.* **1966**, *88*, 3511–3514. (b) Labinger, J. A.; Osborn, J. A. *Inorg. Chem.* **1980**, *19*, 3230–3236. (c) Labinger, J. A.; Osborn, J. A.; Coville, N. J. *Inorg. Chem.* **1980**, *19*, 3236–3243. (d) Labinger, J. A. *Organometallics* **2015**, *34*, 4784–4795.

[10] Collman, J. P.; Sears, C. T. *Inorg. Chem.* **1968**, *7*, 27-32.

[11] van Koten, G.; Terheijden, J.; van Beek, J. A. M.; Wehman-Ooyevaar, I. C. M.; Muller, F.; Stam, C. H. *Organometallics* **1990**, *9*, 903–912.

[12] (a) Farrugia, L. J. *J. Appl. Cryst.* **2012**, *45*, 849-854. (b) Farrugia, L. J. *J. Appl. Cryst.* **1997**, *30*, 565.

[13] Addison, A. W.; Rao, T. N.; Reedijk, J.; van Rijn, J.; Verschoor, G. C. *J. Chem. Soc., Dalton Trans.* **1984**, 1349–1356.

[14] Roddick, D. M.; Zargarian, D. *Inorg. Chim. Acta* **2014**, *422*, 251–264.

[15] (a) Hansch, C.; Leo, A.; Taft, R. W. *Chem. Rev.* **1991**, *91*, 165–195. (b) Hammett, L. P. *Chem. Rev.* **1935**, *17*, 125–136.

[16] Imhoff, P.; Gülpen, J. H.; Vrieze, K.; Smeets, W. J. J.; Spek, A. L.; Elsevier, C. J. *Inorg. Chim. Acta* **1995**, *235*, 77-88.

[17] van Beek, J. A. M.; van Koten, G.; Smeets, W. J. J.; Spek, A. L. *J. Am. Chem. Soc.* **1986**, *108*, 5010–5011.

[18] Gossage, R. A.; Ryabov, A. D.; Spek, A. L.; Stufkens, D. J.; van Beek, J. A. M.; van Eldik, R.; van Koten, G. *J. Am. Chem. Soc.* **1999**, *121*, 2488–2497.

[19] Nabavizadeh, S. M.; Amini, H.; Rashidi, M.; Pellarin, K. R.; McCready, M. S.; Cooper, B. F. T.; Puddephatt, R. J. *J. Organomet. Chem.* **2012**, *713*, 60–67.

[20] Svensson, P. H.; Kloo, L. *Chem. Rev.* **2003**, *103*, 1649–1684.

[21] Goldberg, K. I.; Heinekey, D. M.; Weliange, N. M.; Ahmed, T. J.; Camp, E. R.; Wong, G.; Lao, D. Methods for selective removal of hydroxyls from polyols. US WO 2013130972 A1, September 6, 2013.

[22] Lao, D. B.; Owens, A. C. E.; Heinekey, D. M.; Goldberg, K. I. *ACS Catal.* **2013**, *3*, 2391–2396.

Bibliography

Abdur-Rashid, K.; Fong, T. P.; Greaves, B.; Gusev, D. G.; Hinman, J. G.; Landau, S. E.; Lough, A. J.; Morris, R. H. *J. Am. Chem. Soc.* **2000**, *122*, 9155−9171.

Adams, J. J.; Arulsamy, N.; Roddick, D. M. *Organometallics* **2011**, *30*, 697−711.

Adams, J. J.; Lau, A.; Arulsamy, N.; Roddick, D. M. *Organometallics* **2011**, *30*, 689-696.

Addison, A. W.; Rao, T. N.; Reedijk, J.; van Rijn, J.; Verschoor, G. C. *J. Chem. Soc., Dalton Trans.* **1984**, 1349–1356.

Adduci, L. L.; Bender, T. A.; Dabrowski, J. A.; Gagné, M. R. *Nat. Chem.* **2015**, *7*, 576–581.

Ahmed-Foskey, T. J.; Heinekey, D. M.; Goldberg, K. I. *ACS Catal.* **2012**, *2*, 1285–1289.

Ahuja, R.; Punji, B.; Findlater, M.; Supplee, C.; Schinski, W.; Brookhart, M.; Goldman, A. S. *Nat. Chem.* **2011**, *3*, 167-171.

Anastas, P. T.; Warner, J. C. *Green Chemistry: Theory and Practice*, Oxford University Press: New York, 1998; pp 30.

Arundhathi, R.; Mizugaki, T.; Mitsudome, T.; Jitsukawa, K.; Kaneda, K. *ChemSusChem* **2013**, *6*, 1345–1347.

Baber, R. A.; Bedford, R. B.; Betham, M.; Blake, M. E.; Coles, S. J.; Haddow, M. F.; Hursthouse, M. B.; Orpen, A. G.; Pilarski, L. T.; Pringle, P. G.; Wingad, R. L. *Chem. Commun.* **2006**, *2*, 3880-3882.

Bailey, W. D.; Parkes, M. V.; Kemp, R. A.; Goldberg, K. I. Reactions of Square Planar d^8 Pincer Complexes with Oxygen and Hydrogen. In *Pincer and Pincer-Type Complexes: Application in Organic Synthesis and Catalysis*; Szabo, K. J., Wendt, O. F., Eds.; Wiley-VCH: Weinheim, Germany, 2014; pp 281−298.

Baumgarth, H.; Braun, T.; Braun, B.; Laubenstein, R.; Herrmann, R. *Eur. J. Inorg. Chem.* **2015**, 3157–3168.

Bayse, C. A.; Luck, R. L.; Schelter, E. J. *Inorg. Chem.* **2001**, *845*, 3463–3467.

Bedford, R. B.; Chang, Y.-N.; Haddow, M. F.; McMullin, C. L. *Dalton Trans.* **2011**, *40*, 9034-9041.

Behr, A.; Eilting, J.; Irawadi, K.; Leschinski, J.; Lindner, F. *Green Chem.* **2008**, *10*, 13–30.

Belkova, N. V; Epstein, L. M.; Filippov, O. A.; Shubina, E. S. *Chem. Rev.* **2016**, *116*, 8545–8587.

Ben-Ari, E.; Leitus, G.; Shimon, L. J. W.; Milstein, D. *J. Am. Chem. Soc.* **2006**, *128*, 15390−15391.

Besson, M.; Gallezot, P.; Pigamo, A.; Reifsnyder, S. *Appl. Catal. A: Gen.* **2003**, *250*, 117–124.

Besson, M.; Gallezot, P.; Pinel, C. *Chem. Rev.* **2014**, *114*, 1827–1870.

Bhagan, S.; Wayland, B. B. *Inorg. Chem.* **2011**, *50*, 11011-11020.

Blake, D. M.; Kubota, M. *Inorg. Chem.* **1970**, *9*, 989-991.

Blum, O.; Milstein, D. *J. Am. Chem. Soc.* **2002**, *124*, 11456–11467.

Böhrsch, V.; Serwa, R.; Majkut, P.; Krause, E.; Hackenberger, C. P. R. *Chem. Commun.* **2010**, *46*, 3176-3178.

Brown, J. M.; Dayrit, F. M.; Lightowler, D. *J. Chem. Soc., Chem. Commun.* **1983**, 414−415.

Bullock, R. M.; Song, J.-S.; Szalda, D. J. *Organometallics* **1996**, *15*, 2504–2516.

Carriker, J. L.; Wagenknecht, P. S.; Hosseini, M. A.; Fleming, P. E. *J. Mol. Catal. A Chem.* **2007**, *267*, 218–223.

Celaje, J. J. A.; Lu, Z.; Kedzie, Elyse, A.; Terrile, N. J.; Lo, J. N.; Williams, T. J. *Nat. Commun.* **2016**, *7*, 11308.

Celińska, E. *Biotechnol. Adv.* **2010**, *28*, 519–530.

Černý, M.; Málek, J. *Tetrahedron Lett.* **1969**, *10*, 1739-1742.

Che, T. M. Production of propanediols. US 4642394, February 10, 1987.

Chen, Z.; Liu, D. *Biotechnol. Biofuels* **2016**, *9*, 205.

Cherry, S. D. T.; Kaminsky, W.; Heinekey, D. M. *Organometallics* **2016**, *35*, 2165-2169.

Chianese, A. R.; Shaner, S. E.; Tendler, J. A.; Pudalov, D. M.; Shopov, D. Y.; Kim, D.; Rogers, S. L.; Mo, A. *Organometallics* **2012**, *31*, 7359-7367.

Chock, P. B.; Halpern, J. *J. Am. Chem. Soc.* **1966**, *88*, 3511–3514.

Choi, J.; MacArthur, A. H. R.; Brookhart, M.; Goldman, A. S. *Chem. Rev.* **2011**, *111*, 1761–1779.

Choi, J.; Wang, D. Y.; Kundu, S.; Choliy, Y.; Emge, T. J.; Krogh-Jespersen, K.; Goldman, A. S. *Science* **2011**, *332*, 1545-1548.

Ciriminna, R.; Pina, C. Della; Rossi, M.; Pagliaro, M. *Eur. J. Lipid Sci. Technol.* **2014**, *116*, 1432–1439.

Coll, D.; Delbecq, F.; Aray, Y.; Sautet, P. *Phys. Chem. Chem. Phys.* **2011**, *13*, 1448–1456.

Collman, J. P. *Acc. Chem. Res.* **1968**, *1*, 136–143.

Collman, J. P.; Sears, C. T. *Inorg. Chem.* **1968**, *7*, 27-32.

Crabtree, R. H. *Chem. Rev.* **2016**, *116*, 8750−8769.

Crabtree, R. H.; Siegbahn, P. E. M.; Eisenstein, O.; Rheingold, A. L.; Koetzle, T. F. *Acc. Chem. Res.* **1996**, *29*, 348–354.

de Geest, D. J.; O'Keefe, B. J.; Steel, P. J. *J. Organomet. Chem.* **1999**, *579*, 97-105.

Denney, M. C.; Pons, V.; Hebden, T. J.; Heinekey, D. M.; Goldberg, K. I. *J. Am. Chem. Soc.* **2006**, *128*, 12048-12049.

Desrosiers, P. J.; Cai, L.; Lin, Z.; Richards, R.; Halpern, J. *J. Am. Chem. Soc.* **1991**, *113*, 4173–4184.

Deutsch, P. P.; Eisenberg, R. *Chem. Rev.* **1988**, *88*, 1147−1161.

Dobereiner, G. E.; Yuan, J.; Schrock, R. R.; Goldman, A. S.; Hackenberg, J. D. *J. Am. Chem. Soc.* **2013**, *135*, 12572-12575.

Drago, R. S., Physical Methods for Chemists. 2nd ed.; Surfside Scientific Publishers: Gainesville, Fl, 1992.

Drent, E.; Jager, W. W. Hydrogenolysis of glycerol. US 6080898, June 27, 2000.

Epstein, L. M.; Shubina, E. S. *Coord. Chem. Rev.* **2002**, *231*, 165–181.

Fantasia, S.; Egbert, J. D.; Jurčík, V.; Cazin, C. S. J.; Jacobsen, H.; Cavallo, L.; Heinekey, D. M.; Nolan, S. P. *Angew. Chem. Int. Ed.* **2009**, *48*, 5182−5186.

Farrugia, L. J. *J. Appl. Cryst.* **1997**, *30*, 565.

Farrugia, L. J. *J. Appl. Cryst.* **2012**, *45*, 849-854.

Feller, M.; Diskin-Posner, Y.; Leitus, G.; Shimon, L. J. W.; Milstein, D. *J. Am. Chem. Soc.* **2013**, *135*, 11040-11047.

Findlater, M.; Bernskoetter, W. H.; Brookhart, M. *J. Am. Chem. Soc.* **2010**, *132*, 4534−4535.

Frech, C. M.; Milstein, D. *J. Am. Chem. Soc.* **2006**, *128*, 12434-12435.

Frost, B. J.; Mebi, C. A. *Organometallics* **2004**, *23*, 5317–5323.

Fulmer, G. R.; Miller, A. J. M.; Sherden, N. H.; Gottlieb, H. E.; Nudelman, A.; Stoltz, B. M.; Bercaw, J. E.; Goldberg, K. I. *Organometallics* **2010**, *29*, 2176-2179.

Gallezot, P. *Chem. Soc. Rev.* **2012**, *41*, 1538–1558.

García-Fernández, S.; Gandarias, I.; Requies, J.; Soulimani, F.; Arias, P. L.; Weckhuysen, B. M. *Appl. Catal. B Environ.* **2017**, *204*, 260–272.

Gessen, J. P.; Jacquesy, J. C.; Jouannetaud, M. P. *J. Chem. Soc., Chem. Commun.* **1980**, 1128-1129.

Ghosh, R.; Emge, T. J.; Krogh-Jespersen, K.; Goldman, A. S. *J. Am. Chem. Soc.* **2008**, *130*, 11317-11327.

Goldberg, J. M.; Cherry, S. D. T.; Guard, L. M.; Kaminsky, W.; Goldberg, K. I.; Heinekey, D. M. *Organometallics* **2016**, *35*, 3546–3556.

Goldberg, J. M.; Wong, G. W.; Brastow, K. E.; Kaminsky, W.; Goldberg, K. I.; Heinekey, D. M. *Organometallics* **2015**, *34*, 753–762.

Goldberg, K. I.; Heinekey, D. M.; Weliange, N. M.; Ahmed, T. J.; Camp, E. R.; Wong, G.; Lao, D. Methods for selective removal of hydroxyls from polyols. US WO 2013130972 A1, September 6, 2013.

Goldman, A. S.; Roy, A. H.; Huang, Z.; Ahuja, R.; Schinski, W.; Brookhart, M. *Science* **2006**, *312*, 257–261.

Gong, L.; Lu, Y.; Ding, Y.; Lin, R.; Li, J.; Dong, W.; Wang, T.; Chen, W. *Appl. Catal. A: Gen.* **2010**, *390*, 119–126.

Gossage, R. A.; Ryabov, A. D.; Spek, A. L.; Stufkens, D. J.; van Beek, J. A. M.; van Eldik, R.; van Koten, G. *J. Am. Chem. Soc.* **1999**, *121*, 2488–2497.

Göttker-Schnetmann, I.; White, P.; Brookhart, M. *J. Am. Chem. Soc.* **2004**, *126*, 1804-1811.

Göttker-Schnetmann, I.; White, P. S.; Brookhart, M. *Organometallics* **2004**, *23*, 1766-1776.

Grönberg, K. L. C.; Henderson, R. A.; Oglieve, K. E. *J. Chem. Soc., Dalton Trans.* **1998**, 3093−3104.

Gupta, M.; Hagen, C.; Flesher, R. J.; Kaska, W. C.; Jensen, C. M. *Chem. Commun.* **1996**, 2083-2084.

Hackenberg, J. D.; Kundu, S.; Emge, T. J.; Krogh-Jespersen, K.; Goldman, A. S. *J. Am. Chem. Soc.* **2014**, *136*, 8891−8894.

Haibach, M. C.; Wang, D. Y.; Emge, T. J.; Krogh- Jespersen, K.; Goldman, A. S. *Chem. Sci.* **2013**, *4*, 3683−3692.

Hale, L. V. A.; Szymczak, N. K. *J. Am. Chem. Soc.* **2016**, *138*, 13489–13492.

Hammett, L. P. *Chem. Rev.* **1935**, *17*, 125–136.

Hansch, C.; Leo, A.; Taft, R. W. *Chem. Rev.* **1991**, *91*, 165–195.

Harisekhar, M.; Kumar, V. P.; Priya, S. S.; Chary, K. V. R. *J. Chem. Technol. Biotechnol.* **2015**, *90*, 1906–1917.

Hartley, F. R. *Chem. Soc. Rev.* **1973**, *2*, 163-179.

Henning, J.; Schubert, H.; Eichele, K.; Winter, F.; Pöttgen, R.; Mayer, H. A.; Wesemann, L. *Inorg. Chem.* **2012**, *51*, 5787-5794.

Hocking, R. K.; Hambley, T. W. *Organometallics* **2007**, *26*, 2815-2823.

Holmes, A. J.; Rayner, P. J.; Cowley, M. J.; Green, G. G. R.; Whitwood, A. C.; Duckett, S. B. *Dalton Trans.* **2015**, *44*, 1077−1083.

Huang, Z.; White, P. S.; Brookhart, M. *Nature* **2010**, *465*, 598-601.

Ibers, J. A.; La Placa, S. J. *Science* **1964**, *145*, 920-921.

Imhoff, P.; Gülpen, J. H.; Vrieze, K.; Smeets, W. J. J.; Spek, A. L.; Elsevier, C. J. *Inorg. Chim. Acta* **1995**, *235*, 77-88.

Iron, M. A.; Ben-Ari, E.; Cohen, R.; Milstein, D. *Dalton Trans.* **2009**, 9433-9439.

Jessop, P. G.; Morris, R. H. *Coord. Chem. Rev.* **1992**, *121*, 155−284.

Jia, G.; Lau, C.-P. Coord. *Chem. Rev.* **1999**, *190−192*, 83− 108. (b) Li, T.; Lough, A. J.; Morris, R. H. *Chem. Eur. J.* **2007**, *13*, 3796−3803.

Kaljurand, I.; Kütt, A.; Sooväli, L.; Rodima, T.; Mäemets, V.; Leito, I.; Koppel, I. A. *J. Org. Chem.* **2005**, *70*, 1019−1028.

Kivistö, A.; Santala, V.; Karp, M. *J. Biotechnol.* **2012**, *158*, 242–247.

Kloek, S. M.; Heinekey, D. M.; Goldberg, K. I. *Organometallics* **2006**, *25*, 3007−3011.

Koehne, I.; Schmeier, T. J.; Bielinski, E. A.; Pan, C. J.; Lagaditis, P. O.; Bernskoetter, W. H.; Takase, M. K.; Würtele, C.; Hazari, N.; Schneider, S. *Inorg. Chem.* **2014**, *53*, 2133−2143.

Kovács, G.; Nádasdi, L.; Laurenczy, G.; Joó, F. *Green Chem.* **2003**, *5*, 213–217.

Kraus, G. A. *Clean - Soil, Air, Water* **2008**, *36*, 648–651.

Krogh-Jespersen, K.; Czerw, M.; Zhu, K.; Singh, B.; Kanzelberger, M.; Darji, N.; Achord, P. D.; Renkema, K. B.; Goldman, A. S. *J. Am. Chem. Soc.* **2002**, *124*, 10797-10809.

Kubas, G. J. *Chem. Rev.* **2007**, *107*, 4152–4205.

Kubas, G. J. *Proc. Natl. Acad. Sci.* **2007**, *104*, 6901–6907.

Kuklin, S. A.; Sheloumov, A. M.; Dolgushin, F. M.; Ezernitskaya, M. G.; Peregudov, A. S.; Petrovskii, P. V.; Koridze, A. A.; August, R. V. *Organometallics* **2006**, *25*, 5466-5476.

Kundu, S.; Choi, J.; Wang, D. Y.; Choliy, Y.; Emge, T. J.; Krogh-Jespersen, K.; Goldman, A. S. *J. Am. Chem. Soc.* **2013**, *135*, 5127-5143.

Kundu, S.; Choliy, Y.; Zhuo, G.; Ahuja, R.; Emge, T. J.; Warmuth, R.; Brookhart, M.; Krogh-Jespersen, K.; Goldman, A. S. *Organometallics* **2009**, *28*, 5432-5444.

Labinger, J. A.; Osborn, J. A.; Coville, N. J. *Inorg. Chem.* **1980**, *19*, 3236–3243.

Labinger, J. A.; Osborn, J. A. *Inorg. Chem.* **1980**, *19*, 3230–3236.

Labinger, J. A. *Organometallics* **2015**, *34*, 4784–4795.

Lao, D. B.; Owens, A. C. E.; Heinekey, D. M.; Goldberg, K. I. *ACS Catal.* **2013**, *3*, 2391–2396.

Lebel, H.; Ladjel, C.; Bélanger-Gariépy, F.; Schaper, F. *J. Organomet. Chem.* **2008**, *693*, 2645–2648.

Lee, C. S.; Aroua, M. K.; Daud, W. M. A. W.; Cognet, P.; Pérès-Lucchese, Y.; Fabre, P. L.; Reynes, O.; Latapie, L. *Renew. Sustain. Energy Rev.* **2015**, *42*, 963–972.

Leyssens, T.; Peeters, D.; Orpen, A. G.; Harvey, J. N. *Organometallics* **2007**, *26*, 2637-2645.

Li, S.; Hall, M. B. *Organometallics* **1999**, *18*, 5682−5687.

Li, T.; Lough, A. J.; Morris, R. H. *Chem. Eur. J.* **2007**, *13*, 3796–3803.

Li, T.; Lough, A. J.; Zuccaccia, C.; Macchioni, A.; Morris, R. H. *Can. J. Chem.* **2006**, *84*, 164–175.

Lide, D. R. *Structure of Free Molecules in the Gas Phase*; CRC Press: Boca Raton, FL, 2014.

Liu, F.; Goldman, A. S. *Chem. Commun.* **1999**, 655−656.

Liu, F.; Pak, E. B.; Singh, B.; Jensen, C. M.; Goldman, A. S. *J. Am. Chem. Soc.* **1999**, *121*, 4086-4087.

Lough, A. J.; Park, S.; Ramachandran, R.; Morris, R. H. *J. Am. Chem. Soc.* **1994**, *116*, 8356–8357.

Luterbacher, J. S.; Martin Alonso, D.; Dumesic, J. A. *Green Chem.* **2014**, *16*, 4816–4838.

Lyons, T. W.; Guironnet, D.; Findlater, M.; Brookhart, M. *J. Am. Chem.* Chem. Soc. **2012**, *134*, 15708-15711.

Mag, M.; Engels, J. W. *Nucleic Acids Res.* **1989**, *17*, 5973-5988.

Mantina, M.; Valero, R.; Cramer, C. J.; Truhlar, D. G. *Atomic Radii of the Elements*; CRC Press: Boca Raton, FL, 2014.

Mazzini, F.; Salvadori, P. *Synthesis* **2005**, 2479–2481.

McLaughlin, M. P.; Adduci, L. L.; Becker, J. J.; Gagné, M. R. *J. Am. Chem. Soc.* **2013**, *135*, 1225–1227.

Meakin, P.; Muetterties, E. L.; Jesson, J. P. *J. Am. Chem. Soc.* **1973**, *95*, 75−88.

Montag, M.; Efremenko, I.; Cohen, R.; Shimon, L. J. W.; Leitus, G.; Diskin-Posner, Y.; Ben-David, Y.; Salem, H.; Martin, J. M. L.; Milstein, D. *Chem. Eur. J.* **2010**, *16*, 328-353.

Montag, M.; Schwartsburd, L.; Cohen, R.; Leitus, G.; Ben-David, Y.; Martin, J. M. L.; Milstein, D. *Angew. Chem. Int. Ed.* **2007**, *46*, 1901-1904.

Morales-Morales, D.; Redón, R.; Wang, Z.; Lee, D. W.; Yung, C.; Magnuson, K.; Jensen, C. M. *Can. J. Chem.* **2001**, *79*, 823−829.

Morales-Morales, D.; Redón, R.; Yung, C.; Jensen, C. M. *Inorg. Chim. Acta* **2004**, *357*, 2953-2956.

Morris, R. H. *J. Am. Chem. Soc.* **2014**, *136*, 1948−1959.

Morris, R. H. *Chem. Rev.* **2016**, *116*, 8588−8654.

Moulton, C. J.; Shaw, B. L. *J. Chem. Soc., Dalton Trans.* **1976**, 1020-1024.

Murray, J.; King, D. *Nature* **2012**, 433-435.

Nabavizadeh, S. M.; Amini, H.; Rashidi, M.; Pellarin, K. R.; McCready, M. S.; Cooper, B. F. T.; Puddephatt, R. J. *J. Organomet. Chem.* **2012**, *713*, 60–67.

Nakagawa, Y.; Ning, X.; Amada, Y.; Tomishige, K. *Appl. Catal. A: Gen.* **2012**, *433–434*, 128–134.

Oh, J.; Dash, S.; Lee, H. *Green Chem.* **2011**, *13*, 2004-2007.

O'Reilly, M. E.; Veige, A. S. *Chem. Soc. Rev.* **2014**, *43*, 6325-6369.

Organometallic Pincer Chemistry; Topics in Organometallic Chemistry; van Koten, G.; Milstein, D., Eds.; Springer: Heidelberg, 2013; Vol. *40*.

Park, S.; Bézier, D.; Brookhart, M. *J. Am. Chem. Soc.* **2012**, *134*, 11404-11407.

Paterniti, D. P.; Roman, P. J., Jr.; Atwood, J. D. *Organometallics* **1997**, *16*, 3371–3376.

Peris, E.; Wessel, J.; Patel, B. P.; Crabtree, R. H. *J. Chem. Soc., Chem. Commun.* **1995**, 2175–2176.

Polukeev, A. V.; Petrovskii, P. V.; Peregudov, A. S.; Ezernitskaya, M. G.; Koridze, A. A. *Organometallics* **2013**, *32*, 1000-1015.

Pons, V.; Heinekey, D. M. *J. Am. Chem. Soc.* **2003**, *125*, 8428–8429.

Powell, J.; Shaw, B. L. *J. Chem. Soc. A* **1968**, 617−622.

Qian, H.; Hopfield, J. J. *J. Chem. Phys.* **1996**, *105*, 9292−9298.

Ren, D.; Wong, N. T.; Handoko, A. D.; Huang, Y.; Yeo, B. S. *J. Phys. Chem. Lett.* **2016**, *7*, 20–24.

Roberto, D.; Cariati, E.; Psaro, R.; Ugo, R. *Organometallics* **1994**, *13*, 4227-4231.

Roddick, D. M. *Top. Organomet. Chem.* **2013**, *40*, 49-88.

Roddick, D. M.; Zargarian, D. *Inorg. Chim. Acta* **2014**, *422*, 251–264.

Rodima, T.; Kaljurand, I.; Pihl, A.; Mäemets, V.; Leito, I.; Koppel, I. A. *J. Org. Chem.* **2002**, *67*, 1873−1881.

Rodriguez, A.; Wojtusik, M.; Masca, F.; Santos, V. E.; Garcia-Ochoa, F. *Biochem. Eng. J.* **2017**, *117*, 57–65.

Romero, P. E.; Whited, M. T.; Grubbs, R. H. *Organometallics* **2008**, *27*, 3422−3429.

Ruppert, A, M.; Weinberg, K.; Palkovits, R. *Angew. Chem. Int. Ed.* **2012**, *51*, 2564−2601.

Rybtchinski, B.; Ben-David, Y.; Milstein, D. *Organometallics* **1997**, *16*, 3786-3793.

Salem, H.; Shimon, L. J. W.; Diskin-Posner, Y.; Leitus, G.; Ben-David, Y.; Milstein, D. *Organometallics* **2009**, *28*, 4791−4806.

Saouma, C. T.; Kaminsky, W.; Mayer, J. M. *J. Am. Chem. Soc.* **2012**, *134*, 7293-7296.

Schlaf, M. *Dalton Trans.* **2006**, 4645–4653.

Schlaf, M.; Ghosh, P.; Fagan, P. J.; Hauptman, E.; Bullock, R. M. *Adv. Synth. Catal.* **2009**, *351*, 789–800.

Schlaf, M.; Ghosh, P.; Fagan, P. J.; Hauptman, E.; Bullock, R. M. *Angew. Chem. Int. Ed.* **2001**, *40*, 3887–3890.

Schmeier, T. J.; Dobereiner, G. E.; Crabtree, R. H.; Hazari, N. *J. Am. Chem. Soc.* **2011**, *133*, 9274–9277.

Schwartsburd, L.; Iron, M. A.; Konstantinovski, L.; Diskin-Posner, Y.; Leitus, G.; Shimon, L. J. W.; Milstein, D. *Organometallics* **2010**, *29*, 3817−3827.

Simões, J. A. M.; Beauchamp, J. L. *Chem. Rev.* **1990**, *90*, 629-688.

Sutton, A. D.; Waldie, F. D.; Wu, R.; Schlaf, M.; Silks, L. A. P.; Gordon, J. C. *Nat. Chem.* **2013**, *5*, 428–432.

Svensson, P. H.; Kloo, L. *Chem. Rev.* **2003**, *103*, 1649–1684.

Sykes, A. C.; White, P.; Brookhart, M. *Organometallics* **2006**, *25*, 1664-1675.

Tabah, B.; Varvak, A.; Pulidindi, I. N.; Foran, E.; Banin, E.; Gedanken, A. *Green Chem.* **2016**, *18*, 4657–4666.

Thorn, D. L. *J. Am. Chem. Soc.* **1980**, *102*, 7109–7110.

Timpa, S. D.; Zhou, J.; Bhuvanesh, N.; Ozerov, O. V. *Organometallics* **2014**, *33*, 6210-6217.

Titova, E. M.; Silantyev, G. A.; Filippov, O. A.; Gulyaeva, E. S.; Gutsul, E. I.; Dolgushin, F. M.; Belkova, N. V. Eur. J. *Inorg. Chem.* **2016**, *2016*, 56−63.

Tse, S. K. S.; Xue, P.; Lin, Z.; Jia, G. *Adv. Synth. Catal.* **2010**, *352*, 1512–1522.

Underwood, H. W., Jr.; Baril, O. L. *J. Am. Chem. Soc.* **1930**, *52*, 395–397.

Underwood, H. W., Jr.; Baril, O. L. *J. Am. Chem. Soc.* **1931**, 53, 2200-2202.

Vabre, B.; Lambert, M. L.; Petit, A.; Ess, D. H.; Zargarian, D. *Organometallics* **2012**, *31*, 6041-6053.

van Beek, J. A. M.; van Koten, G.; Smeets, W. J. J.; Spek, A. L. *J. Am. Chem. Soc.* **1986**, *108*, 5010–5011.

van der Boom, M. E.; Milstein, D. *Chem. Rev.* **2003**, *103*, 1759-1792.

van Koten, G.; Terheijden, J.; van Beek, J. A. M.; Wehman-Ooyevaar, I. C. M.; Muller, F.; Stam, C. H. *Organometallics* **1990**, *9*, 903–912.

Vaska, L. *J. Am. Chem. Soc.* **1966**, *88*, 5325–5327.

Vaska, L. *Science* **1963**, *140*, 809–810.

Vaska, L.; Werneke, M. F. *Ann. N. Y. Acad. Sci.* **1971**, *172*, 546−562.

Vuzman, D.; Poverenov, E.; Diskin-Posner, Y.; Leitus, G.; Shimon, L. J. W.; Milstein, D. *Dalton Trans.* **2007**, 5692-5700.

Wang, Y.; Zhou, J.; Guo, X. *RSC Adv.* **2015**, *5*, 74611–74628.

Williams, B. S.; Goldberg, K. I. *J. Am. Chem. Soc.* **2001**, *123*, 2576–2587.

Williams, D. B.; Kaminsky, W.; Mayer, J. M.; Goldberg, K. I. *Chem. Commun.* **2008**, 4195-4197.

Wood, B. M.; Kirwan, K.; Maggs, S.; Meredith, J.; Coles, S. R. *J. Clean. Prod.* **2015**, *93*, 167–173.

Yang, F.; Hanna, M. A.; Sun, R. *Biotechnol. Biofuels* **2012**, *5*, 13.

Yonker, C. R.; Linehan, J. C. *J. Organomet. Chem.* **2002**, *650*, 249-257.

Yonker, C. R.; Linehan, J. C. *Prog. Nucl. Magn. Reson. Spectrosc.* **2005**, *47*, 95–109.

Zeng, H.; Miller, R. S.; Flowers, R. A., II; Gong, B. *J. Am. Chem. Soc.* **2000**, *122*, 2635-2644.

Zhou, C. H.; Beltramini, J. N.; Fan, Y. X.; Lu, G. Q. *Chem. Soc. Rev.* **2008**, *37*, 527–549.

Zhu, K.; Achord, P. D.; Zhang, X.; Krogh- Jespersen, K.; Goldman, A. S. *J. Am. Chem. Soc.* **2004**, *126*, 13044-13053.

Appendix A: Supporting Data for Chapter 2

Table A1. Crystallographic data for complexes 2a, 2c, 6a, and 9.

	2a	**2c**	**6a**	**9**
Empirical formula	$C_{19}H_{32}ClIrO_7P_2$	$C_{39}H_{60}ClIrO_{15}P_2$	$C_{19}H_{32}ClIrO_3P_2$	$C_{27}H_{43}IrO_7P_2$
Formula weight	662.04	1058.46	598.04	733.75
Temperature (K)	100(2)	100(2)	100(2)	100(2)
Wavelength (Å)	0.71073	0.71073	0.71073	0.71073
Crystal system	Orthorhombic	Orthorhombic	Monoclinic	Monoclinic
Space group	P c a 2_1	P 2_1 2_1 2_1	P 2_1/c	P 2_1/c
Unit cell axes (Å)	a = 9.3982(1) b = 20.578(2) c = 13.2708(14)	a = 9.2119(14) b = 17.394(3) c = 27.774(5)	a = 8.7214(7) b = 12.5800(11) c = 21.1323(18)	a = 8.1769(6) b = 33.692(2) c = 11.5909(8)
Unit cell angles (°)	α = 90 β = 90 γ = 90	α = 90 β = 90 γ = 90	α = 90 β = 101.316(4) γ = 90	α = 90 β = 107.356(3) γ = 90
Volume ($Å^3$)	2566.6(5)	4450.2(13)	2273.5(3)	3047.8(4)
Z	4	4	4	4
Density (calculated) (Mg/m^3)	1.713	1.580	1.747	1.599
Absorption coefficient (mm^{-1})	5.465	3.197	6.146	4.526
F(000)	1304	2152	1176	1472
Crystal size (mm^3)	0.20 x 0.08 x 0.02	0.15 x 0.10 x 0.05	0.18 x 0.15 x 0.12	0.30 x 0.18 x 0.02
Theta range for data collection	2.38 to 34.59°	1.88 to 28.21°	2.89 to 30.75°	2.20 to 30.56°
Reflections collected	74919	188919	63343	148583
Independent reflections	10855	10800	6895	9328
R_{int}	0.0447	0.0811	0.0853	0.0577
Completeness to theta (%)	99.9 to 25.00°	100.0 to 25.00°	97.2 to 25.00°	100.0 to 25.00°
Max. and min. transmission	0.8986 and 0.4078	0.8565 and 0.6456	0.5258 and 0.4042	0.9149 and 0.3438
Data / restraints / parameters	10855 / 1 / 285	10800 / 0 / 541	6895 / 9 / 258	9328 / 15 / 368
Goodness-of-fit on F^2	1.088	1.025	1.039	1.122
Final R indices [I>2sigma(I)]	R1 = 0.0233, wR2 = 0.0475	R1 = 0.0262, wR2 = 0.0422	R1 = 0.0471, wR2 = 0.0944	R1 = 0.0260, wR2 = 0.0528
R indices (all data)	R1 = 0.0297, wR2 = 0.0494	R1 = 0.0405, wR2 = 0.0454	R1 = 0.0846, wR2 = 0.1079	R1 = 0.0324, wR2 = 0.0553
Largest diff. peak and hole (e. $Å^{-3}$)	1.499 and -2.137	0.667 and -0.636	1.958 and -2.765	1.177 and -2.299

Table A2. Crystallographic data for complexes 10, 12, 13, and 14.

	10	**12**	**13**	**14**
Empirical formula	$C_{24}H_{38}Cl_3IrO_7P_2$	$C_{23}H_{40}BF_4IrO_3P_2$	$C_{19}H_{34}BF_4IrO_4P_2$	$C_{25}H_{42}BCl_2F_4IrO_4P_2$
Formula weight	799.03	705.50	667.41	818.44
Temperature (K)	100(2)	100(2)	100(2)	100(2)
Wavelength (Å)	0.71073	0.71073	0.71073	0.71073
Crystal system	Monoclinic	Monoclinic	Triclinic	Monoclinic
Space group	P 2_1/n	P 2_1/c	P $\bar{1}$	P 2_1/n
Unit cell axes (Å)	a = 7.8402(5) b = 20.3459(13) c = 19.7129(12)	a = 8.3197(9) b = 26.391(3) c = 12.5000(13)	a = 8.6030(6) b = 12.1556(9) c = 12.7217(9)	a = 11.313(2) b = 20.531(4) c = 14.041(2)
Unit cell angles (°)	α = 90 β = 91.330(3) γ = 90	α = 90 β = 91.365(5) γ = 90	α = 98.823(3) β = 93.861(4) γ = 105.923(3)	α = 90 β = 105.506(8) γ = 90
Volume ($Å^3$)	3143.7(3)	2743.8(5)	1255.78(16)	3142.7
Z	4	4	2	4
Density (calculated) (Mg/m^3)	1.688	1.708	1.765	1.730
Absorption coefficient (mm^{-1})	4.642	5.032	5.495	4.573
F(000)	1584	1400	656	1624
Crystal size (mm^3)	0.15 x 0.09 x 0.03	0.15 x 0.10 x 0.04	0.24 x 0.15 x 0.11	0.60 x 0.12 x 0.10
Theta range for data collection	2.00 to 30.59°	1.80 to 30.68°	2.48 to 28.40°	1.80 to 28.59°
Reflections collected	71980	145206	41686	157716
Independent reflections	9544	8454	6221	7979
R_{int}	0.0499	0.0344	0.0250	0.0349
Completeness to theta (%)	98.7 to 30.59°	99.8 to 25.00°	99.8 to 25.00°	99.9 to 25.00°
Max. and min. transmission	0.8733 and 0.5427	0.8241 and 0.5190	0.5832 and 0.3522	0.6577 and 0.1700
Data / restraints / parameters	9544 / 0 / 349	8454 / 126 / 361	6221 / 0 / 300	7979 / 21 / 395
Goodness-of-fit on F^2	1.074	1.157	1.043	1.089
Final R indices [I>2sigma(I)]	R1 = 0.0312, wR2 = 0.0630	R1 = 0.0185, wR2 = 0.0361	R1 = 0.0177, wR2 = 0.0413	R1 = 0.0147, wR2 = 0.0360
R indices (all data)	R1 = 0.0462, wR2 = 0.0681	R1 = 0.0244, wR2 = 0.0382	R1 = 0.0201, wR2 = 0.0420	R1 = 0.0169, wR2 = 0.0377
Largest diff. peak and hole (e. $Å^{-3}$)	1.358 and -1.321	0.923 and -0.723	1.258 and -1.178	0.842 and -0.799

Appendix B: Supporting Data for Chapter 3

Table B1. Crystallographic data for complexes *trans*-7, 10-BF_4, and 15.

	***trans*-7**	**10-BF_4**	**15**
Empirical formula	$C_{19}H_{33}IrO_3P_2$	$C_{24}H_{37}BF_4IrNO_3P_2$	$C_{62}H_{102}B_2Cl_4F_8Ir_2N_2O_2P_4$
Formula weight	563.59	728.49	1731.15
Temperature (K)	100(2)	100(2)	100(2)
Wavelength (Å)	0.71073	0.71073	0.71073
Crystal system	Triclinic	Triclinic	Triclinic
Space group	P -1	P -1	P -1
Unit cell axes (Å)	a = 7.8388(5) b = 9.9117(7) c = 15.1225(10)	a = 10.7054(9) b = 14.1797(10) c = 18.4651(16)	a = 12.9175(9) b = 14.7329(10) c = 20.1421(14)
Unit cell angles (°)	α = 105.935(3) β = 92.176(3) γ = 107.411(3)	α = 89.544(4) β = 88.624(4) γ = 88.014(3)	α = 109.001(4) β = 96.628(4) γ = 90.772(4)
Volume ($Å^3$)	1068.76(12)	2800.4(4)	3594.9(4)
Z	2	4	2
Density (calculated) (Mg/m^3)	1.751	1.728	1.599
Absorption coefficient (mm^{-1})	6.411	4.935	3.998
F(000)	556	1440	1736.0
Crystal size (mm^3)	0.18 × 0.15 × 0.10	0.16 × 0.13 × 0.020	0.4 × 0.3 × 0.03
Theta range for data collection	2.26 to 28.42°	1.437 to 28.342°	2.928 to 56.87°
Index Ranges	-10 ≤ h ≤ 10 -13 ≤ k ≤ 13 -20 ≤ l ≤ 20	-14 ≤ h ≤ 14 -18 ≤ k ≤ 18 0 ≤ l ≤ 24	-17 ≤ h ≤ 17 -19 ≤ k ≤ 19 -26 ≤ l ≤ 26
Reflections collected	46232	70125	156408
Independent reflections	5353	13356	17805
R_{int}	0.0274	0.0778	0.0693
Data / restraints / parameters	5353 / 0 / 242	13356 / 25 / 672	17805 / 1 / 807
Goodness-of-fit on F^2	1.045	1.016	1.032
Final R indices [I>2σ(I)]	R_1 = 0.0132, wR_2 = 0.0268	R_1 = 0.0494, wR_2 = 0.1201	R_1 = 0.0344, wR_2 = 0.0726
R indices (all data)	R_1 = 0.0143, wR_2 = 0.0271	R_1 = 0.0756, wR_2 = 0.1358	R_1 = 0.0545, wR_2 = 0.0820
Largest diff. peak and hole (e. $Å^{-3}$)	0.558 and -0.560	3.090 and -2.688	2.33 and -2.14

Solubility Observations from pK_a Studies

Studies of the pK_a values for **5-BF$_4$** showed that limited solubility of salts could give misleading results. When deprotonation of **5-BF$_4$** was screened with a series of bases, solid precipitates formed even in the presence of weak bases. Once the more soluble **5-BArF$_{20}$** was studied for deprotonation, there was no driving force for salt formation. Pyridine was not a suitable base for deprotonation, since it coordinated as a sixth ligand to an unsaturated Ir center to give **11**. When **1** was reacted with [Hpyr]BF_4 in CD_2Cl_2, protonation was not obtained, likely due to the limited solubility of [Hpyr]BF_4 and the corresponding Ir(III) adduct. Protonation of **1** with pyridinium is complicated by the complexation of pyridine. While pyridine is a better base than **1** based on the experimentally determined pK_a of **5-BArF$_{20}$** and a simple acid-base reaction would not be expected, formation of **11** is observed. This is likely due to formation of a soluble octahedral Ir(III) compound where pyridine can stabilize an unsaturated Ir(III) metal center. Further support for the competition of an acid-base reaction versus stabilization of an unsaturated metal center was found when **5-BArF$_{20}$** was completely deprotonated by the non-coordinating base 2,6-lutidine rather than coordination of the lutidine moiety in the sixth coordination site. In this case, deprotonation is favored over coordination of a sixth ligand since 2,6-lutidine is sterically hindered.

Appendix C: Supporting Data for Chapter 5

Table C1. Crystallographic data for complexes 4, 6, 8, and 10.

	4	**6**	**8**	**10**
Empirical formula	$C_{23}H_{39}I_2IrO_3P_2$	$C_{25}H_{38}I_2IrO_5P_2$	$C_{25}H_{44}I_6IrNO_3P_2$	$C_{51}H_{80}Br_8Cl_2Ir_2O_{10}P_4$
Formula weight	871.48	926.49	1422.15	2071.61
Temperature (K)	100(2)	100(2)	100(2)	100(2)
Wavelength (Å)	0.71073	0.71073	0.71073	0.71073
Crystal system	Monoclinic	Monoclinic	Monoclinic	Orthorhombic
Space group	P 2_1/n	P 2_1/c	P 2_1/n	P b c n
Unit cell axes (Å)	a = 8.9580(7) b = 25.997(2) c = 12.2529(10)	a = 9.4617(4) b = 18.6805(8) c = 17.9283(8)	a = 7.8947(5) b = 25.7322(16) c = 19.1820(12)	a = 37.123(4) b = 12.0368(11) c = 15.0715(17)
Unit cell angles (°)	α = 90 β = 105.337(4) γ = 90	α = 90 β = 90.510(3) γ = 90	α = 90 β = 95.190(3) γ = 90	α = 90 β = 90 γ = 90
Volume ($Å^3$)	2751.8(4)	3168.7(2)	3880.8(4)	6734.6(12)
Z	4	4	4	4
Density (calculated) (Mg/m^3)	2.104	1.942	2.434	2.043
Absorption coefficient (mm^{-1})	7.234	6.293	8.321	8.919
F(000)	1656	1764	2600	3976
Crystal size (mm^3)	0.06 × 0.05 × 0.03	0.12 × 0.08 × 0.06	0.23 × 0.03 × 0.01	0.52 × 0.22 × 0.15
Theta range for data collection	1.89 to 28.39°	2.15 to 26.46°	2.13 to 28.64°	1.78 to 28.48°
Index Ranges	-11 ≤ h ≤ 11 0 ≤ k ≤ 34 0 ≤ l ≤ 16	-11 ≤ h ≤ 11 -23 ≤ k ≤ 23 -22 ≤ l ≤ 22	-10 ≤ h ≤ 10 -34 ≤ k ≤ 34 -25 ≤ l ≤ 25	-49 ≤ h ≤ 49 -16 ≤ k ≤ 16 -20 ≤ l ≤ 20
Reflections collected	513822	60200	110065	484496
Independent reflections	6877	6544	9753	8375
R_{int}	0.0430	0.0594	0.0863	0.0721
Data / restraints / parameters	6877 / 0 / 295	6544 / 0 / 328	9753 / 28 / 392	8375 / 29 / 382
Goodness-of-fit on F^2	1.155	1.147	1.039	1.088
Final R indices [I>2σ(I)]	R_1 = 0.0314, wR_2 = 0.0914	R_1 = 0.0493, wR_2 = 0.0976	R_1 = 0.0418, wR_2 = 0.0766	R_1 = 0.0330, wR_2 = 0.0763
R indices (all data)	R_1 = 0.0344, wR_2 = 0.0932	R_1 = 0.0614, wR_2 = 0.1018	R_1 = 0.0702, wR_2 = 0.0851	R_1 = 0.0395, wR_2 = 0.0792
Largest diff. peak and hole (e. $Å^{-3}$)	1.572 and -2.210	1.547 and -1.417	1.469 and -2.223	2.367 and -1.694

Vita

Jonathan M. Goldberg was born in 1990 in New York, NY. In 2008, he graduated from Churchville-Chili Senior High School in the suburbs of Rochester, NY. He then attended the University of Rochester in Rochester, NY where he graduated with a Bachelor of Science degree in chemistry in 2012. While at UR, he worked with Prof. Patrick L. Holland on examining C-F bond activation reactions with low-coordinate cobalt complexes. Jonathan then attended graduate school at the University of Washington in Seattle, WA. While at UW, he worked jointly with Profs. D. Michael Heinekey and Karen I. Goldberg on synthesizing iridium pincer complexes and examining their applications to glycerol deoxygenation. Jonathan obtained a Doctor of Philosophy degree in chemistry in 2017.